Natural compounds as pathoblockers of streptococcal infections

Dissertation

zur Erlangung des Grades

des Doktors der Naturwissenschaften

der Naturwissenschaftlich-Technischen Fakultät III

Chemie, Pharmazie, Bio- und Werkstoffwissenschaften

der Universität des Saarlandes

von

Katharina Rox

Saarbrücken

2015

Tag des Kolloquiums:	16. September 2015
Dekan:	Prof. Dr.-Ing. Dirk Bähre
Berichterstatter:	Prof. Dr. Rolf Müller
	Prof. Dr. Manfred Rohde
Vorsitz:	Prof. Dr. Rolf Hartmann
Akad. Mitarbeiter:	Dr. Martin Frotscher

Diese Arbeit entstand unter Anleitung von Prof. Dr. Rolf Müller (in Kooperation mit Prof. Dr. Gursharan Singh Chhatwal in der Abteilung Medizinische Mikrobiologie des Helmholtz-Zentrums für Infektionsforschung; Januar 2012 bis Juni 2013) in der Fachrichtung 8.2 Pharmazeutische Biotechnologie der Naturwissenschaftlich-Technischen Fakultät III der Universität des Saarlandes von Januar 2012 bis März 2015.

meinen Eltern

und

meiner Schwester Barbara

Zusammenfassung

Millionen Menschen weltweit sind von Krankheiten betroffen, die durch Streptokokken verursacht werden und bisweilen schwere Verlaufsformen aufweisen. Letalitätsraten von bis zu 30 % für schwere Verläufe und wiederkehrende Infektionen, die oft zu Spätkomplikationen wie der rheumatischen Herzkrankheit führen, zeigen, dass die derzeitigen antibiotischen Möglichkeiten nicht ausreichen. Daher wird nun ein neuer Ansatz verfolgt: Diesem liegt die These zugrunde, dass das Angreifen an konservierten Virulenzmechanismen das Auftreten von Resistenzen vermeidet. Für diesen Ansatz werden so genannte „kleine Moleküle“ benötigt. Myxobakterien haben sich als verlässliche Produzenten solcher „kleinen Moleküle“ erwiesen, wobei sie zudem oft neu chemische Grundstrukturen und neuartige Wirkmechanismen bieten.

Daher wurden myxobakterielle Extrakte und Substanzen auf ihre Aktivität in Bezug auf zwei Virulenzmechanismen von *S.pyogenes* untersucht: die Invasion in Epithelzellen und die Ausnutzung des menschlichen Plasmin(ogen)-Systems. Dabei wurden mikro-, zellbiologische und analytische Methoden kombiniert. Aktive Substanzen wurden mittels einer bioaktivitätsgeleiteten Isolierungsstrategie in Verbindung mit analytischen Methoden identifiziert.

Diese Arbeit zeigt, dass myxobakterielle Substanzen erfolgreich mit zwei Virulenzmechanismen von *S.pyogenes* interferieren können: (1) Zwei Substanzen hemmen die Invasion, indem sie an einem Protein angreifen, dessen Rolle in diesem Prozess bisher unbekannt war. (2) Mehrere Substanzen können als neue Hemmstoffe des Plasmin(ogen)s dienen und zeigen zudem eine bessere Aktivität als bisher bekannte Antifibrinolytika. Des Weiteren verlängerten zwei dieser Substanzen signifikant das Überleben in einem Maus-Hautinfektionsmodell, welches (sonst) zu einer Sepsis führt.

Diese Ergebnisse zeigen, dass diese neue Klasse von Anti-Infektiva, die Virulenzmechanismen angreift - die „Pathoblocker“ - durch die myxobakteriellen Substanzen bereichert und die Therapiemöglichkeiten von durch Streptokokken hervorgerufenen Krankheiten verbessern wird.

Abstract

Worldwide millions of people are affected by streptococcal diseases ranging from mild to severe. Lethality rates up to 30 % for invasive diseases and recurrent infections often leading to post-infection sequelae like rheumatic heart disease show that current antibiotic treatment is not sufficient. Therefore, a new concept has to be applied: It is assumed that resistance will not arise if conserved virulence mechanisms are targeted. To influence them small molecules are needed. Myxobacteria are proven producers of small molecules offering new chemical scaffolds and unknown modes-of-action.

Consequently, by combining microbiological, cell-biological and analytical methods myxobacterial extracts and compounds were screened for activity with regard to two virulence mechanisms of *S.pyogenes*: invasion into epithelial cells and exploitation of the host's plasmin(ogen) system. Active compounds were identified by linking a bioactivity-guided isolation strategy with analytical methods.

This work demonstrates that myxobacterial compounds interfere successfully with two virulence mechanisms of *S.pyogenes*: (1) Two compounds inhibit streptococcal invasion by targeting a protein not known to be involved in this process so far. (2) Several compounds can serve as new inhibitors of plasmin(ogen) showing better inhibitory activity than known antifibrinolytics. Moreover, two of these compounds significantly prolonged survival in an *in vivo* skin infection model usually leading to systemic severity.

There is rising evidence that the new class of anti-infectives targeting virulence - the 'pathoblockers' - will be enriched by myxobacterial compounds and improve the therapy of diseases caused by *S.pyogenes*.

Table of contents

A List of Abbreviations

α	alpha
a.c.	after clotting
A40	*S.pyogenes* strain A40
A8	*S.pyogenes* strain A8
Ang852	*Angiococcus* strain Ang852
Anm9	*Angiococcus* strain Anm9
approx.	approximately
APSGN	acute poststreptococcal glomerulonephritis
ARF	acute rheumatic fever
Arg	arginine (amino acid)
Asp	asparagine (amino acid)
ATP	adenosine-triphosphate
β	beta
B_{12}	vitamin B_{12}
bp	base pairs
BLAST	basic local alignment search tool
BSA	bovine serum albumin
C3	complement factor C3
C4BP	C4b binding protein
calcd.	calculated
Cdc42	cell division protein 42
CFU/cfu	colony forming unit
Cma13	*Chondromyces robustus* strain 13
conc.	concentration
COSY	correlation spectroscopy (NMR method)
covRS	gene for the control of virulence regulatory system
ctrl	control
Cy/H	Cy/H medium
Da	Dalton
DisA	disorazole A
DisZ	disorazole Z
DMDS	dimethyl disulfide
DMEM	Dulbecco's Modified Eagle Medium
DMOX	dimethyloxazoline
DMSO	dimethylsulfoxid
DNA	deoxyribonucleic acid
dNTP	deoxy nucleoside triphosphate
e.Coli	*Escherichia Coli*
e.g.	*exempli gratia* (latin)
EACA	ε-amino caproic acid
EC_{50}	half maximal effective concentration
ECM	extracellular matrix
EE	ethylacetate
emm	gene for the M protein of group A *streptococcus*
ESI	electron spray ionization
FAK	focal adhesion kinase
FBS	fetal bovine serum
FCS	fetal calf serum
FESEM	field emission scanning electron microscopy/microscopic

fig.	figure/s
γ	gamma
GAPDH	glyceraldehyde-3-phosphate dehydrogenase
GAS	group A streptococci/*streptococcus*
GC	gas chromatography
Gly	glycine (amino acid)
GMAK	Genome Analytics (research group)
GTPase	guanosine triphosphate hydrolyzing enzyme
h	hour(s)
H	H medium
H_2O	water
HCS	high-content screening
HIPS	Helmholtz Institute for Pharmaceutical Research Saarland
His	histidine (amino acid)
HLA	human leukocyte antigen
HMBC	heteronuclear multiple bond correlation (NMR method)
HPLC	high performance liquid chromatography
HSQC	heteronuclear single quantum coherence (NMR method)
HTS	high-throughput screening
HR-ESIMS	high resolution electron spray ionization mass spectrometry
huPlg	human plasminogen
HUVEC	human umbilical vein endothelial cells
HZI	Helmholtz Centre for Infection Research
i.e.	*id est* (latin)
IC_{50}	concentration where 50 % of the target molecule are inhibited
IgA	immunoglobulin A
IgG	immunoglobulin G
Ile	isoleucine (amino acid)
ILK	integrin-linked kinase
INI	Infection Immunology (research group)
IPTG	isopropyl β-D1-thioalactopyranoside
IVIG	intravenous immunoglobulin
κ	kappa
k	kilo
l	Liter
L.lactis	*Lactococcus lactis*
LA	linoleic acid
Lac	*Lactococcus lactis* which is not expressing the SfbI protein
Lac-SfbI	*Lactococcus lactis* expressing the SfbI protein
LAMP-1	lysosomal-associated membrane protein 1
LB	Luria broth/ lysogeny broth
LC	liquid chromatography
LC-HRMS	liquid chromatography coupled to high-resolution mass spectrometry
LEA	linoelaidic acid
LPLC	low performance liquid chromatography
LTA	lipoteichoic acid
µg	microgram
Mac-1/2	IgG degrading enzyme of *S.pyogenes* 1/2
min	minute/s
MINS	Department of Microbial Natural Products
MISG	Microbial Strain Collection (research group)
ml	milliliter

MMIK	Department of Medical Microbiology
MMP	matrix metalloproteinase
MOI	multiplicity of infection
MS	mass spectrometry
MSCRAMM	microbial surface component recognizing adhesive matrix molecules
MTT	thiazolyl blue tetrazolium blue
MWIS	Department of Microbial Drugs
myxobase	internal database for myxobacteria of the groups MWIS and MISG (HZI) and MINS (HIPS)
n	number
NCBI	National Center for Biotechnology Information
NET	neutrophil extracellular trap
NFκB	nuclear factor 'kappa-light-chain-enhancer' of activated B-cells
nm	nanometer (wavelength)
NMR	nuclear magnetic resonance
NRPS	non-ribosomal peptide synthetase
ns	not significant
p-gp	p-glycoprotein
PA	palmitoleic acid
PAGE	polyacrylamide gel electrophoresis
PAM	plasminogen-binding group A streptococcal M or M-like protein
PBS	phosphate buffered saline
PCP	peptidyl carrier protein
PCR	polymerase chain reaction
PEA	palmitelaidic acid
PFA	paraformaldehyde
PI_3K	phosphatidyl-inositol-3-kinase
PKS	polyketide synthase
Pl6894	*Polyangium* strain Pl6894
PlD3	*Polyangium* strain PlD3
Plvo18	*Polyangium* strain Plvo18
Plvt3	*Kofleria flava* strain Plvt3
PMN	polymorphonuclear leukocyte
Pol	Pol medium
RHD	rheumatic heart disease
RNA	ribonucleic acid
RNASeq	sequencing of RNA, also whole transcriptome shotgun sequencing
RP	reversed phase
RP-HPLC	reversed phase high performance liquid chromatography
SAR	structure-activity-relationship(s)
s.c.	subcutaneous(ly)
ScpA	streptococcal C5a peptidase
SDS	sodium dodecyl sulfate
sec	second/s
SEM	scanning electron microscopy/microscopic
SEN	streptococcal surface enolase
Ser	serine (amino acid)
SfbI	fibronectin binding protein I of *S.pyogenes*
Sic	streptococcal inhibitor of complement
ska	gene for streptokinase from group A *streptococcus*
SLO	streptolysin O
SLS	streptolysin S

Soce	*Sorangium cellulosum*
Soce554	*Sorangium cellulosum* strain Soce554
Soce923	*Sorangium cellulosum* strain Soce923
Soce997	*Sorangium cellulosum* strain Soce997
SpeB	streptococcal pyrogenic exotoxin B
S.pneumoniae	*Streptococcus pneumoniae*
S.pyogenes	*Streptococcus pyogenes*
src kinase	sarcoma kinase
STSS	streptococcal toxic shock syndrome
TA	tranexamic acid
tab.	table/s
THB	Todd Hewitt Broth
THY	Todd Hewitt Yeast medium
TLR	Toll-like receptor
TNFα	tumor necrosis factor alpha
TOF	time of flight (detector for MS)
tPA	tissue plasminogen activator
TSB	Todd Soy Broth
TSY	Todd Soy Yeast medium
U	unit(s)
uPA	urokinase
US	United States (of America)
Val	valine (amino acid)
Vit	vitamin solution prepared after Schlegel
vs.	versus
w/o	without/ untreated
ZEIM	Central facility for microscopy

B List of tables and figures

B 1 Tables

Introduction

Materials and methods

Results

B 2 Figures

Introduction

Materials and methods

Results

Inhibitors of group A streptococcal invasion

Salinimyxantins as inhibitors of plasmin(ogen)

Fatty acids as inhibitors of plasmin(ogen)

Discussion

Supplemental information

Appendix

1 Introduction

1.1 Streptococci

Streptococci are a heterogeneous group of bacteria causing a wide range of diseases. The following paragraphs will give a short introduction to the genus *Streptococcus* first, before focusing on *Streptococcus pyogenes*, its epidemiology and pathogen-host-interactions.

1.1.1 The genus *Streptococcus*

The genus *Streptococcus* belongs to one of the most invasive groups of bacteria (Krzyściak *et al.*, 2013). Taxonomically, it can be divided into β-hemolytic and non-β-hemolytic groups (α- or γ-hemolysis; Schottmüller, 1903). Streptococci which show β-hemolysis on blood agar plates are able to lyse red blood cells completely, whereas streptococci exhibiting α-hemolysis are not able to lyse erythrocytes entirely and cause a green zone around the partially lysed cells. γ-hemolytic streptococci are not able to lyse red blood cells at all. Furthermore, streptococci can be characterized by their carbohydrate 'group' antigens and are classified after Rebecca Lancefield (Lancefield, 1933). The β-hemolytic group comprises *inter alia* *S.pyogenes, S.agalactiae, S.dysgalactiae subsp. dysgalactiae, S.dysgalactiae* subsp. *equisimilis,* the *S.anginosus* group and other streptococci like *S.canis* or *S.porcinus* which play a major role in zoonotic diseases but also in humans (Facklam, 2002). The non-β-hemolytic group comprises *S.pneumoniae*, different zoonotic streptococci like the *S.bovis* group and *S. suis*, and furthermore the viridans streptococci which are usually found in the oral cavity. Table 1-1 shows some characteristics and diseases caused by different species. Additionally, streptococci can be divided into six groups (pyogenic, anginosus, mitis, mutans,

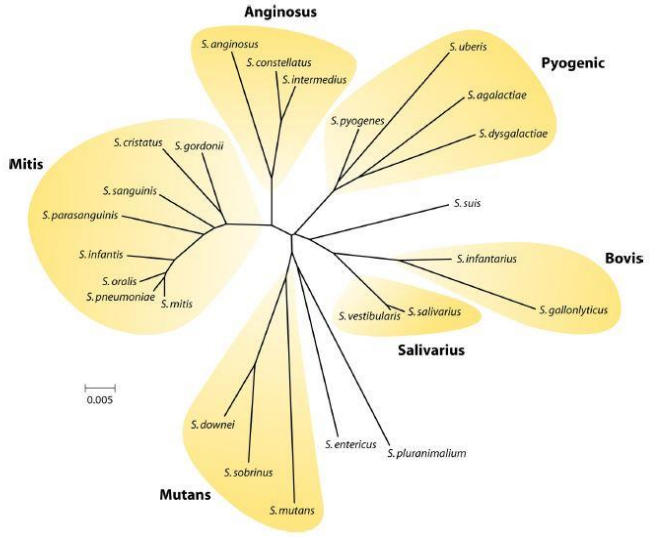

Figure 1-1. Classification of streptococci into groups based on their 16S rRNA sequence.
Adapted from Nobbs A.H. *et al*., 2009 (Copyright © 2009, American Society for Microbiology; reproduced with permission): The figure shows the classification of different streptococcal species based on their 16S rRNA sequence into the following six different groups: anginosus, pyogenic, bovis, salivarius, mitis and mutans. The different branches show specific groups as well as the degree of relationship of different species.

salivarius and bovis) based on 16S rRNA sequencing (fig. 1-1). Among all streptococci the species *S.pyogenes* which is also known as group A *streptococcus* is the most pathogenic bacterium in the genus. The following paragraph gives a deeper insight into characteristics, diseases caused by and pathogenesis of *S.pyogenes*.

Table 1-1. Characteristics and origins of different streptococcal species (after Facklam *et al.*, 2002). The following table gives details about different streptococcal species, their origins and their characteristics.

species	characteristics	origin
S.agalactiae	β-hemolytic Lancefield's group B antigen major cause of neonatal sepsis	human, bovine
***S.anginosus* group**	β-hemolytic and non-β-hemolytic strains Lancefield's group A, C, F or G antigen or none	human
***S.bovis* group**	non-β-hemolytic Lancefield's group D antigen	equine, bovine, koala, human
S.canis	Lancefield's group G antigen	dog, human
S.dysgalactiae* subsp. *dysgalactiae	not β-hemolytic although in the β-hemolytic group α-hemolytic Lancefield's group C antigen virulence factors similar to *S.pyogenes* like M-like proteins	animals
S.dysgalactiae* subsp. *equisimilis	β-hemolytic Lancefield's group A, C, G or L antigen found, but C most commonly found	human, animals
S.pneumoniae	non-β-hemolytic increasing prevalence of multi-drug resistance (Whitney *et al.*, 2000; Mera *et al.*, 2005) leading cause of community-acquired pneumonia (Yayan, 2014; Torres *et al.*, 2015)	human
S.pyogenes	β-hemolytic Lancefield's group A antigen causes severe (i.e. cellulitis, necrotizing fasciitis) as well as mild (i.e. pharyngitis) infections	human
S.suis	α-hemolytic Lancefield's group R antigen	swine, human
Viridans group streptococci	non-β-hemolytic Lancefield's group A, C, F or G antigen or none consists of the mutans group, salivarius group, sanguinis group and mitis group (anginosus group partially classified as β-hemolytic) often found in the oral cavity cause of bacterial endocarditis	human, rat, monkey, swine, avian

1.1.2 *Streptococcus pyogenes*

S.pyogenes is a gram-positive, non-motile, non-spore-forming coccus harboring the Lancefield group A antigen. Therefore, it is also called group A *streptococcus* (GAS). The antigen is a carbohydrate which consists of N-acetyl-β-D-glucosamine linked to a polymeric rhamnose chain. Individual cells are 0.6-1.0 µm in diameter and round to ovoid. They grow in pairs or short chains. Longer chains are found when streptococci are grown in enriched media. As GAS belongs to the lactobacilli, it is facultative anaerobe and obtains its energy from homolactic fermentation of sugars (i.e glucose; Olsen and Musser, 2010).

S.pyogenes can be further classified based on typing of the *emm* gene. To date, more than 250 different M types are known. Recently, it was described that different *emm* genes can be grouped into clusters which, thereby, pave the way for a better functional classification which could also improve the understanding of GAS epidemiology (Sanderson-Smith *et al.*, 2014; Shulman *et al.*, 2014).

S.pyogenes is equipped with several virulence factors to trick and escape the host's immune defense

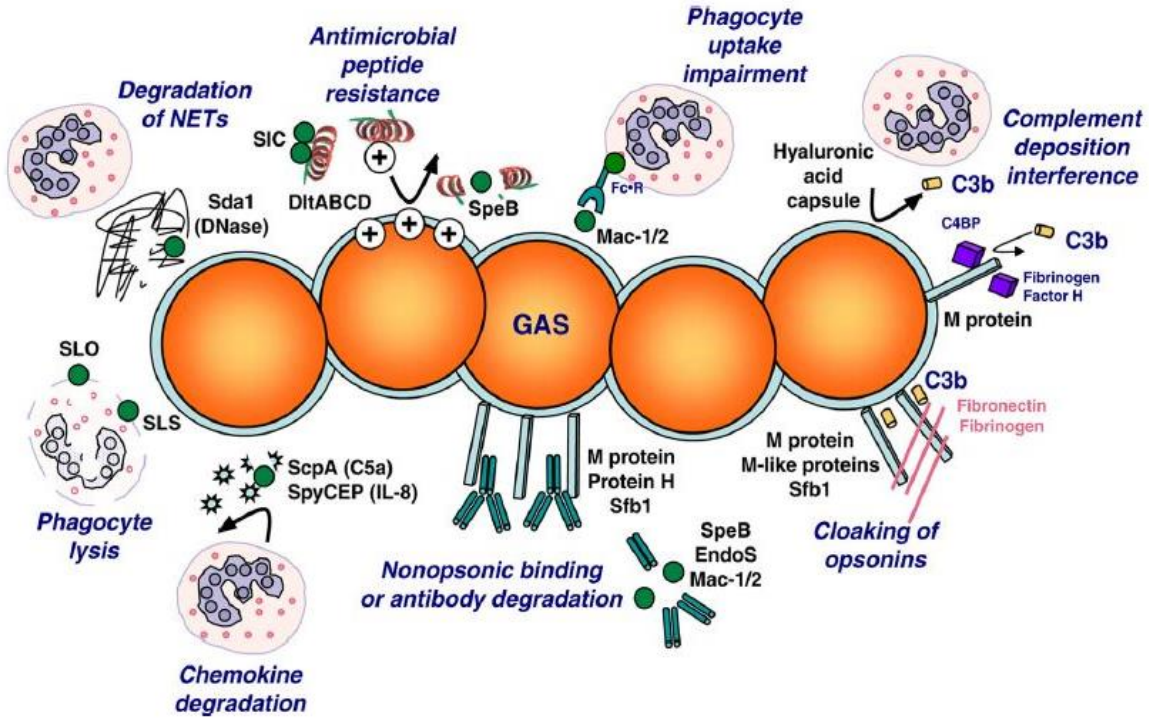

Figure 1-2. Virulence factors of *S.pyogenes* to thwart the host's immune response.
Adapted from Walker *et al*., 2014 (Copyright © 2014, American Society for Microbiology; reproduced with permission): The figure shows several virulence factors contributing to resistance against the host's immune defense mechanisms. Virulence factors involved in the subversion of the plasminogen activation system are not displayed here. The proteases SpyCEP and ScpA degrade IL-8 and C5a and therefore, hinder phagocyte recruitment. SpeB, a secreted protease, degrades immunoglobulins whereas M proteins or SfBI bind to them. Both, the M protein as well as the hyaluronic acid capsule, inhibit complement deposition. Mac-1/2 degrades immunoglobulins, binds the phagocyte Fc receptor and blocks phagocytosis. SpeB degrades antimicrobial peptides. The DNase Sda1 degrades neutrophil extracellular traps (NETs). The toxins SLO and SLS mediate phagocyte lysis and apoptosis.

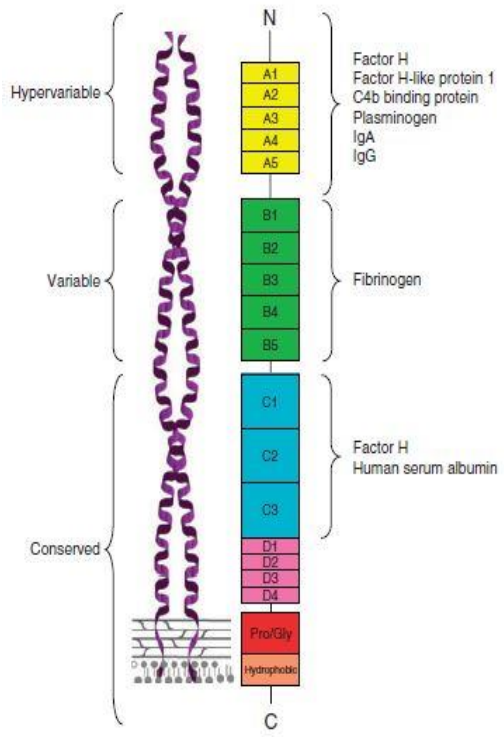

Figure 1-3. Structural and functional characteristics of the M protein.
Adapted from McArthur and Walker, 2006 (Copyright © 2005, John Wiley and Sons; reproduced with permission): The M protein consists of three different regions: a conserved region with C and D repeats, a variable region with B repeats and a hypervariable region with A repeats. The figure shows which host components can be bound by the different regions, e.g. the B repeats bind fibrinogen whereas the A repeats can bind plasminogen or IgG.

(fig. 1-2). It can resist phagocytosis and antimicrobial peptides, degrade neutrophil extracellular traps (NETs) and chemokines, bind immunoglobulins and interfere with the complement system. Furthermore, it is able to destroy tissue and induce vascular leakage and a hyperinflammation by secreting virulence factors and exploit host factors (Walker *et al.*, 2014). The M protein, SfbI (a fibronectin binding protein), streptokinase and the secreted proteinase SpeB play prominent roles in this combat against the host.

One of these major virulence factors is the M protein (fig. 1-3). Structurally, it is a dimer composed of two polypeptide chains that are complexed into an α-helical coiled-coil structure. This structure extends beyond the GAS surface where it is anchored in the cell membrane by an LPxTG motif (x can be any amino acid). More than 250 different M types exist: This is a result of the structural characteristics of the M protein as it typically consists of four different repeat regions (called A to D) which vary in size and amino acid composition (Fischetti, 1989; McArthur and Walker, 2006). In general, the A repeat region is composed of five repeats of 14 amino acids; the B repeat usually has four repeats of 25 amino acids; the C repeat consists of two repeats of 35 amino acids and the D repeat region bears four repeats of seven amino acids. However, variations are also possible resulting in a lack of different repeat regions or a reduced number of repeats within a region. As a consequence of these structural differences, a subdivision into the A-C , D and E pattern can be used for further classification (Smeesters *et al.*, 2010; McMillan *et al.*, 2013). Beside these structural characteristics, the M protein exhibits several functional properties: the A and B repeat regions of the M1 protein are able to bind fibronectin (a host glycoprotein; see below) and thereby, facilitate invasion of streptococci into human cells (vide 1.1.2.2.1; Cue *et al.*, 2001); the plasminogen-binding group A streptococcal M or M-like protein (PAM) can bind plasminogen and consequently, acquire plasmin on the surface of GAS. This favors dissemination of streptococci into deeper tissue (vide 1.1.2.2.2; Sanderson-Smith *et al.*, 2008). Additionally, the M protein can interfere with the complement pathway to prevent efficient opsonophagocytosis: some M types bind C4b binding protein (C4BP) at their highly variable N-terminal region (Johnsson *et al.*, 1996) whereas

others bind factor H at their C repeat region (Horstmann *et al.*, 1988; Fischetti *et al.*, 1995). Moreover, the M protein is able to resist phagocytosis by binding fibrinogen (Horstmann *et al.*, 1992; Carlsson *et al.*, 2005). If the M protein is secreted and detached from the surface, it can bind fibrinogen, form complexes and cause vascular leakage which is important for development of invasive diseases (Herwald *et al.*, 2004). Further virulence determinants of the M protein are binding of IgG and IgA (Smeesters *et al.*, 2010) and induction of inflammation through e.g. interaction with TLR (Pahlman *et al.*, 2006).

The M protein belongs to the group of fibronectin binding proteins. Fibronectin itself is abundant in plasma, other body fluids, and is part of the ECM. Structurally, it is a dimer consisting of two nearly identical 250 kDa units which are linked at their C termini via disulfide bonds. Each monomer consists of three different types of repeating units whereby its RGD motif is located in the third repeating unit. This motif (consisting of the three amino acids Arg-Gly-Asp) is important for interaction with the $\alpha_5\beta_1$-integrin receptor which also plays an important role in streptococcal invasion (vide 1.1.2.2.1; Pankov and Yamada, 2002).

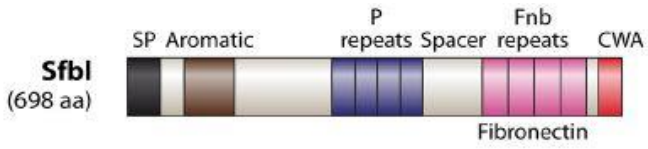

Figure 1-4. Structural characteristics of the SfBI protein.
Adapted from Nobbs *et al.*, 2009 (Copyright © 2009, American Society for Microbiology; reproduced with permission): The figure shows the structural characteristics of the SfBI protein: SP is the signal peptide at the N terminus, followed by the aromatic domain containing aromatic acid-rich amino acids. The P repeats are the proline-rich repeats whereas the Fnb repeats are the fibronectin binding repeats. CWA: cell wall anchor at the C terminus. Two spacer regions can be found between the aromatic domain and the P repeats, and the P repeats and the FnB repeats.

So far, 11 fibronectin binding proteins have been characterized for GAS; most of them are anchored to the cell surface via an LPxTG motif. They can be divided into fibronectin binding proteins containing fibronectin binding repeats like SfbI or into those without repeats like the M protein. Each fibronectin binding repeat is able to bind one fibronectin dimer via a so-called “tandem β-zipper”, a specific protein-protein interaction where additional antiparallel β-strands on sequential β-sheet motifs at the N terminus of fibronectin are formed by a repeat sequence (Schwarz-Linek *et al.*, 2003; Walker *et al.*, 2014). Besides, environmental factors are able to influence the expression of fibronectin binding proteins (Kreikemeyer *et al.*, 2003).

The fibronectin binding protein SfbI is one of the major fibronectin binding proteins of GAS: It consists of an N-terminal aromatic domain (containing several aromatic amino acids), several proline-rich repeats and of the aforementioned fibronectin binding repeats (fig. 1-4; Talay *et al.*, 1994). SfbI is able to mediate adherence and invasion into human cells via binding of fibronectin and subsequent downstream signaling (vide 1.1.2.2.1; Talay *et al.*, 2000). Moreover, it is able to bind the Fc part of IgG in a non-immune fashion and prevents, thereby, phagocytosis and antibody-dependent cell-mediated cytotoxicity by macrophages (Medina *et al.*, 1999). Additionally, SfbI is able to bind

fibrinogen (Katerov *et al.*, 1998) and might, thereby, play a role in plasminogen-mediated virulence (for plasminogen-mediated virulence mechanisms of *S.pyogenes* vide 1.1.2.2.2.)

GAS secretes streptokinase, a specific human plasminogen activator, which is crucial in plasminogen-mediated virulence. It is a single-chain, 414-amino-acid protein which is composed of three different domains: an α-, β- and a γ-domain. All domains are similarly folded and separated by two coiled-coils. Although the term '-kinase' implies that streptokinase has kinase activity, it is neither a kinase nor a protease. Only the formation of a complex with plasminogen or plasmin can lead to the activation of plasminogen (vide 1.1.2.2.2). The streptokinase α-domain mainly binds with two β-strands to a loop region whereas the γ-domain binds near the activation cleavage site of plasminogen. This might induce a conformational change in the binding pocket of plasminogen and consequently, activate it to plasmin (Wang *et al.*, 1998). Phylogenetic studies of the *ska* gene have revealed that streptokinase can be subdivided into three different clusters (1, 2a, 2b) resulting in different modes of activation of plasminogen to plasmin (vide 1.1.2.2.2; McArthur *et al.*, 2008). Moreover, the expression of *ska* is negatively regulated by the *covRS* system (which regulates about 15 % of the GAS genome, either directly or indirectly, and is required for GAS survival under general stress conditions; Dalton and Scott, 2004). In addition, SpeB (positively regulated by *covRS*) is able to degrade and inactivate streptokinase. As a result, *covRS* mutants have an enhanced ability to activate plasminogen and can trigger the development of invasive diseases (Cole *et al.*, 2006; Dalton *et al.*, 2006).

Additional factors interacting with the plasminogen/plasmin system are the α-enolase/streptococcal surface enolase (SEN) and glyceraldehyde-3-phosphate dehydrogenase (GAPDH). Both are able to bind plasminogen. Moreover, both belong to the group of anchorless adhesins: they can be released by the pathogen and then are bound back to the surface if necessary. Thus, a better exploitation of environmental host factors might be possible (Rohde and Chhatwal, 2013).

SpeB is produced as an inactive 40-kDa zymogen which gets activated auto-catalytically to the 28-kDa active protease. It is secreted in the late logarithmic to stationary phase (Chaussee *et al.*, 1997) and has a broad specificity. Beside inactivation of streptokinase, SpeB also degrades ECM components like vitronectin or fibronectin (Kapur *et al.*, 1993) and activates matrix metalloproteinases which lead to further degradation and destruction of tissues (Burns *et al.*, 1996).

All these factors circumventing the host's immune response lead to the fact that *S.pyogenes* is still one of the most important pathogens causing a wide range of infections from mild to severe (Walker *et al.*, 2014). The following paragraph will lead through epidemiology, pathogenesis and important virulence factors playing a role in GAS infections.

1.1.2.1 Epidemiology, treatment and pathogenesis of GAS infections

Every year millions of people around the globe are affected by streptococcal diseases. The spectrum ranges from rather mild infections, like pharyngitis or impetigo, to severe life-threatening diseases, like sepsis or necrotizing fasciitis. The latter are also called invasive diseases as the streptococci are able to migrate to usually sterile sites like deep tissues or the blood stream (Walker *et al.*, 2014). It is estimated that over 600 million cases of GAS pharyngitis occur every year among people older than 4 years and that more than 550 million of these affect people in less-developed countries (Carapetis *et al.*, 2005). Although pharyngitis is a relatively mild disease and can be treated with penicillin quite efficiently, in less-developed countries treatment is not that facile due to the restricted access to the health system (Steer and Carapetis, 2009; Ellis *et al.*, 2010). It is hypothesized that there are different stages in the pathogenesis of pharyngitis: primarily, streptococci adhere to and invade host cells; then they acquire nutrients to proliferate in the host and evade the host's immune response. To do so, streptococci are equipped with several virulence factors facilitating the adherence and invasion and the evasion of the recognition by the host's immune system (*inter alia* fibronectin binding proteins, M-protein; vide 1.1.2 and 1.1.2.2) (Bisno *et al.*, 2003; Olsen *et al.*, 2009; Henningham *et al.*, 2012). If mild GAS infections are not treated properly, post-infection sequelae, i.e. acute rheumatic fever (ARF) and acute poststreptococcal glomerulonephritis (APSGN), can develop (Cunningham, 2008).

ARF is characterized as an immune-mediated, multisystem inflammatory disease that follows untreated GAS infections. Major manifestations of inflammation are found in the joints (arthritis), in the heart (carditis) or in the central nervous system (chorea) (Lee *et al.*, 2009). ARF may result in a long-term damage of the heart valves which causes rheumatic heart disease (RHD) if it is not treated properly with penicillin (or another antibiotic in case of penicillin allergy) for more than 10 days (Steer and Carapetis, 2009). It is estimated that 471.000 cases of ARF occur every year of which 60 % can possibly develop RHD. Furthermore, it is estimated that over 15.6 million people are suffering from RHD; 79 % of all cases occur in less-developed countries or in indigenous populations (Gillen *et al.*, 2002; Carapetis *et al.*, 2005). Although the pathogenesis of ARF/RHD is not completely understood, it is known that it is *inter alia* a result of autoimmunity (Dinkla *et al.*, 2007). In comparison to ARF/RHD APSGN plays a minor role: the prevalence and incidence of APSGN have decreased over the years. To date, it is estimated that 470.000 cases occur annually with a mortality rate of 1 %. However, 97 % of these cases occur in less-developed countries where an appropriate treatment of the disease is not always facile (Carapetis *et al.*, 2005). As APSGN is an inflammatory immune-mediated disease affecting the kidneys which can develop after a skin or pharyngeal infection with GAS, the clinical symptoms include *inter alia* hypertension and proteinuria as a

response to the inflammation in the kidneys (Nordstrand *et al.*, 1999). Therefore, the treatment consists of administration of antihypertensive drugs (nifedipin as a calcium channel modulator, diuretics). The application of antimicrobials is not advantageous (Zaffanello *et al.*, 2010). Although the pathogenesis of APSGN is not completely understood yet, it is believed that the deposition of immune complexes (C3 and IgG) in the glomeruli plays an important role which might be a result of autoantibodies against proteins in the glomeruli like collagen IV (Kefalides *et al.*, 1986). These autoantibodies are a consequence of cross-reactivity between basement membrane proteins and the M-protein of streptococci. However, it has been observed that only few M proteins are nephritogenic and causative for APSGN. Furthermore, it is assumed that streptokinase from GAS is important in the pathogenesis of APSGN (Ohkuni *et al.*, 1991): as streptokinase is able to convert plasminogen into plasmin, plasmin will then be able to cleave C3, activate the alternative complement pathway and contribute to inflammation. Moreover, plasmin can degrade additional extracellular matrix proteins and activate matrix metalloproteinases. Thereby, plasmin enhances the inflammatory and destructive process of the glomeruli. However, it is still not completely defined if streptokinase is the enzyme to convert plasminogen or if also other proteins capable of binding plasminogen or plasmin like SpeB or GAPDH play an even more predominant role (Cunningham, 2000; Eison *et al.*, 2011; Walker *et al.*, 2014).

Beside mild infections and post-infection sequelae, severe life-threatening invasive diseases of GAS like necrotizing fasciitis are of major concern: it is estimated that there are over 660.000 cases of invasive GAS infections every year and over 160.000 deaths each year (Carapetis *et al.*, 2005). Over all, invasive GAS infections have become more severe over the years and exhibit a high mortality rate of about 15-20 %; the mortality rate of sepsis is even higher than 30 % (Carapetis, 2004). A study from the United States detected a case-fatality rate of around 24 % for necrotizing fasciitis and of around 36 % for streptococcal toxic shock syndrome (STSS) (O'Loughlin *et al.*, 2007). The mortality rate for necrotizing fasciitis can even exceed 50 % with increasing age of the patient. Necrotizing fasciitis often occurs in patients who do not have predisposing factors like open wounds, but seemed to be fit and healthy (Lamagni *et al.*, 2008). As it is a rapidly progressing disease characterized by an inflammation and necrosis of fascial tissues, an early diagnosis and treatment are crucial: treatment consists of intravenous application of penicillin and clindamycin (as the latter seems to suppress the expression of several virulence factors of *S.pyogenes* like M protein) as well as rapid surgical intervention (Young *et al.*, 2006; Stevens *et al.*, 2014). Additionally, treatment with intravenous immunoglobulins (IVIG) is used because it is suggested that it may enhance the bactericidal activity of serum by a higher rate of opsonization of streptococci or neutralization of superantigens secreted by streptococci. Moreover, hyperbaric oxygen therapy is applied as an adjunctive therapy: as the infected tissue represents a hypoxic environment in which killing by neutrophil radical oxygen species

or phagocytosis is reduced, it is assumed that hyperbaric oxygen might counteract these effects (Norrby-Teglund *et al.*, 1996; Waddington *et al.*, 2014). It is thought that host (e.g. plasmin) and bacterial proteases (e.g. SpeB) are involved in the pathogenesis of necrotizing fasciitis. Furthermore, tissue-damaging enzymes which are released by activated host neutrophils and a so-called "cytokine storm" as a result of uncontrolled T-cell responses to superantigens of streptococci are important in progression of the disease (Walker *et al.*, 2014).

Even if streptococci have remained susceptible to penicillin over the years (Macris *et al.*, 1998) and even if only a few cases of possible treatment failures have emerged (Pichichero, 1991; Kaplan and Johnson, 2001) (which can also be a result of streptococci using the β-lactamase of other bacteria (Schaar *et al.*, 2014)), treatment options decrease rapidly as soon as patients react allergically to penicillin: antibiotic resistance is increasing for different classes of antibiotics such as macrolides (Silva-Costa *et al.*, 2015), lincosamides (Cantón *et al.*, 2002; Arêas *et al.*, 2014) or trimethoprim (Bergmann *et al.*, 2014) (although the latter is usually not used in treating GAS infections; Gerber, 1996; Randel and Infectious Disease Society of America, 2013); and susceptibility for fluoroquinolones is decreasing in certain areas (Montes *et al.*, 2010). Additionally, there are two possible reasons for failure of treatment with penicillin: (a) sufficient concentrations of penicillin cannot be achieved in extracellular fluids (Stjernquist-Desatnik *et al.*, 1993) or (b) if streptococci invade into epithelial cells, they cannot be effectively killed by penicillin (Kaplan *et al.*, 2006; Ogawa *et al.*, 2011). This implies that streptococci which are not eradicated can become persistent. This enables streptococci to cause recurrent infections in the throat or for example to be transported to other parts of the body by ingestion by PMNs (Medina, Rohde *et al.*, 2003). Then they can become systemic (Medina, Goldmann *et al.*, 2003; Rohde and Chhatwal, 2013). The reason for some patients developing systemic infections like necrotizing fasciitis is still unknown as most of them do not display recent injuries or traumata. Therefore, hypothetically, these kinds of infections could be caused by persistent *S.pyogenes* disseminating into deeper tissue and causing inflammation followed by systemic severity (Johansson and Norrby-Teglund, 2013).

As treatment of GAS infections and mainly of invasive diseases is still not satisfactory, intensive research is going on to find other treatment options or a suitable method to prevent GAS infections – such as an effective vaccine. However, such a vaccine is still not available. The reason for this is the versatility of *S.pyogenes* itself: So far, the M protein has been the target as a vaccine candidate. However, the development harbors several problems: more than 250 different serotypes of M proteins exist; different serotypes cause distinct streptococcal diseases ranging from mild to severe. Additionally, these M types are not specific for a certain disease but can vary depending on the (geographical) region. Other potential targets for a vaccine are the carbohydrate antigen or other surface proteins like fibronectin binding proteins which are important for the virulence of *S.pyogenes*

(McArthur *et al.*, 2004; Dale *et al.*, 2013; Walker *et al.*, 2014). Until a safe vaccine is on market, it is necessary to gain a deeper understanding of the underlying pathogenic mechanisms and to enhance the treatment options of GAS diseases.

New grounds have to be broken as conventional antibiotics are not effective in treating invasive diseases and do not assure an efficient eradication of *S.pyogenes*. The facts show clearly that the high disease burden of group A streptococci is undeniable. Consequently, new drugs are needed that differ in their targets from commonly used anti-infectives to treat the 'untreatable'. Possible targets are key pathogenic mechanisms (Clatworthy *et al.*, 2007; Beckham and Roe, 2014) like adherence and invasion of streptococci (vide 1.1.2.2.1) or the exploitation of the plasminogen activation system (vide 1.1.2.2.2). As elaborated above, these two mechanisms play prominent roles in the pathogenesis of mild and severe group A streptococcal diseases.

1.1.2.2 Pathogen-host interactions of Streptococcus pyogenes

The following paragraphs will give a deeper insight into interactions between the host and the pathogen *S.pyogenes*. Thereby, the focus is on two mechanisms playing a role in and for streptococcal virulence: (1) adherence to and invasion into host cells and (2) exploitation of the plasminogen activation system.

1.1.2.2.1 Adherence and invasion of *Streptococcus pyogenes* into non-phagocytic human cells

Adherence to and invasion into non-phagocytic human cells is crucial for all infections caused by *S.pyogenes*: GAS strains invade epithelial cells (LaPenta *et al.*, 1994) and can cause recurrent infections or be the cause for a dissemination into deeper tissue as well as GAS strains invading the skin and causing superficial skin infections (Rohde and Chhatwal, 2013). Furthermore, it is thought that GAS residing in endothelial cells are able to escape from the intracellular environment into the bloodstream to cause invasive diseases (Ochel *et al.*, 2014). The exact mechanisms for the establishment of this great variety of infections are not completely understood yet. However, it is clear that, for initiation of GAS infection, *S.pyogenes* needs to attach to different cell types, invade them in some cases and hide from the immune system. Then an infection cannot be cleared rapidly. GAS are equipped with several virulence factors to exploit and circumvent the human host. The artifice of these will be highlighted in detail below.

It is believed that initial bacterial attachment to the host cell surface is a two-step process: first, weak and/or long-range interactions between pathogen and host are taking place before a more specific, high-affinity binding occurs (Hasty *et al.*, 1992). Lipoteichoic acid (LTA) which is a membrane-bound glycolipid (Scott and Barnett, 2006) may initiate the first weak interaction between host and

pathogen and thereby, contribute to initial adherence (Courtney *et al.*, 1992; Nobbs *et al.*, 2009). More specific high-affinity binding is possible by several proteins of GAS interacting with multiple host components. There are cell-wall-anchored as well as anchorless adhesins (e.g. GAPDH or α-enolase which play an important role in the subversion of the plasminogen/plasmin system, vide 1.1.2 and 1.1.2.2.2). The cell-wall-anchored proteins are (a) covalently bound to the cell wall peptidoglycan by a C-terminal LPxTG motif (where x is any amino acid) recognized by sortase A; (b) linked to the cell membrane through N-terminal modifications with lipid; (c) tethered on the surface by an unknown mechanism or (d) bound back to the cell surface as a result of non-covalent interactions with cell surface compounds like polysaccharides or other proteins (Rohde and Chhatwal, 2013). Surface proteins bound by a LPxTG motif can be pili (which have been shown to mediate adhesion to tonsils and human skin (Abbot *et al.*, 2007)), M proteins or other MSCRAMMs (microbial surface components recognizing adhesive matrix molecules) (Nobbs *et al.*, 2009; Walker *et al.*, 2014). The latter are able to interact directly with ECM components like laminin, collagen or fibronectin. Moreover, MSCRAMMs interacting with fibronectin have been shown to be not only able to mediate adhesion but also invasion into human cells (like the M protein). Furthermore, it was shown that the hyaluronic acid capsule of *S.pyogenes* is able to trigger tissue invasion by CD44-mediated cell signaling. This caused cytoskeletal rearrangements opening intercellular junctions and, thereby, enabled paracellular transport from the epithelial cell surface into deeper tissue (Cywes and Wessels, 2001).

S.pyogenes has evolved diverse mechanisms to invade into non-phagocytic human cells (fig. 1-5): invasion by (a) a zipper-like mechanism (M protein-mediated), (b) induction of caveolae (SfbI-mediated) or (c) membrane ruffling (Rohde and Chhatwal, 2013).

It is known that the M protein is able to bind the ECM component laminin as well as fibronectin (vide 1.1.2). However, M protein-mediated invasion by binding of laminin is distinct from the one by binding of fibronectin and involves different β_1-integrin receptors. If invasion occurs as a result of fibronectin binding, fibronectin is recognized via its RGD motif by $\alpha_5\beta_1$-integrin receptors on the cell surface (Cue *et al.*, 1998). A zipper-like mechanism has been observed for M protein-mediated invasion. It is assumed that binding to fibronectin and to the integrin receptors at the cell surface promotes a closer contact between streptococci and the human cell. As a result, an intimate contact to host cell microvilli on the cell surface can be established which are then able to engulf the streptococci. Furthermore, streptococci are associated with polymerized actin at the entry port. Internalized streptococci can be found near the cell membrane in vacuoles associated with actin; those found farther within the cell were positive for LAMP-1, a marker for lysosomes and late endosomes. Consequently, it is likely that streptococci first traffic in a phagosome which then fuses

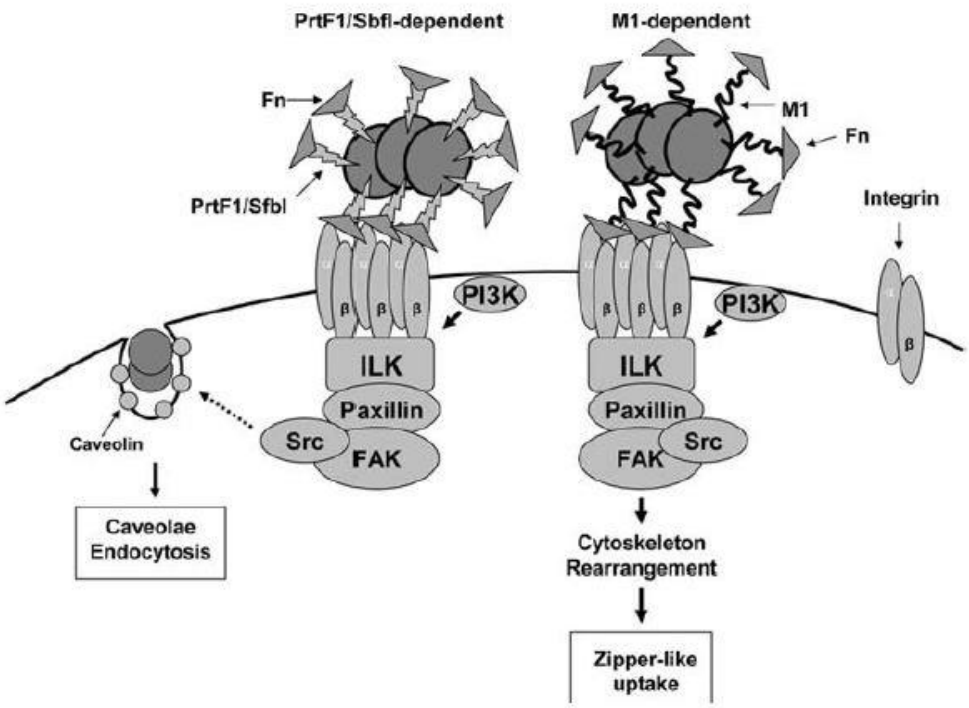

Figure 1-5. Invasion mechanisms and signaling pathways of *S.pyogenes*.
Adapted from Wang *et al.*, 2007 (Copyright © 2007, John Wiley and Sons; reproduced with permission): The figure shows two different invasion mechanisms and their signaling pathways in *S.pyogenes*:
The M1-dependent pathway results in a zipper-like uptake. After the M1 protein binds to fibronectin, the latter is able to interact with $\alpha_5\beta_1$-integrin receptors. PI_3K phosphorylates ILK which leads to phosphorylation of paxillin and recruitment of FAK and src kinase. Consequently, *S.pyogenes* is taken up by a zipper-like mechanism as a result of cytoskeletal rearrangements.
The SfBI-dependent pathway results in an uptake via caveolae. After binding of fibronectin by the SfBI protein and interaction with $\alpha_5\beta_1$-integrin receptors PI_3K phosphorylates ILK as well. This results in recruitment of paxillin, FAK and src kinase. The latter one promotes endocytosis of *S.pyogenes* via caveolae.

with a lysosome. Therefore, it seems that internalized streptococci reside in a phagolysosome (Dombek *et al.*, 1999).

Although both, SfbI and the M protein bind fibronectin (Talay *et al.*, 2000; Marjenberg *et al.*, 2011), a different mechanism of internalization of streptococci can be observed for SfbI: Similar to the M protein, fibronectin bound to SfbI on the surface of GAS is recognized via its RGD motif by $\alpha_5\beta_1$-integrin receptors. Binding to the integrin receptors leads to subsequent cell signaling which, in the case of SfbI-mediation, leads to formation of caveolae: large invaginations on the cell surface that ingest *S.pyogenes* (Ozeri *et al.*, 1998; Molinari *et al.*, 2000). Streptococci reside inside the cell within caveosomes. These are distinct from phago- or lysosomes, distinct from the classical phago-/lysosomal pathway as they are not positive for phago- or lysosomal markers; though, they are positive for caveolin-1, a marker for caveosomes (Pelkmans *et al.*, 2001; Rohde *et al.*, 2003).

The signaling for these two distinct invasion mechanisms (SfbI- and M protein-mediated) is nearly identical (fig. 1-5): after binding to the $\alpha_5\beta_1$-integrin receptor, integrin-linked kinase (ILK) is activated dependent on PI_3K (Purushothaman *et al.*, 2003; Wang *et al.*, 2006). In the event of the M1 protein-mediated pathway paxillin, a signal transduction adaptor protein, is phosphorylated by focal

adhesion kinase (FAK) and assembled into streptococcal focal adhesion. This leads to rearrangement of the actin cytoskeleton and subsequent uptake of *S.pyogenes* via a zipper-like mechanism (Wang *et al.*, 2007). Nevertheless, this signaling cascade is not identical for all M proteins: slightly different signaling cascades have been described, e.g. for invasion of an M3 serotype of *S.pyogenes* into endothelial cells (Nerlich *et al.*, 2009). In the case of the SfbI-mediated pathway the src tyrosine kinase is recruited which leads to phosphorylation of caveolin-1 and endocytosis via caveolae. Beside activation of FAK, paxillin is also recruited. However, it does not seem to be necessary for the SfbI-mediated uptake (Li *et al.*, 1996; Wang *et al.*, 2007). Additionally, vinculin as part of the focal adhesions which is able to link integrins to the cytoskeleton (Critchley, 2000; Ziegler *et al.*, 2006) (*inter alia* it is binding paxillin (Wood *et al.*, 1994), α-actinin (Wachsstock *et al.*, 1987; Kelly *et al.*, 2006) and F-actin (Janssen *et al.*, 2006)) is also recruited to the site of entry. Nevertheless, it is not essential for uptake. Tubulin is absent from the site of entry and therefore, it is thought that it is not involved in invasion. α-actinin is not recruited as well. Additionally, a second pathway for SfbI-mediated invasion is possible involving Rac and Cdc42 which both belong to the family of Rho GTPases and are able to regulate integrin-mediated signals in the way that actin rearrangement and bacterial uptake are taking place (Hall, 1998; Ozeri *et al.*, 2001).

Although proteins belonging to the ERM family (ezrin, moesin and radixin) have not been investigated for their role in streptococcal invasion, it is known that these are able to expose binding sites for actin and other proteins and might, therefore, be involved in formation of focal adhesions. Conformational changes in these proteins can be a result of downstream signaling of Rho GTPases (Hirao *et al.*, 1996; Schoenwaelder and Burridge, 1999; Arpin *et al.*, 2011). Furthermore, it has been shown for ezrin that it can colocalize with actin and that it is enriched in microvilli and membrane ruffles under certain conditions (Berryman *et al.*, 1993; Franck *et al.*, 1993). Ezrin plays a role in regulation of microvilli as well (Viswanatha *et al.*, 2014).

The third mechanism of invasion is independent of fibronectin and of integrins. After group A streptococci attach to the surface, the cell surface undergoes morphological changes: microvilli interact with the bacteria and engulf them by forming pseudopod-like protrusions. It is known that reorganization of the actin cytoskeleton is involved in this process. Although this mechanism has similarities with the M protein-mediated internalization, the factors (to date not elucidated) inducing this invasion pathway must be distinct as fibronectin is not involved (Molinari *et al.*, 2000).

In addition to the different mechanisms of adherence and invasion which enable streptococci to attach to, access and hide within the host's cells, *S.pyogenes* has evolved further mechanisms to take advantage of the human host. One of these is the exploitation of the plasminogen activation system which will be highlighted in the following paragraph.

1.1.2.2.2 Exploitation of the plasminogen activation system

Plasminogen activation and plasmin formation are important in several physiological and pathological processes: plasmin is able to lyse fibrin clots and, therefore, is an essential part of fibrinolysis and a counterpart of coagulation (see below). Beside its primary task in fibrinolysis, plasmin is *inter alia* able to activate mediators of the complement system (Amara *et al.*, 2008) and matrix-metalloproteinases (MMPs) degrading ECM components and leading to tissue destruction (Monea *et al.*, 2002). Physiologically, plasminogen gets activated by urokinase (uPA) or tissue plasminogen activator (tPA). Both activators cleave the Arg_{561}-Val_{562} bond of plasminogen proteolytically and, thereby, activate it to plasmin (Parry *et al.*, 2000). tPA is synthesized in vascular endothelial cells and secreted into the circulating blood stream. It consists of 527 amino acids and is a single-chain glycoprotein. uPA is synthesized as a single-chain glycoprotein as well. However, both activators are secreted as zymogens: by cleavage which results in formation of two-chain-tPA and two-chain-uPA, respectively, both get activated and exhibit their plasminogen activation properties (Spraggon *et al.*, 1995; Lamba *et al.*, 1996). In addition, several gram-positive bacteria are also able to activate plasminogen: group A, C and G streptococci secrete streptokinase whereas staphylococci secrete staphlyokinase. Both '-kinases', though, activate plasminogen non-proteolytically by formation of a plasminogen-staphylo-/streptokinase-complex (for streptokinase see below). Moreover, some *Yersinia* species secrete a protease, termed *Pla*, which activates plasminogen directly (Boyle and Lottenberg, 1997; Coleman and Benach, 1999).

Plasminogen itself is a 92 kDa single-chain glycoprotein consisting of 791 amino acids. Several different carbohydrate configurations are possible (Hayes and Castellino, 1979a, 1979c, 1979b). When plasminogen gets activated to plasmin the Arg_{561}-Val_{562} bond is cleaved enabling a conformational change and thereby exposing the catalytic triad His_{603}-Asp_{646}-Ser_{741} (Ponting *et al.*, 1992). Structurally, it consists of a so-called Pan-apple domain followed by 5 kringles and a serine protease domain. Four out of five of these kringles are able to bind lysines which are necessary for interaction with fibrin molecules or inhibitors of plasminogen/plasmin activation (Law *et al.*, 2012). Native plasminogen has an N-terminal glutamic acid and is therefore termed 'Glu-plasminogen' (Rijken and Lijnen, 2009). By cleaving the first 77 N-terminal amino acids 'Lys-plasminogen' is generated. Similarly, Glu-plasmin and Lys-plasmin exist (Ponting *et al.*, 1992). Lys-plasminogen gets activated more easily in comparison to Glu-plasminogen as Lys-plasminogen adopts the so-called relaxed conformation when the Pan-apple domain is cleaved. By contrast, Glu-plasminogen can adopt a tensed or relaxed conformation, depending on conditions like e.g. chloride ion concentration, whereas the relaxed conformation renders activation to plasmin more facile for activators (Gaffney *et al.*, 1988; Law *et al.*, 2012).

To control plasminogen activation and the action of plasmin, α_2-antiplasmin, a single-chain glycoprotein, serves as an endogenous inhibitor. By forming a stoichiometric complex with plasmin, plasmin cannot exhibit its proteolytic function anymore (Lijnen and Collen, 1982). Other commercially available inhibitors of plasminogen/plasmin are aprotinin, ε-amino caproic acid (EACA) and tranexamic acid (TA). As a result of their lysine-analogue structures, EACA and TA interfere with the kringle domains of plasminogen and thereby, inhibit its action (Violand *et al.*, 1978; Markus *et al.*, 1979; Takada *et al.*, 1986). Aprotinin is isolated from the bovine lung and acts as a serine protease inhibitor; similarly to α_2-antiplasmin, it is able to inactivate free circulating plasmin but has little effect on bound plasmin (Longstaff, 1994; Royston, 2015).

It has been discovered in the early 30ies that streptococci are secreting a factor that is able to lyse fibrin clots (Tillett and Garner, 1933). This 'factor' is nowadays known as streptokinase activating plasminogen to plasmin. Streptokinase can be classified into three so-called 'cluster types'. This classification relies on sequence similarities or differences in the β-domain of streptokinase. Depending on the respective cluster type (vide 1.1.2), plasminogen is activated in different ways (fig. 1-6): cluster 1 type streptokinase is secreted by streptococci and able to form a complex with plasminogen. By forming this complex plasminogen undergoes a conformational change and is able to cleave the Arg_{561}-Val_{562} bond of another plasminogen molecule activating it to plasmin. In detail, Ile_1 is inserted into the N-terminal binding cleft of plasminogen, thereby forming a salt bridge with Asp_{740} of plasminogen and triggering the formation of the active site (Boxrud *et al.*, 2004; McArthur *et al.*, 2012). Cluster 2 type streptokinase needs fibrinogen for activation of plasminogen:

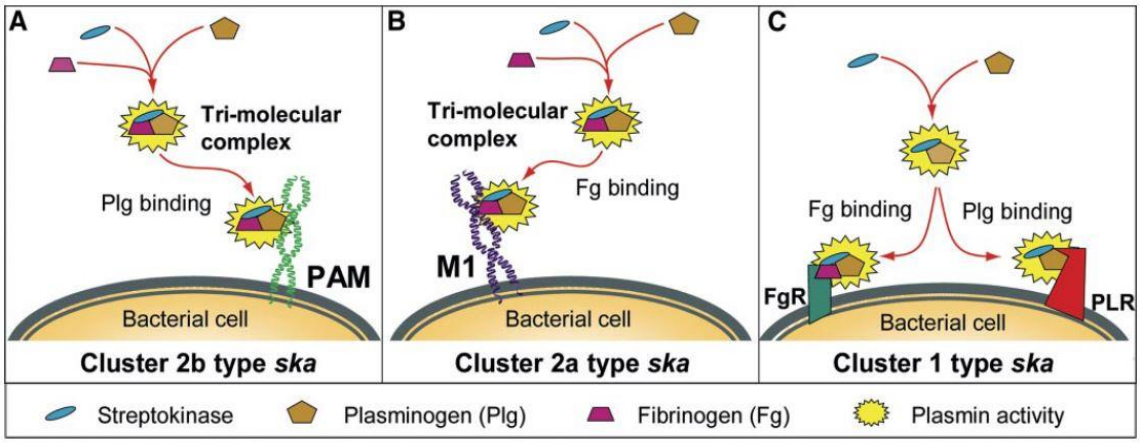

Figure 1-6. Cluster-dependent activation of plasminogen by streptokinase.
Adapted from McArthur *et al.*, 2008 (Copyright © 2008, Federation of American Societies for Experimental Biology; reproduced with permission): A: Cluster 2b type ska: streptokinase (ska) forms a tri-molecular complex with plasminogen and fibrinogen. This complex is bound via PAM to the streptococcal surface where plasmin activity is acquired. B: cluster 2a type ska: streptokinase forms a complex with fibrinogen and plasminogen and acquires plasmin activity. The complex can be bound to the bacterial surface e.g. via the M1 protein. C: Cluster 1 type ska: streptokinase forms a complex with plasminogen and acquires plasmin activity. Surface-bound plasmin activity can be acquired via binding of the complex to plasminogen receptors (PLR) or formation of a complex with fibrinogen and binding to fibrinogen receptors (FgR).

cluster 2a type streptokinase is secreted as well and forms a tri-molecular complex with fibrinogen and plasminogen to activate plasminogen to plasmin. Cluster 2b type streptokinase is only able to activate plasminogen on the bacterial cell surface: plasminogen is bound to the streptococcal cell surface via PAM (vide 1.1.2). Then a tri-molecular complex is formed (fibrinogen-plasminogen-streptokinase) which acts as an activator for further plasminogen molecules (Kalia and Bessen, 2004; McArthur *et al.*, 2008). However, it has also been postulated that strains harboring a cluster 2a type streptokinase are also able to activate plasminogen directly as (at least in one study by Lizano and Johnston) the β-domain had only little effect in plasminogen activation. It is thought that sequence differences outside the β-domain might also contribute to variable plasminogen activation properties (Lizano and Johnston, 2005). Additionally, it has been shown that cluster 2a type streptokinase can activate Glu-plasminogen in absence of fibrinogen even if it does not act as fast as cluster 1 type streptokinase (Cook *et al.*, 2014). Streptokinase is able to form a complex with plasmin as well. This complex can activate plasminogen more rapidly than a streptokinase-plasminogen-complex (Boxrud *et al.*, 2000). All three cluster types are able to activate soluble plasminogen when forming a streptokinase-plasmin-complex. Thereby, they gain soluble plasminogen activation activity (Cook *et al.*, 2012). Though, streptokinase can also be cleaved by plasmin which results in a loss of plasminogen activation activity (Shi *et al.*, 1994). In contrast to plasmin alone, the streptokinase-plasmin-complex of cluster 2a type streptokinase is not susceptible to α_2-antiplasmin inhibition. Surprisingly, streptokinase-plasmin-complexes formed with either cluster 2b or cluster 1 type streptokinase can be inhibited by α_2-antiplasmin (Cook *et al.*, 2012). Nevertheless, one has to bear in mind that streptokinase is specific for the human host (Yakovlev *et al.*, 1995). Therefore, it is necessary to utilize a humanized plasminogen mouse model to investigate the function of streptokinase *in vivo*. One such model demonstrated that *S.pyogenes* secreting streptokinase exploits plasminogen during invasive disease (Sun *et al.*, 2004).

An additional mechanism for streptococci to acquire surface-bound plasmin activity is binding of plasminogen to its plasminogen binding proteins GAPDH, SEN or PAM (Pancholi and Chhatwal, 2003; Sanderson-Smith *et al.*, 2012). The benefit of binding plasmin(ogen) to their surface is that it cannot get inactivated that easily anymore by α_2-antiplasmin (Wiman and Collen, 1978; Hall *et al.*, 1991). Consequently, a better exploitation of plasmin activity is possible: this enables GAS to become invasive by using plasmin which can destroy tissue and activate MMPs (Sanderson-Smith *et al.*, 2012). Whereas PAM is binding kringle 2 of plasminogen via its plasminogen binding domains in the A repeat region (Sanderson-Smith *et al.*, 2006, 2008), SEN binds plasminogen via its lysine residues in the carboxy-terminal region (Pancholi and Fischetti, 1997, 1998; Derbise *et al.*, 2004). Like SEN, GAPDH is also binding plasminogen via its lysine residues (Pancholi and Fischetti, 1992; Winram and Lottenberg, 1998). Both have a preference in binding Lys-plasminogen in contrast to Glu-

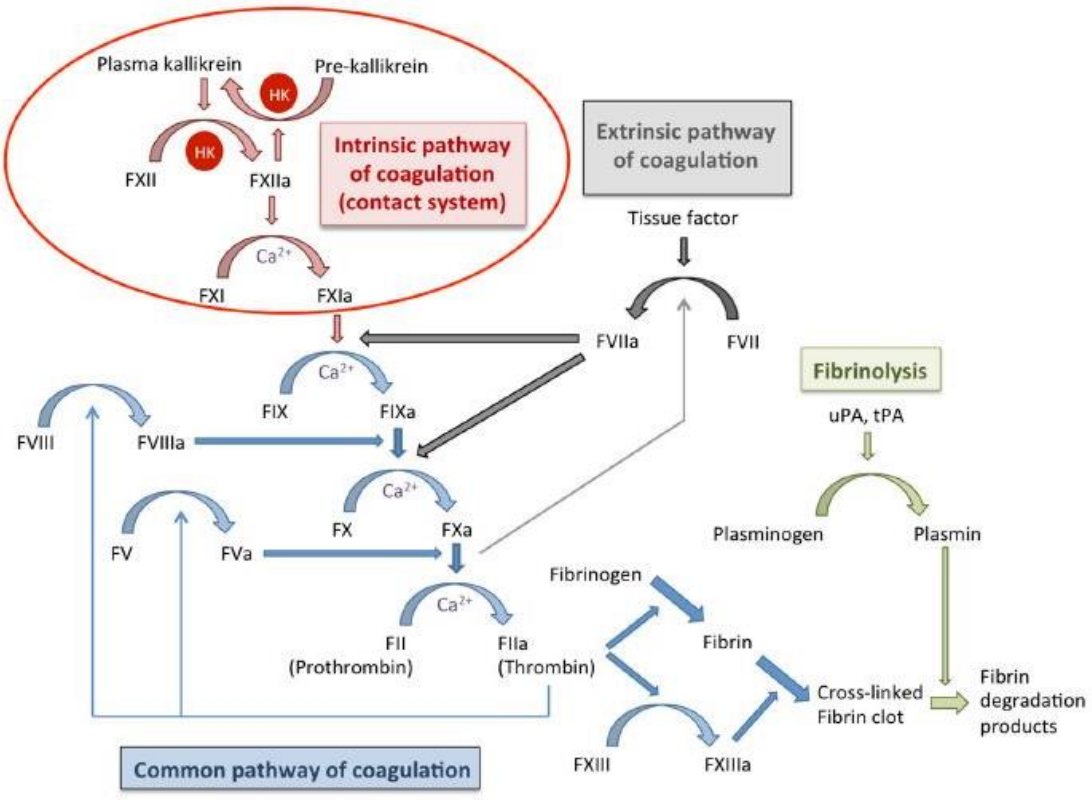

Figure 1-7. Pathways of coagulation.
Adapted from Loof *et al.*, 2014 (Copyright © 2014 Loof, Deicke and Medina; reproduced with permission): The common pathway of coagulation (depicted in blue) can be activated via the intrinsic pathway of coagulation (depicted in red) or by the extrinsic pathway of coagulation (depicted in grey). The extrinsic pathway starts with the activation of FVII to FVIIa by tissue factor. The intrinsic pathway is activated upon contact which leads to activation of FXII to FXIIa and activation of pre-kallikrein to kallikrein, respectively. Fibrinolysis starts with activation of plasminogen to plasmin, e.g. mediated by uPA or tPA. Plasmin can degrade fibrin clots. Further details concerning the coagulation cascade are described in the text.

plasminogen. The binding of plasminogen to GADPH or SEN can be inhibited via EACA. As this one has also one lysine residue, it can successfully interfere and compete with GAPDH and SEN (Sanderson-Smith *et al.*, 2012). Additionally, it has been demonstrated that EACA can inhibit the binding between PAM and plasminogen (Berge and Sjöbring, 1993). When plasminogen is bound to these receptors, it can get activated by the endogenous activators like uPA. This ensures the acquisition of plasmin activity even in the absence of streptokinase (Sanderson-Smith *et al.*, 2013). Besides, PAM is binding the streptokinase-fibrinogen-plasminogen-complex which is formed by cluster 2b type streptokinase as this one is not exhibiting soluble plasminogen activation activity (McArthur *et al.*, 2008).

As *S.pyogenes* exploits the plasminogen activation system, the host uses the coagulation system to defend himself. Upon injury, the host has to react rapidly to close and seal the wound and to prevent invasion of microorganisms into the blood stream. This is accomplished by formation of a stable clot and has been termed ‘immunothrombosis’ (Engelmann and Massberg, 2013). In general, the coagulation system can be activated via two pathways: the extrinsic and the intrinsic one (fig. 1-7). The extrinsic pathway is initiated by the release of tissue factor from injured endothelial cells. Tissue

factor leads to activation of FVII to FVIIa. The latter is able to activate FX and FIX. The intrinsic pathway or contact system is activated upon binding of FXII to negatively charged surfaces like DNA, kaolin, collagen or dextran-sulfate. In addition, streptococci are also able to activate the contact system: *S.pyogenes* can bind FXII to its surface where it undergoes autoactivation (Loof *et al.*, 2014). Then, FXIIa can activate pre-kallikrein to kallikrein via surface bound high molecular weight kininogen (HK) (Ben Nasr *et al.*, 1997). FXIIa then activates FXI which leads to FIXa. With the common pathway of activation, FIXa activates FX leading to generation of thrombin (FII). This one is able to convert fibrinogen to fibrin. To obtain a stable clot, fibrin is cross-linked by FXIIIa. Fibrinolysis occurs when plasminogen gets activated to plasmin which is able to degrade fibrin (Loof *et al.*, 2014). Activation of the contact system by *S.pyogenes* does also result in mobilization of the whole coagulation cascade. Consequently, GAS are entrapped within a clot. Efficient entrapment seems to prevent dissemination as streptococci can also be killed within the clot (Loof *et al.*, 2011). As it has been shown that generation of thrombin plays an important role in the host's defense against GAS, it is hypothesized that local fibrin deposition might be the cause for reduced survival and reduced dissemination of *S.pyogenes* (Sun *et al.*, 2009). Nevertheless, by secreting streptokinase and using the plasminogen activation system to dissolve clots, streptococci are enabled to escape the entrapment (as described above) (Khil *et al.*, 2003). Therefore, it is thought to date that plasminogen can be deployed as a virulence factor by *S.pyogenes* for invasive diseases (Sun *et al.*, 2004; Walker *et al.*, 2005).

Plasmin(ogen) is not only used by GAS to dissolve clots, but also in the clinics to dissolve those clots that have formed after e.g. myocardial infarction or ischemic stroke (Wardlaw *et al.*, 2014). To activate plasminogen, several activators like uPA, tPA, recombinant forms thereof or streptokinase (although from group C *streptococcus*) are used. Thereby, streptokinase is the cheapest application form. Utilization of streptokinase harbors one important problem: immunogenicity. After administration, antibodies directed against streptokinase can be generated or antibodies against streptokinase could already be present in plasma as a result of previous infections with streptococci. Therefore, higher doses of streptokinase might be necessary or – in the worst case – regularly administered doses will not be efficient as they will be neutralized by antibodies (McArthur *et al.*, 2012). Additionally, treatment with activators of plasminogen is always tricky: if too much plasminogen is activated, serious complications as systemic bleeding might arise. Consequently, in the case of overdosing, it is necessary to use inhibitors of activation like TA and EACA or inhibitors of plasmin like aprotinin. Besides, overdosing can always result in thromboembolic complications. As a result, the equilibrium between thrombolysis and thromboembolic events is fragile. Though, the abovementioned inhibitors harbor also some risks: aprotinin can cause anaphylactic reactions upon second exposure (Dietrich *et al.*, 2007; Royston, 2015). There has also been reported one case in which an anaphylactic reaction already arose upon primary exposure (Kaddoum *et al.*, 2007). One

study showed that administration of aprotinin in high-risk cardiac surgery patients led to a higher mortality rate than EACA or TA. Although the latter two were not as effective as aprotinin in reduction of massive bleeding they had a lower risk of causing mortality than aprotinin (Fergusson *et al.*, 2008). In contrast to aprotinin and EACA, especially tranexamic acid seems to be quite effective in preventing the complication of massive bleeding – at least for treatment of trauma-associated bleeding: in a recent study, it reduced the probability of receiving a blood transfusion by one third. However, this should not hide the fact that effects on thromboembolic events and mortality still remain uncertain. Additionally, high doses of TA can cause neurotoxic effects. Therefore, it is necessary to pay attention to dosing while using TA during bleeding complications (CRASH-2 collaborators *et al.*, 2011; Franchini and Mannucci, 2014; Tengborn *et al.*, 2015).

Several antifibrinolytic agents are currently on the market. Although tranexamic acid is associated with some complications and is not the most effective one in reduction of bleeding, it is, currently, still the drug of choice.

Inhibitors directed against virulence mechanisms of GAS interacting with the plasminogen activation system can also be beneficial in an antifibrinolytic context. To date no small molecules directly interfering with these virulence mechanisms of group A *streptococcus* exist – apart from several (structurally similar) inhibitors of streptokinase gene expression (Sun *et al.*, 2012; Yestrepsky *et al.*, 2014). In addition, no agents directed against other important group A streptococcal virulence mechanisms, e.g. adherence and invasion (vide 1.1.2.2.1), have been published so far. Though, these could be powerful new weapons: in the case of adherence and invasion, these agents could reduce persistence and dissemination (Gerber, 1996; Medina, Goldmann *et al.*, 2003; Rohde and Chhatwal, 2013).

However, these new drugs with the special mode-of-action in targeting virulence have to be discovered first. There are several possibilities: one could be the use of synthetic chemical compounds whereas another could consist of compounds derived from natural products. As natural products offer new chemical scaffolds and often novel modes of action (Butler and Buss, 2006; Weissman and Müller, 2010; Cragg and Newman, 2013), they may aid in the quest for such new weapons. To evolve these new anti-virulence agents, it will be beneficial to take a (side) glance to natural products.

1.2 Natural products

Natural products have always played a role in the therapy of (human) diseases. To date, a lot of drugs in contemporary academic medicine originate from natural sources or have been inspired by them. Consequently, the following paragraphs will give an overview of natural products used in the past and today to cure infectious diseases. Furthermore, they will highlight the inherent potential of natural products with a focus on those derived from myxobacteria regarding new anti-virulence agents.

1.2.1 Natural products as therapeutics

The discovery of penicillin from the fungus *Penicillum notatum* as an antibiotic agent by Alexander Fleming and its characterization by Chain and Florey led to the so-called 'golden era of antibiotics' ranging from the 40ies to the 60ies of the 20th century. Furthermore, it marked a milestone in the therapy of infectious diseases: life-threatening infections with e.g. staphylococci and streptococci were cured (Chain *et al.*, 1940; Ligon, 2004). The group of penicillins expanded by the discovery of cephalosporins; also derived from a fungus. However, soon resistance mechanisms, like secretion of β-lactamase, evolved in several microorganisms. The race against resistance development began: by modifying structures of penicillins and by identifying clavulanic acid (isolated from actinomycetes) as a natural inhibitor of β-lactamases (Brown *et al.*, 1976; Lewis, 2013).

Nevertheless, fungi were and are not the only producers of anti-infectives: actinomycetes are producing a much higher number of structurally different, active substances: streptomycin successfully used against tuberculosis was one of the first to be discovered (Schatz *et al.*, 2005). Other antibiotics from actinomycetes like erythromycin (N.N., 1952) or vancomycin (Fairbrother and Williams, 1956) followed. Though, antibiotic resistance against these drugs emerged as well: bacteria developed e.g. efflux pumps to efficiently transport antibiotics outwards by exchanging and mutating their genes. Again the only 'remedy' to overcome these mechanisms seemed to be chemical modification of the respective antibiotic. Thereby, re-development of resistance was not prevented and went on (Poole, 2005; Alekshun and Levy, 2007; Chang *et al.*, 2015).

Between 1981 and 2010, 270 anti-infective drugs were approved and accessed the market (including drugs against parasites, bacteria, viruses and fungi). Although more than 30 % were a natural product itself or were derived from or inspired by a natural product, this percentage should not deceive about the fact that only six new drugs were approved from 2006 to 2010 in the area of new anti-bacterial agents (Newman and Cragg, 2012). Yet, novel agents are urgently needed with regard to increasing resistance and microorganisms developing new methods to exploit the host. Especially,

the emergence of the multiresistant ESKAPE pathogens (*Enterococcus faecium*, *Staphylococcus aureus*, *Klebsiella pneumoniae*, *Acinetobacter baumanii*, *Pseudomonas aeruginosa*, *Enterobacter* ssp.) raises major concern. But also the increase of invasive diseases caused by GAS proves the rising need for not only 'classical' antibacterial remedies, but also agents that target new mechanisms, i.e. virulence (Clatworthy *et al.*, 2007; Pendleton *et al.*, 2013; Waddington *et al.*, 2014; World Health Organization, 2014).

To keep up with (or possibly stay at least one step ahead of) the microbes, it is necessary to find new chemical scaffolds. Although natural products are a good source for new scaffolds, to date, natural products research has become rare in pharmaceutical industry. Some of the following reasons have fueled this process:

As an optimization of this process, high-throughput screening (HTS) was implemented in pharmaceutical industry. Natural products turned out as difficult candidates for HTS: if crude extracts were screened, diversity within the library was ensured, but laborious re-screening was necessary to finally discover the active component. Therefore, the process was not as fast as expected. Furthermore, natural products often interact with several targets. Consequently, it is likely that HTS developed for defined targets might overlook a potent compound (Koehn and Carter, 2005). Although most of the natural products do not follow the first four rules of Lipinski's 'rule of five', hits derived from natural products still have a 50 % chance to become an orally applicable drug (Lipinski *et al.*, 2001; Macarron, 2006; Ganesan, 2008). However, pharmaceutical industry was looking for more beneficial ways and libraries for HTS. Consequently, libraries of synthetic chemicals were used which seemed to be more suitable for screening than natural extract libraries. In addition, combinatorial chemistry seemed to offer a large chemical diversity in construction of libraries. And finally, a decline in interest in infectious disease research – the main domain of natural products – led most of the pharmaceutical industries to abandon research with focus on natural products (Projan, 2003; Koehn and Carter, 2005).

Although natural products harbor an enormous structural diversity, initially, as described, HTS was not so successful. Several metabolites seemed to be inactive. This might be explained by the so-called 'screening hypothesis' assuming that any potent biological activity is a rare feature for any molecule to possess (Jones and Firn, 1991; Firn and Jones, 2003). Nevertheless, innovative strategies and approaches were and are implemented to spur the pipeline of new anti-bacterial agents although not all of these offer high-throughput (Bode and Müller, 2005; Baker *et al.*, 2007; Kirst, 2013; Müller and Wink, 2014). Among these are *inter alia* secondary metabolomics (Krug and Müller, 2014), variation of culture conditions (termed 'one strain – many compounds' approach (OSMAC) (Bode *et al.*, 2002)), genomic engineering (Aigle and Corre, 2012), combinatorial (bio)synthesis (Ganesan, 2004; Baltz, 2014) and high-content screening (HCS) (Zanella *et al.*, 2010; Brodin and

Christophe, 2011). To enhance the biodiversity within the libraries, bacterial strains are now also collected from so far unexplored habitats like marine ones (Bull and Stach, 2007; Garcia, Krug *et al.*, 2009; Cragg and Newman, 2013). Furthermore, the focus is not only on actinomycetes, but also on other microbial sources like myxobacteria which have already produced at least one compound that has been approved for cancer therapy (Ixempra®, Bristol-Myers Squibb) and is now on the market (although after structural modification and as an anti-cancer drug) (Gerth *et al.*, 1996; Trédan *et al.*, 2015). In addition, myxobacteria produce further substances with promising anti-infective activity not only against bacteria but also against parasites (Baumann *et al.*, 2014; Held *et al.*, 2014; Surup *et al.*, 2014). After a brief overview of the myxobacterial classification, the following paragraph will give an insight into production and potential therapeutic use of myxobacterial (secondary) metabolites.

1.2.2 Myxobacteria – their characterization, the production and potential therapeutic use of their secondary metabolites

Myxobacteria are gram-negative, mainly aerobic, rod-shaped bacteria which live in the soil or on e.g. rotting wood and can move swarmwise by gliding (Reichenbach, 1999). They also secrete a broad range of secondary metabolites. These are often attractive lead structures for drug discovery as they exhibit rare or novel modes of action (see below) (Weissman and Müller, 2010).

Myxobacteria belong to the δ-subclass of proteobacteria and can be divided into three suborders and altogether eleven families (*Cystobacterineae*: *Anaeromyxobacteraceae, Cysterbacteraceae, Myxococcaceae, Vulgatibacteraceae;* *Nannocystineae*: *Haliangiaceae, Kofleriaceae, Nannocystaceae;* *Sorangiineae*: *Labilitrichaeceae, Phaselicystidaceae, Polyangiaceae* and *Sandaracinaceae*; fig. 1-8) (Reichenbach and Höfle, 1993; Sanford *et al.*, 2002; Garcia, Reichenbach *et al.*, 2009; Mohr *et al.*, 2012; Garcia and Müller, 2014a, 2014b, 2014c, 2014d, 2014e; Knupp dos Santos *et al.*, 2014; Lang, 2014; Sood *et al.*, 2014; Yamamoto *et al.*, 2014). The slime excreted during gliding motility supports the proteolytic activities of most of the myxobacteria: native proteins of lysed prey cells are denatured and thereby proteolytic exoenzymes are supplied with substrates (Gnosspelius, 1978; Dawid, 2000). Although psychrophilic myxobacteria exist which grow below 6°C, the majority is considered as mesophiles generally growing within a temperature range of 6°C and 38°C. Thereby, it has to be considered that each species has its own distinct temperature optimum to grow (McDonald, 1967; McCurdy, 1969; Janssen *et al.*, 1977; Dawid *et al.*, 1988; Fudou *et al.*, 2002; Gerth and Müller, 2005; Garcia, Reichenbach *et al.*, 2009). Furthermore, myxobacteria display social behavior by e.g. cooperative motility, excretion of proteolytic exoenzymes and collective food uptake. Under nutrient-limiting conditions they start to aggregate. This leads to the formation of

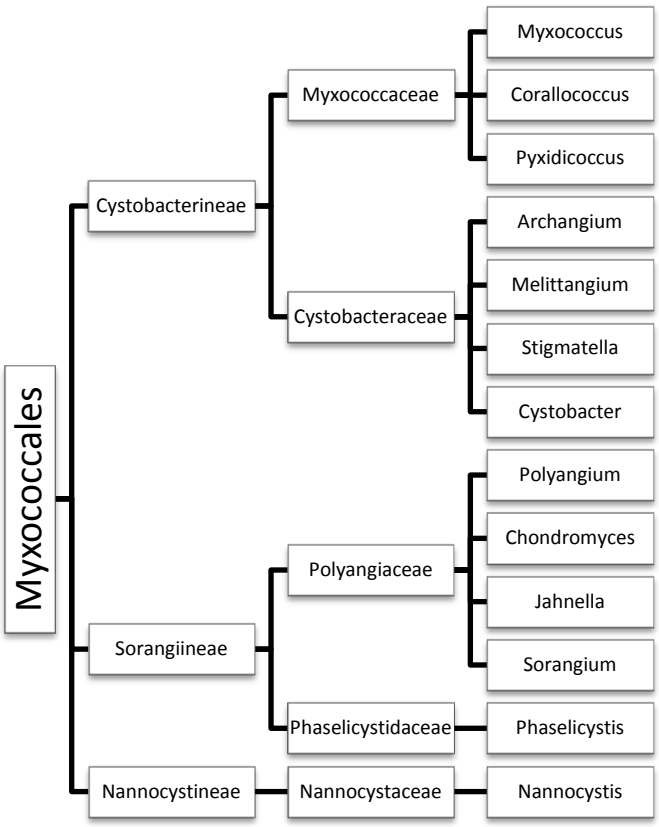

Figure 1-8. Taxonomic classification of the *Myxococcales*.
The order *Myxococcales* can be divided into three suborders (*Cystobacterineae, Nannocystineae* and *Sorangiineae*) and into eleven families, five of these covering most of the known species are displayed here. The *Myxococcales* were classified after Garcia, Reichenbach *et al.*, 2009 and Reichenbach and Höfle, 1993 and using NCBI taxonomy browser.

multicellular and often complex fruiting bodies (fig. 1-9). By formation of fruiting bodies, it is guaranteed that a new life cycle starts with a bacterial swarm rather than a single cell (Reichenbach, 1999). Within these fruiting bodies so-called myxospores are formed. In comparison to vegetative cells, they are much shorter and thicker and rounded and surrounded by a thin capsule. They differ from eubacterial endospores by their way of formation, structure and physiological properties. Myxospores are dehydrated and resistant against environmental factors like dryness, heat or UV radiation. Therefore, they are perfect survival cells to overcome unfavorable environmental or nutritional conditions (Dawid, 2000; Pathak *et al.*, 2012). In correlation to other bacteria, myxobacteria harbor large genomes (typically a bacterial ring chromosome) with a GC-content between 64 and 72 % (Dawid, 2000). In 2007, the complete genome of the model strain *Sorangium cellulosum* (Soce56) was sequenced and was the largest genome ever sequenced in those days (Schneiker *et al.*, 2007). The genome of the strain *Myxococcus xanthus* had been sequenced earlier (Goldman *et al.*, 2006). Nevertheless, no global synteny was apparent between those two strains representing two myxobacterial families (Schneiker *et al.*, 2007).

According to the genome database (from NCBI), 16 different myxobacterial strains have been sequenced to date. The existence of whole genome sequences of different myxobacterial strains facilitates screening for new secondary metabolites: as most of the compounds produced by myxobacteria are synthesized on molecular assembly lines, like polyketide synthases (PKSs), non-ribosomal peptide synthetases (NRPSs) or a combination of both, screening for such biosynthetic clusters has become much easier. Additionally, secondary metabolites are not only synthesized on biosynthetic gene clusters, but can also be altered later by post-translational modifications (Wenzel and Müller, 2009a). Basically, a NRPS is at least composed of the following domains: an adenylation (A) domain which activates the amino acid, a thiolation (T) domain which represents the

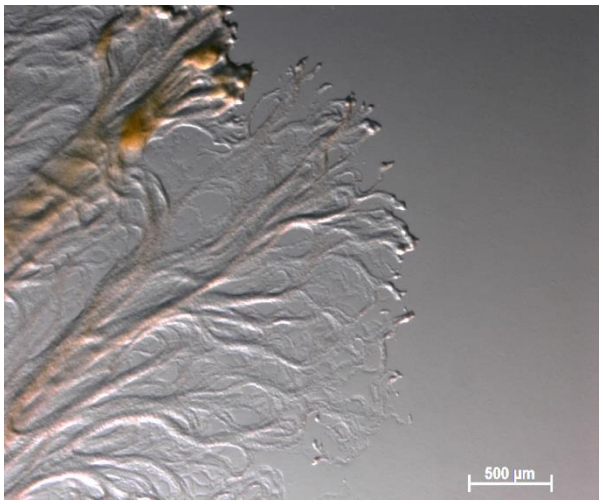

Figure 1-9. Swarming of Soce554 on Cy-agar
The picture shows the growth and swarming of the strain Soce554 (Sorangium cellulosum) on Cy-agar after two weeks of inoculation at 30°C. The scale bar indicates 500 µm.
Image by Diana Telkemeyer and Katharina Rox, HZI, Braunschweig.

peptidyl carrier protein (PCP) where the activated amino acid is covalently attached, and a condensation (C) domain catalyzing the peptide bond formation. Further domains like a methyl transferase domain (MT) or an epimerization (E) domain might also be present. Similar to an NRPS, a PKS module is composed of an acyl transferase (AT) domain which transfers an acyl carrier protein (ACP) to the amino acid and a ketoacyl synthase (KS) domain which condensates an extender unit with the acyl thioester from the upstream molecule. As a result a β-keto acid is formed. This can be further processed by a β-ketoacyl reductase (KR), β-hydroxyacyl dehydratase (DH), enoyl reductase (ER) or/and a methyl transferase (MT) domain. The last module usually is responsible to release the newly formed molecule. This can be done by e.g. a thioesterase (TE) domain. However, it has been observed that the abovementioned scheme is much more diverse in nature. Therefore, every myxobacterial gene cluster might harbor unusual genetic or biochemical properties (Wenzel and Müller, 2007).

Beside the possibility of understanding how myxobacterial secondary metabolites are produced, the availability of the genome sequences offers more: strains can be engineered metabolically and/or biosynthetic clusters can be heterologously expressed. Moreover, primary metabolic pathways can be exploited in a better way by identification of key precursors for the secondary metabolism (Wenzel and Müller, 2009b). Furthermore, genome mining renders possible the uncovering of so far unknown biosynthetic gene clusters which can lead to the discovery of new compounds finally (Pistorius and Müller, 2012). In addition to exploring the genome, investigation of the metabolome also reveals a great potential for new secondary metabolites, e.g. a study of different strains of *Myxococcus xanthus* exhibiting the enormous capacity for new so far unknown natural products (Krug *et al.*, 2008). Like genome mining, metabolome mining is equally able to detect new compounds – in the case of myxoprincomide, a combined approach using targeted mutagenesis, LC-HRMS and statistical data analysis enabled the identification of a compound which is only present in low amounts (Cortina *et al.*, 2012). As bioinformatic tools (Hufsky *et al.*, 2014) and MS methods (Hoffmann *et al.*, 2014) for natural product discovery are developing rapidly, combined approaches using *inter alia* genome and metabolome mining might be even more successful and also more rapid in the detection of new compounds (Krug and Müller, 2014). Bioactivity-guided screening of extracts

is not as fast as the aforementioned promising new methods: positively screened extracts have to be reproduced on a larger scale and to be fractionated and then further purified to finally obtain an active compound. Nevertheless, it has been proven successful within the last decades (Weissman and Müller, 2010; Schäberle *et al.*, 2014).

Especially in the bioactivity-guided screening approach structures of active compounds have to be elucidated and efficient purification-strategies have to be implemented for compounds of interest produced in large scale. Thereby, NMR and HR-ESIMS are used to determine the structure and the molecular formula (Breton and Reynolds, 2013; Seger *et al.*, 2013; Halabalaki *et al.*, 2014). However, in some cases NMR spectroscopy might not be sufficient for structure elucidation. Such a case is the presence of an unsaturated fatty acid: often the location of double bonds cannot be determined by NMR. Therefore, GC-MS combined with different derivatization strategies has to be used to assign double bonds to their respective positions (Andersson and Holman, 1974; Dunkelblum *et al.*, 1985; Leonhardt and DeVilbiss, 1985; Fay and Richli, 1991). In addition, GC-MS is a suitable method to identify volatile metabolites (Nawrath *et al.*, 2010).

Different isolation- and purification-strategies of active compounds from crude extracts can be used. One of these is the classical extraction with organic solvents. Though, several other methods have been developed like solid phase and ultrasound-assisted extraction. Isolation of natural products comprises the use of several chromatographic methods starting with low-pressure liquid chromatography (LPLC) (e.g. LH-20 gel chromatography), proceeding with MPLC and finally using HPLC. Whereas LPLC is suitable for crude extracts, MPLC serves for enrichment of secondary metabolites which can be purified by HPLC afterwards (Sticher, 2008; Bucar *et al.*, 2013). This strategy can lead to pure compounds. Although flash-LC was always used for purification of crude extracts like LPLC (Bucar *et al.*, 2013), recently available high performance cartridges also assure a high resolution for samples difficult to purify. Depending on the compound to be purified, flash-LC using these high performance cartridges can be an alternative to conventional preparative HPLC.

Beside epothilone (vide 1.2.1), additional substances derived from myxobacteria have been isolated and show good activity in the fight against diseases of various therapeutic areas. Several myxobacterial compounds have been isolated to fight cancer. In addition to epothilone, other promising compounds like e.g. disorazole are currently in development for clinical trials (Seitz *et al.*, 2014). Disorazole has been isolated from *Sorangium cellulosum* (Jansen *et al.*, 1994) and targets the cytoskeleton, i.e. tubulin. However, in contrast to epothilone, it destabilizes the microtubules and thereby, blocks mitosis and finally induces apoptosis (Elnakady *et al.*, 2004).

Furthermore, several myxobacterial compounds have been discovered with promising activity to combat infectious diseases. Thereby, these target different mechanisms like the bacterial protein synthesis (e.g. althiomycin (Fujimoto *et al.*, 1970; Zarantonello *et al.*, 2002)), the bacterial RNA

polymerase (e.g. sorangicins (Irschik *et al.*, 1987; Campbell *et al.*, 2005)) the respiratory chain (e.g. thuggacins (Irschik *et al.*, 2007)), the bacterial topoisomerase IIa (like the recently discovered cystobactamids (Baumann *et al.*, 2014)) or biofilm formation (e.g. carolacton (Jansen *et al.*, 2010; Kunze *et al.*, 2010)). Inhibiting biofilm formation, though, represents a novel mechanism in anti-infective therapy: 'conventional' therapies have bacteriostatic or bactericidal effects which lead to rapid development of resistance. Targeting quorum-sensing, a conserved mechanism of bacteria, might inhibit biofilm formation without induction of resistance. However, in the case of carolacton, disruption of biofilm formation also led to the bacteria's death (Kunze *et al.*, 2010). Thus, it is a good example for inhibitors of bacterial virulence. In addition, it shows that natural products from myxobacteria can be a good source for new anti-virulence agents. This raises hope that myxobacterial natural products can also serve as pathoblockers against *S.pyogenes* by targeting its conserved key pathogenic mechanisms (vide 1.1.2).

1.3 Objectives of this thesis

The objective of this thesis is the quest for natural compounds from myxobacteria as pathoblockers of streptococcal infections which are still not sufficiently treatable. The latter underlines the fundamental importance of this subject.

S.pyogenes has evolved several mechanisms to defend itself and to circumvent the host's immune defense (Walker *et al.*, 2014): Adherence to and invasion into epithelial cells and secretion of streptokinase are two of these important mechanisms in streptococcal virulence which are addressed in this thesis.

'Pathoblockers' are meant to block pathogenic or virulence mechanisms of *S.pyogenes*. As some pathogenic or virulence mechanisms seem to be conserved in bacteria and as targeting these mechanisms might result in a lower selection pressure, it is assumed that resistance against these will not arise (Clatworthy *et al.*, 2007). Myxobacteria produce a broad-range of secondary metabolites (Wenzel and Müller, 2009a; Weissman and Müller, 2010; Müller and Wink, 2014). This fact turns them into ideal candidates for novel agents in the combat against streptococcal diseases. Therefore, myxobacterial extracts and substances were screened for their 'pathoblocking' activities against the two abovementioned streptococcal virulence mechanisms. Besides screening, new bioactive compounds were isolated and their structure was elucidated. Active compounds were characterized with regard to their possible targets *in vitro* and, if applicable, *in vivo*.

To achieve the goal to find potent inhibitors for these virulence mechanisms, several methods were combined, apparently for the first time in only one work which is presented in this thesis:

(1) classical microbiological and cell-biological methods were linked to natural products biology to investigate activities and to perform initial mode-of-action-studies and structure-activity-relationship studies of different compounds
(2) analytical methods were used to recognize, isolate and identify active compounds
(3) non-toxic 'hit compounds' were further characterized in *in vivo* experiments

The major aim of this thesis was to determine if and how natural products from myxobacteria interfere with certain aspects of streptococcal pathogenesis. If myxobacterial compounds succeed in blocking key pathogenic mechanisms, this will open the avenue for new therapeutic strategies to combat invasive group A streptococcal infections. If successful, myxobacterial compounds might become one of the first 'pathoblockers' - new anti-infectives targeting virulence.

2 Materials and methods

2.1 Materials

2.1.1 Chemicals, media and buffers

Chemicals and solutions

Solvents were obtained from J.T.Baker and had p.a. quality. Chemicals and solutions that were used are indicated in tab. 2-1.

Table 2-1 Chemicals and solutions.

Chemical/solution	manufacturer
acetic acid	Merck
acrylamide 30 % (Rotiphorese Gel 30)	Roth
Agar-Agar, Kobe I	Roth
agarose Broad range (NEEO Ultra quality)	Roth
Amberlite XAD-16 adsorber resin	Sigma
ammoniumpersulfate (APS)	Serva
ampicillin	Applichem
Bacto™ Tryptic Soy Broth	Becton Dickinson
Bacto™ Tryptone	Becton Dickinson
β-mercaptoethanol	Serva
bovine serum albumin (BSA)	Sigma Aldrich
bromophenol blue	Sigma Aldrich
Coomassie Brilliant Blue R-250	Sigma Aldrich
Columbia blood agar plates	Becton Dickinson
Difco™ M17 broth	Becton Dickinson
dimethyl disulfide (DMDS)	Sigma Aldrich
dimethylsulfoxid	Sigma Aldrich
di-sodiumhydrogenphosphat (Na_2HPO_4)	Merck
dNTPs	Fermentas
erythromycin	Sigma Aldrich
ethanol 96 % (EtOH)	J.T.Baker
ethidum bromide	Applichem
fetal calf serum (FCS)	PAA
fibrinogen	Sigma Aldrich
hydrochloric acid (HCl), 37%	Merck
GeneRuler™ DNA ladder mix, 100-1000 bp	Fermentas
gentamicin solution 10 mg/ml	Sigma Aldrich
glucose	Roth
L-glutamine (200 mM)	PAA
glycerol 85 %	Roth

HEPES-BSS	Promocell
Immersol 518F	Zeiss
isopropyl alcohol	Merck
lactose	Roth
6x loading dye (agarose gel electrophoresis)	Fermentas
magnesium chloride ($MgCl_2$) solution for PCR	Qiagen
methanol (MeOH)	J.T.Baker
paraformaldehyde (PFA) solution, 4% in PBS	USB Corporation
penicillin G	Sigma Aldrich
penicillin/streptomycin (100x)	Pan Biotech GmbH
5x phusion high fidelity PCR buffer	Thermo Scientific
Phusion® Hot Start II High fidelity DNA Polymerase	Thermo Scientific
plasminogen, EACA- and lysin-free	Biopur
plasmin	Biopur
ProLong®Gold antifade reagent	Invitrogen
proteinase K	Fluka
RNase (DNase-free)	Applichem
S-2251	Chromogenix
saponin	Fluka
sodium citrate	Fluka
sodium dodecyl sulfate (SDS)	Sigma Aldrich
sodium hydroxide (NaOH)	Merck
T4 DNA ligase	New England Biolabs
TEMED	Biorad
thiazolyl blue tetrazolium blue (MTT)	Sigma Aldrich
thionyl chloride	Fluka
thrombin	Haemochrom Diagnostica
Todd Hewitt Broth (THB)	Roth
Tris	Sigma Aldrich
Triton X-100	Sigma Aldrich
trizma Base	Sigma Aldrich
tryphan blue (0.4%)	Sigma Aldrich
trpysin/EDTA in HEPES-BSS	Promocell
trypsin/EDTA in PBS	Gibco
yeast extract	Roth

Media

All media for cultivation of *E.coli*, group A streptococci and lactococci were autoclaved prior to use at 121°C for 15 min.

Media for cultivation of *E.coli*

LB medium

10 g	Tryptone
5 g	yeast extract
10 g	sodium chloride
ad 1 l	distilled water

LB agar

LB-Medium + 16-18 g/l agar

Media for cultivation of group A streptococci

THY medium

36.4 g	Todd-Hewitt broth
5 g	yeast extract
ad 1 l	distilled water

TSB medium

30 g	Todd-Soy broth
ad 1 l	distilled water

THY agar

THY medium + 16-18 g/l agar

Media for cultivation of lactococci

M17 broth

37.25 g	M17 broth
ad	950 ml distilled water

Then the medium is mixed, heated and boiled for 1 min to completely dissolve the power. After autoclaving, the medium is cooled to 50°C. Then 50 ml of a sterile 10 % lactose solution are added.

M17 agar

37.25 g	M17 broth
16 g	agar
ad	950 ml distilled water

Then the same procedure is performed as for M17 broth.

Media for cultivation of myxobacteria

Media components for cultivation of myxobacteria were obtained from BD Biosciences, Roth or Sigma Aldrich.

Cy medium

0.3 %	casitone	
0.1 %	yeast extract	
0.1 %	calcium chloride	
50 mM	HEPES (11,8 g/l)	
1.6 %	agar	
ad 200 ml	distilled water	pH 7.2

H medium

0.2 %	soya flour	
0.2 %	glucose	
0.8 %	starch	
0.2%	yeast extract	
0.1 %	calcium chloride	
0.1 %	magnesium sulfate	
50 mM	HEPES (11,8 g/l)	
8 mg/l	Fe-EDTA	
ad 200 ml	distilled water	pH 7.4

P medium		
0.2 %	pepton marcor	
0.8 %	starch	
0.4 %	probion	
0.2 %	yeast extract	
0.1 %	calcium chloride	
0.1 %	magnesium sulfate	
100 mM	HEPES (23,8 g/l)	
8 mg/l	Fe-EDTA	
ad 200 ml	distilled water	pH 7.5

Pol medium		
0.3 %	starch, soluble	
0.3 %	probion	
0.05 %	calcium chloride	
0.2 %	magnesium sulfate	
50 mM	HEPES (11,8 g/l)	
ad 200 ml	distilled water	pH 7.2

Cy/H medium

50 % Cy medium + 50 % H medium

Vy/2 agar		
0.5 %	bakers' yeast	
0.1 %	calcium chloride	
0.5 mg/ml	cyanocobalamin	
1.5 %	agar	
ad 500 ml	distilled water	pH 7.2

Cy agar		
0.3 %	casitone	
0.1 %	yeast extract	
0.1 %	calcium chloride	
1.5 %	agar	
ad 500 ml	distilled water	pH 7.2

B_{12} solution	
50 mg	vitamin B_{12}
ad 100 ml	distilled water

Vit solution (Schlegel, 1992)

0.2 mg	biotin
2.0 mg	nicotinic acid
1.0 mg	thiamine
1.0 mg	4-amino benzoic acid
0.5 mg	pantothenate
5.0 mg	pyridoxamine
2.0 mg	cyanocobalamine
ad 100 ml	distilled water

Media for cultivation of cell lines or primary cells

Media, buffers and solutions used for cultivation of HEp2- and A549-cells:

DMEM, #31885, Gibco
DMEM with HEPES, #22320, Gibco
DMEM with HEPES + 5 mM glutamine + 10 % FCS (termed 'infection medium')
DMEM + 5 mM glutamine + 10 % FCS (termed 'seeding medium')
DMEM + 5mM glutamine + 10 % FCS + penicillin (10000 U/ml) + streptomycin (0.1 mg/ml) (termed 'cultivation medium')

Media, buffers and solutions used for cultivation of HUVEC:

EGM-2, #C22111, PromoCell
EGM-2 + Supplement-Mix (#C39216, PromoCell) (termed 'cultivation medium')
HEPES buffered saline solution, #C-40020, PromoCell
Trypsin/EDTA in HEPES buffered saline solution (HEPES-BSS), C-41022, PromoCell

Buffers

1% agarose buffer (in TBE)

1 %	agarose
ad 500 ml	TBE buffer

boiled in microwave until agarose is melted, then kept at 50°C.

PBS (1x)

10 %	PBS (10x)
ad 1 l	distilled water

SDS running buffer (1x)

10 %	SDS running buffer (10x)
ad 1 l	distilled water

SDS running buffer (10x)

30 g	Trizma base
150 g	glycine
10 g	SDS
ad 1 l	distilled water

TBE buffer (10x)

108 g	Tris base
55 g	boric acid
7 g	EDTA
ad 1 l	distilled water

PBS (10x)

80 g	sodium chloride	
2 g	kalium chloride	
7.6 g	sodium hydrogen diphosphate dihydrate	
2 g	kalium dihydrogen phosphate	
ad 1000 ml	distilled water	pH 7.4

5x SDS-PAGE loading buffer

1.75 ml	Tris-HCl (0.5 M, pH 6.8)
4 ml	glycerol
2 ml	SDS (0.25 g dissolved in 1 ml Tris-HCl)
0.5 ml	distilled water
0.5 ml	0.25 % bromophenol blue (25 mg in 10 ml H_2O)
1.25 ml	β-mercaptoethanol

12.9 mM sodium citrate buffer

3.3 g	sodium citrate
ad 1l	distilled water

TBE buffer (1x)

10 %	TBE (10x)
ad 1 l	distilled water

2.1.2 Bacterial strains

2.1.2.1 Group A streptococci, lactococci and E.coli strains

Strains of *Streptococcus pyogenes* were obtained from the HZI strain collection within the MMIK department (tab. 2-2).

Table 2-2: Streptococcal strains.

strain	additional information
AP1	clinical isolate, used for *in vivo* assays, secretes cluster 2a streptokinase (vide 6.1), originally: 40/58 strain from the WHO Collaborating Center for references and research on Streptococci, Institute of Hygiene and Epidemiology, Prague, Czech Republic; kindly provided by H. Herwald, Lund university
5448	used for *in vivo* assays, cluster 2a streptokinase, M1T1 clone (Aziz *et al.*, 2004)
A8	used in invasion assays, invades cells via cytoskeletal rearrangements (Molinari *et al.*, 2000)
A40	used in invasion assays, invades cells via the SfbI-mediated pathway (Molinari *et al.*, 2000)
A614	secretes cluster 2a streptokinase (vide 6.1)
A666	secretes cluster 2b streptokinase (vide 6.1)
A314	secretes cluster 2b streptokinase, NS1133 (McArthur *et al.*, 2008)

The following *E.coli* strain was obtained from the HZI strain collection (MMIK department; tab. 2-3).

Table 2-3: E.coli strain used for cloning of the *ska* gene.

strain	additional information
***E.coli* DH5α-pQE 30-TEV**	*E.coli* Top10 (Qiagen) with a pQE30-TEV vector was used for cloning the *ska* gene; 100 µg/ml ampicillin are necessary for cultivation; the strain contains the pQe30-vector (Qiagen) with a gene for a TEV-protease to cleave histidine-tags; the gene for the TEV-protease was cloned into the abovementioned vector by Giuseppe Gulotta and PD Dr. Patric Nitsche-Schmitz (MMIK, HZI)

The following lactococcal strains were kindly provided by Dr. René Bergmann (ZEIM, HZI, Braunschweig; tab. 2-4):

Table 2-4: Lactococcal strains.

strain	additional information
***Lactococcus lactis* expressing SfbI (Lac-SfbI)**	SfbI was cloned into a vector with an erythromycin resistance gene
Lactococcus lactis (Lac)	

Both lactococcal strains were used for invasion assays.

2.1.2.2 Myxobacterial strains

The following myxobacterial strains were obtained from the MWIS/MISG strain collection within the HZI. The strains were regularly grown in the indicated culture medium. For production of compounds they were grown in the indicated 'production medium' which was supplemented with 1 % Amberlite XAD-16 adsorber resin (tab. 2-5; for detailed description of the composition of the medium vide section 2.1.1).

Table 2-5: Myxobacterial strains.

Abbreviation	Strain name	culture medium	production medium
706	belongs to the *Sorangiineae* (Jansen *et al.*, 2014)	Cy/H	Pol
Ang852	*Angiococcus* 852	Pol + Vit + B_{12}	P
Anm9	*Angiococcus* 9	Pol + Vit	P + Vit
Cma13	*Chondromyces robustus* 13	Pol + Vit + B_{12}	Pol + Vit + B_{12}
Pl6894	*Polyangium* 6894	Pol + B_{12}	Pol + Vit
PlD3	*Polyangium* 3	Pol + Vit	Pol + Vit
Plvo18	*Polyangium* 18	Pol + B_{12}	Pol + B_{12}
Plvt3	*Kolferia flava* 3	Cy/H + Vit	Pol + Vit
Soce554	*Sorangium cellulosum* 554	Cy/H + Vit	H + Vit
Soce712	*Sorangium cellulosum* 712	Cy/H	H
Soce923	*Sorangium cellulosum* 923	Cy/H	H

2.1.3 Cell lines/primary cells for cell culture

The following cell lines and primary cells were used (tab. 2-6).

Table 2-6: Cell lines and primary cells used for cell culture.

name of the cells	additional information
HEp2-cells	human larynx carcinoma epithelial cell line, kindly provided by Ina Schleicher (ZEIM, HZI, Braunschweig)
A549-cells	human lung adenocarcinoma epithelial cell line, kindly provided by Ina Schleicher (ZEIM, HZI, Braunschweig)
HUVEC	human umbilical vein endothelial cells, primary cells, purchased from PromoCell

2.1.4 Myxobacterial extracts and compounds

Vinblastine, ε-amino caproic acid (EACA) and tranexamic acid (TA) were purchased from Sigma Aldrich. Tubulysin A was obtained from Dr. Jennifer Herrmann (MINS, HIPS). RC 11.1 and RC 11.2 as well as disorazole A and Z were obtained from Dr. Rolf Jansen (MWIS, HZI). Salinimyxantins (sAP01-sAP05, myxobase keys ## 3074, 3064, 3177, 3238) were obtained from Dr. Alberto Plaza and Suvd Nadmid (MINS, HIPS). Linoleic acid (LA) and palmitoleic acid (PA) were purchased from Acros Organics. Linoelaidic acid (LEA) and palmitelaidic acid (PEA) were purchased from Biomol.

Myxobacterial extracts and myxobacterial compounds for screening purposes were obtained from Dr. Klaus Gerth (MWIS, HZI) and Dr. Jennifer Herrmann/Prof. Dr. Rolf Müller (MINS, HIPS).

Prior to performing a plasminogen activation assay (vide 2.4.3) LA, LEA, PA and PEA were treated as follows to assure that they are protonated: every substance was dried under nitrogen flow at 40°C. Then they were dissolved in methanol containing 5 % H_2O and 10 % HCOOH. The methanol phase was extracted 5 times with n-heptane. n-heptane phases were separated from the methanol phase, united and dried under nitrogen flow at 40°C. Then, the dried substances were dissolved in the appropriate solvent (usually PBS) before being used for the plasminogen activation assay.

2.1.5 Instruments

Instruments repeatedly used for different methods are specified in tab. 2-7.

Table 2-7: Instruments repeatedly used for different methods.

Agarose gel chambers (Horizon^{TM} 58)	Autoclave-steam sterilizer (Biomedis)
Centrifuge 5417R (Eppendorf)	Centrifuge 5804R (Eppendorf)
HERA Cell 150i CO_2 incubator (Thermo Scientific)	Kodak IS2000R gel documentation unit (Intas)
Microwave Pro825 (Whirlpool)	Nano Drop ® (Thermo Scientific)
Novaspec II spectrophotometer (Amersham Pharmacia Biotech)	pH-meter 766 (Calimatic Knick)
Power pack 200 (BioRad)	Power pack 300 (BioRad)
SDS gel chambers (BioRad)	Thermocycler (Biometra)
Transferpette® S-8 (multichannel pipette, Brand)	Vortex Genie 2^{TM} (Bender + Hobein AG)
Water bath (GFL)	

2.2 General methods

All assays were performed in biological triplicates if not otherwise stated. Consequently, standard deviations were calculated from independent experiments.
In addition, all assays with disorazole A or Z, vinblastine, tubulysin A, salinimyxantins or fatty acids were performed using Sapphire Pipette Tips, 10 µl, low retention from Greiner BioOne instead of commonly used 10 µl pipette tips.

2.2.1 Microbiological methods

Handling of microorganisms was always performed in a biosafety cabinet.

2.2.1.1 Cultivation of group A streptococci and lactococci

Preparation of glycerol cultures for long-term preservation

Group A streptococcal strains were obtained in a glycerol culture from the MMIK department's strain collection (vide 2.1.2.1); lactococcal strains were obtained from Dr. René Bergmann (ZEIM, HZI, Braunschweig; vide 2.1.2.1). Streptococcal strains were streaked out onto sheep blood agar plates and were incubated overnight at 37°C. Lactococcal strains were streaked out onto M17 agar plates (agar plates for Lac-SfbI were supplemented with 3 µg/ml erythromycin) and were incubated overnight at 30°C.
The following day the respective streptococcal strain grown on the blood agar plate was inoculated in liquid culture with THY medium and incubated overnight at 37°C and 5 % CO_2. Lactococcal strains were inoculated in M17 medium with 0.5 % glucose at 30°C (*Lactococcus lactis* expressing SfbI (Lac-SfbI) was supplemented with 3 µg/ml erythromycin during cultivation). After overnight culture, the strain grown in the respective medium was mixed with 85 % glycerol (relation 3:1; liquid culture:glycerol), sealed in a vial and stored at -80°C.

Preparation of liquid cultures (streptococci)

A short piece of a glycerol culture of the respective streptococcal strain was inoculated in liquid culture with either THY or TSB medium and incubated at 37°C and 5 % CO_2 overnight to obtain a stationary phase culture.
For midlog phase cultures or to determine the growth of a certain strain, streptococci from an overnight culture were re-inoculated in a fresh liquid culture with either THY or TSB medium and

incubated at 37°C and 5 % CO_2 until they had grown to the specified OD. To measure the OD 1 ml of the culture was measured against a reference consisting of the respective medium.

Preparation of liquid cultures (lactococci)

Liquid cultures of lactococci were prepared in a similar way as the ones of streptococci. Briefly, a piece of a glycerol culture of the respective lactococcal strain was inoculated in M17 medium + 0.5 % glucose at 30°C overnight. The strain Lac-SfbI was supplemented with 3 µg/ml erythromycin during cultivation.

Preparation of cultures on agar plates

To prepare a culture on an agar plate the respective streptococcal strain was streaked out onto a sheep blood agar plate or a THY agar plate from a glycerol culture or a liquid culture. Then the plate was incubated overnight at 37°C. Lactococci were streaked out onto M17 agar plates and incubated overnight at 30°C. Lactococci expressing SfbI were streaked out on M17 agar plates supplemented with additional 3 µg/ml erythromycin for growth.

2.2.1.2 Cultivation of myxobacteria

Preparation of cultures on plates

To cultivate different myxobacterial strains on agar plates, some cells of the respective defrosted cryoculture were placed onto Vy/2 or Cy agar plates. They were incubated at 30°C until growth and/or swarming could be observed.

Preparation of liquid cultures for long-term cultivation

The respective strain was inoculated from a cryoculture in the indicated medium as described in section 2.1.2.2 and incubated at 30°C and 180 rpm until growth could be observed (typically after one week). If no growth could be observed after inoculation from a cryoculture, the respective strain was inoculated in the indicated medium from a culture on an agar plate of the respective strain.

2.2.1.3 Preparation of myxobacterial extracts

Preparation of liquid cultures for production of secondary metabolites

In case of cultivation in liquid media for production of secondary metabolites the respective strain was re-inoculated from a previous liquid culture in the respective ‘production medium’ (vide 2.1.2.2) and incubated at 30°C and 180 rpm until growth was observed and production of the desired metabolites was detected.

Harvesting a myxobacterial liquid culture

After a 100 ml myxobacterial liquid culture supplied with Amberlite XAD-16 adsorber resin had been grown for the designated amount of time (typically 1-4 weeks depending on the strain; until sufficient growth was observed) the culture was harvested by sieving the culture medium, the cells and the XAD through a 200 µm sieve. The sieve was washed twice before drying it with tissue from below. Then the residuum upon the sieve was transferred into a flask. Acetone was added for 1 h in order to extract the metabolites. Afterwards, the acetone and the remaining content of the flask were filtered into a round bottom flask. The acetone was removed by evaporation with a rotavapor (Heidolph) until the round bottom flask was dry. The remaining content in the round bottom flask was dissolved in 1 ml of methanol and transferred into a vial for testing in bioassays.

2.2.2 Cellbiological methods

All media, buffers and trypsin were heated to 37°C in a water bath prior to use. All cell lines and primary cells were handled in a biosafety cabinet.

2.2.2.1 Cultivation of A549- and HEp2-cells

Splitting of cell lines

Cells were splitted in a cell culture dish as soon as 80-90 % confluence was obtained (HEp2- and A549-cells). The 'cultivation medium' (vide 2.1.1) was removed and the cells were washed once with PBS. Afterwards, PBS was removed and trypsin was added. When the cells started to detach, 'cultivation medium' was added to stop the reaction. Loosely attached cells were washed away from the surface with 'cultivation medium'. Then the cells were splitted 1:10 or 1:20 depending on the growth rate of the respective cell line to obtain 80-90 % confluence within 3-4 days at 37°C and 5 % CO_2. Cells were not used after passage 10.

Freezing and thawing of cell lines

For long-term preservation cell lines (HEp2- and A549-cells) were stored in liquid nitrogen. Therefore, the respective cell line was cultivated as described above and detached of the cell culture dish with trypsin. Then the cells were transferred into a falcon tube and centrifuged for 9 min at 700 rpm. The supernatant was discarded and the cells were resuspended in 'cultivation medium' (vide 2.1.1) supplemented with 5 % DMSO. 1 ml suspension (containing $3x10^6$ cells) of the respective cell line was frozen in a cryo vial (Nunc). These vials were stored in an isopropanol filled freezing container for 24 h at -80°C. The freezing container assures a controlled cooling of 1°C per minute which prevents

cell damage by accumulation of ice crystals. After 24 h the cryo vials were transferred to liquid nitrogen.

The respective cell line was thawed by seeding the content of a cryo vial into a cell culture dish filled with 'cultivation medium' which had been pre-warmed to 37°C before. Cells were then incubated at 37°C and 5 % CO_2. 6 h after thawing the cells, the medium was replaced by fresh 'cultivation medium'.

2.2.2.2 Cultivation of HUVEC

Splitting of HUVEC

Cells were splitted when they had reached 80-90 % confluence in a cell culture dish. Cells were washed once with HEPES buffer before 3 ml of trypsin/EDTA were added. When cells started to detach, 7 ml of EGM with supplements were added. Cells were centrifuged at 900 rpm for 9 min. Supernatant was removed and cells were resuspended in 4 ml of EGM with supplements. Then cells were added to a new cell culture dish containing EGM with supplements. The medium was changed every 3 days. Cells were not used after passage 6.

Thawing of HUVEC

The content of a cryo vial of HUVEC was seeded into a cell culture dish containing pre-warmed EGM-2 medium with supplements. Cells were then incubated at 37°C and 5 % CO_2. 6 h after thawing the cells, the medium was replaced by fresh one.

2.2.3 Analytical methods

2.2.3.1 Analytical HPLC

Myxobacterial extracts were analyzed by RP-HPLC on an Agilent 1260 system (Agilent Technologies) equipped with a diode array UV detector and a Corona ultra-detector (Dionex). 1 µl of each extract was injected. The following conditions were used: column Nucleodur 120 EC, 125x2mm, 5 µm, C_{18} (Macherey-Nagel); temperature: 40°C; solvent A: 95% H_2O, 5% acetonitrile, 5 mM ammonium acetate, 40 µl/l acetic acid; solvent B: 95% acetonitrile, 5% H_2O; 5 mM ammonium acetate, 40 µl/l acetic acid; gradient 10-100 % B for 30 min, 100 % B for 10 min; 10 % B post-run for 10 min; flow 0.3 ml/min; UV detection 200-450 nm.

Fractions obtained after fermentation and during purification of fermenter products were analyzed by analytical RP-UPLC on an Agilent 1260 HPLC system (Agilent Technologies) equipped with a diode array UV detector and a corona ultra-detector (Dionex). 1 µl of each fraction was injected. The

following conditions were used: column Waters Acquity UPLC BEH C18, 130 Å, 1.7 µm, 50x2.1 mm; temperature: 40°C; solvent A: 95% H_2O, 5% acetonitrile, 5 mM ammonium acetate, 40 µl/l acetic acid; solvent B: 95% acetonitrile, 5% H_2O; 5 mM ammonium acetate, 40 µl/l acetic acid; gradient: 90 % A for 10 min, 10-100 % B for 30 min, 100 % B for 10 min; 10 % B post-run for 10 min; flow 0.3 ml/min; UV detection 200-450 nm. In addition RC 11.1, RC 11.2, RC 25.1, RC 25.3, RC 28.1, RC 28.5, RC 36.1 and RC 36.2 (vide 2.4.2) were analyzed by analytical RP-UPLC under the same conditions.

2.2.3.2 Fractionation via HPLC

Fractionation via HPLC was performed analogously to an analytical RP-HPLC. For fractionation, a fraction-collector was replaced by the Corona ultra-detector (Dionex). 10 µl of the crude extract or of the pre-purified fraction to be tested (e.g. RC 11.1 or RC 11.2) were injected. Fractions were collected every 30 sec in a 96well-plate. After the end of the HPLC-run the plate containing the solvent of the fractions was dried under nitrogen flow at 37°C for 1 h.

Myxobacterial extracts were fractionated using the same column and the same conditions as described in section 2.2.3.1.

For fractionation of RC-fractions the following conditions were used: column Waters Acquity UPLC BEH C18, 130 Å, 1.7 µm, 50x2.1 mm; temperature: 40°C; solvent A: 95% H_2O, 5% acetonitrile, 5 mM ammonium acetate, 40 µl/l acetic acid; solvent B: 95% acetonitrile, 5% H_2O; 5 mM ammonium acetate, 40 µl/l acetic acid; gradient 10-100 % B for 30 min, 100 % B for 10 min; 10 % B post-run for 10 min; flow 0.3 ml/min; UV detection 200-450 nm.

2.2.4 Statistical analysis

Statistical analysis for all assays described below (with exception of the survival data of the *in vivo* assays) was performed using Microsoft Excel 2010. Significance was determined by using a two-tailed, paired student's t-test.

Survival data were analyzed using GraphPad Prism7 Software. Significance was determined by using a Mantel-Cox- and a Wilcoxon-Test.

Results were considered to be significant when they had a p-value lower than 0.05. The following asterisks are corresponding to the following p-values:

*	0.05	< p <	0.01	**	0.01 < p < 0.001
***	0.001	< p <	0.0001	****	p < 0.0001

2.3 Methods for inhibitors of group A streptococcal invasion

2.3.1 Infection assays

2.3.1.1 Invasion assay with S.pyogenes strain A40 and A8

Invasion assay

Cells (HEp2 or A549) were detached from the cell culture dishes as described in section 2.2.2.1. The trypsin reaction was stopped with 'seeding medium' (vide 2.1.1). The cells were counted in a Neubauer Chamber. Afterwards, they were seeded into each well of a 24well-plate onto sterile glass coverslips (HEp2-cells: 62500 cells/well; A549-cells: 75000 cells/well). Then they were incubated for 24 h at 37°C and 5 % CO_2 until they reached 80 % confluence. In parallel, the streptococcal strains A40 and A8 were inoculated in TSB medium and incubated overnight at 37°C and 5 % CO_2.

The following day, the cells were washed twice with 'infection medium' (vide 2.1.1). Then the substances or extracts to be tested were added to the respective wells in the respective concentration (vide tab. 2-8). For screening purposes 2.5 µl of each extract or each compound were added to the cells. The cells were incubated for 30 min at 37°C and 5 % CO_2. Meanwhile, the streptococcal strains were centrifuged at 5000 rpm for 10 min and washed with PBS. Then they were adjusted to a transmission of 10 % at 600 nm and diluted 1:150 in 'infection medium'. Dilution resulted in an MOI of 20-40 for infection of HEp2-cells or 5-10 for infection of A549-cells. MOI was determined by counting the cells in technical triplicates and by plating the bacteria in serial dilutions in technical duplicates. Plates were incubated overnight at 37°C. The following day, colonies were counted.

For infection the cells were washed twice with 'infection medium'. Then the 'infection medium' containing the respective strain was added. Additionally, the substances/extracts to be tested were added to the respective wells in the same concentrations/amounts as described above. Then the cells were incubated for 2 h at 37°C and 5 % CO_2. To stop the infection the cells were washed twice with PBS and fixed with 1 % paraformaldehyde overnight at 4°C.

Table 2-8: Concentrations of compounds and amounts of extracts used in invasion assays.

name of extract/compound	amount/final concentration per well
Soce554	2.5 µl
Soce923	2.5 µl
fractions of Soce554	2.5 µl
fractions of Soce923	2.5 µl
disorazole A	0.001-5 µg/ml
disorazole Z	0.001-5 µg/ml
tubulysin A	0.5-250 ng/ml
vinblastine	0.5-250 ng/ml

Modified invasion assay with different pre-incubation strategies of substances

The assay was performed as described above with the following modifications: Both streptococcal strains (A40 and A8) were grown overnight at 37°C in TSB medium as described above or were supplemented with 2.5 µg/ml disorazole Z. Additionally, cells that were infected with *S.pyogenes* strains A40 or A8 were treated as described above. Cells that were infected with *S.pyogenes* strains supplemented with disorazole Z during cultivation were not treated. Infection was performed as described above. After addition of the bacteria, cells were incubated for 2 h at 37°C and 5 % CO_2 before being washed twice with PBS and fixed with 1 % paraformaldehyde as described above.

2.3.1.2 Invasion assay with lactococci

The assay was performed as described in section 2.3.1.1. In addition to the *S.pyogenes* strains A40 and A8, cells were infected with either *L.lactis* (Lac) or *L.lactis* expressing SfbI (Lac-SfbI). Therefore, both lactococcal strains were inoculated one day before infection in M17 medium and incubated overnight at 30°C. Lac-SfbI was supplemented with 3 µg/ml erythromycin to assure that only lactococci expressing SfbI grow (vide 2.1.2.1). Cells were treated with 2.5 µg/ml disorazole A or Z 30 min prior and during infection. Infection and fixation were performed as described in section 2.3.1.1.

2.3.1.3 Quantification of intracellular viable bacteria (survival assay)

The assay was performed as described above in section 2.3.1.1. Concentrations of tested compounds (disorazole A and Z, tubulysin A and vinblastine) are indicated in tab. 2-8. Cells were not seeded onto glass coverslips. After 2 h of infection, the medium was removed and 'infection medium' (vide 2.1.1) containing penicillin and gentamicin was added to the cells to kill extracellular streptococci or lactococci. The concentration of penicillin per well was 50 µg/ml whereas the one of gentamicin was 100 µg/ml. The cells were incubated for further 2 h at 37°C and 5 % CO_2. Then they were washed twice with 'infection medium' before being detached by adding 100 µl trypsin per well for 5 min at 37°C and 5 % CO_2. Then 400 µl/well of a 1 % saponin solution were added to lyse the cells and release the remaining intracellular bacteria. The cells were incubated for 20 min at 37°C and 5 % CO_2. Afterwards, the intracellular bacteria were plated on agar plates in serial dilutions in technical replicates (THY agar for streptococci and M17 agar for lactococci) and incubated overnight at 37°C. The following day, the colonies were counted to determine the amount of intracellular viable bacteria. Data were indicated in % as intracellular survival of group A streptococci in comparison to the untreated control (infected cells were treated with methanol only).

2.3.1.4 (Double-)Immunofluorescence staining and microscopic analysis

Tab. 2-9 shows the antibodies that were used for immunofluorescence staining. Antibodies were diluted in PBS containing 10 % FCS.

Table 2-9: Antibodies used for immunofluorescence staining.

antibody	additional information
Rabbit anti-*S.pyogenes* serum, polyclonal anti-GAS	dilution 1:100 (Molinari *et al.*, 1997)
Rabbit anti-*Lactococcus lactis* serum	dilution 1:100; kindly provided by Dr. Susanne Talay (HZI, Braunschweig)
Alexa Fluor ®488 anti-human CD29 antibody	dilution, against human β_1-integrin; BioLegend
Mouse anti-α-tubulin, polyclonal antibody	diluted 1:100; Sigma Aldrich
Mouse anti-vinculin, clone hVIN-1, monoclonal antibody	diluted 1:100; Sigma Aldrich
Mouse anti-ezrin/p81/80K/Cytovillin AB-1, Clone 3C12, monoclonal antibody	diluted 1:100; Thermo Scientific
Alexa Fluor ®488 phalloidin	dilution 1:100; Invitrogen
Alexa Fluor ®488 goat anti-rabbit IgG (H+L)	dilution 1:200; Invitrogen
Alexa Fluor ®568 goat anti-rabbit IgG (H+L)	dilution 1:300; Invitrogen
Alexa Fluor ®488 goat anti-mouse IgG (H+L)	dilution 1:200; Invitrogen

Fluorescence microscopic analysis was performed by using the following two fluorescence microscopes and software: (a) Zeiss Axiophot fluorescence microscope with a Zeiss AxioCam HRc digital camera and Zeiss Axiovision software 4.8; (b) Zeiss AxioImager A2 with a Zeiss AxioCam MRm camera and Zen 2011 software.

Double-immunofluorescence staining of extra- and intracellular streptococci and of actin or tubulin

For double-immunofluorescence staining, coverslips were removed from the 24well-plate. Coverslips were washed twice with PBS before and after the staining procedure and between the different steps of staining. The staining procedure was started by incubating the coverslips first with a primary antibody against GAS for 1.5 h, followed by a secondary Alexa Fluor®488 goat anti-rabbit antibody for 30 min. Permeabilization was performed by incubation with Triton X-100 0.1 % for 5 min. Afterwards, coverslips were incubated with the same primary antibody as described above for 1.5 h, followed by a secondary Alexa Fluor®568 goat anti-rabbit IgG antibody for 45 min. Finally, the cells were stained with phalloidin-Alexa-488 antibody for 30 min to visualize the actin cytoskeleton. For staining of tubulin instead of actin, coverslips were incubated with a mouse anti-α-tubulin antibody for 30 min, followed by a secondary Alexa Fluor®488 goat anti-mouse antibody for 30 min. The coverslips were mounted into ProLong® gold antifade reagent on microscope slides. The mounting medium was allowed to solidify overnight at room temperature. The following day the coverslips on the

microscope slides were sealed with nail polish. Then they were stored at 4°C in the dark until fluorescence microscopic analysis.
Samples were analyzed by a fluorescence microscope to determine intracellular and extracellular streptococci or to examine the integrity of the actin cytoskeleton or the tubulin matrix.

Double-immunofluorescence staining of extra- and intracellular lactococci and of actin

Double-immunofluorescence staining of extra- and intracellular lactococci and of actin was done analogously to the one of streptococci (as described above). Instead of using an anti-GAS antibody, the rabbit anti-*Lactococcus lactis* serum was used. Coverslips were incubated with this serum for 1 h.

Immunofluorescence staining of streptococci and of vinculin, ezrin or β_1-integrin

To reduce non-specific background a modified method for fixation of cells compared to the one described in section 2.3.1.1 was used. The fixation was performed analogously to Stradal *et al.*, 2003. Briefly, after 2 h of infection cells were washed once with pre-warmed 'infection medium' (vide 2.1.1). Then a 4 % paraformaldehyde solution was added and the cells were incubated at room temperature for 20 min. Afterwards, a 4 % paraformaldehyde solution containing 0.1 % Triton X-100 was added for 5 min. Cells were washed three times with pre-warmed PBS before fixation with 4 % paraformaldehyde at 4°C overnight.
In general, the staining procedures for vinculin, ezrin or β_1-integrin and streptococci were similar to those described above (vide 'double-immunofluorescence staining of extra- and intracellular streptococci and of actin or tubulin'). Though, different antibodies and incubation times were used:
Cells that were stained for vinculin or ezrin were incubated for 1 h with an anti-vinculin or an anti-ezrin antibody, respectively, followed by an Alexa Fluor® 488 goat anti-mouse IgG antibody for 30 min. After permeabilization with Triton X-100 0.1 % for 5 min, cells were incubated with an anti-GAS antibody for 1.5 h. Before mounting the coverslips, they were stained with an Alexa Fluor® 568 goat anti-rabbit antibody for 35 min.
Staining for β_1-integrin was performed analogously to the one for ezrin or vinculin. Instead of using an anti-ezrin or anti-vinculin antibody, an Alexa Fluor® 488 anti-human CD29 antibody was added to the cells for 30 min.

2.3.1.5 Field emission scanning electron microscopic (FESEM) analysis

For FESEM a different fixation method was used compared to the one described in section 2.3.1.1: Prior to fixation, cells were washed twice with pre-warmed 'infection medium' (vide 2.1.1). Cells were fixed in a solution containing 2 % glutaraldehyde and 5 % paraformaldehyde in cacodylate buffer (0.1 M cacodylate, 0.09 M sucrose, 0.01 M calcium chloride, 0.01 M magnesium chloride,

pH 6.9) for at least 1 h at 4°C. Processing of samples was done by Ina Schleicher in the Central facility for Microscopy (ZEIM, HZI) as described in Rohde *et al.*, 2003. SEM images were recorded by Prof. Dr. Manfred Rohde on a Zeiss field emission scanning electron microscope DSM992 Gemini at an acceleration voltage of 5kV.

2.3.2 MTT assays

MTT is used to measure viability of cells. Upon addition of MTT (yellow colored), it is converted to a dark blue, water-insoluble MTT formazan by mitochondrial dehydrogenase. Acidified isopropanol solubilizes the blue crystals which can be measured colorimetrically (Mosmann, 1983).
Two different MTT assays were used: the first one was performed to assess cytotoxicity of compounds when cells were treated for 24 h whereas the second one determined cytotoxicity under infection conditions.

MTT assay to test cytotoxicity

HEp2-cells were seeded into a 24well-plate as described in section 2.3.1.1. They were incubated at 37°C and 5% CO_2 for approximately 24 h until they reached 80-90 % confluence. Then the cells were incubated with disorazole A or Z or were left untreated for 24 h at 37°C and 5 % CO_2. Disorazole A and Z were tested in the following concentrations: 2.5 µg/ml and 0.01 µg/ml. Untreated cells, pure medium and completely damaged cells served as controls. To damage cells, they were treated with 0.5 % Triton X-100 1 h prior to addition of MTT.
After 24 h of incubation with the compounds, MTT diluted in PBS (stock solution 5 mg/ml) was added to the wells at a final concentration of 1 mg/ml. The cells were incubated for 4 h at 37°C and 5 % CO_2. Afterwards, the medium was removed and 0.04 M HCl in 2-propanol was added. The cells were incubated at room temperature for 15 min. Then the supernatant was transferred to a 96well-plate. The samples were measured at 560 nm and at 670 nm as a reference wavelength on a Tecan Sunrise ELISAReader using Magellan software. Data was normalized using the following formula: (A-B)/(C-B) with ‘A’ as the respective data point, ‘B’ as the value of the uninfected Triton X-100-treated control and ‘C’ as the untreated and uninfected control.

Modified MTT assay to test cytotoxicity under infection conditions

HEp2-cells were seeded, treated with disorazole A and Z and infected with *S.pyogenes* strains A40 and A8 as described in section 2.3.1.1. For treated cells, the respective disorazole was added in final concentrations of 2.5 and 0.01 µg/ml. In addition, cells were left uninfected and untreated. At the end of the infection time, cells were washed twice with ‘infection medium’ (vide 2.1.1). Then MTT

diluted in PBS (stock solution 5 mg/ml) was added to the wells as described above. The same controls as in the original MTT assay (see above) were used. After addition of MTT, the assay was continued as described for the abovementioned MTT assay (vide 'MTT assay to test cytotoxicity').

2.3.3 Antimicrobial testing

The MIC of disorazole Z was tested against the *S.pyogenes* strains A40 and A8. Therefore, the streptococcal strains A40 and A8 were grown in THY medium at 37°C and 5 % CO_2 until OD 0.6. 300 µl of the respective strain was diluted in 20 ml THY medium ('streptococcus-medium mixture'). MIC tests were conducted in 96-well microtiter well plates in THY medium analogously as described by Okanya *et al.*, 2011. Briefly, 3 µl of disorazole Z (concentration stock solution in methanol: 1 mg/ml) were pipetted into the first row (A) of the plate. Negative controls were left blank. Using a multichannel pipet, 150 µl of the 'streptococcus-medium-mixture' (as described above) were aliquoted into all rows. To the first row, additional 150 µl of the 'streptococcus-medium mixture' were added and mixed by repeated pipetting before transferring the same amount to the second row. A 1:1 serial dilution was done in the subsequent rows, and 150 µl discarded after the last row (H). The plates were incubated for 24 h at 37°C and 5 % CO_2. The lowest concentration of disorazole Z preventing visible growth of the respective streptococcal strain was determined as the MIC. The concentrations tested ranged from 0.078 µg/ml to 10 µg/ml.

In addition, streptococci (strains A40 and A8) were inoculated in liquid culture (TSB medium) and were not supplemented or supplemented with 2.5 µg/ml disorazole Z and incubated at 37°C and 5 % CO_2 for 8 h. Then bacteria were plated in serial dilutions and plates were incubated at 37°C and 5 % CO_2 overnight. The following day, colonies were counted.

2.4 Methods used to identify inhibitors of plasmin(ogen)

2.4.1 Fermentation of the myxobacterial strain 706

Extract kinetic prior to fermentation

Prior to fermentation of the myxobacterial strain 706 an extract kinetic was run to assess the optimal time point for harvest. Therefore, the strain 706 was inoculated in 1:10 in 100 ml Pol medium containing 1 % Amberlite XAD-16 adsorber resin in 4x250 ml flasks at 30°C and 180 rpm. After three, six, eight and ten days an extract was prepared of each flask as described in section 2.2.1.3. The extract was tested in a plasminogen activation assay to assess its activity (vide 2.4.3).

Fermentation of the myxobacterial strain 706

The strain 706 was cultivated in 100 ml of Cy/H medium in a 250 ml flask at 30°C and 180 rpm. For production of metabolites, it was inoculated 1:10 in 1 l of Pol medium in 10x2.5 l flasks at 30°C and 180 rpm. The strain 706 was cultivated in a fermenter in 70 l of Pol medium with Amberlite XAD-16 adsorber resin at 30°C and 170 rpm. The fermenter was inoculated with 10 l of culture of the strain 706. Every day samples of 100 ml were taken for analysis of activity. An extract was prepared from every sample as described in section 2.2.1.3. As daily sampling did not yield in equal amounts of XAD, the content of the different extracts was always normalized to 100 g of total weight (liquid culture containing XAD; e.g. sample of day 8 only had 86.5 g of total weight, for the plasminogen activation assay a correction factor of 1.15 (as a result of 100g/86.5g) was used). The extract was tested in the plasminogen activation assay in concentrations ranging from 0.05-2 % (vide 2.4.3). The fermenter was harvested on day 9. Then, the XAD extract was purified (vide 2.4.2). Fermentation was done in cooperation with Reinhard Sterlinski and Steffen Bernecker (MWIS, HZI).

2.4.2 Purification and structure elucidation of products obtained by fermentation

2.4.2.1 Purification of compounds via LH-20 gel chromatography, RP-MPLC and Si-flash-LC

Fig. 2-1 shows the purification process of the XAD extract obtained by fermentation of strain 706 schematically.

588 g of Amberlite XAD-16 adsorber resin and some residual cells were extracted in a column with 2.5 l acetone. The acetone was evaporated by using a rotavapor (Heidolph). The residue was dissolved in H_2O and extracted three times with ethyl acetate. The ethyl acetate fraction (RC 22; 5.2 g) was evaporated. Before proceeding with further purification RC 22 and the H_2O were tested for biological activity in a plasminogen activation assay (vide 2.4.3).

Then RC 22 was dissolved in methanol containing 5 % H_2O and extracted three times with n-heptane. The methanol-phase was termed RC 23. Fraction RC 23 (2.6 g) was evaporated and dissolved in methanol. The extracted n-heptane fraction (RC 24; 2.4 g) was evaporated as well. For testing biological activity RC 24 was dissolved in methanol. Afterwards, RC 23 and RC 24 were tested for biological activity in a plasminogen activation assay (vide 2.4.3).

RC 23 (dissolved in methanol containing 5 % H_2O) was separated by Sephadex LH-20 chromatography (column 7 x 60 cm; flow 5.8 ml/min; UV detection 254 nm, solvent: 95 % methanol, 5 % H_2O). Fractions (RC 23.x, with x = fraction number) were collected for peaks, shoulders, valleys and baseline of the chromatogram and were tested for biological activity in a plasminogen activation assay (vide 2.4.3).

RC 24 (dissolved in dichloromethane) was separated by Si-Flash chromatography using a Grace Reveleris system (column Reveleris Silica 40 g; solvent A dichloromethane; solvent B acetone; gradient: 4% B A for 1 min, 4-10 % B for 20 min, 10 % B for 10 min, 10-100 % B for 10 min, 100 % B for 25 min; flow 15 ml/min; UV detection 210 nm, 254 nm, 280 nm; ELSD detection (ELSD threshold 5 mV, sensitivity low)). Fractions (RC 24.x, with x = fraction number) were collected for peaks, shoulders, valleys and baseline. Fractions were evaporated, dissolved in methanol and then tested for biological activity in a plasminogen activation assay (vide 2.4.3).

1 g of the fraction RC 23.8 dissolved in methanol was separated by RP-MPLC (column 480 x 30 mm; Nucleodur C_{18} (Macherey-Nagel); solvent A: 50 % H_2O/50 % MeOH + 5% HCOOH; solvent B: 100% MeOH + 5% HCOOH; gradient: 75% B for 50 min, 75-100 % B for 5 min; 100 % B for 30 min; flow 30 ml/min; UV detection 205 nm). Fractions (RC 25.x, with x = fraction number) were collected for peaks, shoulders and valleys of the chromatogram. Fractions were evaporated, dissolved in methanol and then tested for biological activity in a plasminogen activation assay (vide 2.4.3).

For further purification RC 25.1 and RC 25.3 were separated by Si-Flash chromatography using a Grace Reveleris system (column Reveleris Silica HP 4 g (20 µm); solvent A dichloromethane; solvent B acetone; gradient: 100 % A for 4 min, 0-5 % B for 10 min, 5 % B for 5 min, 5-100 % B for 10 min, 100 % B for 25 min; flow 15 ml/min; UV detection 210 nm, 220 nm, 254 nm; ELSD detection (ELSD threshold 5 mV, sensitivity low)). Fractions were collected for peaks, shoulders, valleys and baseline. Fractions were evaporated, dissolved in methanol and then tested for biological activity in a plasminogen activation assay (vide 2.4.3). Fractions obtained from RC 25.1 were termed RC 26.x (with x = fraction number) and those from RC 25.3 RC 27.x (with x = fraction number). Active fractions of RC 26 and RC 27 were united in correlation with the data from the plasminogen activation assay and termed RC 28.1-RC 28.5.

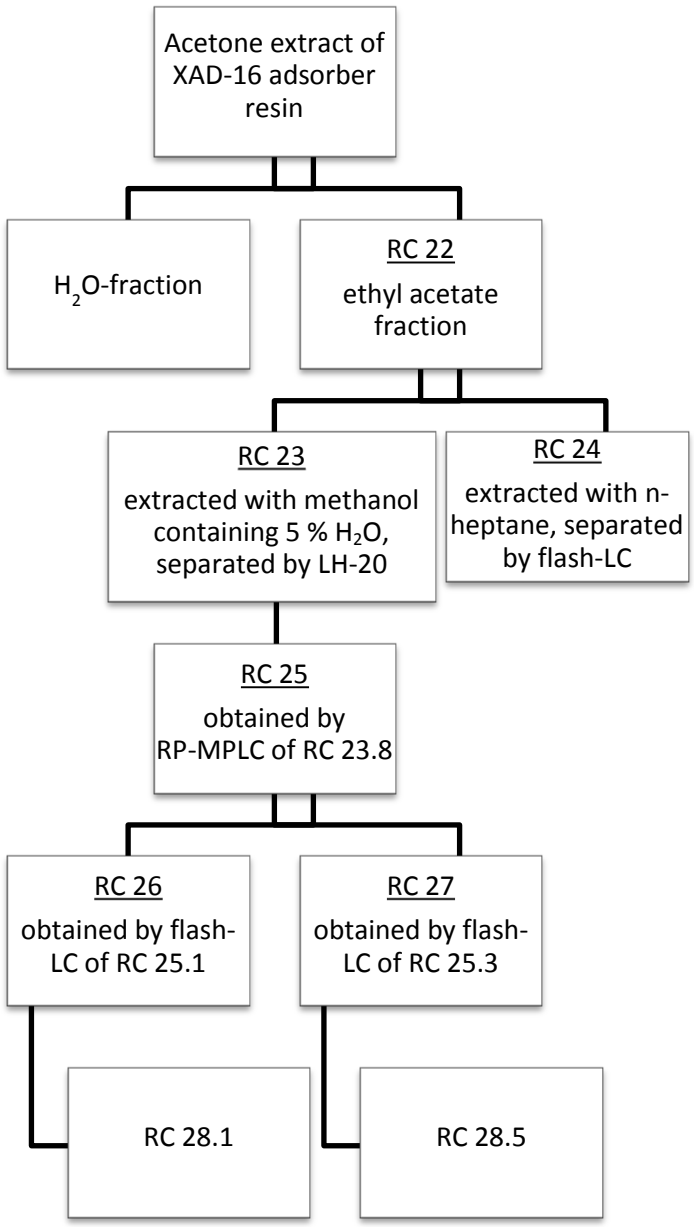

Figure 2-1: Scheme of the purification process of the XAD obtained by fermentation of the strain 706.
The figure displays the names of the respective fractions and by which methods they were obtained.

In addition, RC 23.8 was separated a second time by RP-MPLC (using the same conditions as described above). The fractions were termed RC 33.x (with x = fraction number) and tested in a plasminogen activation assay (vide 2.4.3).

RC 33.1 and RC 33.3 were identical to RC 25.1 and RC 25.3. These two fractions (RC 33.1 and RC 33.3) were separated by Si-flash-LC using the same conditions as described for RC 25.1 and RC 25.3. The fractions obtained from RC 33.1 were termed RC 34.x (with x = fraction number) and those obtained from RC 33.3 were termed RC 35.x (with x = fraction number). Active fractions of RC 34 and RC 35 were united in correlation with the data from the plasminogen activation assay and termed RC 36.1 and RC 36.2.

2.4.2.2 Structure elucidation via NMR and HR-ESIMS

^{1}H and ^{13}C NMR spectra of RC 28.1 and RC 28.5 in $CDCl_3$ were recorded on a Bruker Avance 700 MHz spectrometer, locked to the deuterium signal of the solvent. Chemical shifts are given in parts per million (ppm) and coupling constants in Hz. NMR spectra are displayed in section 8.1, fig. 8-1. NMR data are given in section 3.3, tab. 3.3-2 and 3.3-3.

HR-ESIMS data of RC 28.1 and RC 28.5 were recorded on a Maxis ESI TOF mass spectrometer (Bruker Daltonics). Molecular formulas were calculated including the isotopic pattern (Smart Formula algorithm).

2.4.2.3 Methods for location of double bond(s) via GC-MS

GC-MS spectra were recorded on a Trace GC Ultra (Thermo Scientific) equipped with a split/splitless injector coupled to an ITQ 900 (Thermo Scientific; Ion Trap). 1 µl of each sample was injected in split mode using a PAL Combi-XT autosampler. Base temperature of the injector was 275°C with a split flow of 10 ml/min. Helium was used as carrier gas with a flow of 1 ml/min. A TraceGOLD^{TM} TG-5MS column was used (30mx0.25mmx0.25µm, Thermo Scientific).

Mass spectrometric conditions were as follows: The source temperature was held at 200°C during GC-MS runs. The mass selective detector was operated in full scan mode with positive polarity; spectra were acquired in the range of *m/z* 40-700; maximal ion time was 25 ms. Scan control, data acquisition and processing were performed with XCalibur Software (Thermo Scientific).

Derivatization with diazomethane

To obtain diazomethane 1.5 ml of 37 % KOH was added slowly to a mixture of diazald (367 mg, Sigma Aldrich) and carbitol (1 mg, Sigma Aldrich) in the inner tube of a diazomethane generator apparatus (Sigma Aldrich) at 0°C. The outer tube contained 3 ml of diethyl ether. The reaction was run for 50 min. During the reaction the generator apparatus was swung occasionally. When the reaction was terminated, the diazomethane was dissolved in the diethyl ether of the outer tube. Remaining diazomethane was destroyed by adding glacial acetic acid to the outer and the inner tube.

For preparation of methyl esters, diazomethane was added slowly to the samples (RC 28.1 and RC 28.5) dissolved in diethyl ether. Samples were swung for 20 min at room temperature. Then solvents were evaporated under nitrogen flow and samples were dissolved in n-hexane. In addition, a blank sample was prepared as well. Samples were analyzed by GC-MS using the following gradient: 130°C as initial temperature for 2.5 min, 130-240°C ramped with 5 degrees/min, 240-325°C ramped with 30 degrees/min, 325°C held for 5 min.

Derivatization with DMDS

To locate the double bond within the fatty acids, the methyl esters of samples (as described in the preceding paragraph) were dissolved in 50 µl n-hexane and treated with 100 µl dimethyl disulfide (DMDS) and 5 µl of iodine in diethyl ether (60 mg iodine in 1 ml diethyl ether; diethyl ether filtered over Al_2O_3) at 60°C for 8 h. The reaction was terminated by adding 100 µl of 20 % aqueous solution of $Na_2S_2O_3$. The n-hexane phase was separated and the aqueous phase was extracted a second time with 100 µl of n-hexane. Both n-hexane phases were united and dried under nitrogen flow at 40°C. Then each sample was redissolved in 100 µl of n-hexane. In addition, a blank sample was prepared

according to those of the fatty acids. Then all samples were analyzed by GC-MS using the same gradient as the one for methyl ester derivatives (as described in 'Derivatization with diazomethane').

Derivatization with 2-amino-2-methyl-propan-1-ol

Fatty acids (RC 36.1, RC 36.2, LEA, LA, PEA and PA) were treated with 20 µl thionyl chloride for 10 min at 100°C to generate the acid chlorides and dried under nitrogen flow at 40°C. Under cooling to 0°C 500 µl of a freshly prepared solution of 2-amino-2-methyl-propan-1-ol in dichloromethane (10 mg/ml) were added to each sample. Then samples were left on ice for 1 h. Afterwards, they were kept at room temperature for 1 h before they were dried under nitrogen flow at 40°C. 500 µl of trifluoro acetic anhydride were added to each sample. After 3 h at room temperature, they were dried under nitrogen flow at 40°C. Samples were dissolved in 2.14 ml iso-hexane and 0.86 ml water. The organic layer was transferred into a new vial. The water phase of each sample was extracted two more times with iso-hexane. All organic phases were united in a new vial and the solvent was evaporated under nitrogen flow at 40°C. Samples were redissolved in 100 µl of iso-hexane and analyzed by GC-MS using the following gradient: 80°C as initial temperature for 3 min, 80-180°C ramped with 20 degrees/min, 180-280°C ramped with 2 degrees/min, 280°C held for 15 min, 280-325°C ramped with 5 degrees/min, 325°C held for 5 min.

2.4.3 Plasminogen activation assays

(Standard) Plasminogen activation assay with culture supernatants of cluster 2a type streptokinase

To determine if compounds or extracts are able to interfere with plasminogen activation, supernatants of overnight cultures of group A streptococcal strains A614 or AP1 (in THY medium) were used as both secrete cluster 2a type streptokinase. The strain AP1 was used in addition to the strain A614. The assay was performed in a 96well-plate. 75 µl of the respective supernatant were used per well. Then the desired amount of substance or extract to be tested was added (for standard screening purposes 1 µl of extract or of substance; for concentrations of other substances see tab. 2-10). 69 µl PBS, 5 µl S-2251 (10 mM stock solution) and 1 µl plasminogen (1 mg/ml stock solution) were added per well to start the reaction. The assay was run at 37°C. The absorption was measured at the beginning of the reaction and then every hour at 405 nm after 3 sec of shaking on a Tecan Sunrise ELISAReader using Magellan software. The reaction was finished when untreated samples had reached an OD_{405nm} of about 1.

For the standard plasminogen activation assay culture supernatants of the strain A614 were used. Data are displayed in % of the untreated control.

Plasminogen activation assay with culture supernatants of cluster 2b streptokinase

The assay was conducted as described above with the following modifications: Briefly, 75 µl of the culture supernatant of the *S.pyogenes* strain A314 were used. Then substances to be tested were added to the respective well (for concentrations see tab. 2-10). 61.2 µl PBS, 1 µl plasminogen (1 mg/ml stock solution), 5 µl S-2251 (10 mM stock solution) and 8.8 µl fibrinogen (17 µM stock solution; to obtain a final fibrinogen concentration of 1 µM per well) were added to each well to start the reaction. The assay was run and measured at the same conditions as described above.

Plasminogen activation assay with other activators of plasminogen

The assay was conducted as described above with the following modifications: 75 µl of PBS were used instead of culture supernatants. Then the respective activator of plasminogen was added: For urokinase as well as for tPA a final concentration of 1 µg/ml per well was employed. 2 µg/ml per well were used as final concentration for staphylokinase.

Table 2-10: Extracts, substances or fractions and their concentrations used in plasminogen activation assays.
The table displays the respective extract, substance or fractions that were used in plasminogen activation assays. The final concentrations or amount per well used in a plasminogen activation assay are indicated. In parenthesis the concentration/amount used for the assay with the respective activator is displayed.

extract/substance/fractions	amount/final concentration per well
EACA	0.5-1000 µM (cluster 2a and cluster 2b assays) 0.05-25 µM (uPA, tPA, staphylokinase)
TA	0.5-1000 µM (cluster 2a and cluster 2b) 0.05-25 µM (uPA, tPA, staphylokinase)
sAP01	2.5-100 µM (cluster 2a) 2.5-50 µM (cluster 2b, uPA, tPA, staphylokinase)
sAP02	5-50 µg/ml (cluster 2a)
sAP03	0.05-50 µg/ml (cluster 2a)
sAP04	0.5-25 µg/ml (cluster 2a)
sAP05	0.5-50 µg/ml (cluster 2a, uPA, tPA, staphylokinase)
RC 11.1	1.5 µl (cluster 2a)
RC 11.2	1.5 µl (cluster 2a)
RC 36.1	0.25-100 µg/ml (cluster 2a (A614)) 2.5-100 µg/ml (cluster 2a (AP1)) 0.25-50 µg/ml (cluster 2b) 5-100 µg/ml (uPA, tPA, staphylokinase)
RC 36.2	0.25-100 µg/ml (cluster 2a (A614)) 2.5-100 µg/ml (cluster 2a (AP1)) 0.25-50 µg/ml (cluster 2b) 5-100 µg/ml (uPA, tPA, staphylokinase)
LA	2.5-250 µg/ml (cluster 2a (AP1, A614))
LEA	2.5 -250 µg/ml (cluster 2a (AP1, A614)
PA	2.5-250 µg/ml (cluster 2a (AP1, A614))
PEA	2.5-250 µg/ml (cluster 2a (AP1, A614))

Ang852	2.5 µl (cluster 2a)
Anm9	2.5 µl (cluster 2a)
fractions of Anm9	2.5 µl (cluster 2a)
Cma13	2.5 µl (cluster 2a)
Pl6894	2.5 µl (cluster 2a)
PlD3	2.5 µl (cluster 2a)
Plvo18	2.5 µl (cluster 2a)
Plvt3	2.5 µl (cluster 2a)
Soce 997	2.5 µl (cluster 2a)
Soce712	2.5 µl (cluster 2a)
706 (extract kinetic)	1 µl (cluster 2a)
706 (fermenter kinetic)	0.05-2 % (standardized to amount of XAD; cluster 2a)
H_2O-phase	1 µl
ethyl acetate phase	1 µl
fractions of RC 23	1 µl
fractions of RC 24	1 µl
fractions of RC 25	1 µl
fractions of RC 26	1 µl
fractions of RC 27	1 µl

2.4.4 Clotting assay

To assess whether substances influence the entrapment of bacteria within clots, a 50 ml overnight culture (THY medium) of the *S.pyogenes* strains AP1 or A666 was centrifuged at 5000 rpm for 10 min. The supernatant was discarded and the pellet was washed twice in 12.9 mM sodium citrate buffer. Then the pellet was dissolved in 1 ml 12.9 mM sodium citrate buffer and the bacteria were adjusted to a transmission of 10 % at 600 nm. The suspension was diluted 1:100 in 12.9 mM sodium citrate buffer. For clot induction, 100 µl citrate plasma, 100 µl of the respective bacterial suspension and 50 µl thrombin were used. When clots were formed, 1 ml of 1 % plasma in 12.9 mM sodium citrate buffer was added to each sample. Then clots were left untreated or were treated with RC 11.1 or RC 11.2. For clots formed with *S.pyogenes* strain A666, a final concentration of 60 µg/ml was used for both substances (RC 11.1 and RC 11.2). For those formed with *S.pyogenes* strain AP1, a final concentration of 30 µg/ml was used. 50 µl of the supernatant of each sample were plated onto blood agar plates in serial dilutions at 0, 2, 4 and 6 h after clot induction. Blood agar plates were incubated at 37°C overnight. Colonies were counted the following day to assess the amount of bacteria which had escaped the clot. Data are displayed as $\log_{10}$ CFU of the respective strain per ml. Two independent experiments were performed. Standard deviations were calculated accordingly.
Citrate plasma was obtained from healthy volunteers who gave their informed consent.

2.4.5 Fibrinolysis assay

For a fibrinolysis assay a clot was induced first. Therefore, 50 µl of fibrinogen (17 µM stock solution), 25 µl 12.9 mM sodium citrate buffer and 1 µl thrombin were added. The clot was incubated 1 h at 37°C before 75 µl of 12.9 mM sodium citrate buffer were added. Then clots were treated with RC 36.1 or RC 36.2 (both conc.: 100 µg/ml), EACA (conc.: 100 µM), TA (conc.: 100 µM) or sAP01 (conc.: 10 µM) or were untreated and incubated for 1 h at 37°C. Then 2 µl of plasmin (1 mg/ml stock solution) were added to each clot. To assess changes in turbidity, clots were measured every 30 min at 405 nm on a Tecan Sunrise ELISAReader using Magellan software. Assays were run for 120 min (for untreated clots and those treated with EACA, TA and sAP01) and for 150 min (for untreated clots and those treated with RC 36.1 and RC 36.2).
Data was normalized to the respective data point at 0 min. Data are displayed as loss of OD in % of the respective clot in comparison to the respective control at the data point at 0 min.

2.4.6 Plasmin assay

To assess inhibition of plasmin activity, different concentrations of compounds (see tab. 2-11) were incubated with 0.6 % plasmin (stock solution 1 mg/ml) in PBS for 1 h at 37°C before 3.3 % of S-2251 (10 mM stock solution) were added. Untreated plasmin served as control. The absorption was measured at the beginning of the reaction and then every hour at 405 nm after 3 sec of shaking on a Tecan Sunrise ELISAReader using Magellan software. The reaction was finished when untreated samples had reached an OD_{405nm} of about 1. Data are displayed in % of the untreated control.

Table 2-11: Compounds and concentrations used in the plasmin assay.

compound	concentration
EACA	25-1000 µM
RC 36.1	2.5-100 µg/ml
RC 36.2	2.5-100 µg/ml
sAP01	2.5-50 µM
sAP05	5-50 µg/ml
TA	25-1000 µM

2.4.7 Toxicity assays

2.4.7.1 MTT assay

To assess cytotoxicity of salinimyxantins on HUVEC, two representatives (sAP01 and sAP03) were tested in an MTT assay. Therefore, a 24well-plate was prepared by adding 500 µl EGM with supplements in each well. HUVEC were detached as described in section 2.2.2.2. After resuspension in EGM with supplements, cells were counted in a Neubauer chamber. Approximately 30000 cells were seeded per well. They were incubated at 37°C and 5% CO_2 for approximately 24 h until they reached 70-80 % confluence. Before conducting an MTT assay fresh EGM with supplements was added. The cells were incubated with sAP01 or sAP03 or were left untreated for 24 h at 37°C and 5% CO_2. sAP01 and sAP03 were tested at the following concentrations: 5, 10, 25 and 50 µM. Untreated cells, pure medium and completely damaged cells (treated with Triton X-100 0.5 % 1 h prior to addition of MTT) served as controls. The assay was finalized as described in section 2.3.2.

2.4.7.2 in vivo toxicity test

Before substances are used in *in vivo* infection models, they have to be tested *in vivo* to assess possible (short-term) toxic effects (vide 2.4.8.1) according to the authorities. RC 25.1/RC 36.1 and RC 25.3/RC 36.2 were subjected for *in vivo* infection models. RC 11.1 as a pre-purified fraction was tested for toxicity *in vivo*. RC 11.1 is analogous to RC 25.1.

Therefore, huPlg negative transgenic C57Bl6/J mice (see below) were treated once with 50 µg of RC 11.1 s.c. (in 100 µl PBS) and were monitored for the next following 6 days. In a second trial, mice were treated on days 0, 1, 2, 3, 4, 5 and 6 with 50 µg of RC 11.1 s.c. (in 100 µl PBS) and were monitored for additional 3 days. For administration of RC 11.1, mice were anaesthetized with isoflurane. During the experiment mice were monitored for locomotion, behavior, appearance and weight. Mice were euthanized when they lost more than 20 % of weight.

2.4.8 Animal experiments

2.4.8.1 Bioethical statement

All animal experiments were performed in strict accordance with the guidelines of the European Convention for the “Protection of Vertebrate Animals used for Experimental and other Scientific purposes”, with “the Australian Code of Practice for the Care and Use of Animals for Scientific Purposes” and with the “Guidelines for the Care and Use of Laboratory Animals” (National Health and Medical Research Council, Australia). All experiments conducted in Germany were approved by

the ethical board of "Niedersächsisches Landesamt für Verbraucherschutz und Lebensmittelsicherheit", Oldenburg, Germany. All experiments conducted in Australia were approved by the University of Queensland Animal Ethics Committee, Brisbane, Australia.

2.4.8.2 Genotyping of huPlg transgenic mice

huPlg transgenic mice on a C57Bl6/J background (backcrossed at least 10 generations, Sun *et al.*, 2004) were bred in the animal facility at the HZI. To determine if mice were positive or negative for huPlg, genotyping via PCR was performed.

Therefore, tails of 3-4-week-old transgenic mice were obtained from the animal facility at the HZI. The ThermoScientific Animal Tissue Direct PCR kit (Thermo Scientific) with huPlg specific primers (tab. 2-12) was used for genotyping. Briefly, 20 µl of dilution buffer and 0.5 µl of DNA release additive were added to every tail. Then every sample was centrifuged at 15000 rpm for 1 min, mixed by vortexing and centrifuged again at 15000 rpm for 1 min. Samples were incubated for 5 min at room temperature, followed by incubation at 95°C for 2 min. Before transferring the supernatant into a new reaction tube, samples were centrifuged at 15000 rpm for 1 min.

The genotyping PCR was set up as follows:

2x Phire-PCR-buffer	10 µl
huPlg primer A (10 pmol/µl)	1 µl
huPlg primer B (10 pmol/µl)	1 µl
Phire-DNA-polymerase	0.4 µl
water	6.6 µl
supernatant of the respective sample	1 µl

The following thermal cycling conditions were used (the steps 2-4 were repeated 29 times):

(1) 98°C 5 min
(2) 98°C 20 sec
(3) 54°C 30 sec
(4) 72°C 45 sec
(5) 72°C 5 min
(6) 4°C hold

Afterwards, samples were run on an agarose gel by electrophoresis and stained with ethidium bromide as described in section 2.5.1. Mice were positive for huPlg when two bands were detected at 400 bp and 200 bp.

Tab. 2-12: Primers used for genotyping of huPlg transgenic mice

Primer	Sequence
huPlg primer A	5'-CAC CTC CCT GTG ATT GAG AA-3'
huPlg primer B	5'-GAA GTG TAC TCC TTG TAA AAT G-3'

2.4.8.3 in vivo model with S.pyogenes strain 5448

Eight- to twenty-week-old huPlg positive transgenic mice on a C57Bl6/J background (backcrossed at least 10 generations, Sun *et al.*, 2004) were infected with *S.pyogenes* strain 5448.

An overnight culture of the strain 5448 (in THY medium) was re-inoculated in fresh THY medium and grown until midlog phase (OD 0.4-0.6). Then the bacteria were centrifuged at 5000 rpm for 10 min and washed twice in PBS. They were resuspended in PBS and adjusted to an OD of 1.0. Bacteria were diluted to obtain 3-5x10^8 cfu/ml. The specific inoculum dose was administered in a 100 µl volume. The same culture was plated in serial dilutions on blood agar plates to determine the exact infection dose. The agar plates were incubated overnight at 37°C. The following day the colonies were counted and the infection dose was calculated.

Sex- and age-matched groups of C57Bl6/J huPlg positive transgenic mice were infected s.c. with 3-5x10^7 cfu of *S.pyogenes* strain 5448. Cohorts of 12-13 mice were used. Untreated mice received 100 µl PBS s.c. as a control on the day of infection and on day 2 after infection. Treated mice received either 50 µg of RC 25.1/RC 36.1 or RC 25.3/RC 36.2 s.c. (in a volume of 100 µl) on the day of infection and on day 2 after infection. For s.c. injection of bacteria or compounds, mice were anaesthetized with methoxyflurane (Australia) or isoflurane (Germany). During the experiment mice were monitored for locomotion, behavior, appearance and weight. Mice were euthanized when they lost more than 20 % of weight (German ethics) or when they reached a score of 3 for two of the following parameters: locomotion, appearance or behavior (Australian ethics). The experiment ended after 10 days.

2.4.8.4 in vivo model with S.pyogenes strain AP1

Eight- to sixteen-week-old huPlg positive transgenic mice on a C57Bl6/J background (backcrossed at least 10 generations, Sun *et al.*, 2004) were infected with *S.pyogenes* strain AP1.

The strain AP1 was prepared similarly to the one of 5448 (vide 2.4.8.3). After growth to midlog phase, washing with PBS and adjustment to an OD of 1.0, bacteria were diluted to obtain 1x10^8 cfu/ml. The specific inoculum dose was administered and determined as described in section 2.4.8.3.

Sex- and age-matched groups of C57Bl6/J huPlg positive transgenic mice were infected s.c. with 1x10^7 cfu of *S.pyogenes* strain AP1. Cohorts of 15-16 mice were used. Untreated mice received PBS s.c. as a control on the day of infection. Treated mice received either 50 µg of RC 25.1/RC 36.1 or RC 25.3/RC 36.2 s.c. on the day of infection. Mice were anaesthetized as described above. During the experiment mice were monitored as described above. The experiment ended after 7 days or after all mice had died.

2.5 Supplemental information

2.5.1. Cloning and analysis of the *ska* genes of *S.pyogenes* strains A614 and A666

For analysis of *ska* gene sequences of the *S.pyogenes* strains A614 and A666 and for generating recombinant streptokinase, the respective *ska* gene of these two strains was cloned into a pQe30-TEV vector. Stephanie Peter assisted in cloning recombinant streptokinase.

In detail, overnight cultures of the strains A614 and A666 (in THY medium) were centrifuged at 5000 rpm for 10 min. The supernatant was discarded and the pellet was resuspended in TE-buffer (from DNeasy blood and tissue kit, Qiagen) containing 10 % DNase-free RNase (10 µg/ml). The suspension was transferred to a vial filled with zirconium beads. Bacterial cells were lysed using a fastprep machine (MP Biomedical) twice for 30 sec at 4.0 m/sec. Then AL-buffer (from DNeasy blood and tissue kit, Qiagen) was added and beads were spun down for 30 sec. The lysate was transferred to a new reaction tube and proteinase K was added. The tube was inverted and incubated for 30 min at 56°C. Then 100 % ethanol was added and genomic DNA was isolated according to the protocol of the DNeasy blood and tissue kit (Qiagen).

After isolation of DNA an agarose gel electrophoresis was performed. Therefore, 2 µl of GeneRuler™ and 5 µl of each genomic DNA sample (mixed with 6x Orange DNA loading dye, Thermo Scientific) were loaded on a 1 % agarose gel. The gel was run at 90 V for 30 min and stained with ethidium bromide for 10 min afterwards. An image of the gel was taken by using a KodakImager.

Then a PCR (Mullis and Faloona, 1987) was performed to amplify the respective *ska* gene. Tab. 2-13 shows the sequences of the primers used in this reaction. The reaction was set up as follows:

Phusion Hot Start PCR buffer	5 µl
magnesium chloride 50 mM	2.5 µl
dNTPs	2 µl
ska_M1M6_rev (10 pmol/µl)	1 µl
ska_M6_fwd (for A614)/	
ska_M1_fwd (for A666)	1 µl
Phusion Polymerase	0.25 µl
respective DNA sample	2 µl
water	11.25 µl

The following thermal cycling conditions were used (the steps 2-4 were repeated 29 times):

(1) 98°C 30 sec
(2) 98°C 10 sec
(3) 65°C 30 sec
(4) 72°C 80 sec
(5) 72°C 7 min
(6) 4 °C hold

Then a gel electrophoresis was performed as described above to detect the 1500 bp PCR product, followed by PCR purification using a PCR clean-up, gel extraction kit (Machery-Nagel). Afterwards, the PCR products were digested using the restriction enzymes BamH1 and SaL1 for 3 h at 37°C. FastDigest® enzymes and reaction buffer (both from Fermentas) were used. The reaction was set up as follows:

10x fastDigest® restriction buffer	5 µl
BSA 1 mg/ml	5 µl
fastDigest® BamH1	1 µl
fastDigest® SaL1	1 µl
DNA sample	11 µl
water	27 µl

Then an agarose gel of the digested products was run as described above. The bands of each product were cut out of the gel using a scalpel and were purified using a PCR-clean-up, gel extraction kit (Macherey-Nagel).

The *E.coli* strain DH5α-pQe30-TEV was inoculated from a glycerol culture in LB-medium containing a final concentration of 100 µg/ml ampicillin and incubated at 180 rpm at 37°C overnight. The following day the pQe30-TEV vector was isolated using a QiaPrep Spin MiniPrep Kit (Qiagen). Then the vector was digested using the same digestion conditions as described above. After digestion, an agarose gel electrophoresis of the product was performed; the vector was cut out of the gel using a scalpel and was purified as described above.

The digested PCR products of the *ska* gene were ligated into the vector. The reaction was run for 16 h at 17°C and was set up as follows:

respective digested insert	6.6 µl
digested vector	2 µl
10x T4-DNA-ligase buffer	1 µl
T4-ligase	0.4 µl
ATP (from NewEnglandBiolabs)	0.3 µl

Ligation efficiency was checked by PCR. Therefore, two primers were used that anneal close to the restriction sites of the vector (for sequences see tab. 2-13). The reaction was set up as the one for PhusionPolymerase described above with the following primers: primer no. 94 and 96 (from the MMIK oligonucleotide collection). In addition, 2 µl of the vector containing the respective insert were used. Furthermore, similar thermal cycling conditions were employed as described above with the following modifications: an annealing temperature of 52°C and an elongation time of 210 sec were used.

After the PCR reaction, a gel electrophoresis was performed as described above to check for PCR products at 1500 bp. The PCR products were purified as described above. The concentration of the

PCR products was determined using a NanoDrop®. Sequences of the *ska* genes of the strains A614 and A666 were obtained from the sequencing facility of the HZI (Dr. Robert Geffers, GMAK). The sequence of the *ska* gene of the strain AP1 was obtained from Anne Fiebig (INI, HZI; (Fiebig *et al.*). *Ska* sequences of the strains A614, AP1 and A666 were analyzed using NCBI Blast (Camacho *et al.*, 2009) and BioEdit to determine the cluster type of streptokinase. Sequences were mapped against the streptokinase β-domains of the following streptococcal strains representing different cluster types of streptokinase using BioEdit:

NS414 (cluster 1), GenBank Accession No.: EU352621.1

5448 (cluster 2a), GenBank Accession No.: EU352628.1

NS59 (cluster 2b), GenBank Accession No.: EU352640.1

Table 2-13: Primers used for amplification of the *ska* gene

Primer	Sequence
94	5'-CCC GAA AAG TGC CAC CTG-'3
96	5'-GTT CTG AGG TCA TTA CTG G-'3
ska_M1_fwd (for A666)	5'-GCG GAT CCA TTG CTG GAT ATGGGT GG-'3
ska_M6_fwd (for A614)	5'-GCG GAT CCA TTG CTG GGT ATG GAT GG-'3
ska_M1M6_rev	5'-GCG TCG ACT TAT TTG TCT TTA GGG TTA TC-'3

2.5.2 Characterization of the *S.pyogenes* strain AP1 with regard to SpeB expression and the *covRS* gene

Characterization of the *S.pyogenes* strain AP1 with regard to SpeB expression

Overnight cultures of *S.pyogenes* strains AP1 and 5448 (in THY medium) were centrifuged at 5000 rpm for 10 min. The strain 5448 was used as control as it expresses SpeB (Aziz *et al.*, 2004). 5 ml of each supernatant were filtered through a 0.22 µm filter (Millipore) to remove residual GAS. 1 ml of 10 % trichloro acetic acid was added to 1 ml of supernatant. Every sample was prepared in duplicate. Samples were incubated on ice for 20 min. Then they were centrifuged at 13000 rpm for 15 min at room temperature. The supernatant was discarded and the pellet was washed with 1 ml ice-cold 100 % ethanol followed by centrifugation at 13000 rpm for 5 min at room temperature. The supernatant was discarded and the pellet was allowed to dry for 30 min at room temperature in a fume hood. The first pellet of each strain was resuspended in 40 µl of 100 mM Tris buffer (12.11 g Tris base, ad 100 ml distilled water, pH 7.6). Then these 40 µl were used to resuspend the second pellet of each strain. Prior to running an SDS-PAGE (Laemmli, 1970), 5x SDS-PAGE loading buffer was added to each sample and samples were incubated at 95°C for 10 min.

20 µl of each sample and 7 µl of an unstained SDS-PAGE ruler (Thermo Scientific) were loaded on an SDS-PAGE-gel (12 % resolving and 4 % stacking gel, see tab. 2-14). The gel was run at 100 V for 1.5 h.

Then it was stained with Coomassie staining solution (Coomassie Brilliant Blue R-250 2 g/l, methanol 40 %, acetic acid 10 %, ad 1 l distilled water): first, the gel was heated in a microwave until the solution started to boil, then it was incubated for 20 min on a shaker. Afterwards, the gel was destained with rapid destaining solution (methanol 40 %, acetic acid 10 %, ad 500 ml distilled water), heated in a microwave until the solution started to boil and was then incubated for 20 min on a shaker. The rapid destaining procedure was repeated with final destain (acetic acid 10 %, glycerol 4 %, ad 1 l distilled water). The gel was left in final destain overnight. The following day the gel was washed with water before images were taken.

Table 2-14: Composition for one SDS-PAGE 12 % resolving and 4 % stacking gel

12 % resolving gel	water	1.6 ml
	30 % acrylamide	2.0 ml
	1.5 M Tris (pH 8.8)	1.3 ml
	10 % SDS	0.05 ml
	10 % APS	0.05 ml
	TEMED	0.002 ml
4 % stacking gel	water	0.69 ml
	30 % acrylamide	0.17 ml
	1.0 M Tris (pH 6.8)	0.13 ml
	10 % SDS	0.01 ml
	10 % APS	0.01 ml
	TEMED	0.001 ml

Characterization of the *S.pyogenes* strain AP1 with regard to the *covRS* gene

Genomic DNA from an overnight culture of *S.pyogenes* strain AP1 in THY medium was extracted using DNAeasy blood and tissue kit (Macherey-Nagel). The PCR reaction was set up as follows for amplification of the whole *covRS* gene (primer sequences as described in Walker *et al.*, 2007):

dH_2O	29.5 µl
5x buffer	10 µl
dNTPs	4 µl
covRS primer 1 forward 1 µM	2.5 µl
covRS primer 12 reverse 1 µM	2.5 µl
$MgCl_2$ 50 mM	5 µl
Phusion HotStart Polymerase	0.5 µl
DNA template	1 µl

For amplification of only *covR* and *covS* the PCR reaction was set up identically. For *covR* the primers *covRS* primer 1 forward 1 µM and *covRS* primer 8 reverse 1 µM were employed whereas for *covS* the primers *covRS* primer 3 forward 1 µM and *covRS* primer 12 reverse 1 µM were used.

The following thermal cycling conditions were used (the steps 2-4 were repeated 29 times):

(1) 98°C 30 sec
(2) 98°C 10 sec
(3) 52°C 30 sec
(4) 72°C 2 min
(5) 72°C 5 min
(6) 4 °C hold

After the PCR a gel with 1 % agarose containing ethidium bromide was run. 5 µl of 'HyperLadder™' (Bioline) as a marker and 5 µl of each PCR product were used. The gel was run at 100 V for 30 min.
The PCR products were purified following the instructions of the Wizard SV Gel and PCR clean-up kit (Promega). The amount of DNA was measured using a NanoDrop® (Thermo Scientific). The DNA of each product was diluted to an amount of 30-50 ng/µl.
The sequencing reaction was set up as follows:

Primers 1 µM	4 µl
5x seq buffer	4 µl
BDTv3l	1 µl
H_2O up to	20 µl
Template PCR product	30-50 ng

5x seq buffer and BDTv3l were obtained from the sequencing department within the University of Queensland, Brisbane, Australia.

The following thermal cycling conditions were used (the steps 2-4 were repeated 24 times):

(1) 96°C 5 min
(2) 96°C 10 sec
(3) 50°C 10 sec
(4) 60°C 4 min
(5) 4°C hold

For the sequencing reaction the primers covRS primer 1 to 12 were used:

covRS:	primers 1-12
covR:	primers 1-8
covS:	primers 3-12

Samples were sequenced at the University of Queensland, Brisbane, Australia. Sequences were analyzed using BioEdit and NCBI blast (Camacho *et al.*, 2009). Sequences were aligned to the *covR* gene of SF370 and the *covRS* gene of MGAS 5005 (GenBank accession numbers: AE004092.2 and NC_007297.1).

3 Results

3.1 Inhibitors of group A streptococcal invasion

3.1.1 Screening reveals disorazoles as inhibitors of group A streptococcal invasion

About 300 myxobacterial extracts and 300 myxobacterial compounds were screened in a cell-based infection model for their properties to inhibit invasion of streptococci. Two different *S.pyogenes* strains were used representing two different invasion mechanisms: the strain A40 invades epithelial cells by formation of caveolae (SfbI-mediated) whereas the strain A8 invades epithelial cells via cytoskeletal rearrangements resulting in induction of membrane ruffling (Rohde and Chhatwal, 2013).

Several myxobacterial extracts were able to inhibit invasion. Invasion of both *S.pyogenes* strains A40 and A8 was inhibited when HEp2-cells were treated with a myxobacterial extract, in this case with the extract of Soce923: no intracellular streptococci were detected via double-immunofluorescence staining compared to the untreated and infected controls (fig. 3.1-1a-d). To validate this result, two inhibitory extracts (derived from Soce923 and Soce554) were replicated and tested again. In this case both extracts showed the same inhibitory properties as well (data not shown).

As a next step, these two extracts were fractionated via HPLC to assign the activity to a distinct peak. Double-immunofluorescence staining in combination with HPLC-fractionation of the extracts of Soce554 and Soce923 showed that the active compound was located within the fraction between 18.5 and 19 min (for Soce554) and 19 and 19.5 min (for Soce923), respectively: compared to the untreated control, HEp2-cells treated with these fractions did not bear intracellular streptococci (fig. 3.1-2a-d) and exhibited a similar inhibition of invasion as the crude extract (fig. 3.1-1a-d). In the HPLC-chromatogram of Soce923 a small peak was detected at 19.1 min (fig. 3.1-2e). Therefore, the activity was assigned to this peak.

Almost all extracts that showed activity were derived from *Sorangium cellulosum*. In the compound screening only disorazoles were active. The disorazoles are known to be present in several extracts of *Sorangium cellulosum* (Dr. Klaus Gerth, personal communication; data from the myxobase). Disorazoles usually elute around 18-19 min assuming that the same HPLC-conditions are used as in this study. In addition, disorazoles show a characteristic UV-spectrum (Irschik *et al.*, 1995). Such a characteristic UV-spectrum was observed at 19.1 min for the extract of the strain Soce923 (data not shown).

Figure 3.1-1: Screening reveals inhibitory properties of the extract of Soce923 with regard to group A streptococcal invasion.
If HEp2-cells were treated with the extract of Soce923 (b,d), invasion of *S.pyogenes* strain A40 as well as invasion of the strain A8 was hampered in contrast to untreated cells (a,c).
a-d: Double-immunofluorescence staining of HEp2-cells infected with *S.pyogenes*. red: intracellular streptococci, yellow: extracellular streptococci, green: actin cytoskeleton. a,b: cells were infected with *S.pyogenes* strain A40 for 2 h. c,d: cells were infected with *S.pyogenes* strain A8 for 2 h. a,c: cells were untreated. b,d: cells were treated with the extract of Soce923. All images were taken with 63x magnification on a Zeiss Axiophot Fluorescence microscope. The scale bar indicates 20 µm.

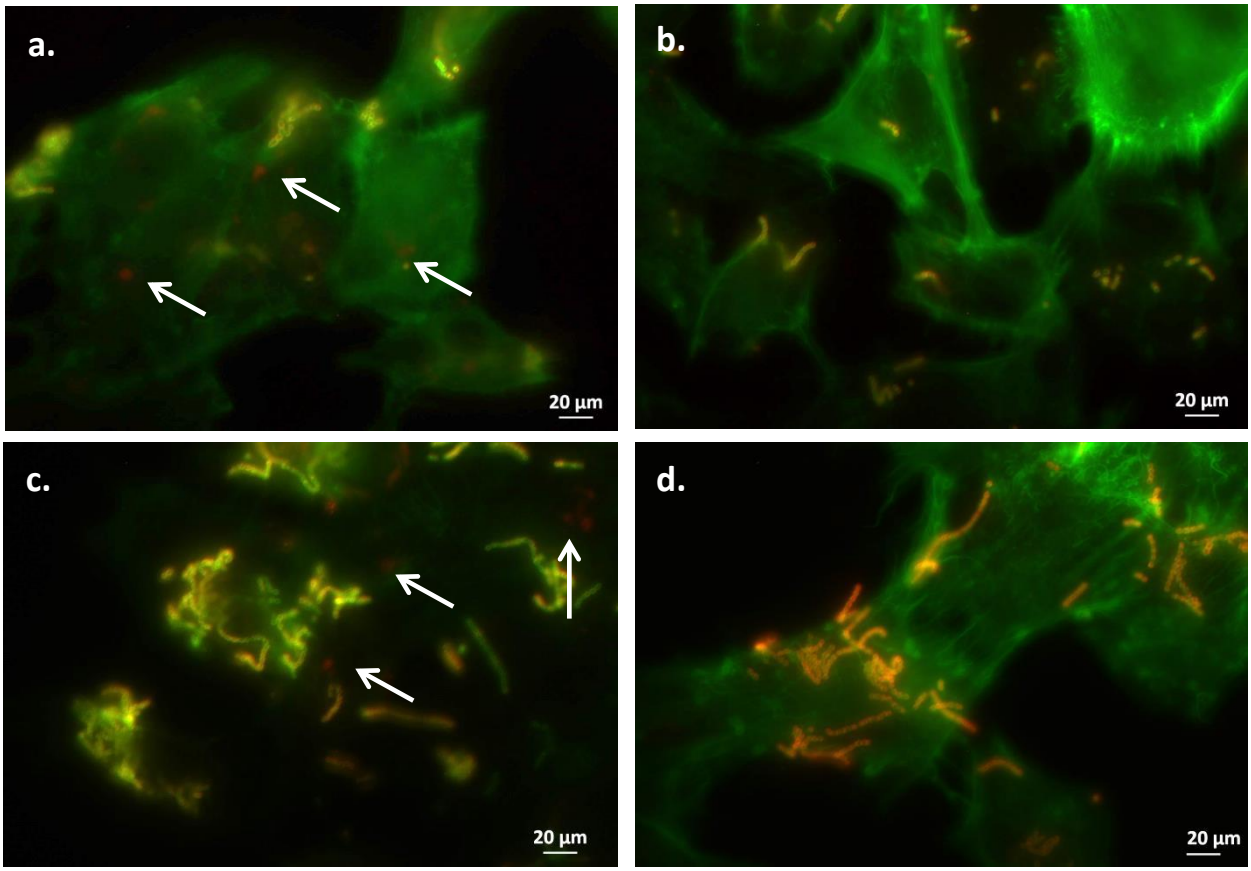

Therefore, it is most likely that disorazole is the active compound in every positively tested extract. It is described that disorazoles are highly cytotoxic (Jansen *et al.*, 1994). Surprisingly, HEp2-cells treated with extracts containing disorazoles did not show immediate toxicity. Slight alterations concerning the cell shape were detected. Though, these were also found in untreated and infected cells (fig. 3.1-1a-d).

Consequently, the disorazoles were characterized in more detail with regard to their cytotoxicity and their inhibitory properties.

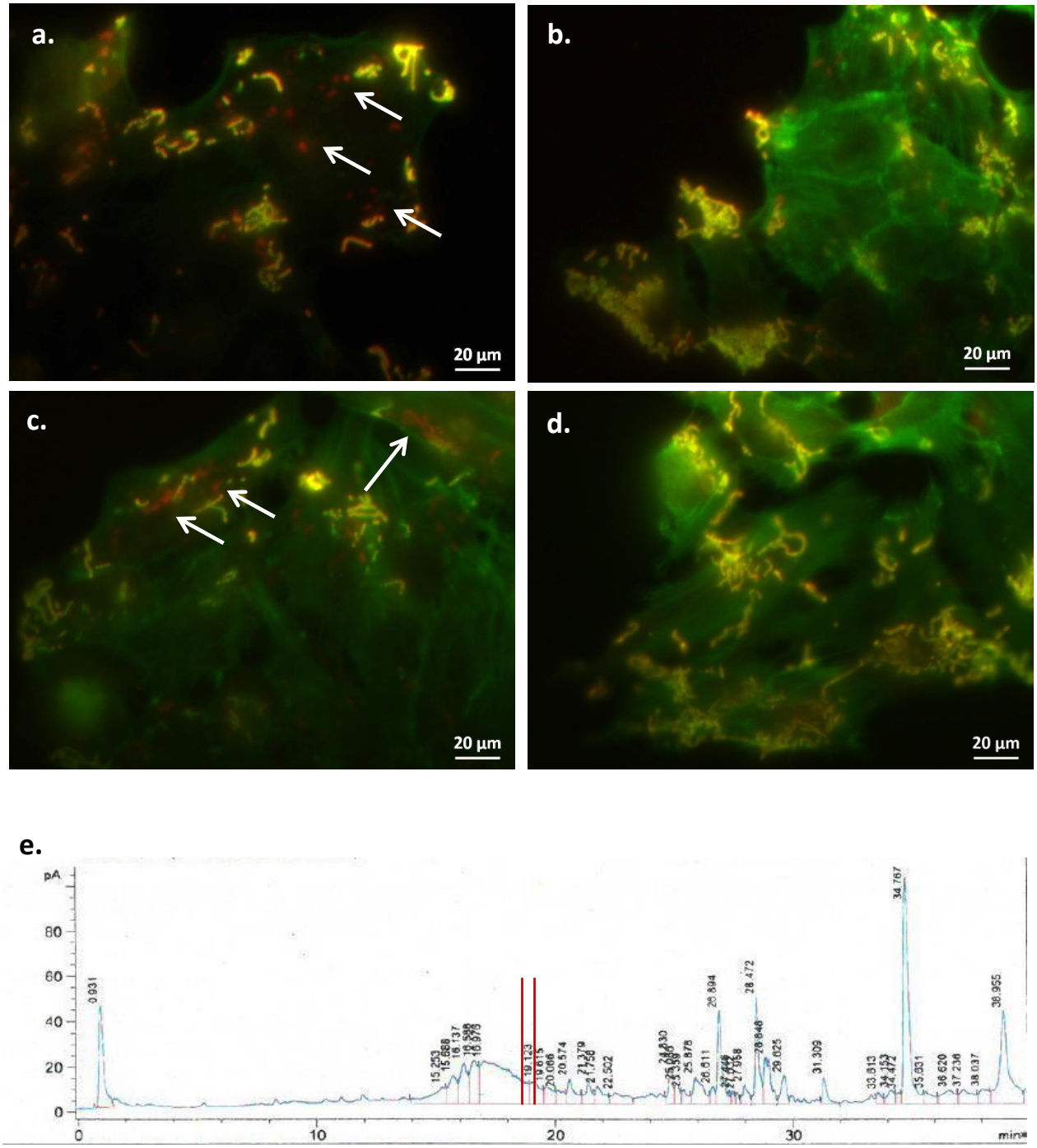

Figure 3.1-2: Combination of double-immunofluorescence staining with HPLC-fractionation reveals the active compound within the extract of Soce923.

The fraction at 19.0-19.5 min of the extract of Soce923 (b,d) inhibited invasion of both *S.pyogenes* strains A40 and A8 into HEp2-cells (a,c). The HPLC-chromatogram of the extract of Soce923 showed a small peak at 19.1 min. In correlation with the double-immunofluorescence images activity was assigned to that peak.

a-d: Double-immunofluorescence staining of HEp2-cells infected with *S.pyogenes*. red: intracellular streptococci, yellow: extracellular streptococci, green: actin cytoskeleton. a,b: cells were infected with *S.pyogenes* strain A40 for 2 h. c,d: cells were infected with *S.pyogenes* strain A8 for 2 h. a,c: cells were untreated. b,d: cells were treated with the fraction at 19.0-19.5 min of the extract of Soce923. All images were taken with 63x magnification on a Zeiss Axiophot Fluorescence microscope. The scale bar indicates 20 µm.

i: HPLC-chromatogram of the extract of Soce923. Peaks were detected with a Corona detector. The active fraction at 19.0-19.5 min is marked with two red bars.

3.1.2 Disorazoles inhibit invasion of *S.pyogenes* into epithelial cells mediated by cytoskeletal rearrangements

For further characterization purified disorazole A and Z were used (fig. 3.1-3). Both were obtained from Dr. Rolf Jansen (MWIS, HZI).

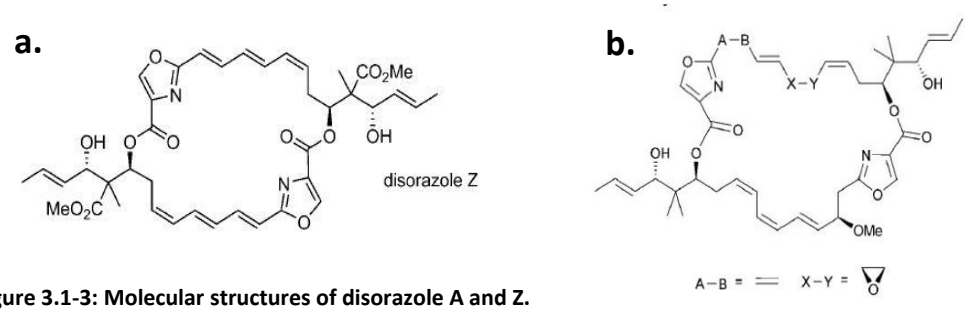

Figure 3.1-3: Molecular structures of disorazole A and Z.
Molecular structures of disorazole Z (a) and disorazole A (b). Adapted from Schäckel *et al.*, 2010 (Copyright © 2010, WILEY-VCH Verlag GmbH & Co. KGaA, Weinheim; reproduced with permission); Weissman and Müller, 2010 (Copyright © 2010, Royal Society of Chemistry; reproduced with permission).

The inhibitory potential of the disorazoles on the invasion pathway mediated by cytoskeletal rearrangements was assessed by performing infection experiments using the *S.pyogenes* strain A8. Disorazole A and Z were added to HEp2-cells 30 min prior to infection in a concentration of 2.5 µg/ml. Double-immunofluorescence pictures demonstrated clearly that nearly all streptococci were found extracellularly upon treatment with disorazoles. By contrast, untreated and infected cells showed intracellular and extracellular streptococci (fig. 3.1-4a-c). In addition, scanning electron microscopy (SEM) images confirmed these observations (fig. 3.1-4d-f). In untreated cells, intracellular streptococci were located right under the cell surface (white arrow; fig. 3.1-4d) whereas in treated cells, streptococci were only associated with the cell surface (fig. 3.1-4e,f). The double-immunofluorescence as well as the SEM pictures did not reveal immediate cytotoxic effects as the cells did not appear to be affected or entirely damaged. Nevertheless, treatment with disorazoles induced changes on the cell surface of HEp2-cells as less and shorter microvilli were detected (fig. 3.1-4f, white arrows).

Figure 3.1-4: Invasion of *S.pyogenes* strain A8 into HEp2-cells is inhibited by disorazoles.
a-g: HEp2-cells were infected with *S.pyogenes* strain A8 for 2 h. Disorazoles efficiently inhibited invasion.
a-f: Cells treated with disorazole A (b,e) or Z (c,f) showed almost no intracellular streptococci in comparison to untreated cells (a,d). a: White arrows indicate intracellular streptococci. d: A white arrow points to streptococci which have been taken up. e: A white arrow indicates streptococci that are not taken up. f: White arrows point to shorter microvilli.
g: Intracellular survival of GAS was determined in comparison to the untreated control (w/o-ctrl). The diagram shows that significantly less intracellular streptococci were found when cells were treated with disorazoles.
a-c: Double-immunofluorescence staining: red: intracellular streptococci, yellow: extracellular streptococci, green: actin cytoskeleton. All images were taken with 63x magnification on a Zeiss Axiophot Fluorescence microscope. The scale bar indicates 20 µm. d-f: SEM pictures. a,d: cells were untreated. b,e: cells were treated with 2.5 µg/ml disorazole A. c,f: cells were treated with 2.5 µg/ml disorazole Z. Images were taken by Manfred Rohde (ZEIM, HZI). d,e: scale bars indicate 2 µm. f: scale bar indicates 1 µm.
g: ns: not significant. *: 0.05 < p < 0.01. **: 0.01 < p < 0.001. ***: 0.001 < p < 0.0001. ****: p < 0.0001

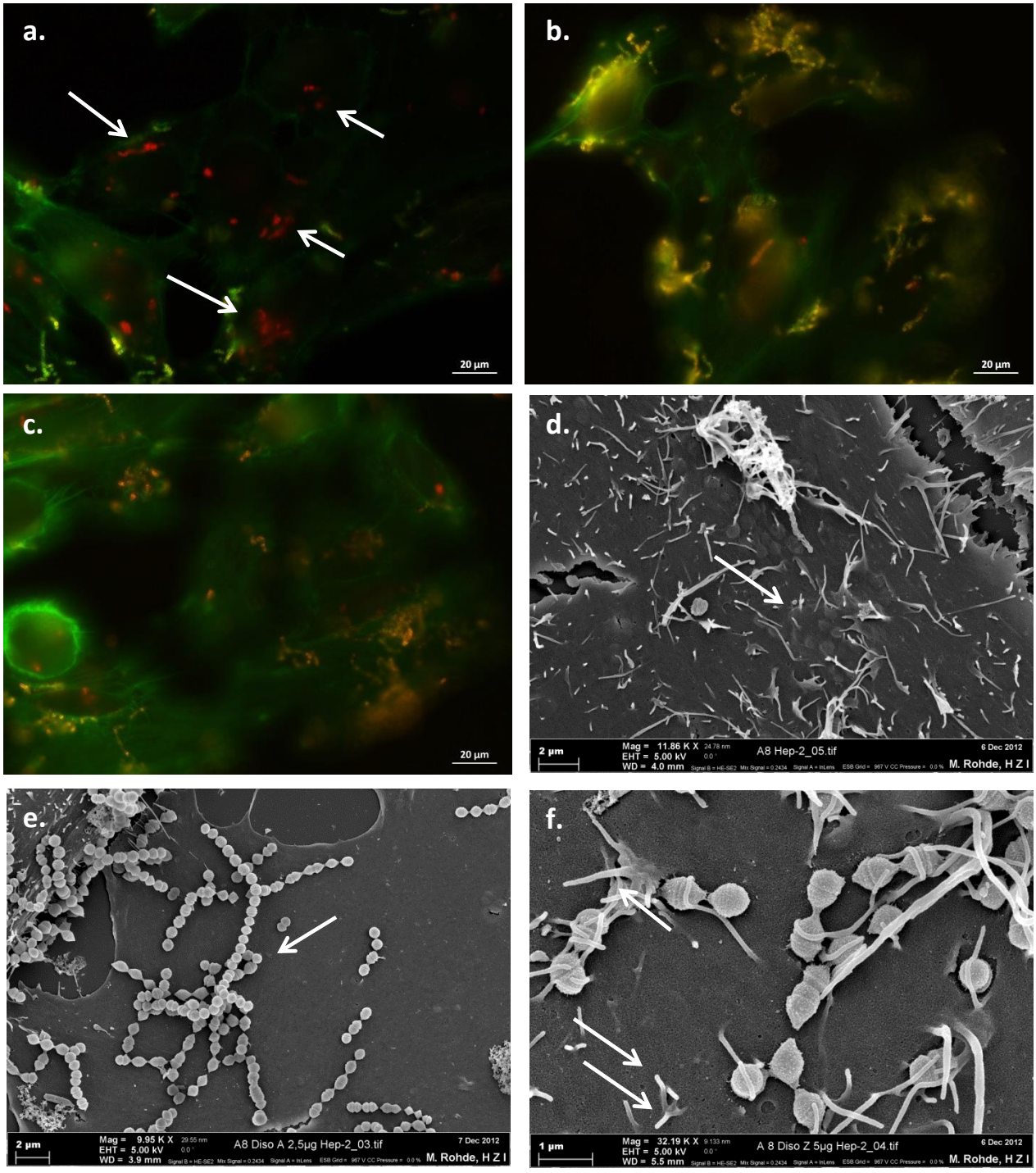

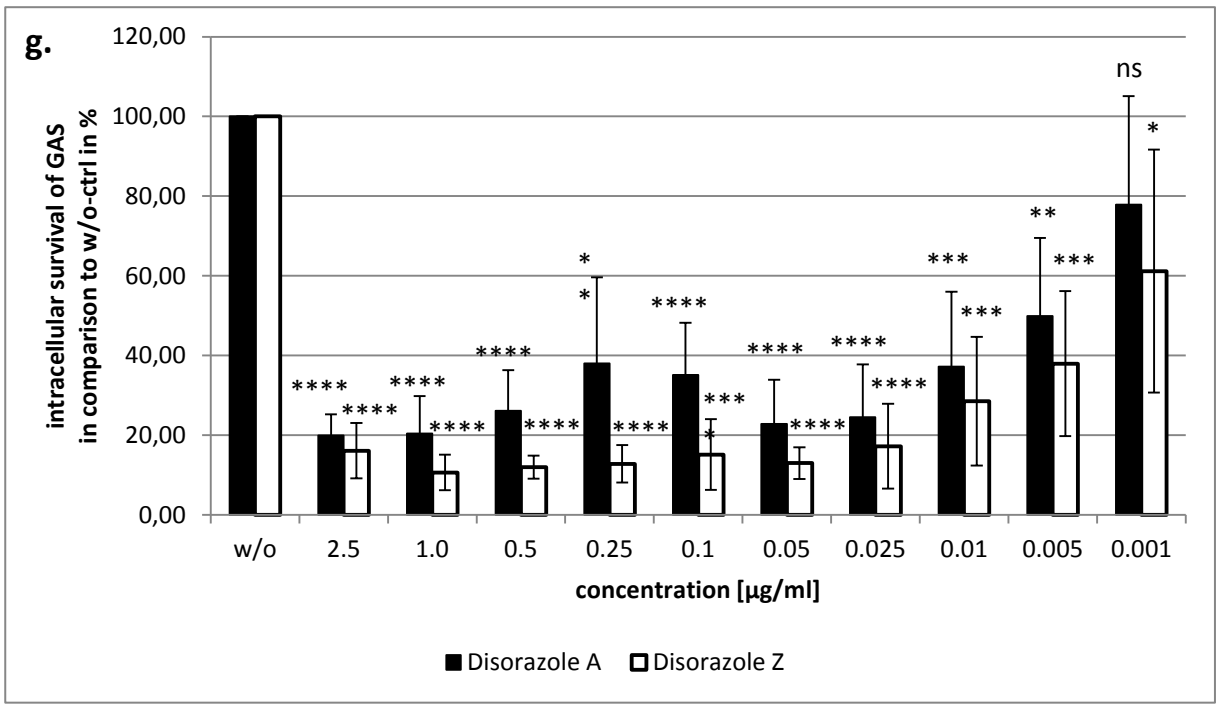

Next, the amount of intracellular viable bacteria was determined in order to quantify the inhibition of invasion. Therefore, a survival assay was performed. Different concentrations of the disorazoles were used to assess the lowest concentration being still effective. Significantly less intracellular viable streptococci were found upon treatment with disorazoles: At high concentrations of 2.5 µg/ml of both disorazoles, around 80 % less intracellular streptococci were detected in comparison to untreated controls. At a concentration of 5 ng/ml, 50 % less intracellular viable streptococci were found for cells treated with disorazole Z versus 30-40 % for those treated with disorazole A. Therefore, both disorazoles have an IC_{50} at around 5 ng/ml (fig. 3.1-4g).

Lower numbers of viable intracellular bacteria were detected upon treatment with different concentrations of disorazole A and Z when HEp2-cells were infected by *S.pyogenes* strain A8. This suggests that invasion is hampered upon treatment with disorazoles.

When streptococci infect the host, they mainly invade into pharyngeal epithelial cells. However, they do not invade them exclusively. Although they cannot invade lung epithelial cells as effectively as pharyngeal epithelial cells, they are still capable to do so (Cue *et al.*, 1998). Therefore, A549-cells were used to assess the inhibitory effects of the disorazoles in an infection assay.

In comparison to similar experiments with HEp2-cells (fig. 3.1-4a) less invasive streptococci were found in A549-cells (fig. 3.1-5a). Upon treatment with disorazole A and Z, less intracellular bacteria were detected compared to the untreated control (fig. 3.1-5a-c). Inhibition of invasion was not as effective in A549-cells as in HEp2-cells (fig. 3.1-4g and 3.1-5d). Upon treatment with disorazoles less intracellular viable streptococci were found in comparison to untreated controls (fig. 3.1-4d). At concentrations ranging from 1 to 5 µg/ml invasion decreased by 40-70 %. At lower concentrations, e.g. 5 ng/ml, almost no inhibition was observed.

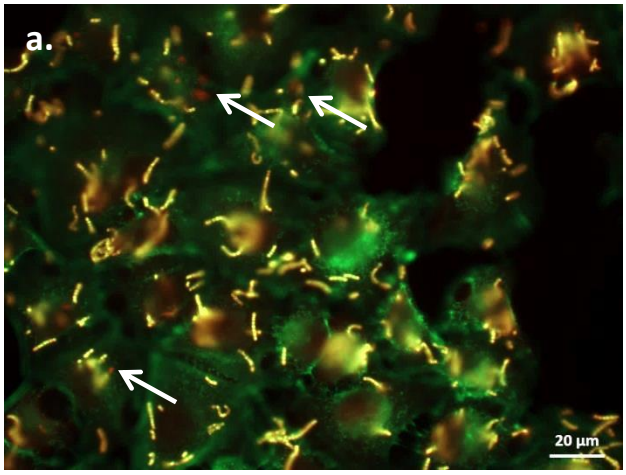

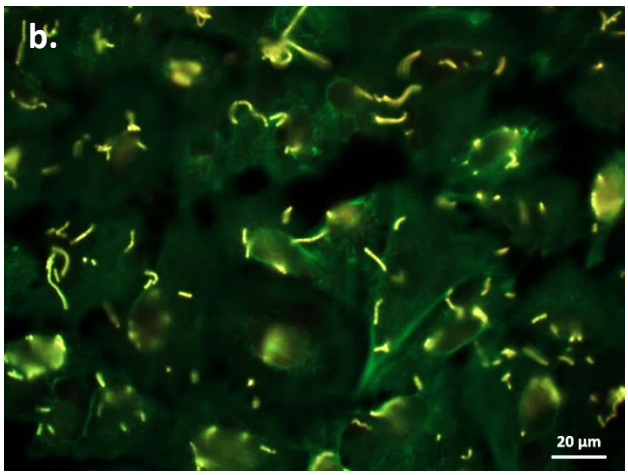

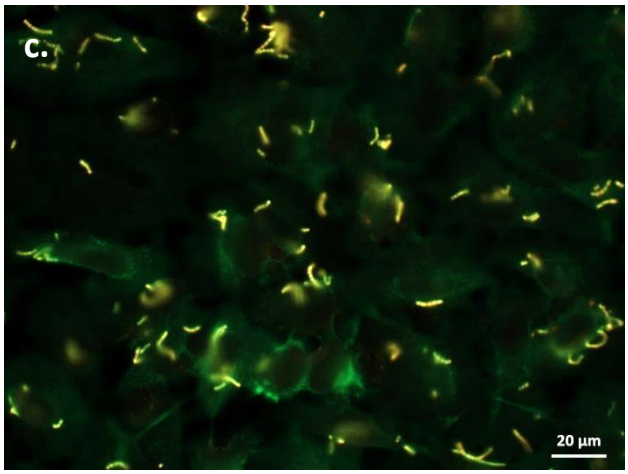

Figure 3.1-5: Disorazoles inhibit invasion of *S.pyogenes* strain A8 into A549-cells.
a-d: A549-cells were infected with *S.pyogenes* strain A8 for 2 h (a-d). Disorazoles inhibited invasion efficiently.
a-c: Cells treated with disorazole A (b) or Z (c) (conc. 2.5 µg/ml for both disorazoles) did not show intracellular streptococci in comparison to untreated (a) cells.
d: Intracellular survival of GAS was determined in comparison to the untreated control (w/o-ctrl). The diagram shows that significantly less intracellular streptococci were found when cells were treated with disorazoles.
a-c: Double-immunofluorescence staining: red: intracellular streptococci, yellow: extracellular streptococci, green: actin cytoskeleton. All images were taken with 63x magnification on a Zeiss AxioImager Fluorescence microscope. The scale bar indicates 20 µm. White arrows point to intracellular streptococci. d: ns: not significant. *: 0.05 < p < 0.01. **: 0.01 < p < 0.001. ***: 0.001 < p < 0.0001. ****: p < 0.0001

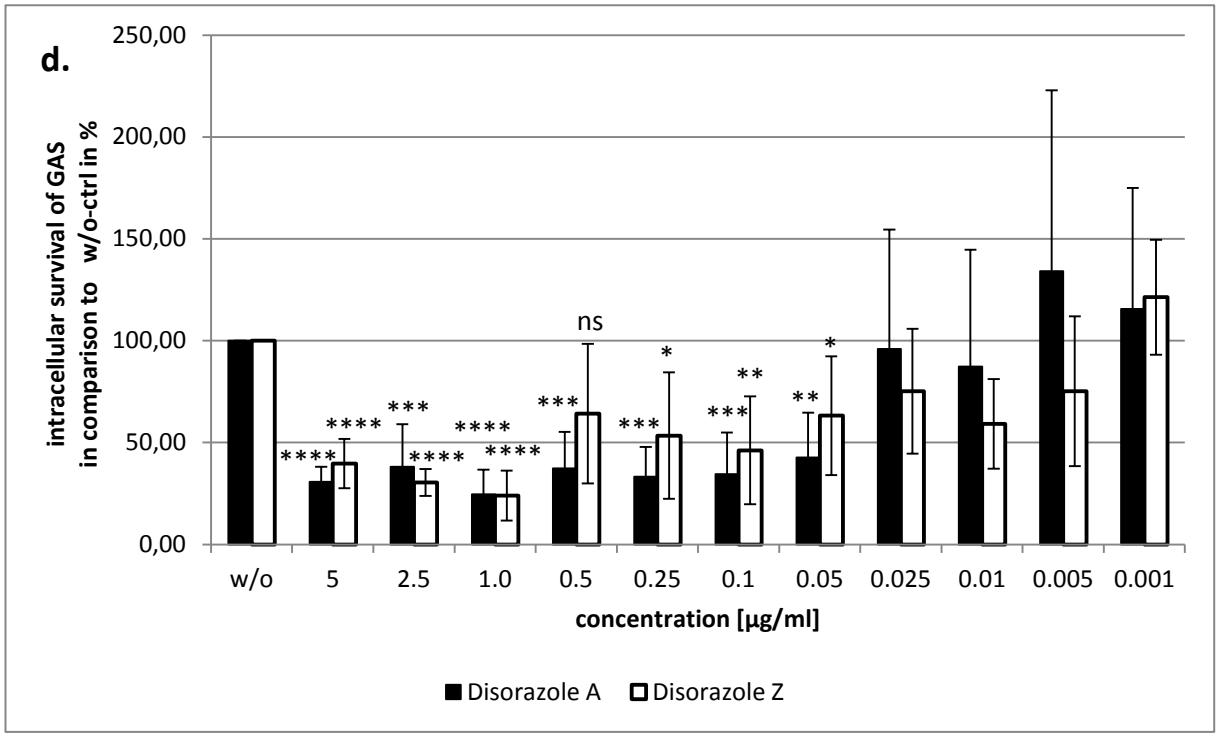

As a result, both disorazoles reduced the amount of intracellular viable streptococci significantly in two different epithelial cell types. This suggests that they inhibited group A streptococcal invasion mediated by cytoskeletal rearrangements.

3.1.3 Influence of disorazoles on the SfbI-mediated pathway of invasion

Disorazoles were also tested for their inhibitory properties regarding the SfbI-mediated pathway of invasion. The disorazoles were added in the same concentrations to the cells as described in section 3.1.2. Instead of the strain A8, the *S.pyogenes* strain A40 was used for infection of HEp2-cells. Invasion of group A streptococci was reduced upon treatment with disorazoles (fig. 3.1-6a-c).
Double-immunofluorescence images showed clearly that invasion is reduced when cells are treated with disorazoles. Upon treatment with disorazoles, fewer intracellular streptococci were detected in comparison to the untreated control. Furthermore, SEM pictures showed that invasion of streptococci was decreased when cells were treated with disorazoles (fig. 3.1-6d-f). If cells were untreated, formation of and uptake via caveolae was observed (fig. 3.1-6d-e). Upon treatment with disorazole A or Z, streptococci were mainly found on the cell surface although intracellular bacteria as well as the process of the uptake of streptococci were observed in a smaller range (fig. 3.1-6f-h).
Double-immunofluorescence and SEM images suggested differences in the amount of intracellular streptococci between disorazole-treated and untreated cells. To determine if this effect was significant, a survival assay was performed with HEp2-cells. Different concentrations of the disorazoles were used to investigate the lowest concentration which still has an effect. As depicted in fig. 3.1-6i disorazole Z was slightly more effective than disorazole A: 30-50 % less intracellular viable bacteria were detected for cells treated with disorazole Z versus 20-40 % less upon treatment with disorazole A (both compounds were used at a concentration of 2.5 µg/ml). Consequently, the IC_{50} for both disorazoles was around 2.5 µg/ml (this IC_{50} is much higher than the IC_{50} determined for the disorazoles in the infection with the strain A8; vide section 3.1.2). These data support the results obtained by double-immunofluorescence and SEM: the amount of intracellular streptococci invading HEp2-cells via the SfbI-mediated pathway was only reduced significantly at high concentrations. This suggests that this pathway is only inhibited partially upon treatment with disorazoles.

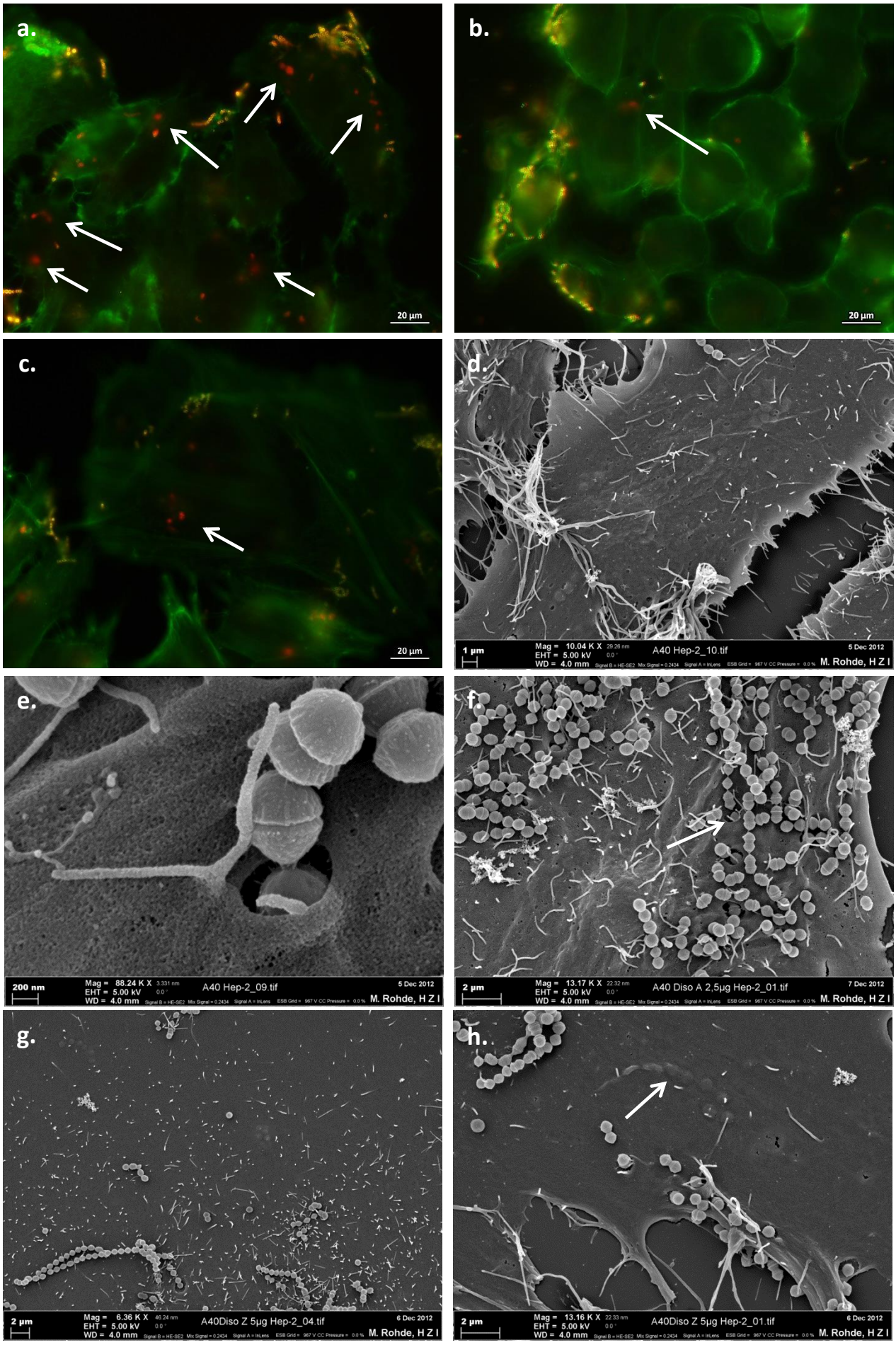
a.
20 µm
b.
20 µm
c.
20 µm
d.
1 µm
Mag = 10.04 K X
EHT = 5.00 kV
WD = 4.0 mm
A40 Hep-2_10.tif
5 Dec 2012
M. Rohde, H Z I
e.
200 nm
Mag = 88.24 K X
EHT = 5.00 kV
WD = 4.0 mm
A40 Hep-2_09.tif
5 Dec 2012
M. Rohde, H Z I
f.
2 µm
Mag = 13.17 K X
EHT = 5.00 kV
WD = 4.0 mm
A40 Diso A 2,5µg Hep-2_01.tif
7 Dec 2012
M. Rohde, H Z I
g.
2 µm
Mag = 6.36 K X
EHT = 5.00 kV
WD = 4.0 mm
A40Diso Z 5µg Hep-2_04.tif
6 Dec 2012
M. Rohde, H Z I
h.
2 µm
Mag = 13.16 K X
EHT = 5.00 kV
WD = 4.0 mm
A40Diso Z 5µg Hep-2_01.tif
6 Dec 2012
M. Rohde, H Z I

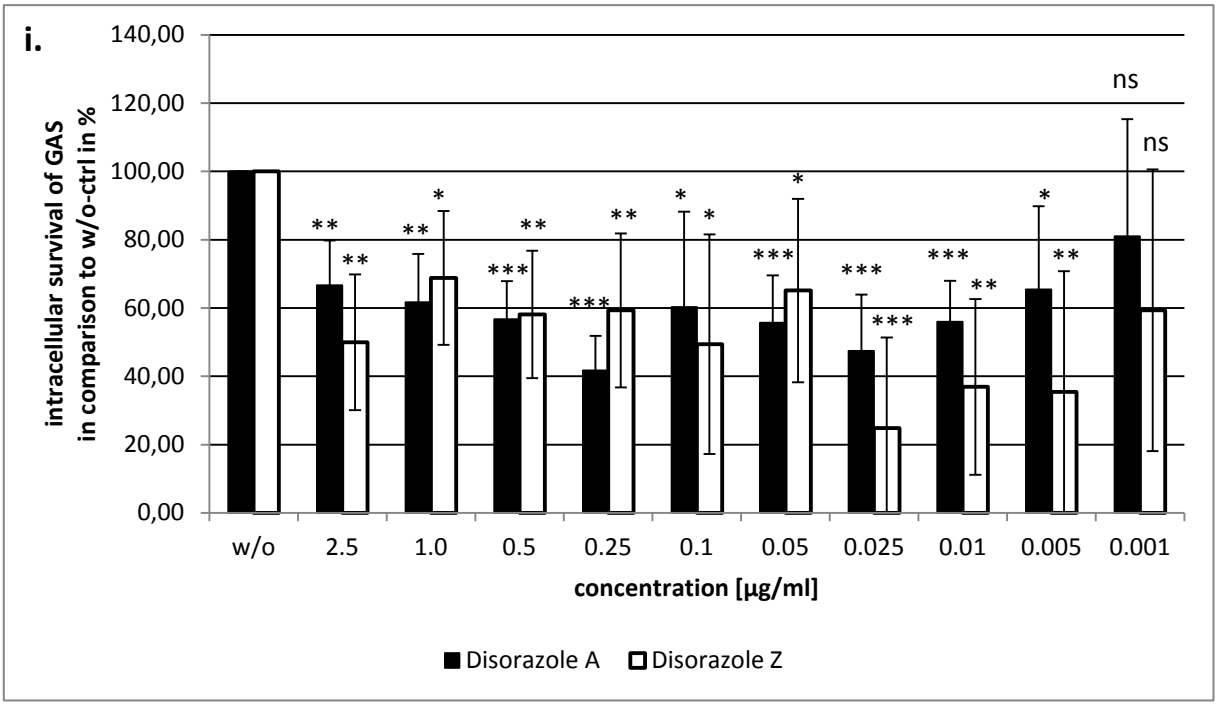

Figure 3.1-6: Influence of treatment with disorazoles upon infection of Hep2-cells with *S.pyogenes* strain A40.
a-i: HEp2-cells were infected with *S.pyogenes* strain A40 for 2 h. Disorazoles reduced the amount of intracellular streptococci.
a-g: Cells treated with disorazole A (b,f) or Z (c,g,h) showed isolated intracellular streptococci in comparison to untreated (a,d,e) cells. a-c: White arrows indicate intracellular streptococci. f: A white arrow points to streptococci which are taken up by formation of caveolae. h: A white arrow indicates streptococci that have been taken up.
i: Intracellular survival of GAS was determined in comparison to the untreated control (w/o-ctrl). The graph shows that significantly less intracellular streptococci were found when cells were treated with disorazoles.
a-c: Double-immunofluorescence staining: red: intracellular streptococci, yellow: extracellular streptococci, green: actin cytoskeleton. All images were taken with 63x magnification on a Zeiss Axiophot Fluorescence microscope. The scale bar indicates 20 µm. d-h: SEM pictures. a,d,e: cells were untreated. b,f: cells were treated with 2.5 µg/ml disorazole A. c,g,h: cells were treated with 2.5 µg/ml disorazole Z. d-h: Images were taken by Manfred Rohde (ZEIM, HZI). d: scale bar indicates 1 µm. e: scale bar indicates 200 nm. f-h: scale bars indicate 2 µm. f: scale bar indicates 1 µm.
i: ns: not significant. *: 0.05 < p < 0.01. **: 0.01 < p < 0.001. ***: 0.001 < p < 0.0001.

To assess the effects of disorazoles during infection of lung epithelial cells, A549-cells were used and infected with *S.pyogenes* strain A40. Treated cells harbored less intracellular streptococci than untreated cells (fig. 3.1-7a-c). Though, isolated intracellular streptococci were still detectable within disorazole Z-treated cells (fig. 3.1-7c). Quantification of intracellular viable streptococci revealed that the amount of intracellular bacteria was reduced only at high concentrations of both disorazoles (fig. 3.1-7d): a reduction by 10-40 % was achieved. Consequently, treatment with disorazoles resulted in a reduction of intracellular streptococci. These effects in A549-cells were comparable to those observed in HEp2-cells (reduction of intracellular streptococci by 30-50 % for HEp2-cells vs. 10-40 % for A549-cells; fig. 3.1-6i and fig. 3.1-7d).

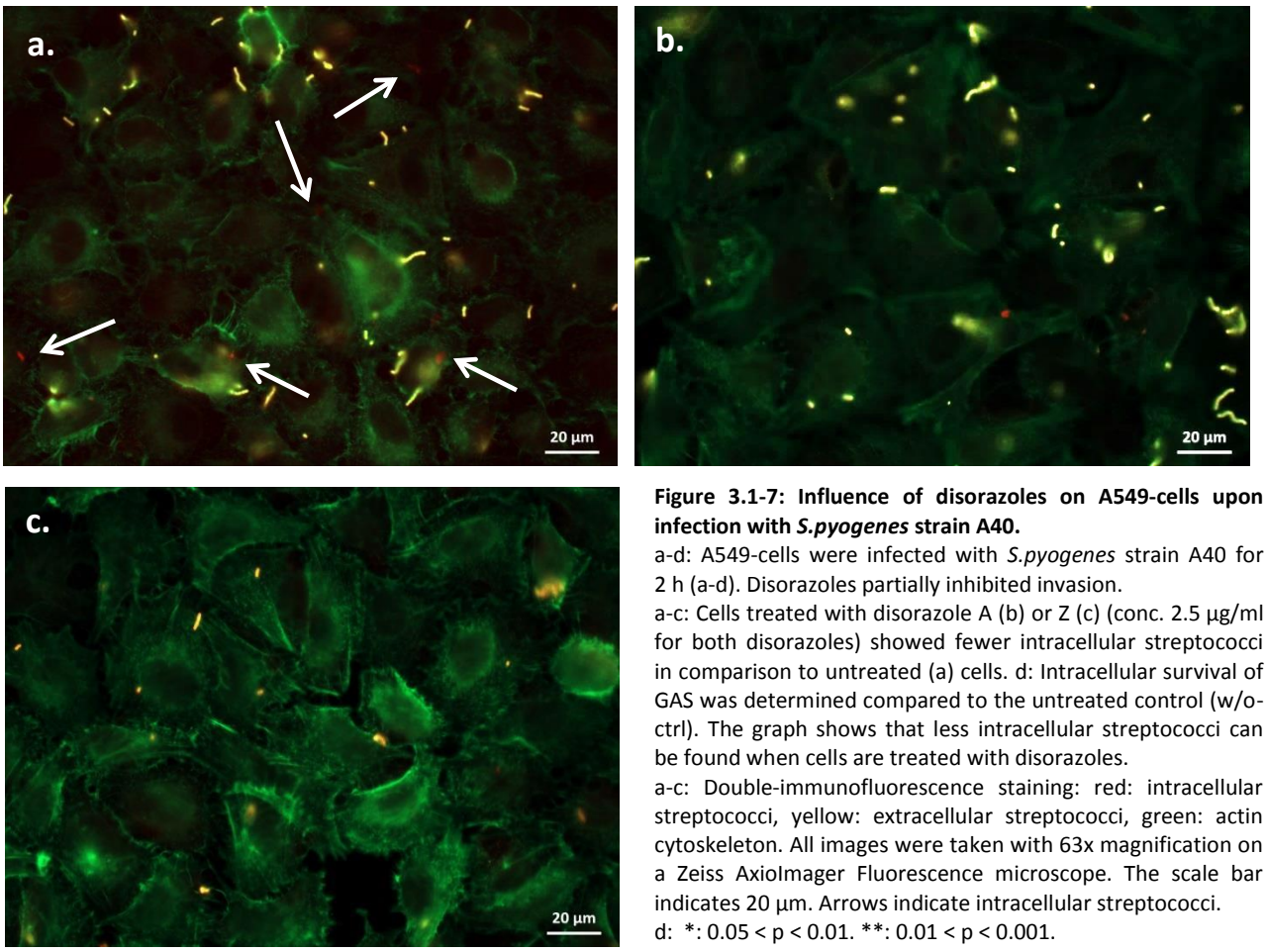

Figure 3.1-7: Influence of disorazoles on A549-cells upon infection with *S.pyogenes* strain A40.

a-d: A549-cells were infected with *S.pyogenes* strain A40 for 2 h (a-d). Disorazoles partially inhibited invasion.

a-c: Cells treated with disorazole A (b) or Z (c) (conc. 2.5 µg/ml for both disorazoles) showed fewer intracellular streptococci in comparison to untreated (a) cells. d: Intracellular survival of GAS was determined compared to the untreated control (w/o-ctrl). The graph shows that less intracellular streptococci can be found when cells are treated with disorazoles.

a-c: Double-immunofluorescence staining: red: intracellular streptococci, yellow: extracellular streptococci, green: actin cytoskeleton. All images were taken with 63x magnification on a Zeiss AxioImager Fluorescence microscope. The scale bar indicates 20 µm. Arrows indicate intracellular streptococci.

d: *: $0.05 < p < 0.01$. **: $0.01 < p < 0.001$.

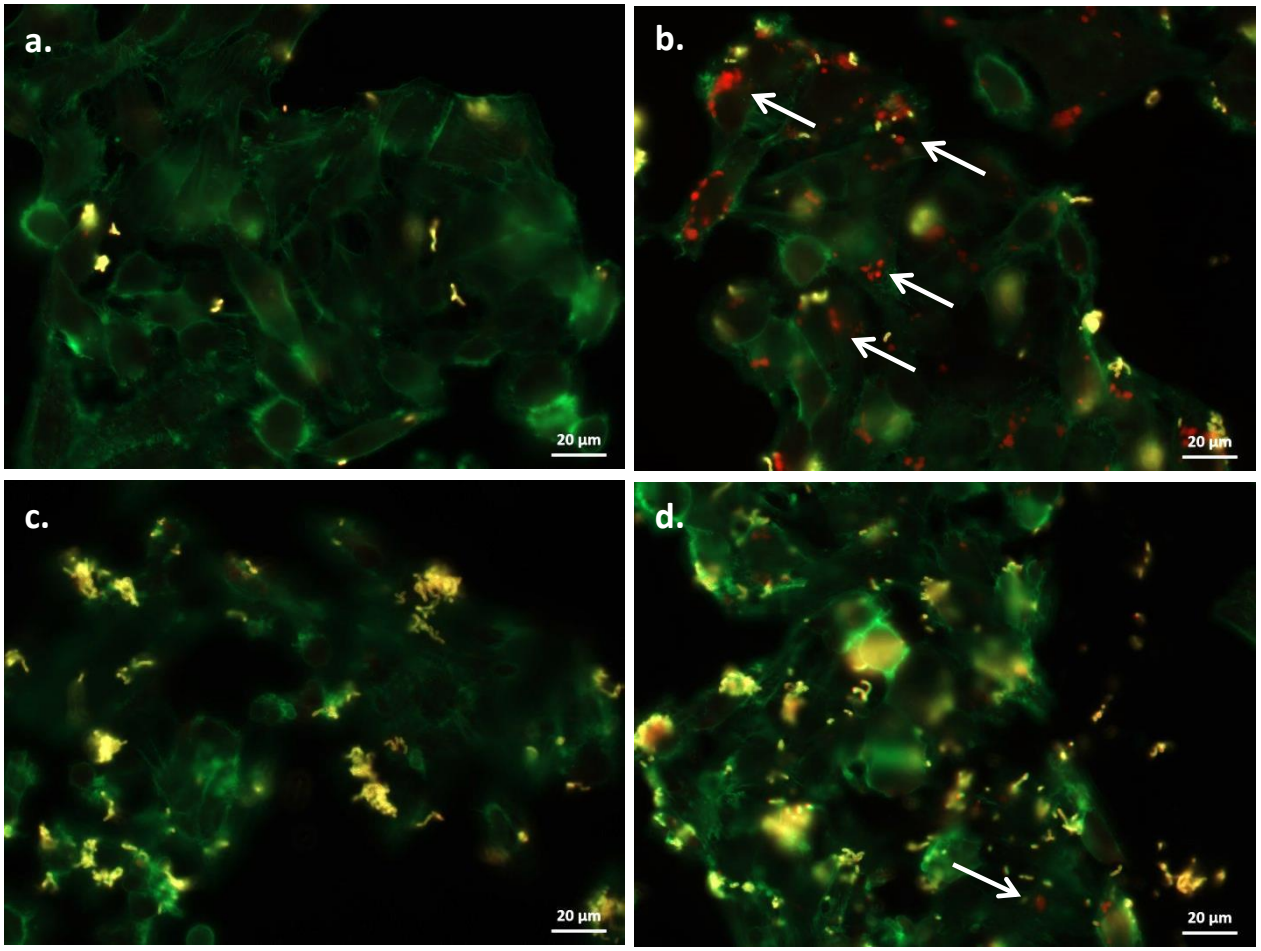
a.
20 µm
b.
20 µm
c.
20 µm
d.
20 µm

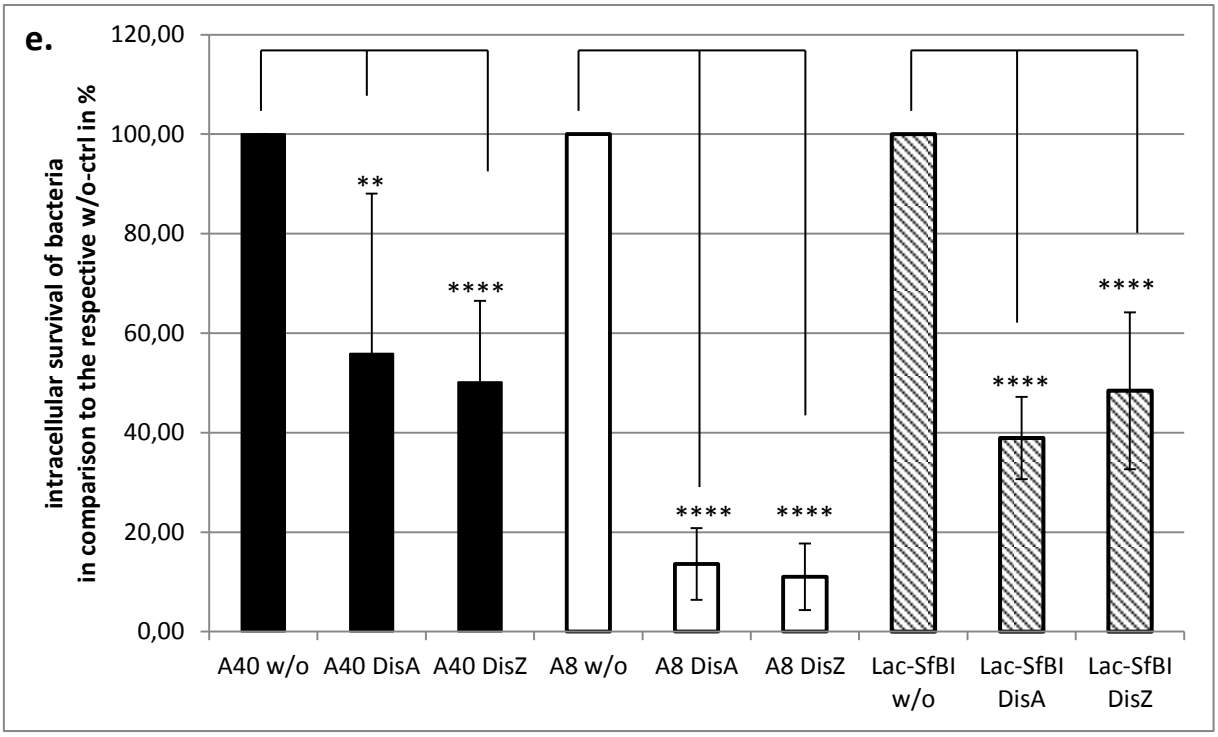
e.
intracellular survival of bacteria
in comparison to the respective w/o-ctrl in %
120,00
100,00
80,00
60,00
40,00
20,00
0,00
**
****
****
****
****
****
A40 w/o
A40 DisA
A40 DisZ
A8 w/o
A8 DisA
A8 DisZ
Lac-SfBI w/o
Lac-SfBI DisA
Lac-SfBI DisZ

Figure 3.1-8: Disorazoles diminish invasion of lacotococci expressing SfBI into HEp2-cells.
a: HEp2-cells were infected with Lac for 2 h. b-d: HEp2-cells were infected with Lac-SfBI for 2 h. e: HEp2-cells were infected with *S.pyogenes* strain A40 or A8 or Lac-SfBI for 2 h and treated either with disorazole A or Z or were left untreated. Intracellular survival of bacteria was determined.
a: Lactococci did not show invasion and only slight adherence. b-d: Cells treated with either disorazole A (c) or Z (d) at a concentration of 2.5 µg/ml showed less intracellular lactococci than the untreated control (b). e: Infected cells treated with disorazoles (conc. 2.5 µg/ml) showed significantly less intracellular bacteria. When cells were infected with *S.pyogenes* strain A8 and treated with disorazoles, invasion was efficiently inhibited. Cells infected with either *S.pyogenes* strain A40 or Lac-SfBI and treated with disorazoles also showed reduced invasion.
a-d: Double-immunofluorescence staining of infected cells. red: intracellular lactococci, yellow: extracellular lactococci; green: actin cytoskeleton. All images were taken with 63x magnification on a Zeiss AxioImager Fluorescence microscope. The scale bar indicates 20 µm. White arrows indicate intracellular streptococci. e: A40: *S.pyogenes* strain A40; A8: *S.pyogenes* strain A8; DisA: disorazole A; DisZ: disorazole Z; w/o: untreated; **: 0.01 < p < 0.001; ****: p < 0.0001.

It is known that *S.pyogenes* strain A40 invades cells via the SfbI-mediated pathway (Molinari *et al.*, 2000). To detect if the same range of inhibition of invasion was also observed if only SfbI as invasin is present, the heterologous expression system in *Lactococcus lactis* (family *streptococcaceae*) was used, taking advantage of the inability of this bacterial species to invade human cells. For this purpose a *L.lactis* strain expressing SfbI on the surface (Lac-SfbI) (obtained from Dr. René Bergmann, ZEIM, HZI) was used.

HEp2-cells were infected with Lac-SfbI for 2 h and treated with disorazoles. Additionally, as a negative control the cells were infected for 2 h with a *Lactococcus lactis* strain not expressing SfbI (Lac). Cells infected with Lac did not show invasive and almost no adhered lactococci whereas cells infected with Lac-SfbI did so (fig. 3.1-8a,b). Similarly to cells infected with *S.pyogenes* strain A40, cells infected with Lac-SfbI and treated with disorazoles (conc. 2.5 µg/ml) showed only few intracellular bacteria (fig. 3.1-8b-d).

To estimate the amount of intracellular viable bacteria, a survival assay was performed comparing the effects of the disorazoles during infection with Lac-SfbI and both *S.pyogenes* strains A40 and A8.

The amount of intracellular bacteria was significantly reduced upon treatment with both disorazoles and infection with the strain A8 (reduction by 80-90 %). This reduction was also observed and statistically significant for both disorazoles and upon infection with either *S.pyogenes* strain A40 or Lac-SfbI (fig. 3.1-8e). At first sight, there seemed to be a minimal difference in the amount of intracellular bacteria between Lac-SfbI and the *S.pyogenes* strain A40: this perceived difference was not statistically significant (A40 DisA against Lac-SfbI DisA: $p = 0.25$; A40 DisZ versus Lac-SfbI DisZ: $p = 0.79$).

As a result, both disorazoles reduced the amount of intracellularly located bacteria significantly. In conjunction with the double-immunofluorescence and the SEM images the survival data suggest that invasion was inhibited upon treatment with disorazoles. Against the background of the data depicted in the preceding paragraph, it was shown that disorazoles inhibit two important invasion pathways of

group A streptococci into two different epithelial cell types (via SfbI and via cytoskeletal rearrangements).

3.1.4 Inhibition of group A streptococcal invasion into epithelial cells is a direct result of disorazoles interfering with the eukaryotic host cells

In the previously described assays, the compounds were added to the respective cells prior to infection. The next step was to investigate the effects of the compounds in the case when only streptococci were treated with disorazoles. As both disorazoles had shown similar inhibitory effects, effects on streptococci were only assessed using disorazole Z.

A MIC-assay was conducted with the *S.pyogenes* strains A40 and A8. Both strains were untreated and treated with disorazole Z. No inhibitory effect on both strains could be determined for disorazole Z ranging up to concentrations of 10 µg/ml (data not shown). Next, both strains were inoculated with and without disorazole Z (conc. 2.5 µg/ml) and bacteria were plated after 8 h. No significant differences in the amount of viable bacteria were detected between inoculation with and without disorazoles (A40 vs. A40 supplemented with disorazole Z: $p = 0.25$; A8 vs. A8 supplemented with disorazole Z: $p = 0.08$). As a result, the disorazoles did not affect the streptococci during growth.

Then, the effects of the disorazoles on streptococci during the infection process were assessed: both streptococcal strains (A40 and A8) were supplemented with disorazole Z during cultivation. In addition, HEp2-cells were not treated prior to infection. These cells were infected with each strain supplemented with disorazole Z during cultivation. The assay was conducted as described in the preceding paragraphs.

Fig. 3.1-9a-d show the infection with *S.pyogenes* strain A40: HEp2-cells treated prior to infection with disorazole A or Z showed less intracellular streptococci (fig. 3.1-9a,c,d). By contrast, in untreated HEp2-cells, which were infected with the strain A40 supplemented with disorazole Z during cultivation, no differences in the amount of intracellular streptococci were observed compared to the untreated and infected control (with the strain A40) (fig. 3.1-9a,b).

Similar effects were observed upon infection with *S.pyogenes* strain A8 (fig. 3.1-9e-h): in HEp2-cells treated with disorazoles almost no intracellularly located streptococci were detected (fig. 3.1-9e,g,h). By contrast, HEp2-cells infected with streptococci supplemented with disorazole Z during cultivation showed a similar amount of intracellular streptococci compared to the untreated and infected control (with the strain A8) (fig. 3.1-9e,f). Consequently, it is more likely that disorazoles interfere directly with the eukaryotic host cells.

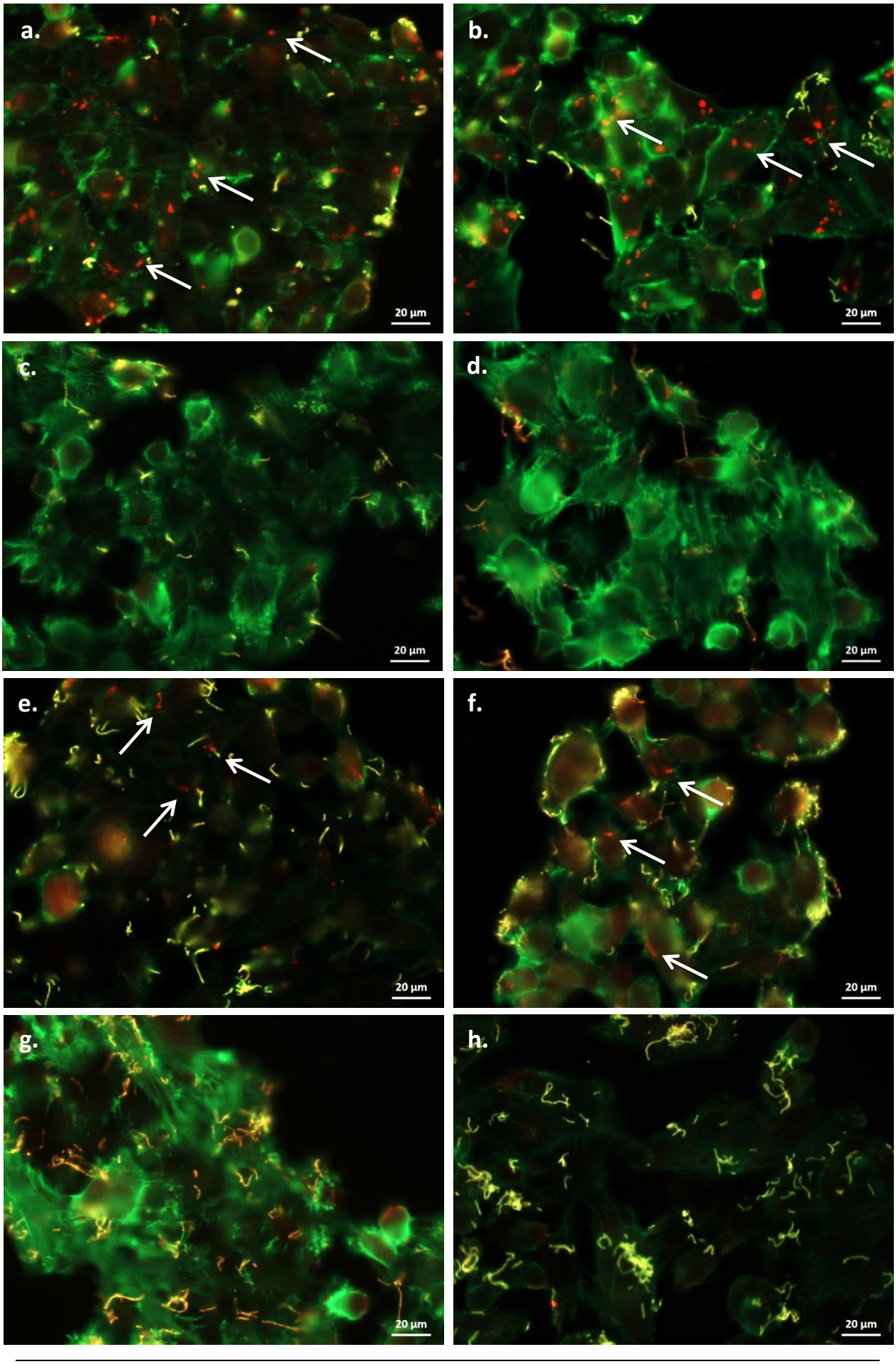
a.
20 µm
b.
20 µm
c.
20 µm
d.
20 µm
e.
20 µm
f.
20 µm
g.
20 µm
h.
20 µm

Figure 3.1-9: Inhibitory effects of disorazoles are a result of interference with eukaryotic cells.
a-h: HEp2 cells were infected with *S.pyogenes* strain A40 (a-d) or A8 (e-h) for 2 h. Cells were treated with disorazole A (c,g) or Z (d,h) in a concentration of 2.5 µg/ml or were untreated (a,e). Cells were infected with the respective *S.pyogenes* strain supplemented with disorazole Z (conc. 2.5 µg/ml) during cultivation (b,f).
a-h: Cells treated with either disorazole A (c,g) or Z (d,h) did not show intracellular streptococci in contrast to the untreated control (a,e). Cells infected with an *S.pyogenes* strain supplemented with disorazole Z during growth (b,f) showed nearly as many intracellular streptococci as the untreated control (a,e).
a-h: Double-immunofluorescence staining of infected cells. red: intracellular streptococci, yellow: extracellular streptococci; green: staining of the actin cytoskeleton. All images were taken with 63x magnification on a Zeiss AxioImager A2 Fluorescence microscope. The scale bar indicates 20 µm. White arrows point to intracellular streptococci.

3.1.5 Cytotoxicity is not the cause of the inhibitory properties of the disorazoles

As disorazoles are well known cytotoxic drugs (Jansen *et al.*, 1994), one could assume that the inhibitory properties of the disorazoles are only a result of cytotoxic effects.

Therefore, a cytotoxicity assay was performed mimicking the same conditions as used in the previous infection assays. All data were normalized to an untreated and uninfected control. Furthermore, treatment with triton X-100 served as a control for maximal cell damage, i.e. maximal cytotoxicity.

Both untreated and treated HEp2-cells infected with the *S.pyogenes* strain A8 did not show a reduced viability compared to the untreated and uninfected control. These effects were observed for both disorazoles at two different concentrations (i.e. 2.5 µg/ml and 10 ng/ml). By contrast, both the untreated and treated HEp2-cells infected with the strain A40 showed a significant decrease in viability compared to uninfected and untreated cells. Thereby, treatment with disorazole A or Z in both tested concentrations (i.e. 2.5 µg/ml and 10 ng/ml) did not lead to an additional reduction in cell viability. It was observed that infection with the strain A40 per se already led to a significant increase in cell death. Nevertheless, it was observed that disorazoles did not lead to decreased cell viability under the conditions used in the infection assays (fig. 3.1-10a).

Infected cells might have been killed after 24 h as the strain A40 already led to decreased viability after 2 h (fig. 3.1-10a). Therefore, cytotoxicity for 24 h was assessed with uninfected cells treated with disorazoles. Under these conditions viability of HEp2-cells upon treatment with disorazoles (conc. 2.5 µg/ml and 10 ng/ml) was decreased by approximately 50-60 % (fig. 3.1-10b).

Although disorazoles did not exhibit cytotoxic effects under the conditions used in the infection assays, they showed these effects 24 h after incubation with HEp2-cells. However, it is very likely that the observed effects upon treatment with the disorazoles regarding group A streptococcal invasion are not a result of cytotoxicity.

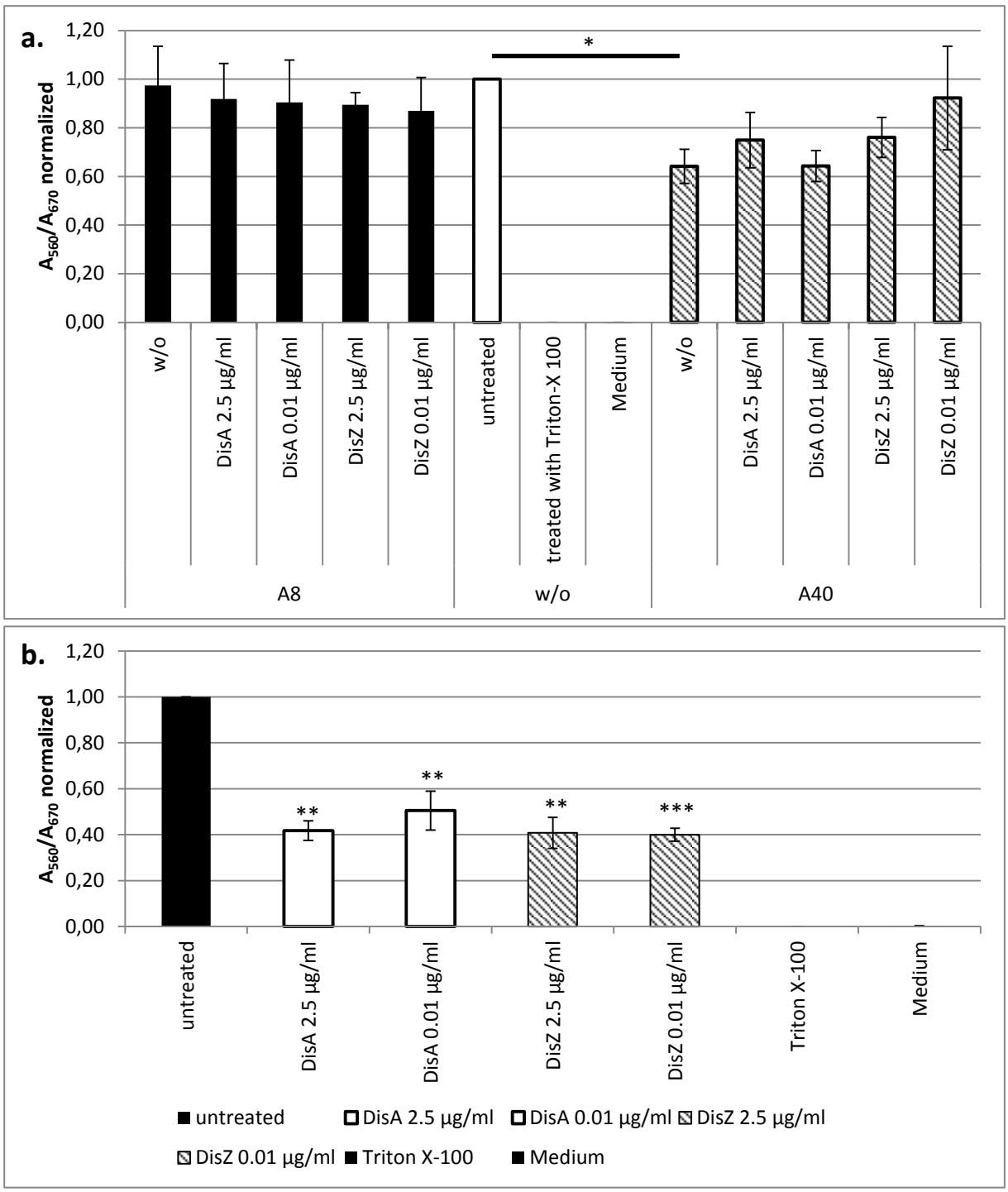

Figure 3.1-10: Effects of disorazoles on cell viability.
a,b: Viability of HEp2-cells was assessed by performance of an MTT assay. Untreated and uninfected cells served as a negative control for maximal cell viability. Cells treated with triton X-100 served as a positive control for maximal cell damage. Medium only without cells served as blank.
a: Treatment of infected HEp2-cells (either with A40 or A8) with disorazoles did not decrease cell viability. Cells infected with A40 showed a significant decrease in cell viability.
b: Treatment of uninfected cells with disorazoles for 24 h reduced cell viability by 40-50 %.
a: Cells were infected with either *S.pyogenes* strain A40 or A8 for 2 h. Infected cells were untreated or treated with either disorazole A or Z. Concentrations used for testing were 2.5 µg/ml or 0.01 µg/ml. Data were normalized against the untreated, uninfected and the triton X-100-control. *: $0.05 < p < 0.01$.
b: Cells were treated with either disorazole A or Z for 24 h. Concentrations used for testing were 2.5 µg/ml or 0.01 µg/ml. Data were normalized against the untreated, uninfected and the triton X-100-control. **: $0.01 < p < 0.001$

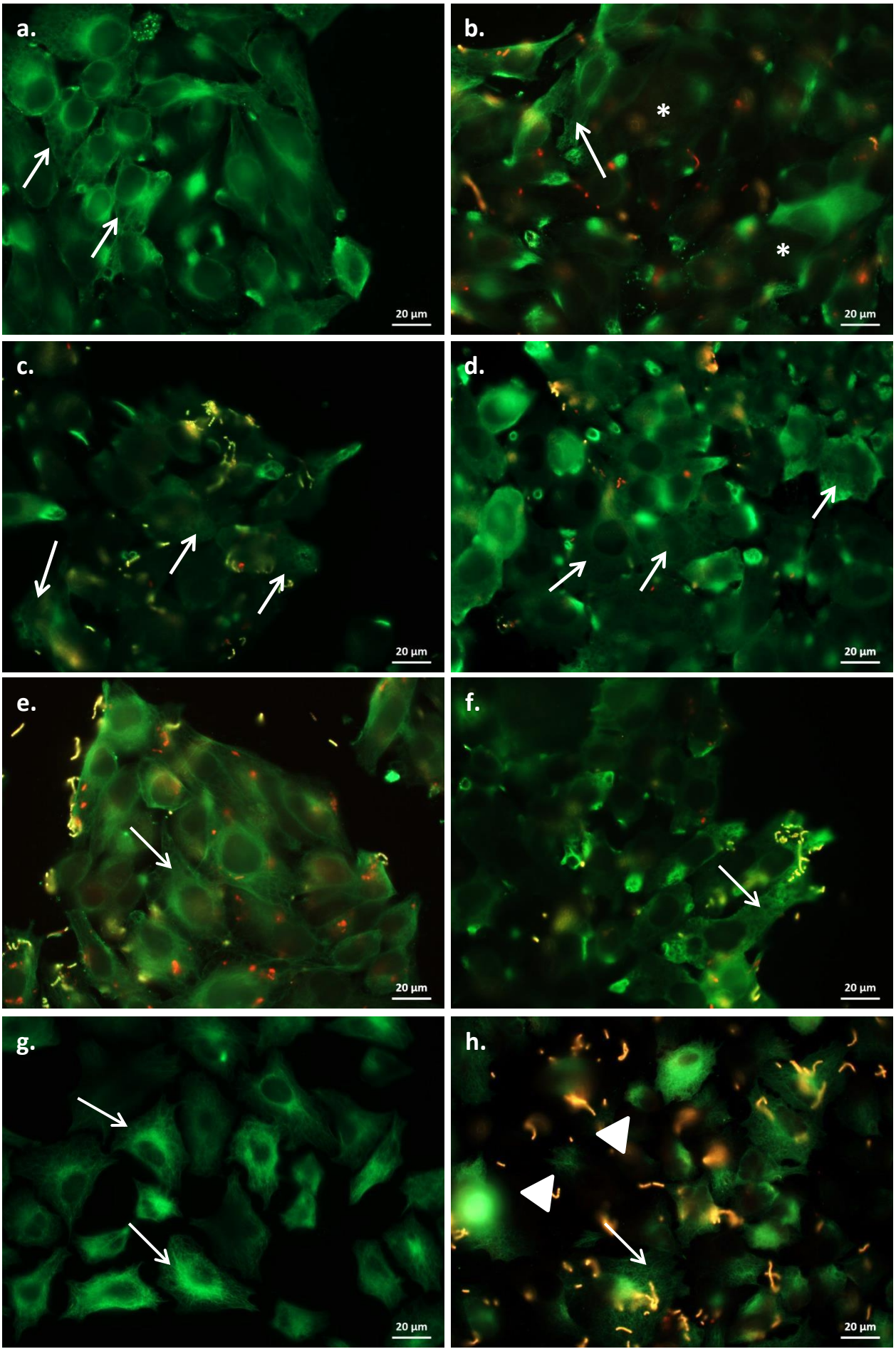
a.
20 µm
b.
*
*
20 µm
c.
20 µm
d.
20 µm
e.
20 µm
f.
20 µm
g.
20 µm
h.
20 µm

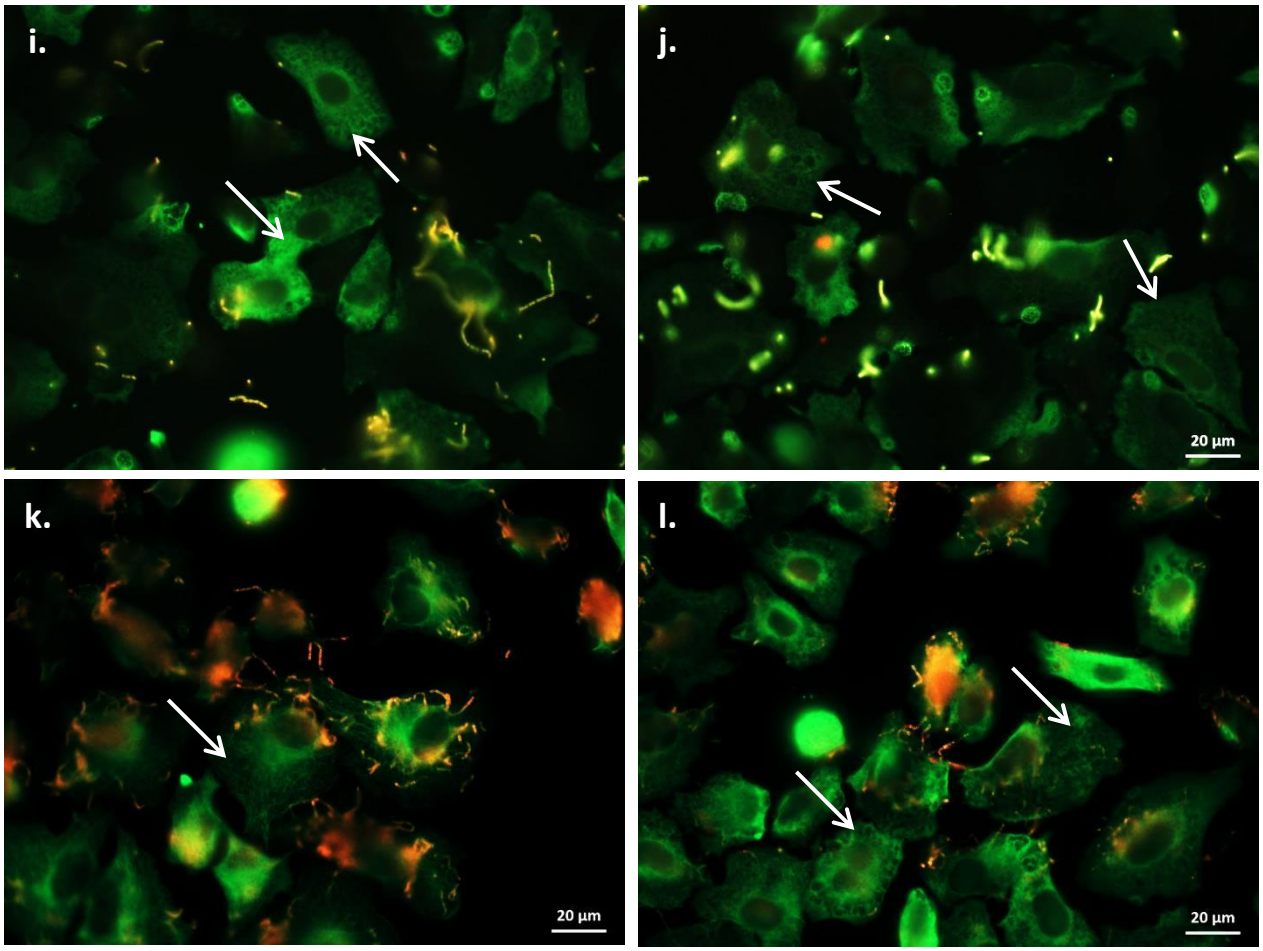

Figure 3.1-11: Effects of disorazoles on tubulin polymerization.
a-h: HEp2 cells (a-f) or A549-cells (g-m) were uninfected (a,g) or infected with *S.pyogenes* strain A40 (e,f,h-j) or A8 (b-d,k,l) for 2 h. Cells were treated with disorazole A (c,i) or Z (d,f,j,l) at a concentration of 2.5 µg/ml or were untreated (b,e,h,k).
a-l: Cells treated with either disorazole A (c,j) or Z (d,f,j,l) showed tubulin polymerization although tubulin fragments were shorter (c,d, white arrow) in contrast to the infected untreated control (b,e,h,k).
a-h: Double-immunofluorescence staining of infected cells. red: intracellular streptococci; yellow: extracellular streptococci; green: staining of α-tubulin. All images were taken with 63x magnification on a Zeiss AxioImager A2 Fluorescence microscope. The scale bar indicates 20 µm. Tubulin polymerization is indicated by a white arrow; diffuse fluorescence is indicated by white asterisks. White arrowheads mark disrupted cells.

It is known that cytotoxic effects of the disorazoles are a result of interaction with the tubulin polymerization: disorazoles destabilize microtubules (Elnakady *et al.*, 2004). Although cytotoxic effects were not detected under the conditions used for infection assays, it is possible that tubulin is already affected by the disorazoles during infection. Tubulin is part of the cytoskeleton. It has been shown that tubulin is not involved in the invasion process (Ozeri *et al.*, 2001). Notwithstanding, the influence of the disorazoles on tubulin during the infection was investigated.

HEp2-cells were infected with either *S.pyogenes* strain A40 or A8 for 2 h. Uninfected HEp2-cells served as a control for intact tubulin organization. Infected cells were left untreated or treated with disorazole A or Z (concentration 2.5 µg/ml). Infection with either *S.pyogenes* strain A40 or A8 already

had a slight influence on the tubulin matrix: untreated cells infected with the strain A8 (fig. 3.1-11b) did not show an entirely undamaged tubulin matrix in comparison to the untreated control (fig. 3.1-11a). Although some cells infected with the strain A8 showed tubulin polymerization (fig. 3.1-11b; indicated by a white arrow), diffuse fluorescence of tubulin was observed as well. This might indicate an incomplete tubulin polymerization (fig. 3.1-11b; indicated by a white asterisk). Cells infected with A8 and treated with disorazole A (fig. 3.1-11c) or Z (fig. 3.1-11d) showed tubulin polymerization (indicated by a white arrow). Moreover, the tubulin polymers of the treated infected cells were shorter than those of the infected, untreated cells (fig. 3.1-11c,d). Though, the tubulin matrix was not damaged.

HEp2-cells infected with the strain A40 (fig. 3.1-11e) showed tubulin polymerization comparable to the one of uninfected cells (fig. 3.1-11a). HEp2-cells treated with disorazole Z and infected with the strain A40 also showed shorter tubulin polymers (fig. 3.1-11f). However, still these appeared to be intact.

In addition, effects on tubulin polymerization were assessed on A549-cells (lung epithelial cells). Untreated and uninfected cells showed an unaltered tubulin polymerization (fig. 3.1-11g). The same was observed for cells infected with the strain A40. Nevertheless, disrupted cells were observed as well (fig. 3.1-11h; marked by white arrowheads). Treated A549-cells infected with the strain A40 showed tubulin polymerization. Again, shorter tubulin polymers were spotted (fig. 3.1-11i,j).

A549-cells infected with the strain A8 (fig. 3.1-11k) showed an intact tubulin network whereas those treated with disorazole Z showed shorter tubulin polymers again (fig. 3.1-11l).

The disorazoles had a slight to moderate influence on the tubulin polymerization. However, the tubulin network still appeared to be intact. Even if it is known that tubulin does not play a role in the invasion process (Ozeri *et al.*, 2001), it had to be proven that the slight influence of the disorazoles on tubulin did not result in reduced streptococcal invasion. Therefore, two other cytotoxic compounds (vinblastine and tubulysin A) known to inhibit tubulin polymerization (Khalil *et al.*, 2006) were tested for their inhibitory properties with regard to streptococcal invasion.

As vinblastine and tubulysin A have lower EC_{50} values for cytotoxicity, lower starting concentrations were used in comparison to the disorazoles.

In HEp2-cells infected with the strain A40 and treated with either vinblastine or tubulysin A (conc. 250 ng/ml) intracellular streptococci were observed (fig. 3.1-12b,c; white arrows point to intracellular streptococci). In similarly treated HEp2-cells (with vinblastine or tubulysin A at a concentration of 250 ng/ml) infected with the strain A8 intracellular streptococci were detected as well (fig. 3.1 12e,f; white arrows indicate intracellular streptococci). For both strains, the amount of intracellular viable streptococci was comparable to untreated cells (fig. 3.1-12a,d).

Figure 3.1-12: Invasion of streptococci into HEp2-cells is not inhibited by vinblastine or tubulysin A.
a-h: HEp2 cells infected with *S.pyogenes* strain A40 (a-c,g) or A8 (d-f,h) for 2 h.
a-f: Cells were treated with vinblastine (b,e) or tubulysin A (c,f) in a concentration of 250 ng/ml or were left untreated (a,d).
g,h: Cells were left untreated or treated with vinblastine or tubulysin A in concentrations ranging from 0.5-250 ng/ml.
a-f: Cells treated with either vinblastine (b,e) or tubulysin A (c,f) did not show fewer intracellular streptococci compared to the untreated control (a,d). Intracellular streptococci are indicated with white arrows.
a-f: Double-immunofluorescence staining of infected cells. red: intracellular streptococci; yellow: extracellular streptococci; green: staining of the actin cytoskeleton. All images were taken with 63x magnification on a Zeiss AxioImager A2 Fluorescence microscope. The scale bar indicates 20 µm.

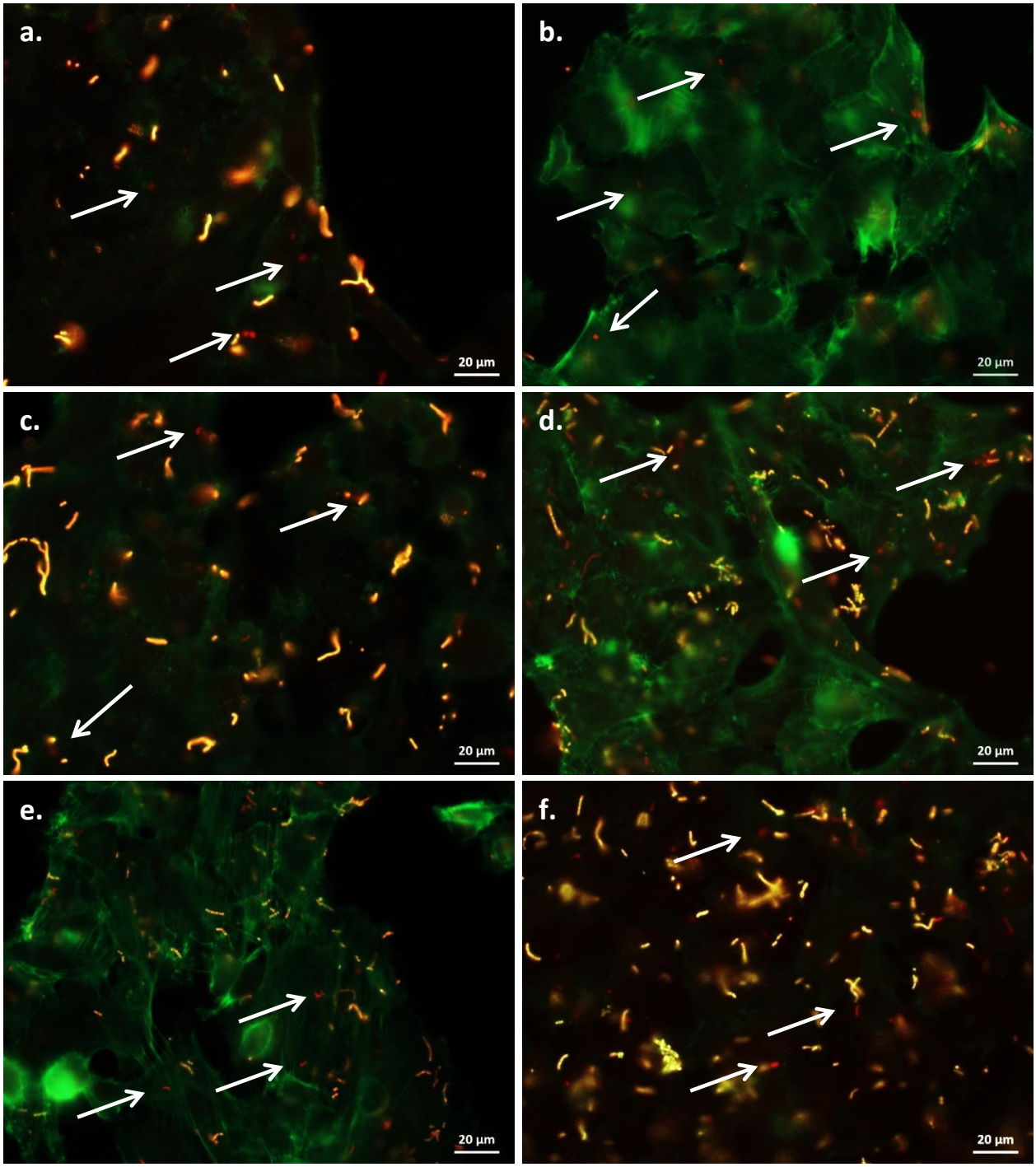

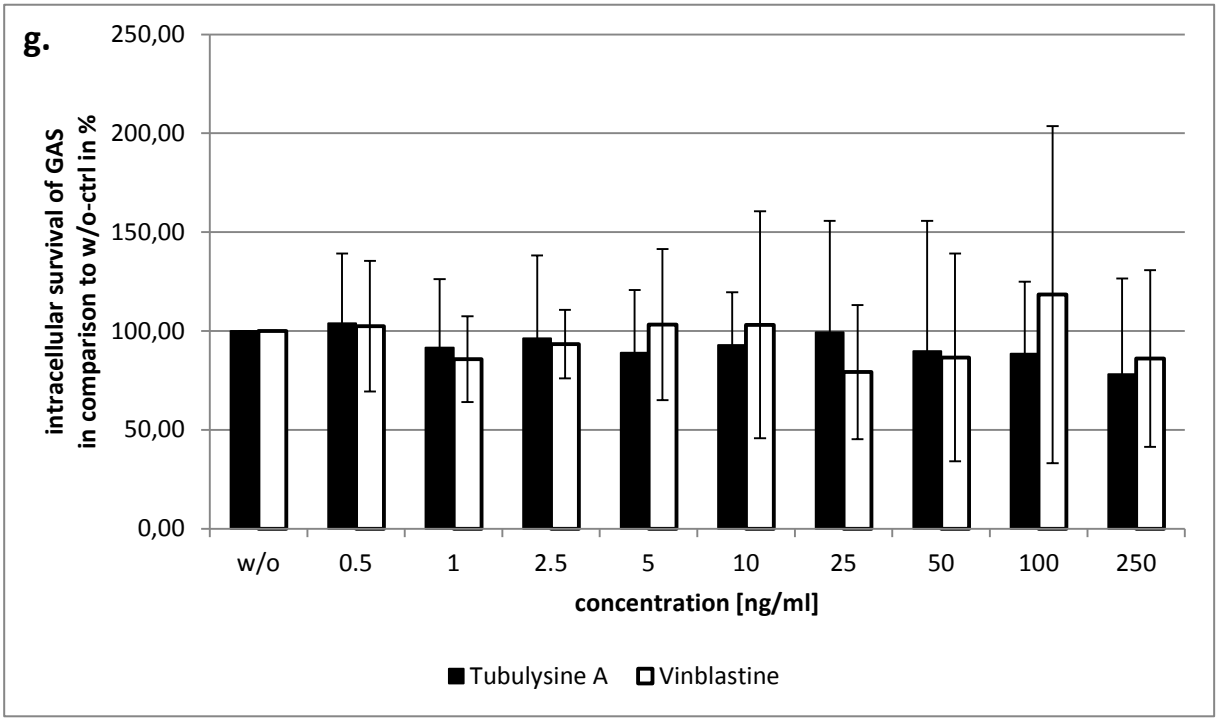

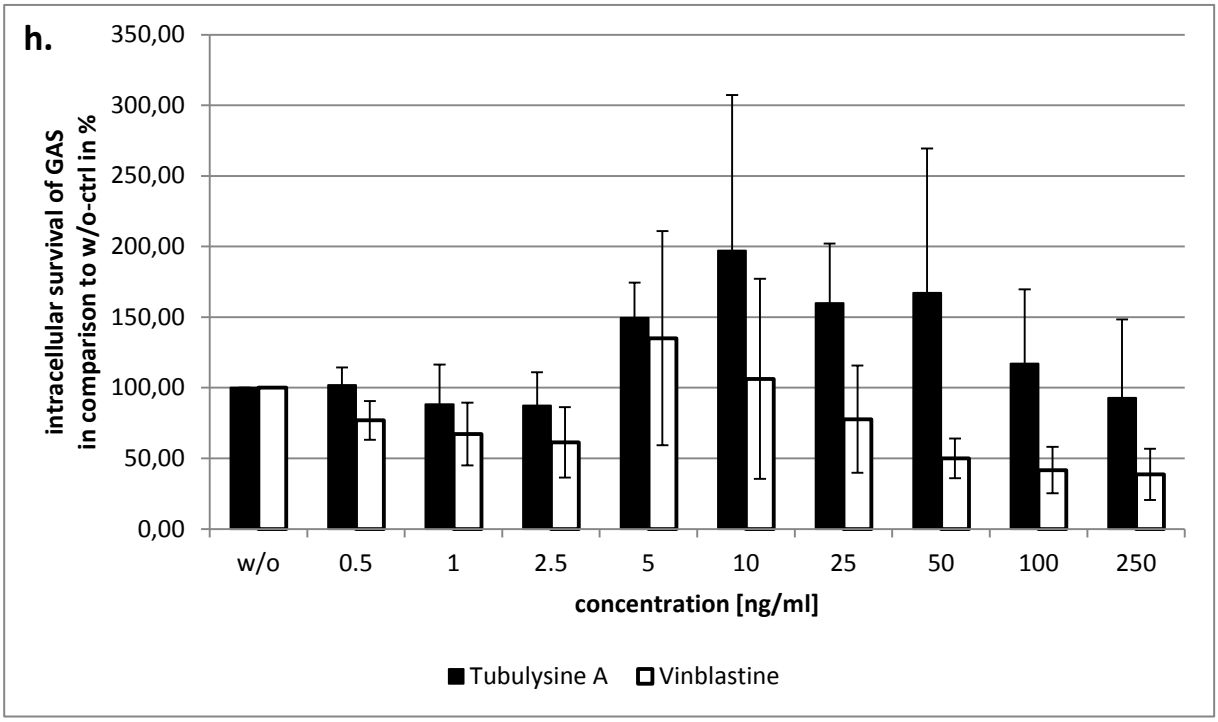

To quantify intracellularly viable streptococci, a survival assay was performed. Concentrations ranging from 0.5-250 ng/ml of tubulysin A and vinblastine were tested. HEp2-cells were infected for 2 h with either *S.pyogenes* strain A40 or A8. Treatment with vinblastine or tubulysin A upon infection with the strain A40 had no effect on the amount of intracellular viable streptococci compared to the untreated control (fig. 3.1-12g). Treatment with tubulysin A upon infection with the strain A8 had no inhibitory effect, either. Treatment with vinblastine, however, had an inhibitory effect at higher concentrations ranging from 50-250 ng/ml at first sight. Though, only 50 % less intracellularly viable

streptococci were detected. Double-immunofluorescence images showed a comparable amount of intracellular streptococci upon treatment with vinblastine by contrast with the untreated control (fig. 3.1-12a,b).

As vinblastine and tubulysin A did not reduce the amount of intracellular streptococci, it is very unlikely that they inhibit streptococcal invasion. Therefore, all evidence supports the conclusion that the inhibitory effects upon treatment with disorazoles are neither a result of cytotoxicity nor of alterations of the tubulin matrix.

3.1.6 Disorazoles and their effects on downstream signaling pathways of invasion

A functional actin cytoskeleton is necessary for uptake of streptococci into host cells (Molinari *et al.*, 2000; Wang *et al.*, 2007). Therefore, it was investigated if infected cells treated with disorazoles were affected in their actin cytoskeleton.

HEp2-cells infected with the strain A40 and treated with disorazole A or Z (conc. 2.5 µg/ml) did not show alterations in the actin cytoskeleton. Intact actin fibers were detected comparable to those of untreated cells (fig. 3.1-13a-c, white arrows point to actin fibers). Similarly, in treated HEp2-cells infected with the strain A8 no alterations in the actin cytoskeleton compared to untreated cells were observed, either (fig. 3.1-13d-f, white arrows point to actin fibers). Consequently, treatment with disorazoles did not affect the actin cytoskeleton.

Integrin clustering is necessary for an efficient uptake of streptococci within the SfbI-mediated pathway of invasion (Wang *et al.*, 2007). Therefore, the possible interference of disorazoles with this process was investigated.

β_1-integrins were detected at the site of streptococcal entry in infected and untreated cells (fig. 3.1-14a). The same was observed for HEp2-cells treated with either disorazole A or Z (fig. 3.1-14b,c). In addition, HEp2-cells treated with disorazoles showed fewer streptococci than untreated cells (fig. 3.1-14a-c). These results suggest that disorazoles do not perturb integrin clustering and that it is unlikely that they interfere with direct integrin signaling. However, it is still possible that they interfere with farther downstream signaling processes. Vinculin as part of the focal adhesions links integrins to the cytoskeleton (Critchley, 2000). Consequently, it was investigated if disorazoles hamper this process.

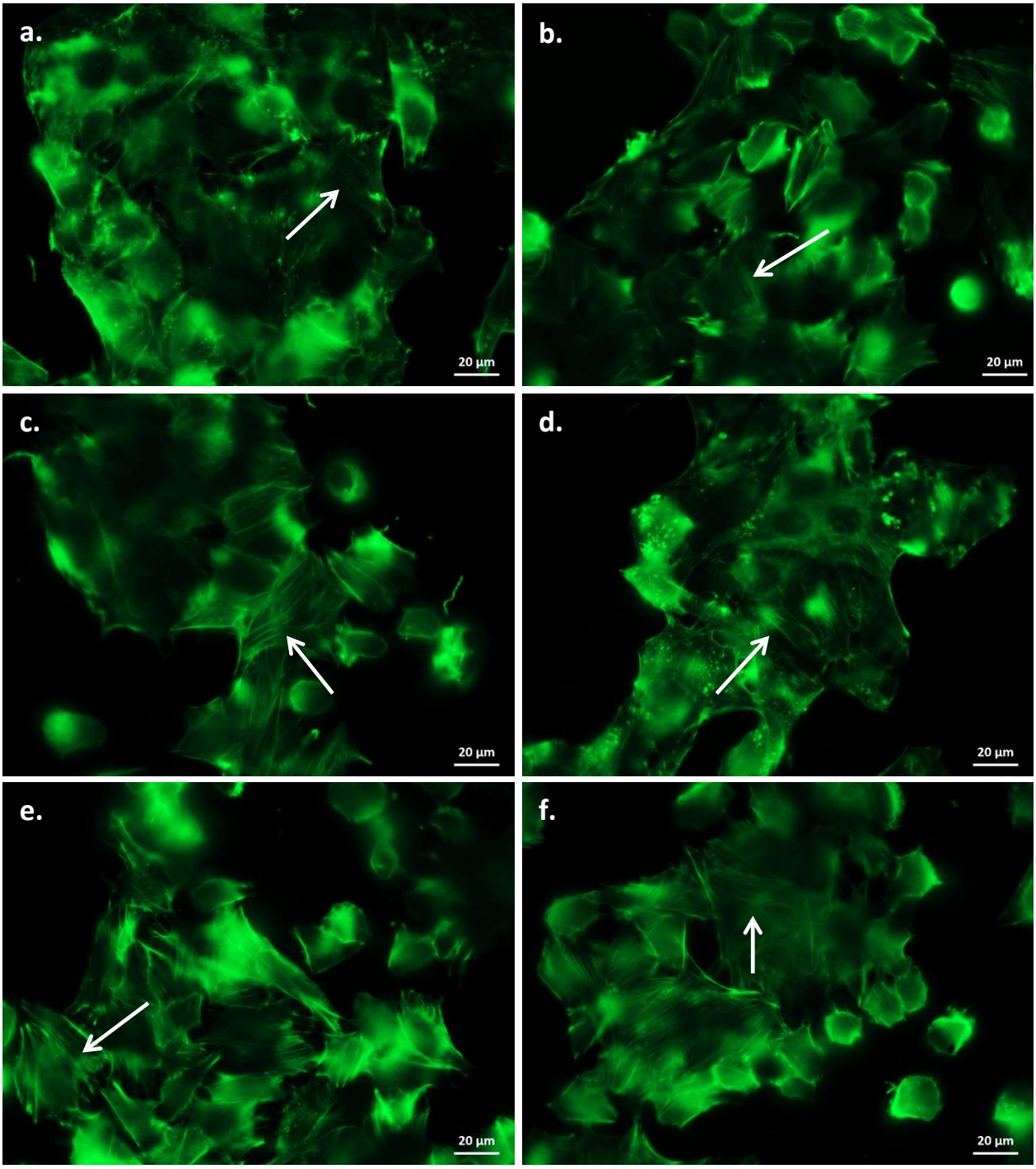

Figure 3.1-13: Disorazoles do not affect the actin cytoskeleton.
a-f: HEp2 cells were infected with *S.pyogenes* strain A40 (a-c) or A8 (d-f) for 2 h. Cells were treated with disorazole A (b,e) or Z (c,f) at a concentration of 2.5 µg/ml or were left untreated (a,d).
a-f: Cells treated with either disorazole A (b,e) or Z (c,f) did not affect the actin cytoskeleton compared to the untreated control (a,d). White arrows point to actin fibers.
a-f: Immunofluorescence staining of infected cells. green: staining of the actin cytoskeleton (and extracellular streptococci). All images were taken with 63x magnification on a Zeiss AxioImager Fluorescence microscope. The scale bar indicates 20 µm.

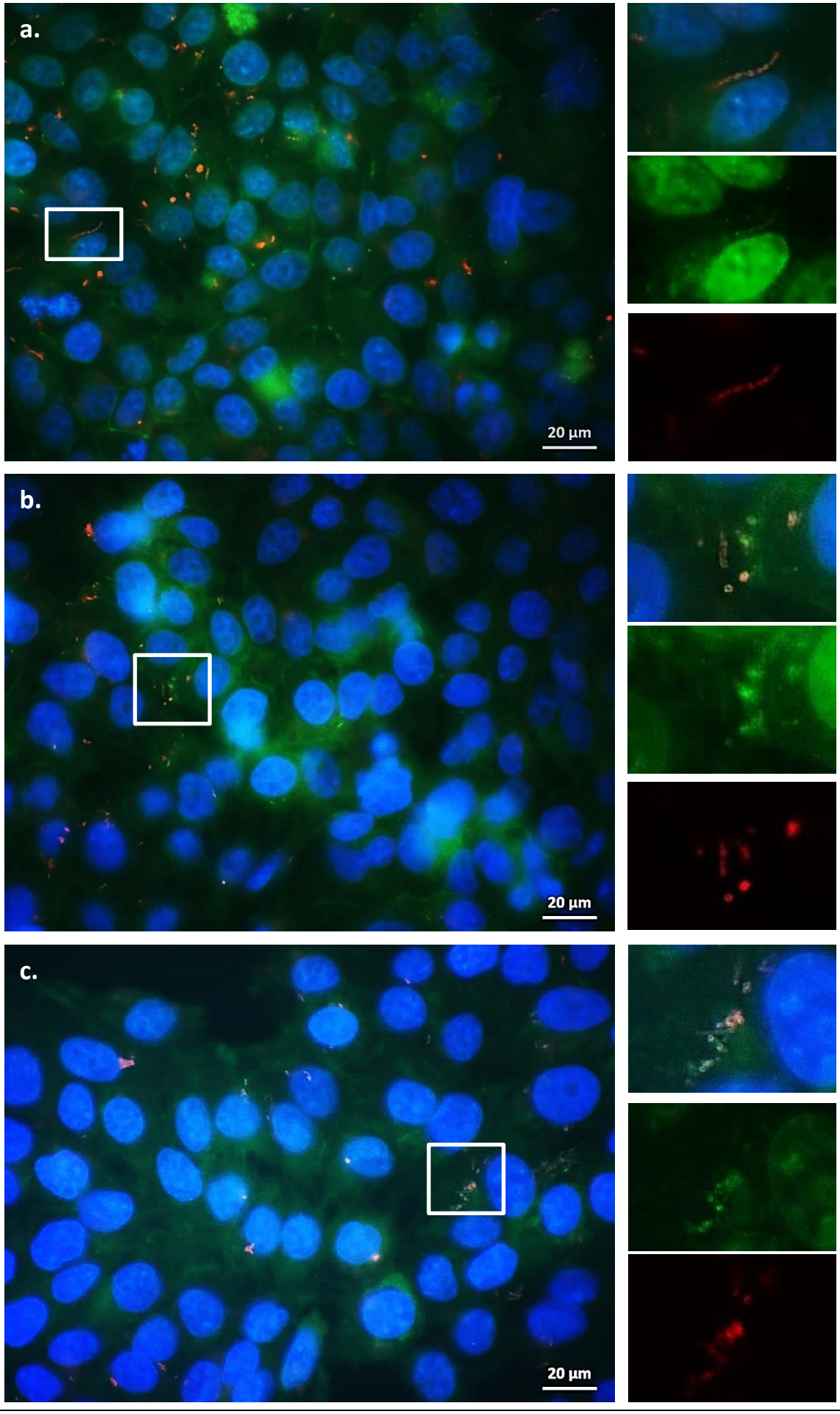
a.
20 µm
b.
20 µm
c.
20 µm

Figure 3.1-14: Integrin clustering is not perturbed upon treatment with disorazoles.
a-c: HEp2 cells were infected with *S.pyogenes* strain A40 (a-c) for 2 h. Cells were treated with disorazole A (b) or Z (c) at a concentration of 2.5 µg/ml or were untreated (a).
a-c: Cells treated with either disorazole A (b) or Z (c) did not perturb integrin clustering compared to the untreated control (a).
a-c: Double-immunofluorescence staining of infected cells. green: staining of the β_1-integrin-subunit; red: streptococci (intra- and extracellular); blue: DAPI (nucleus); yellow: streptococci with integrins. All images were taken with 63x magnification on a Zeiss AxioImager Fluorescence microscope. The scale bar indicates 20 µm. A box with a white frame indicates the position of the detailed pictures of each image on the right hand side. The detailed pictures show the merged picture (upper), the Alexa-488 channel picture displaying the β_1-integrin-stain (middle); the Alexa-568 channel (lower) displaying the stained streptococci.

No differences concerning the distribution of vinculin within HEp2-cells were detected for both untreated and treated cells (disorazole A or Z; conc. 2.5 µg/ml). In addition, both untreated and treated cells showed that vinculin was localized to focal adhesions (fig. 3.1-15a-c). As a result, it is unlikely that formation of focal adhesions is impaired upon treatment with disorazoles. Colocalization of vinculin and streptococci at the site of entry was not determined as confocal microscopy was not used. As disorazoles do not affect the cellular distribution of vinculin, it is most likely that vinculin is still enabled to exert its functions and link integrins to the cytoskeleton. Thus, disorazoles do not inhibit invasion by interacting with vinculin.

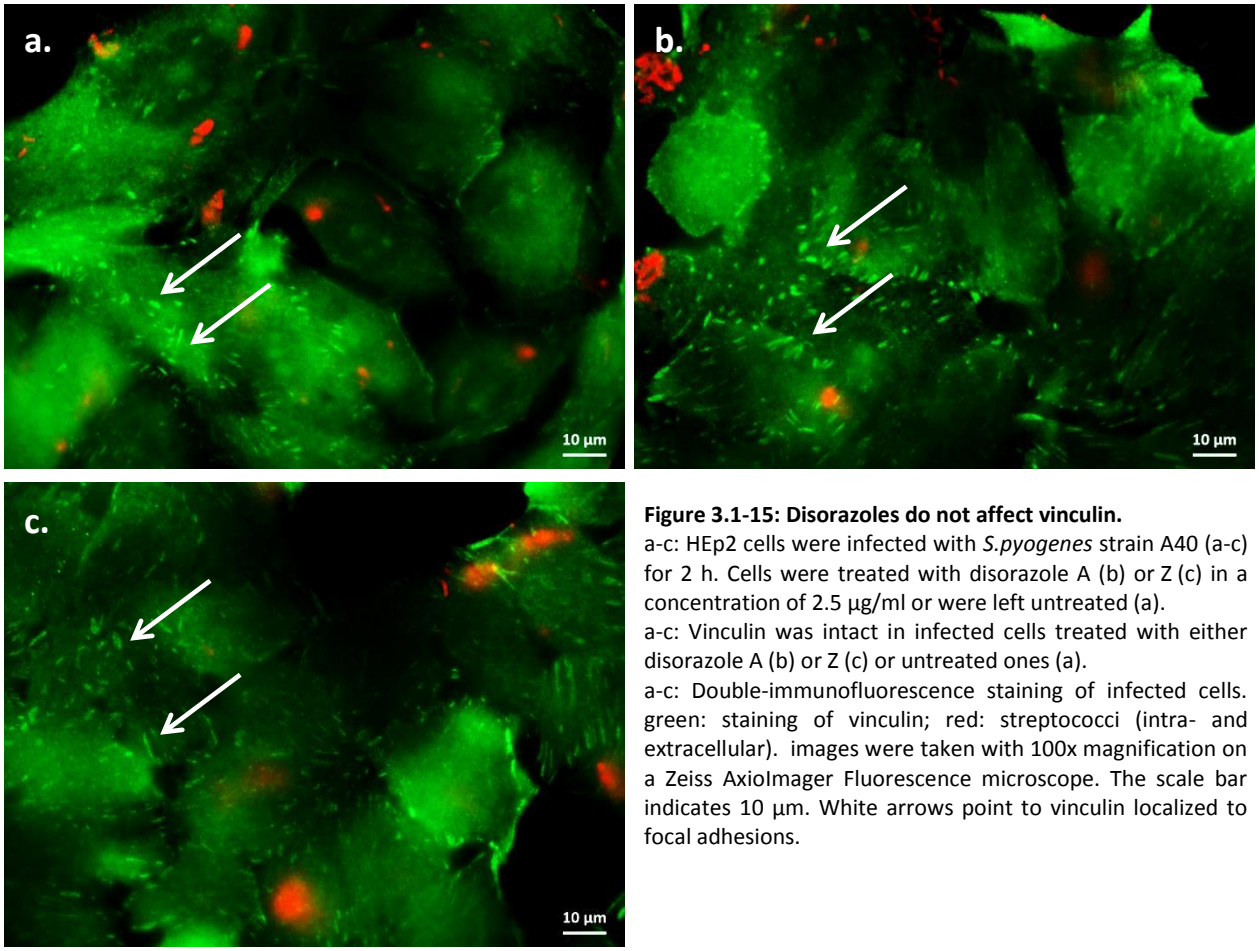

Figure 3.1-15: Disorazoles do not affect vinculin.
a-c: HEp2 cells were infected with *S.pyogenes* strain A40 (a-c) for 2 h. Cells were treated with disorazole A (b) or Z (c) in a concentration of 2.5 µg/ml or were left untreated (a).
a-c: Vinculin was intact in infected cells treated with either disorazole A (b) or Z (c) or untreated ones (a).
a-c: Double-immunofluorescence staining of infected cells. green: staining of vinculin; red: streptococci (intra- and extracellular). images were taken with 100x magnification on a Zeiss AxioImager Fluorescence microscope. The scale bar indicates 10 µm. White arrows point to vinculin localized to focal adhesions.

Another factor in the invasion process might be ezrin. However, it has never been investigated for its role in streptococcal invasion. It is known that ezrin regulates the formation of microvilli (Viswanatha *et al.*, 2014) and is enriched in membrane ruffles under certain conditions (Franck *et al.*, 1993). As shorter microvilli were detected upon treatment with disorazoles (fig. 3.1-4e,f), possible effects of the disorazoles on ezrin were assessed.

Untreated HEp2-cells infected with the strain A40 showed a regular distribution of ezrin (indicated by white arrows; fig. 3.1-16a). Differences were observed in infected cells treated with either disorazole A or Z (conc. 2.5 µg/ml): ezrin formed cluster-like structures. Furthermore, diffuse fluorescence was detected (white arrowheads indicate clusters and white asterisks point to diffuse fluorescence; fig. 3.1-16b,c).

In addition, HEp2-cells were infected with *S.pyogenes* strain A8. Untreated cells showed a regular distribution of ezrin, either (indicated by white arrows; fig. 3.1-16d). However, differences were observed in infected and treated cells: to some extent a regular distribution of ezrin was detected as well as a formation of smaller clusters and a partially diffuse fluorescence (white arrows indicate regular distribution of ezrin, white arrowheads formation of smaller clusters and white asterisks indicate diffuse fluorescence; fig. 3.1-16e,f).

As a result, treated cells showed cluster formation of ezrin and diffuse fluorescence upon infection with the strain A40. Treated cells infected with the strain A8 showed a partially regular distribution of ezrin. Besides, cluster formation and diffuse fluorescence were detected. Hence, ezrin is affected upon treatment with disorazoles. Therefore, it can be assumed that these observed effects are the cause of the inhibition of invasion upon treatment with disorazoles.

Figure 3.1-16: Ezrin is one potential target of the disorazoles and, possibly, involved in the invasion process of *S.pyogenes* into epithelial cells.

a-d: HEp2 cells were infected with *S.pyogenes* strain A40 (a-c) or A8 (d-f) for 2 h. Cells were treated with disorazole A (b,e) or Z (c,f) in a concentration of 2.5 µg/ml or were left untreated (a,d).

a-f: Cells treated with either disorazole A (b,e) or Z (c,f) alter the distribution of ezrin compared to an untreated control (a,d). Furthermore, treated cells (b,c,e,f) show cluster formation of ezrin as well as diffuse fluorescence. Treated cells which are infected with A8 show a partially regular distribution of ezrin (e,f).

a-f: Double-immunofluorescence staining of infected cells. green: staining of ezrin; red: streptococci (intra- and extracellular). All images were taken with 100x magnification on a Zeiss AxioImager Fluorescence microscope. The scale bar indicates 10 µm. White arrows indicate a regular distribution of ezrin. White arrowheads indicate cluster formation of ezrin. White asterisks indicate diffuse fluorescence.

↓

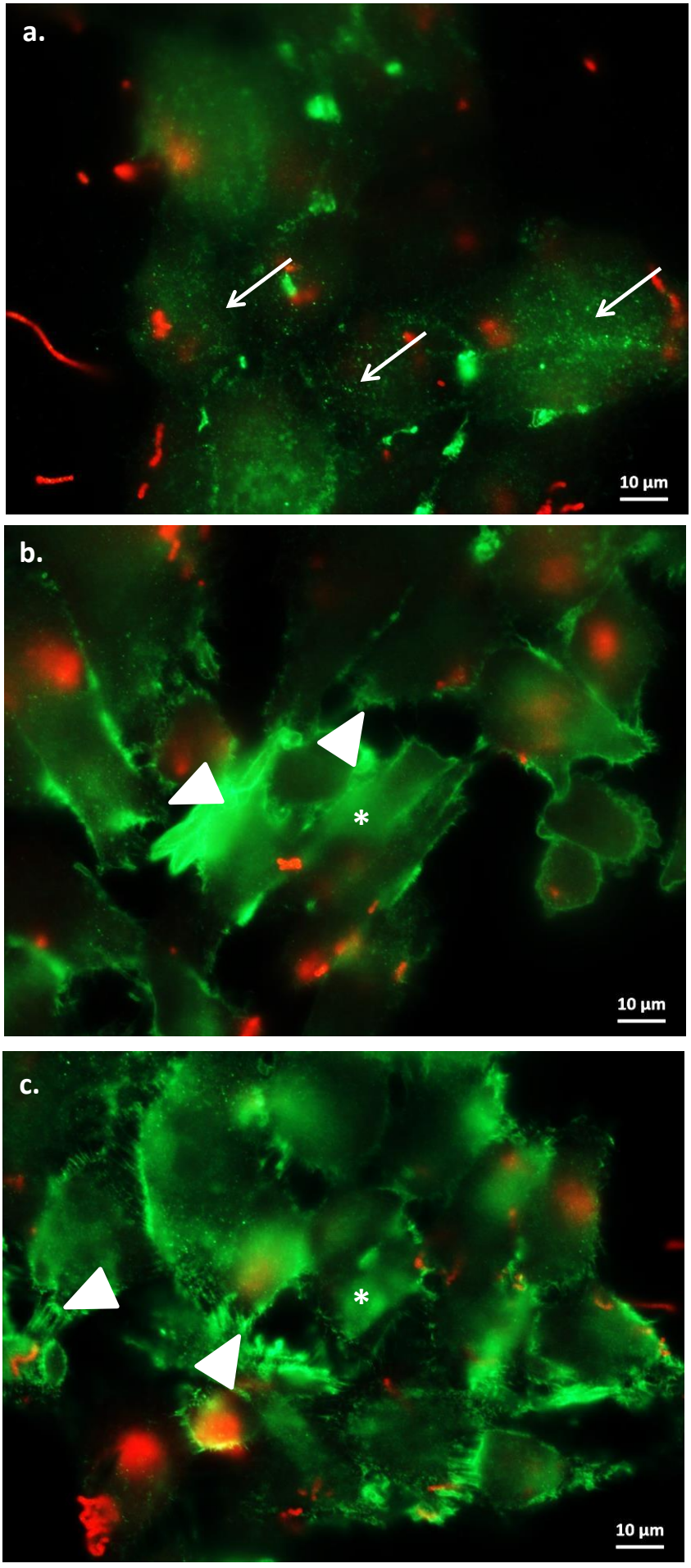
a.
10 µm
b.
*
10 µm
c.
*
10 µm

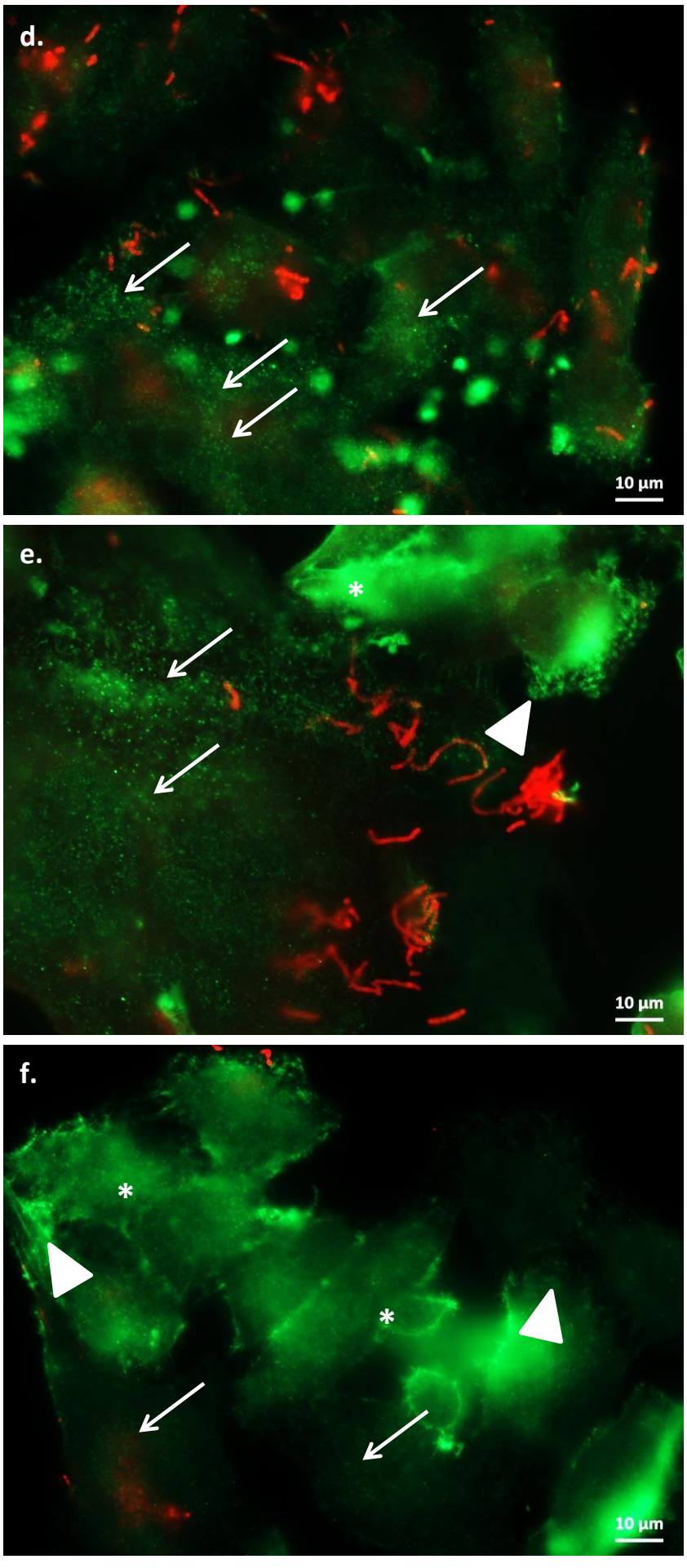
d.
10 µm
e.
*
10 µm
f.
*
*
10 µm

3.2 Salinimyxantins as inhibitors of plasmin(ogen)

3.2.1 SAR-studies on salinimyxantins with regard to inhibition of plasminogen activation

Five related and novel compounds named 'salinimyxantins' were obtained from Dr. Alberto Plaza (MINS, HIPS). As these compounds exhibit unconventional chemical scaffolds for myxobacterial secondary metabolites and as they were not active against gram-positive or gram-negative bacteria (assays performed by Dr. Jennifer Herrmann, MINS, HIPS; data from the myxobase), they were tested for their inhibitory properties with regard to activation of plasminogen. The salinimyxantins sAP01-sAP03 (myxobase keys ##3074, 3064 and 3177) were isolated from the strain MSr9506 (myxobase key #9506, isolated by Dr. Ronald O. Garcia, MINS, HIPS). The compounds sAP04 and sAP05 were obtained by feeding experiments, respectively (performed by Dr. Alberto Plaza, MINS, HIPS). Fig. 3.2-1 shows the molecular structures of the five tested compounds.

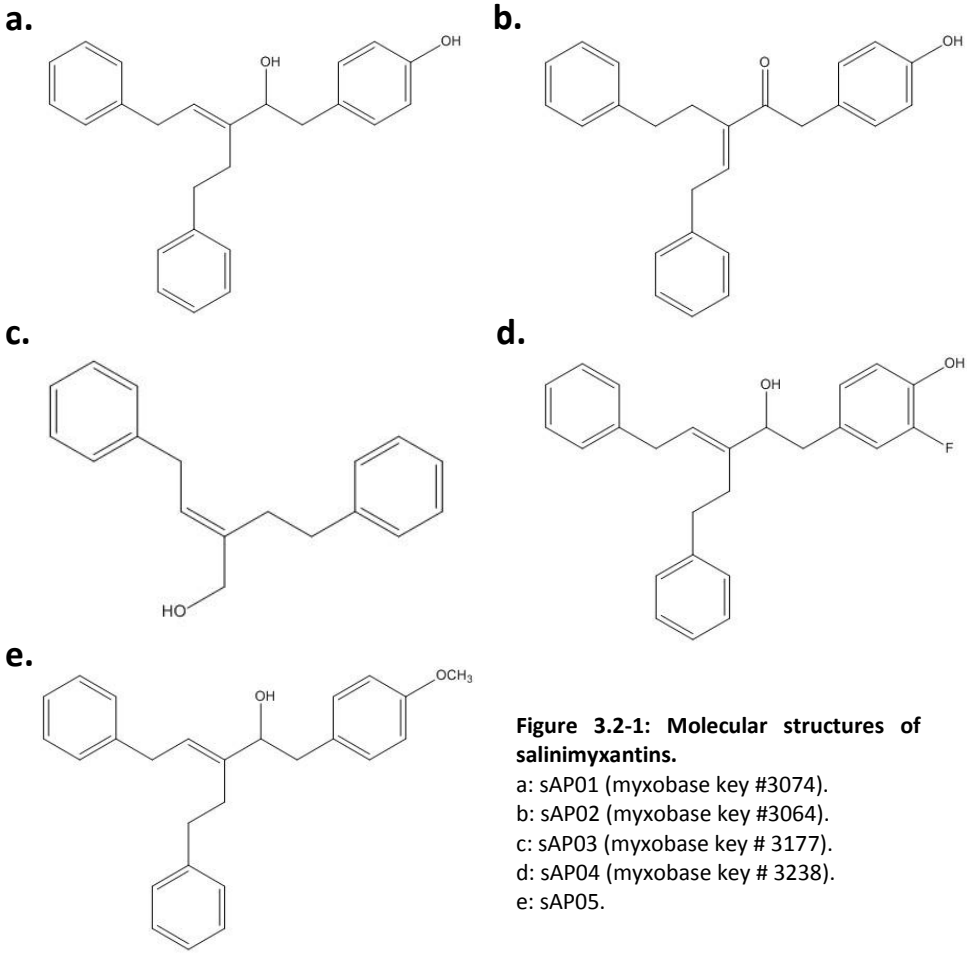

Figure 3.2-1: Molecular structures of salinimyxantins.
a: sAP01 (myxobase key #3074).
b: sAP02 (myxobase key #3064).
c: sAP03 (myxobase key # 3177).
d: sAP04 (myxobase key # 3238).
e: sAP05.

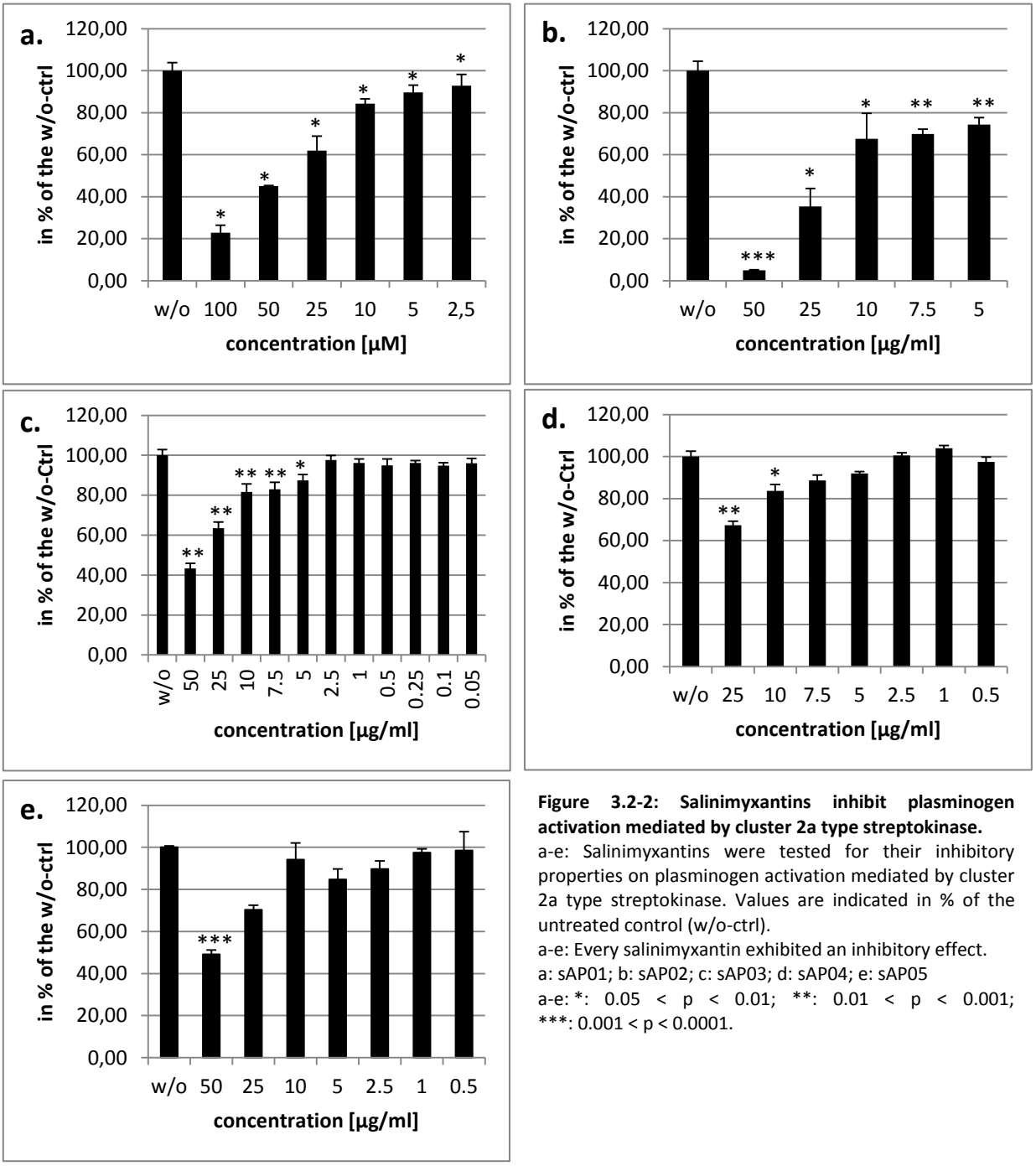

Figure 3.2-2: Salinimyxantins inhibit plasminogen activation mediated by cluster 2a type streptokinase.
a-e: Salinimyxantins were tested for their inhibitory properties on plasminogen activation mediated by cluster 2a type streptokinase. Values are indicated in % of the untreated control (w/o-ctrl).
a-e: Every salinimyxantin exhibited an inhibitory effect.
a: sAP01; b: sAP02; c: sAP03; d: sAP04; e: sAP05
a-e: *: 0.05 < p < 0.01; **: 0.01 < p < 0.001; ***: 0.001 < p < 0.0001.

Initially, it was assessed if the compounds are able to inhibit plasminogen activation by cluster 2a type streptokinase. This cluster type was chosen as it has been shown that cluster 2a type streptokinase (besides cluster 1 type streptokinase) predominantly causes lethality in a murine infection model (Cook *et al.*, 2012) (for a detailed elaboration on the cluster type of the different strains used in this study vide section 6.1).

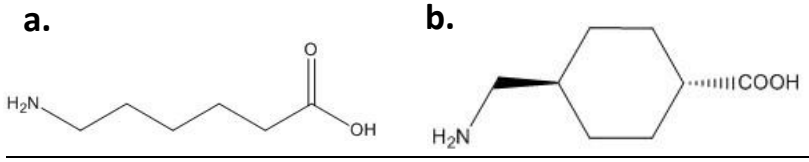

Figure 3.2-3: Molecular structures of EACA and TA.
a: EACA (ε-amino caproic acid)
b: TA (tranexamic acid)

The compound sAP01 showed significant inhibition of plasminogen activation mediated by cluster 2a type streptokinase. The IC_{50} was determined at 25-50 µM (fig. 3.2-2a). Compared to sAP01, the compound sAP02 has a keto- instead of a hydroxyl-group in the carbon chain. sAP02 inhibited plasminogen activation as well and showed an IC_{50} between 10-25 µg/ml (fig. 3.2-2b) which corresponded to 28-70 µM. Compared to sAP01, the compound sAP03 lacks a phenyl-ethyl-group in its scaffold. A reduced IC_{50} of 50 µg/ml (fig. 3.2-2c) corresponding to 198 µM was detected for sAP03. The compound sAP04 has a Fluor-atom in meta-position of the hydroxyl-phenyl-ring. It inhibited plasminogen activation only weakly and had an IC_{50} higher than 25 µg/ml (fig. 3.2-2d) corresponding to an IC_{50} higher than 66 µM. Instead of a hydroxyl-group like in sAP01, sAP05 carries a methoxy-group in para-position in the phenyl-ring. The IC_{50} for sAP05 was determined at around 50 µg/ml (fig. 3.2-2e) corresponding to 134 µM. Structure modifications from the lead structure of sAP01 led to a loss of activity: substituents in the hydroxyl-phenylring withdrawing electrons from the ring (like sAP04) led to higher IC_{50}-values. By contrast, substituents that move electrons into the ring (sAP05) had effects comparable to those of sAP01. Loss of a phenyl-ethyl-group led to a dramatic decrease of activity (sAP03). Therefore, this part is as essential as the hydroxyl-phenyl-group. However, modification of the hydroxyl-group in the carbon chain to a keto-group led to comparable activity (sAP02; fig. 3.2-2).

Tranexamic acid (TA) and ε-amino caproic acid (EACA) were tested as they are known inhibitors of plasminogen activation (Alkjaersig *et al.*, 1959; Markus *et al.*, 1979). Both substances have a carboxylic acid and an amino group (fig. 3.2-3). EACA showed an IC_{50} of more than 1 mM (fig. 3.2-4)

Figure 3.2-4: EACA and TA inhibit plasminogen activation mediated by cluster 2a type streptokinase.
EACA and TA were tested for their inhibitory properties on plasminogen activation mediated by cluster 2a type streptokinase. Values are indicated in % of the untreated control (w/o-ctrl).
TA was more active in inhibition of plasminogen activation mediated by cluster 2a type streptokinase than EACA.

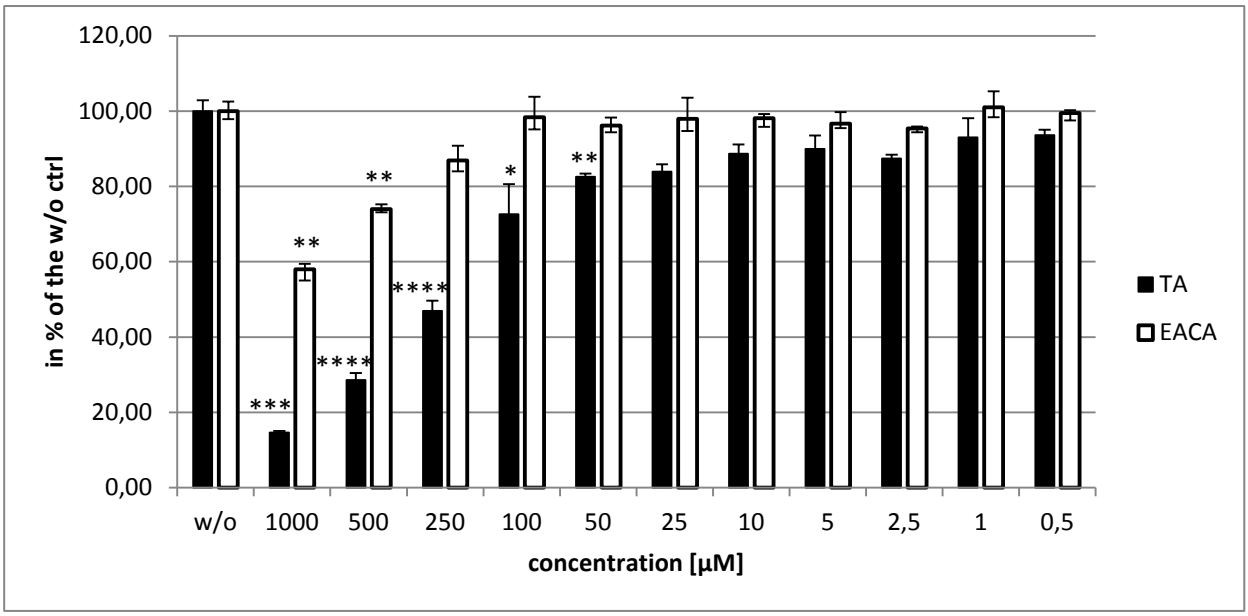

whereas TA showed an IC_{50} of around 250 µM (fig. 3.2-4). Compared to TA, sAP01 has a 5fold stronger activity. In correlation to EACA it is 20fold more active (IC_{50} for sAP01: 25-50 µM).

Furthermore, sAP01 was tested against a cluster 2b type streptokinase. Yet, at a concentration of 50 µM only 20 % of the activity was inhibited (fig. 3.2-5a). At a concentration of 1 mM EACA also inhibited the activity of the cluster 2b type streptokinase by 20 % (fig. 3.2-5b). By contrast, TA achieved an inhibition of about 30 % at a concentration of 1 mM (fig. 3.2-5b). In general, the IC_{50}-values for cluster 2b type streptokinase were much higher than the ones of cluster 2a type streptokinase.

Besides streptokinase, there are also other activators of plasminogen like uPA, tPA or staphylokinase. The salinimyxantins were also tested against these activators in order to detect potential inhibitory effects.

EACA and TA were tested against uPA and tPA (in concentrations ranging up to 25 µM). However, no inhibitory activity was detected (fig. 3.2-6a,b). Though, TA showed an IC_{50} of about 25 µM when plasminogen was activated by staphylokinase. EACA inhibited plasminogen activation by staphylokinase at a concentration of 25 µM by only 20 %. Therefore, the IC_{50} of EACA was higher than 25 µM (fig. 3.2-6c).

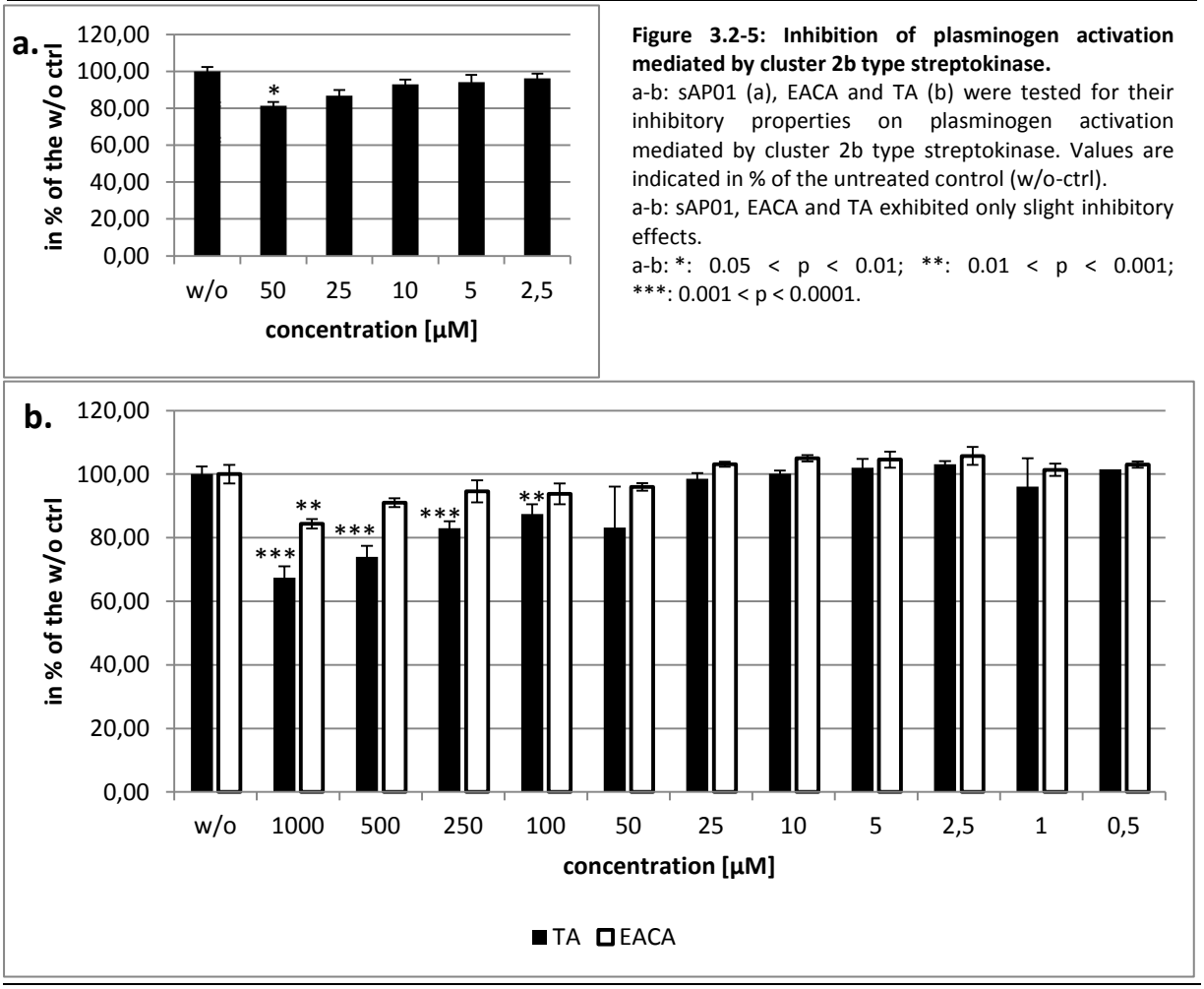

Figure 3.2-5: Inhibition of plasminogen activation mediated by cluster 2b type streptokinase.
a-b: sAP01 (a), EACA and TA (b) were tested for their inhibitory properties on plasminogen activation mediated by cluster 2b type streptokinase. Values are indicated in % of the untreated control (w/o-ctrl).
a-b: sAP01, EACA and TA exhibited only slight inhibitory effects.
a-b: *: 0.05 < p < 0.01; **: 0.01 < p < 0.001; ***: 0.001 < p < 0.0001.

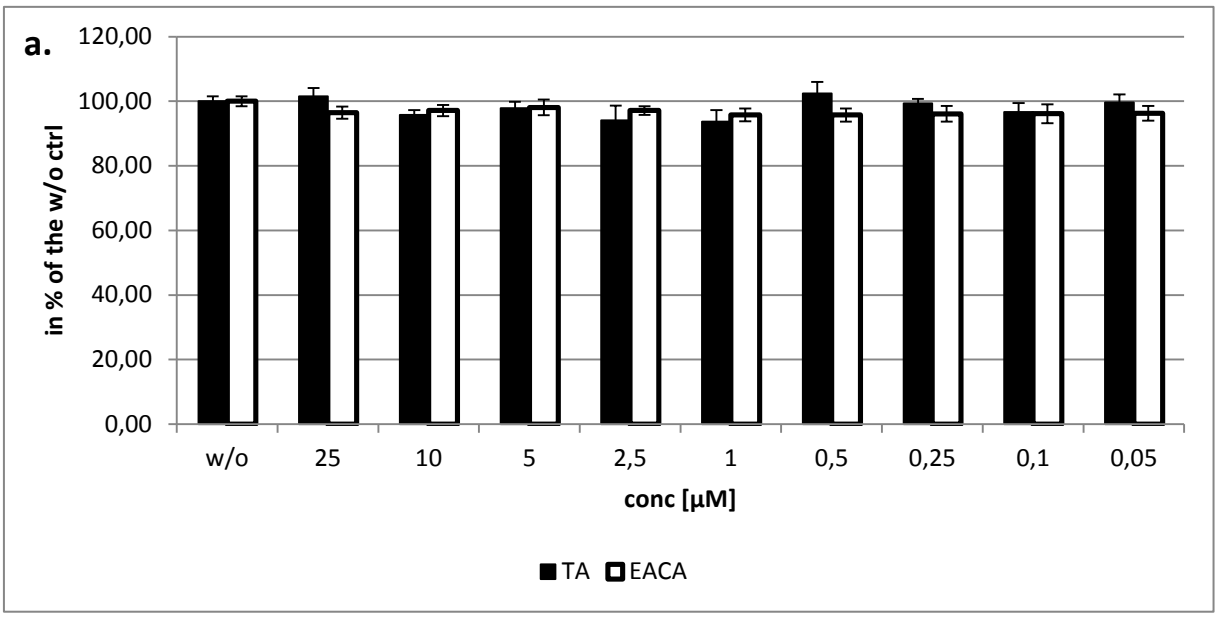
a.
120,00
100,00
80,00
60,00
40,00
20,00
0,00
in % of the w/o ctrl
w/o
25
10
5
2,5
1
0,5
0,25
0,1
0,05
conc [µM]
TA
EACA

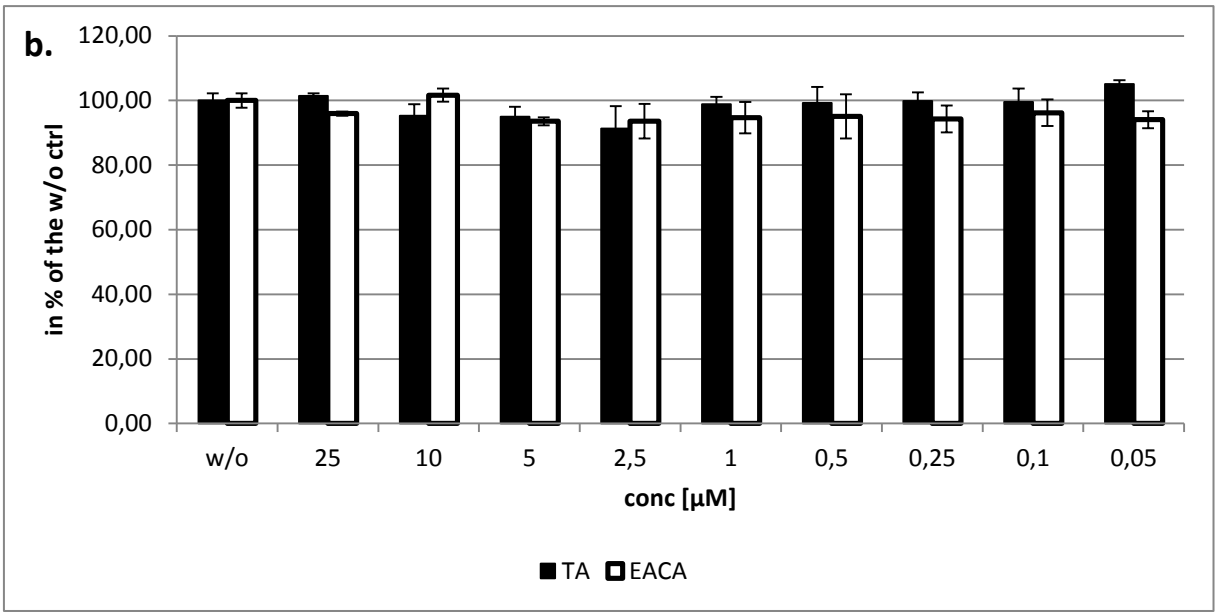
b.
120,00
100,00
80,00
60,00
40,00
20,00
0,00
in % of the w/o ctrl
w/o
25
10
5
2,5
1
0,5
0,25
0,1
0,05
conc [µM]
TA
EACA

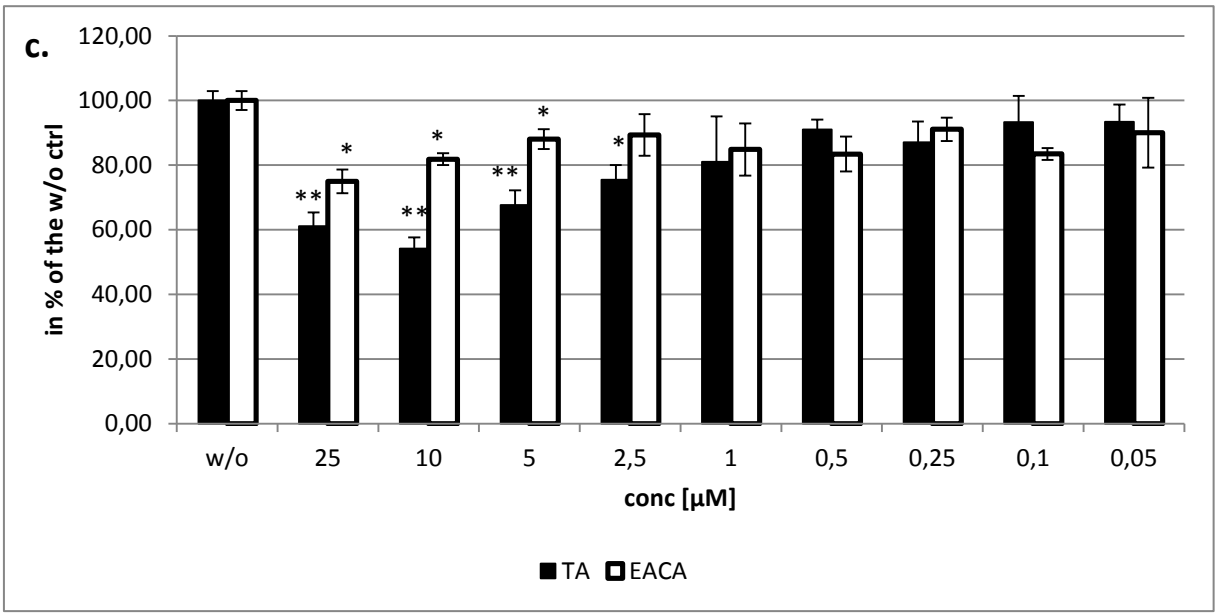
c.
120,00
100,00
80,00
60,00
40,00
20,00
0,00
in % of the w/o ctrl
**
*
w/o
25
10
5
2,5
1
0,5
0,25
0,1
0,05
conc [µM]
TA
EACA

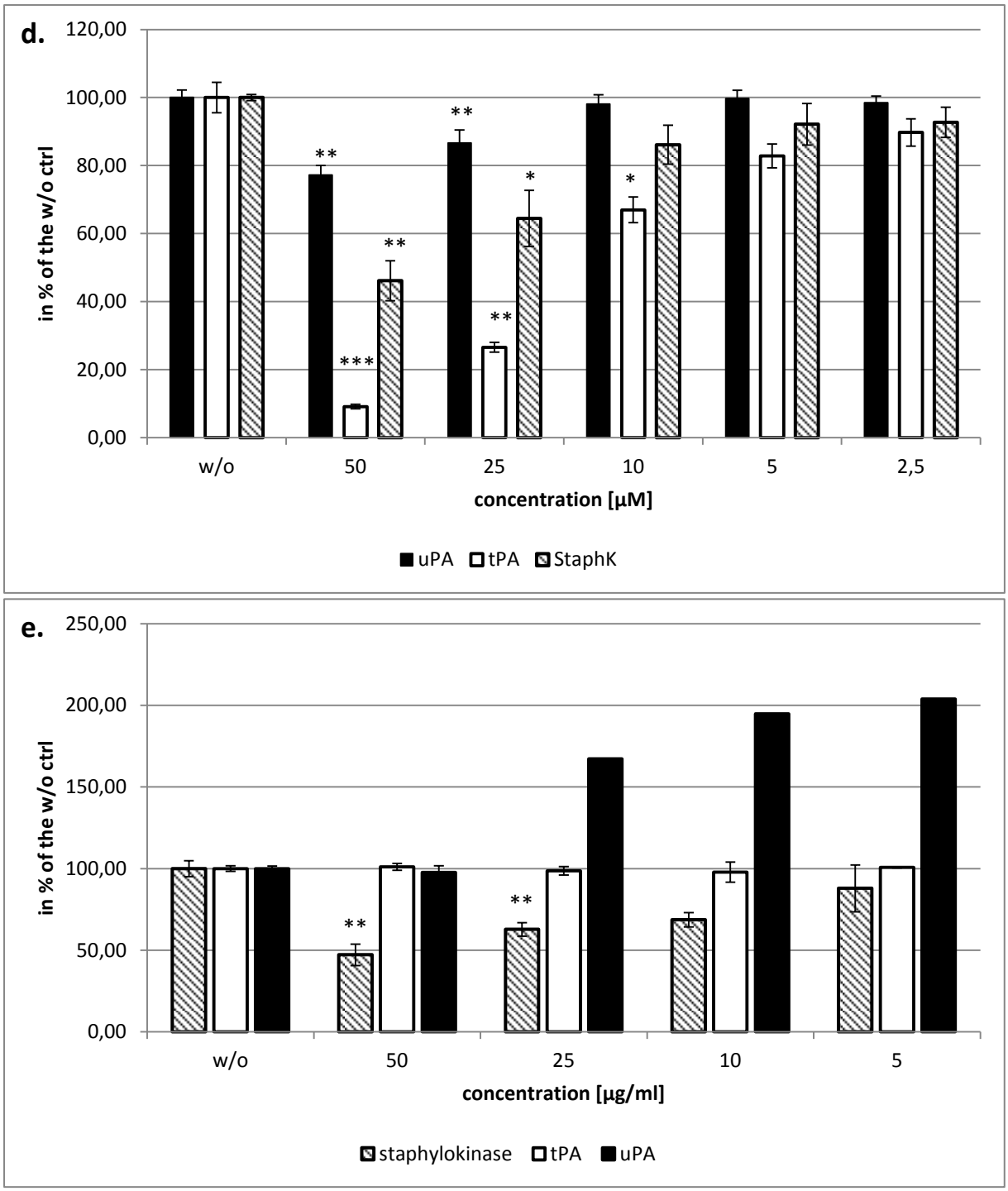

Figure 3.2-6: Effects of EACA, TA, sAP01 and sAP05 on plasminogen activation mediated by uPA, tPA and staphylokinase.
a-e: EACA, TA, sAP01 and sAP05 were tested for their inhibitory properties on plasminogen activation mediated by uPA, tPA and staphylokinase. Values are indicated in % of the untreated control (w/o-ctrl).
a-b: TA and EACA were not able to inhibit plasminogen activation via uPA (a) or tPA (b). c: Plasminogen activation was inhibited by EACA or TA when plasminogen was activated by staphylokinase. d: sAP01 inhibited plasminogen activation by uPA, tPA and staphylokinase. e: sAP05 inhibited plasminogen activation mediated by staphylokinase whereas no effect was observed upon activation via uPA or tPA.
a-e: $0.05 < p < 0.01$; **: $0.01 < p < 0.001$; ***: $0.001 < p < 0.0001$.

sAP01 inhibited plasminogen activation mediated by all three activators: uPA, tPA and staphylokinase. However, different IC_{50}-values were detected for each activator: for uPA the

IC_{50}-value was higher than 50 µM as the activation was inhibited by only 20 % at this concentration. tPA was inhibited quite efficiently by sAP01. An IC_{50} of 10-25 µM was determined. For staphylokinase an IC_{50} of 50 µM was detected (fig. 3.2-6d).

As the salinimyxantin sAP05 differs only in the methoxy-group compared to sAP01, it was tested for its inhibitory properties with regard to all activators. In contrast to sAP01, sAP05 inhibited only the plasminogen activation mediated by staphylokinase. An IC_{50} of 50 µg/ml (approximately 134 µM) was assessed. uPA and tPA were not inhibited at the concentrations tested for sAP05. Furthermore, at lower concentrations of sAP05 (5-25 µg/ml) plasminogen seemed to be activated more rapidly by uPA in contrast to the untreated control (fig. 3.2-6e).

All activators of plasminogen were inhibited – at least by sAP01. Therefore, it is unlikely that the salinimyxantins target streptokinase exclusively. These results suggest a mode of action in which the target of the salinimyxantins is not streptokinase, but plasminogen or plasmin.

3.2.2 Cytotoxic effects of salinimyxantins are only exhibited at high concentrations

EACA and TA are fatty acid derivatives and used as anti-fibrinolytics on the market (Anonick *et al.*, 1992). Furthermore, they are not cytotoxic. The salinimyxantins were more effective than EACA and TA in the inhibition of plasminogen activation (vide 3.2.1). With regard to possible clinical applications of the salinimyxantins, it was important to assess potential cytotoxic effects.

An MTT assay was performed to measure the viability of cells after 24 h of treatment with only two different salinimyxantins, sAP01 and sAP03: sAP01 is the most effective compound of the salinimyxantins with respect to inhibition of plasminogen activation in this study (vide 3.2.1) whereas sAP03 is structurally different from the other salinimyxantins (fig. 3.2-1). Furthermore, the assay was performed with human umbilical vein endothelial cells (HUVEC). As antifibrinolytics are often administered directly into the blood stream, these cells were chosen to mimic possible effects on physiologically relevant endothelial cells.

Both tested salinimyxantins showed cytotoxic effects at high concentrations, i.e. 50 µM, compared to untreated cells. At concentrations of 5 µM cytotoxic effects were not observed in comparison to untreated cells. Furthermore, sAP03 which lacks a phenyl-ethyl-group was less cytotoxic at higher concentrations, i.e. 25-50 µM, than sAP01 (fig. 3.2-7).

After all, the tested salinimyxantins exhibited no cytotoxic effects at low concentrations.

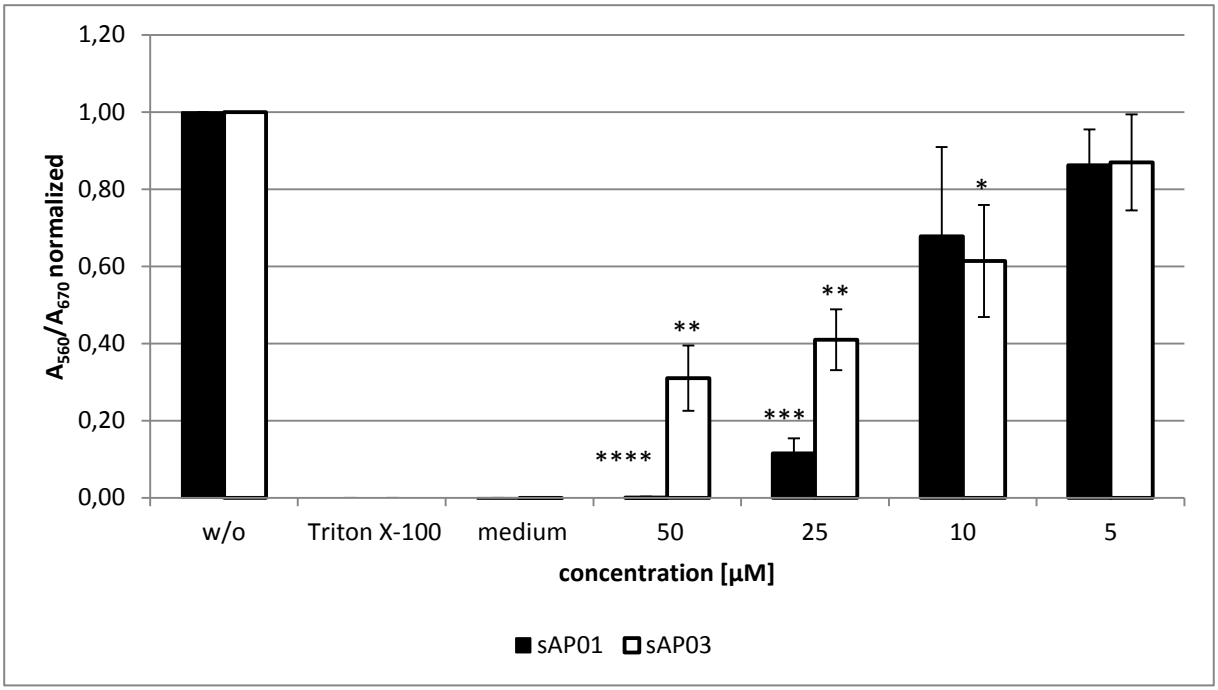

Figure 3.2-7: Effects of two salinimyxantins on viability of HUVEC.
Viability of HUVEC was assessed by performance of an MTT assay. Cells were treated with either sAP01 or sAP03 for 24 h. Untreated cells served as a negative control for maximal cell viability. Cells treated with triton X-100 served as a positive control for maximal cell damage. Another positive control consisted of pure medium without cells.
Treatment of cells with high concentrations of sAP01 or sAP03 decreased cell viability whereas at concentrations of 5 µM almost no decrease in cell viability was observed.
All values were normalized against the untreated uninfected and triton X-100-control. *: $0.05 < p < 0.01$; **: $0.01 < p < 0.001$; ***: $0.001 < p < 0.0001$; ****: $p < 0.0001$

3.2.3 Plasmin as the direct target of the salinimyxantins

Following the results of section 3.2.1, it had to be determined if the salinimyxantins inhibit plasminogen or plasmin directly. Consequently, two salinimyxantins (sAP01 and sAP05) were investigated for their inhibitory properties on plasmin.

First, a fibrinolysis assay was performed. EACA, TA and sAP01 were incubated with a clot before the clot was lysed by plasmin. Clots treated with sAP01 at a concentration of 10 µM did not get lysed entirely 150 min after addition of plasmin. By contrast, clots treated with either EACA or TA were almost lysed completely. Although TA seemed to prevent clot lysis initially, it was lysed after 150 min. An initial decrease of the clot was observed for sAP01. Though, after 30 min the clot increased again. Therefore, sAP01 started to exhibit its full inhibitory activity against plasmin as recently as after 30 min. sAP01 was the only substance in this assay preventing complete clot destruction (fig. 3.2-8a).

EACA and TA are known inhibitors of plasminogen: they interact with lysine-binding sites of plasminogen and thereby, inhibit activation (Alkjaersig *et al.*, 1959; Markus *et al.*, 1979). For both substances (EACA and TA) no direct inhibition of plasmin was observed at concentrations ranging up to 1 mM (fig. 3.2-8b).

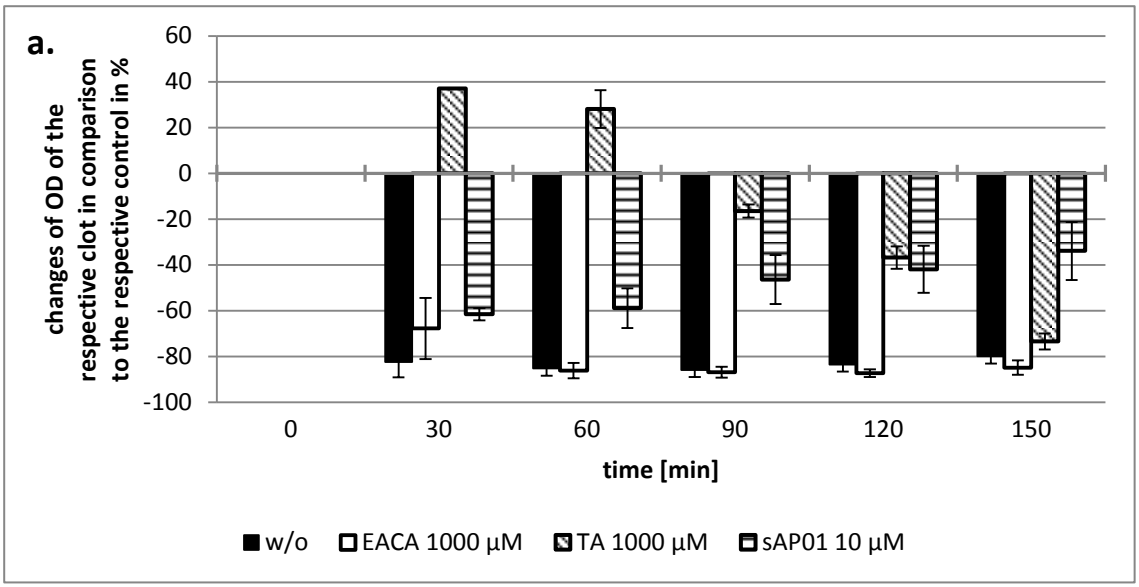
a.
changes of OD of the respective clot in comparison to the respective control in %
60
40
20
0
-20
-40
-60
-80
-100
0
30
60
90
120
150
time [min]
w/o
EACA 1000 µM
TA 1000 µM
sAP01 10 µM

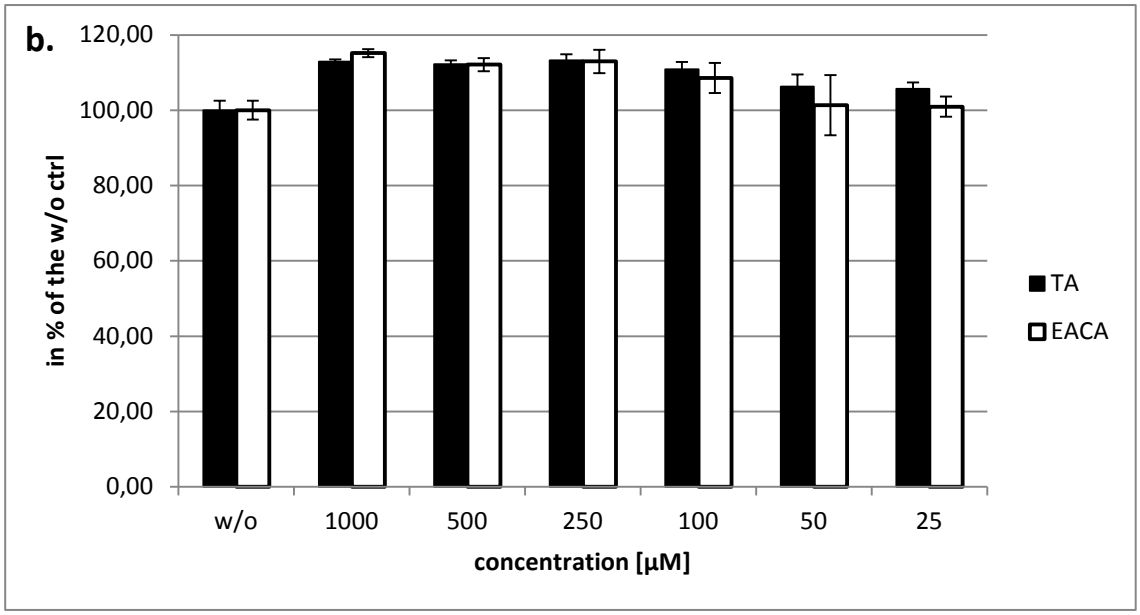
b.
in % of the w/o ctrl
120,00
100,00
80,00
60,00
40,00
20,00
0,00
w/o
1000
500
250
100
50
25
concentration [µM]
TA
EACA

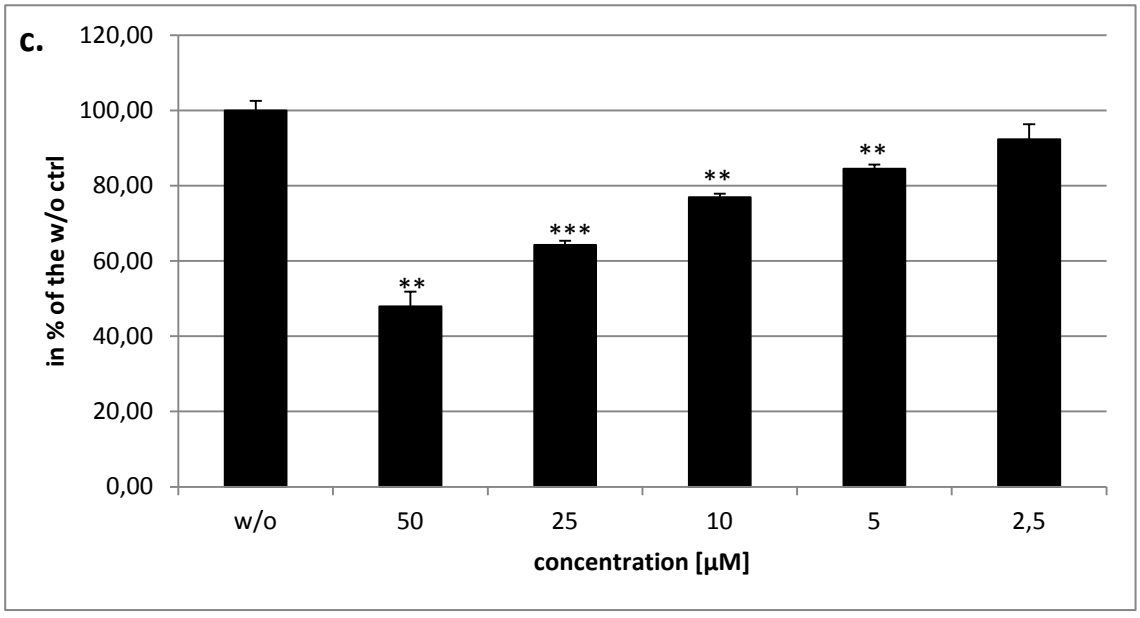
c.
in % of the w/o ctrl
120,00
100,00
80,00
60,00
40,00
20,00
0,00
**
***
**
**
w/o
50
25
10
5
2,5
concentration [µM]

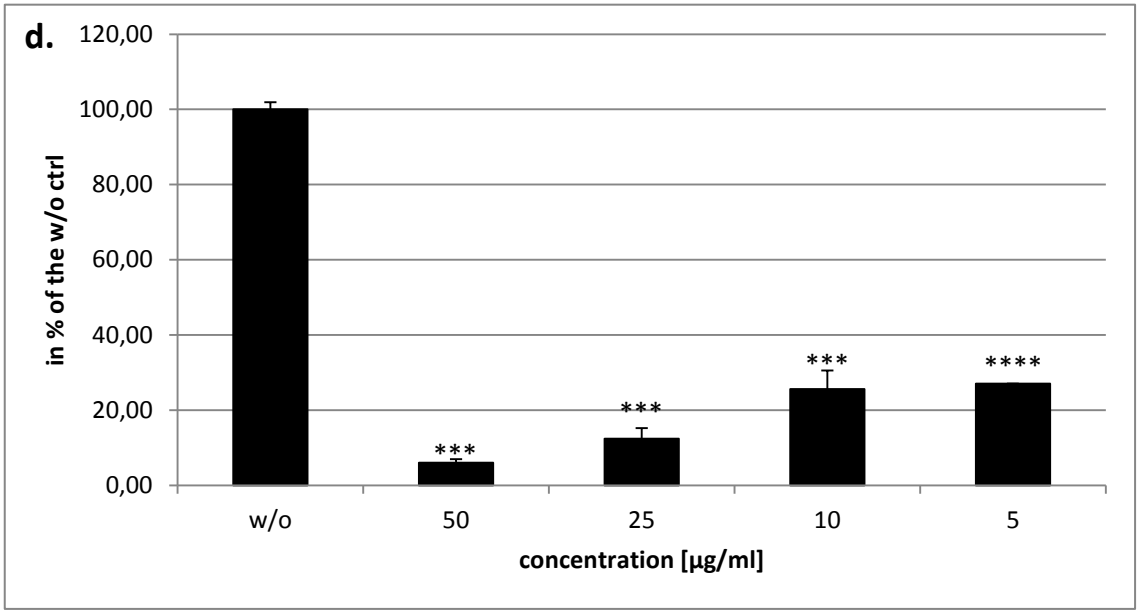

Figure 3.2-8: Plasmin as a direct target of the salinimyxantins.
a: A fibrinolysis assay was performed to test inhibition of plasmin by EACA, TA and sAP01. Turbidity as a result of clot formation or destruction was measured at 405 nm.
b-d: EACA, TA (a), sAP01 (b) and sAP05 (c) were tested for their inhibitory properties on plasmin. Values are indicated in % of the untreated control (w/o-ctrl).
a: sAP01 was the only tested compound which prevented complete clot destruction. b: EACA and TA did not inhibit plasmin. c: sAP01 inhibited plasmin. d: sAP05 diminished plasmin activity by 70-90 %.
a-c: **: $0.01 < p < 0.001$; ***: $0.001 < p < 0.0001$; ****: $p < 0.0001$

By contrast, both tested salinimyxantins inhibited plasmin (fig. 3.2-8c,d). While an IC_{50} of 50 µM was detected for sAP01 which is similar to the IC_{50} of plasminogen activation mediated by cluster 2a type streptokinase (vide 3.2.1), sAP05 was more potent: the IC_{50} was lower than 5 µg/ml, approximately 13 µM. sAP05 decreased plasmin activity by approximately 70 % at a concentration of 5 µg/ml.
As especially sAP05 exhibited a higher inhibitory activity against plasmin than against activators of plasminogen, it is likely that plasmin is the direct target of the salinimyxantins.

3.3 Fatty acids as inhibitors of plasmin(ogen)

3.3.1 Screening reveals several extracts as inhibitors of plasminogen activation via streptokinase

About 600 myxobacterial extracts and 300 myxobacterial compounds were screened for their inhibitory properties in a plasminogen activation assay. Whereas no compound within the screened compound library was active, nine extracts showed significant activity. After validation of these nine 'hit extracts', they were replicated and tested again. All replicated extracts inhibited plasminogen activation via streptokinase (fig. 3.3-1a).

To find the compound responsible for the activity, every 'hit extract' was fractionated by RP-HPLC. The thereby obtained fractions were tested in a plasminogen activation assay. Exemplarily, the results of the fractionation of the extract of strain Anm9 are displayed (fig. 3.3-1b): activity was found at a retention time between 26.5-26 min. The other eight extracts showed activity at similar retention times (data not shown). Consequently, the HPLC chromatograms of the respective strains were examined for peaks at the abovementioned retention times. As depicted in fig. 3.3-1c,d activity was assigned to two peaks which elute directly one after another: for the strain Anm9 activity was correlated with these twin peaks at 25.9 min and 26.6 min (fig. 3.3-1c); for the strain Pl6894 activity was correlated with these twin peaks at 25.7 min and 26.4 min (fig. 3.3-1d). According to the activity assays and to the chromatograms for every tested active extract, these twin peaks were responsible for the activity in all active strains.

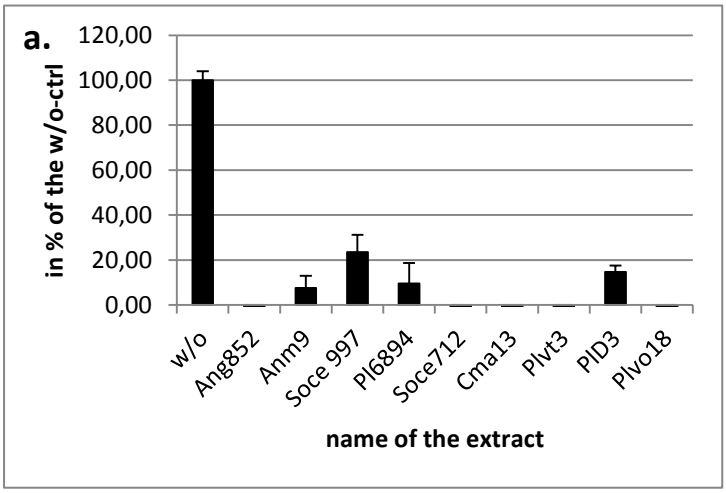

Figure 3.3-1: Myxobacterial extracts inhibit plasminogen activation.
a: Replicated extracts of the indicated strains were tested in a plasminogen activation assay. All extracts showed significant inhibitory activity compared to an untreated control (w/o-ctrl). Values are indicated in % of the w/o-ctrl.
b: Fractions of the extract of Anm9 were tested in a plasminogen activation assay. Results from the fractions at retention times from 18-27 min are displayed. The crude extract was tested as a positive control. Fractions at retention times from 25.0-26.5 min showed good inhibitory activity (and are indicated as white bars). Values are given in % of the w/o-ctrl.
c,d: HPLC-chromatogram of the extract of Anm9 (c) and Pl6894 (d). For both extracts activity was assigned to the same peaks (indicated by black arrows). Peaks were detected at 210 nm.

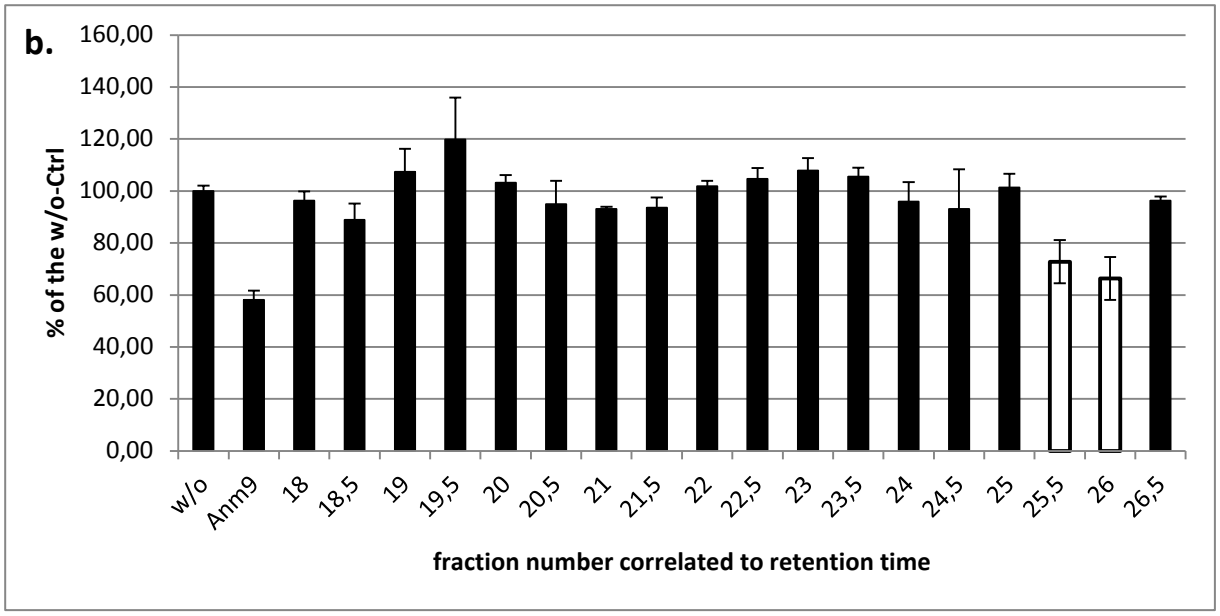
b.
160,00
140,00
120,00
100,00
80,00
60,00
40,00
20,00
0,00
% of the w/o-Ctrl
w/o
Anm9
18
18,5
19
19,5
20
20,5
21
21,5
22
22,5
23
23,5
24
24,5
25
25,5
26
26,5
fraction number correlated to retention time

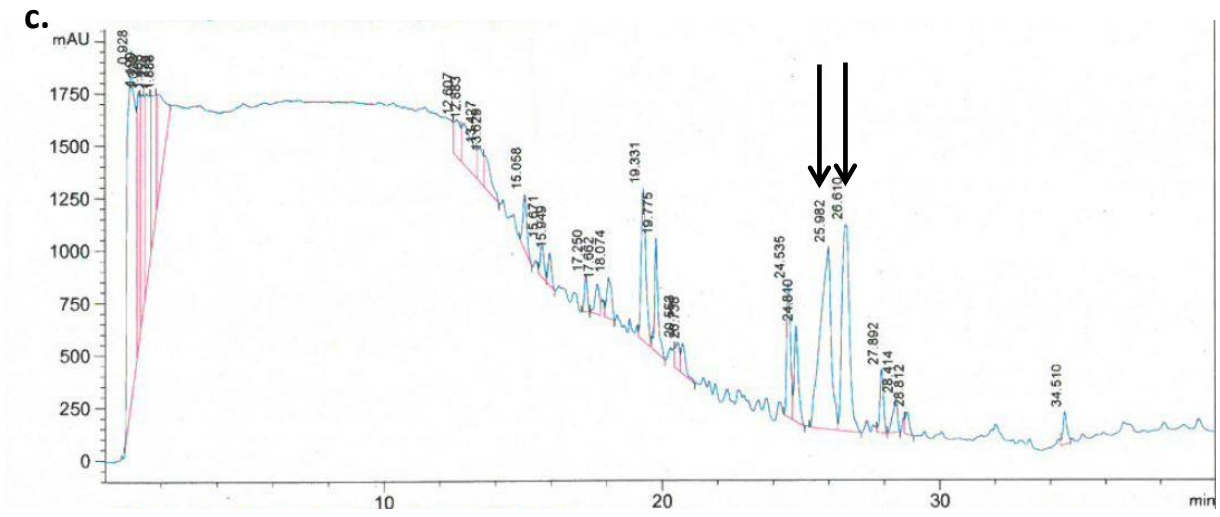
c.
mAU
1750
1500
1250
1000
750
500
250
0
10
20
30
min

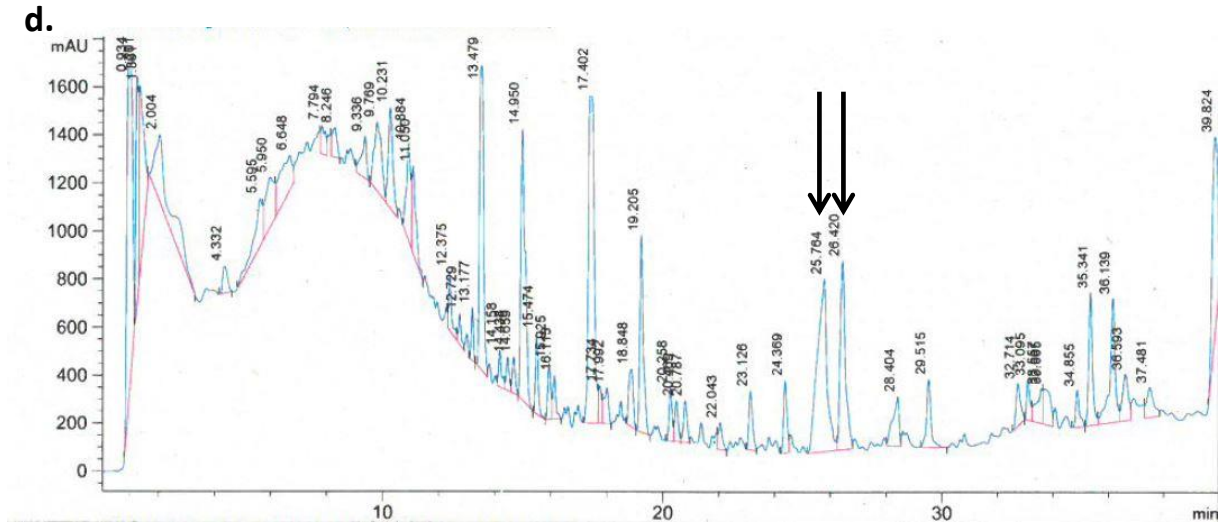
d.
mAU
1600
1400
1200
1000
800
600
400
200
0
10
20
30
min

3.3.2 Active compounds are efficiently purified via LH-20 gel chromatography, RP-MPLC and Si-flash-LC

These twin peaks already had attracted attention in the MWIS group as antibacterial activity against several microorganisms, though in high concentrations only, was found (Dr. Klaus Gerth, MWIS, HZI, personal communication). However, so far their structure had not been elucidated completely. It was known that they are unsaturated fatty acids whereas the location of the double bond(s) had not been determined (NMR by Dr. Rolf Jansen, MWIS, HZI). Furthermore, the fatty acids were not completely purified, but were obtained as enriched fractions.

To determine undoubtedly that those fatty acids were responsible for the inhibitory effects, it was necessary to isolate and purify them. To produce sufficient material for complete structure elucidation and further characterization of the compounds, a large-scale fermentation was performed.

First, a production kinetic was established to estimate the optimal harvest time of the fermenter. The strain 706 (obtained from Dr. Kathrin I. Mohr, MWIS, HZI; so far not classified, belongs to the *Sorangiineae*) also showed the same twin peaks in its chromatogram. As it had already been cultivated in a fermenter once, this strain was chosen. During the fermentation samples were taken daily. Activity of the extract of the strain 706 was already detected 3 days after start of cultivation (fig. 3.3-2a). The activity fluctuated, but did not differ significantly between different harvest points in time. The results also showed that the strain produced the active compounds already on the second day of fermentation (fig. 3.3-2b). Therefore, the active compounds could potentially take part in the primary metabolism. If the active compounds were fatty acids, this could be possible.

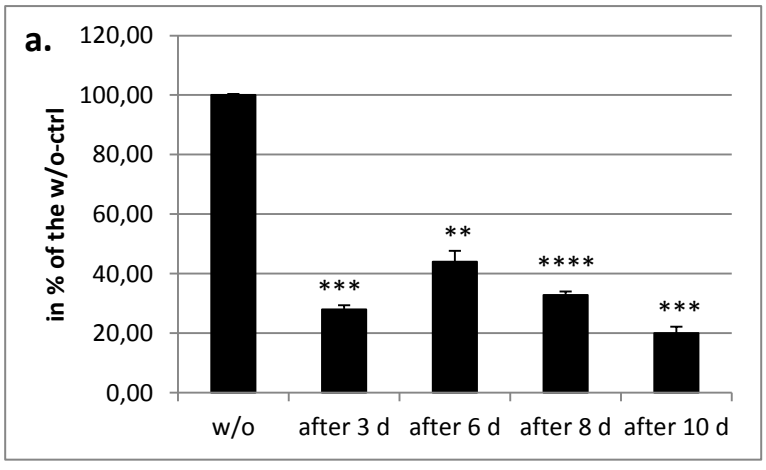

Figure 3.3-2: Extract kinetic of the strain 706.
a,b: Extracts of the strain 706 harvested at different time points were tested in a plasminogen activation assay. Values are indicated in % of the untreated control (w/o-ctrl).
a: Every harvested extract inhibited plasminogen activation.
**: $0.01 < p < 0.001$;
***: $0.001 < p < 0.0001$; ****: $p < 0.0001$.
b: Extracts prepared from a sample taken daily from a fermenter showed that inhibitory activity was already detected on day 1 of fermentation and remained until day 9.

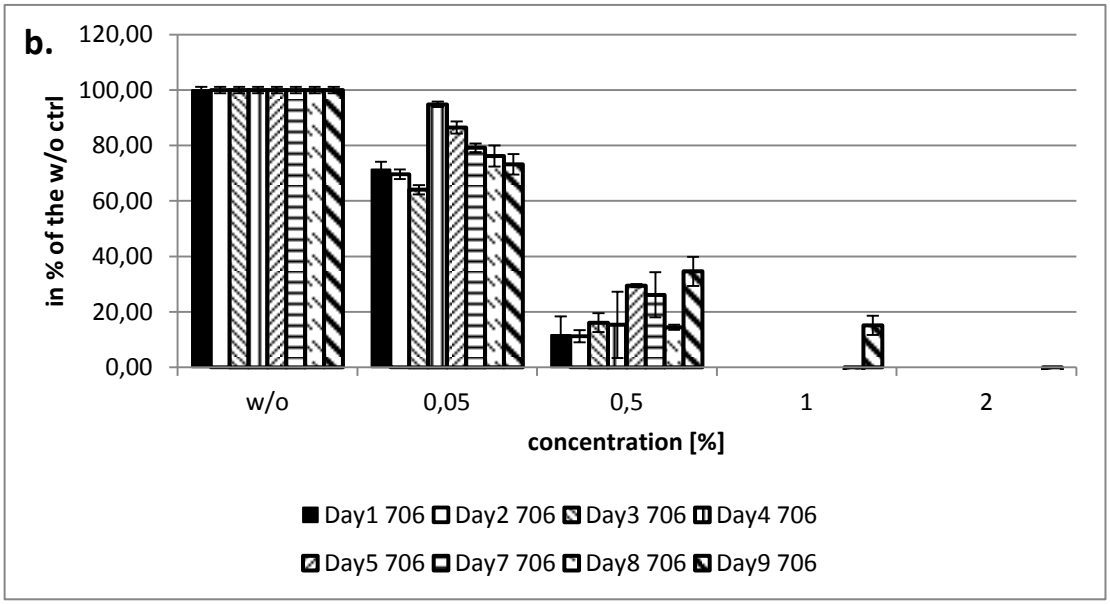

The XAD adsorber resin present during fermentation was harvested and extracted with acetone. After evaporation of the solvent, the wet oily residue was diluted with water and extracted with ethyl acetate. The subsequent isolation of the compounds was activity-guided in correlation with liquid chromatography as analytical method.

The ethyl acetate and the water fraction were both tested in the plasminogen activation assay. Activity was found in the ethyl acetate fraction only (fig. 3.3-3a). In addition, the abovementioned twin peaks were detected in the ethyl acetate fraction (fig. 3.3-3b). Afterwards, the raw extract was partitioned between aqueous methanol and n-heptane. The obtained methanol (RC 23) and n-heptane (RC 24) fractions both showed the twin peaks in the analytical chromatogram (fig. 3.3-3c,d).

RC 23 was separated by LH-20 gel chromatography whereas RC 24 was separated via Si-flash-LC. The fractions RC 23.8 and RC 23.9 showed the best inhibitory activity comparable to the activity of the methanol fraction (RC 23) (fig. 3.3-3e). Furthermore, the Si-flash fractions RC 24.5-24.9 showed an inhibitory activity comparable to the one of the n-heptane fraction (fig. 3.3-3f).

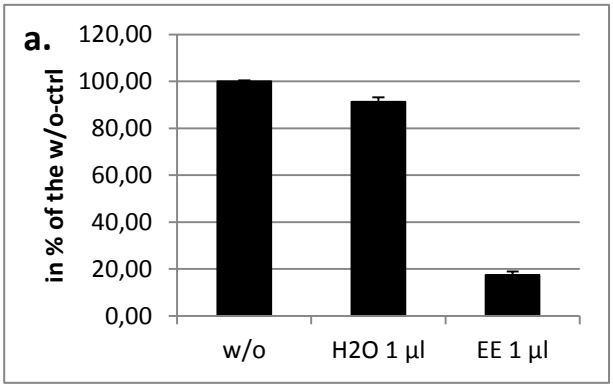

Figure 3.3-3: Extraction and partitioning of the active compounds after fermentation.
a: 1 µl of the H_2O- and the ethyl acetate fraction were tested in a plasminogen activation assay. The ethyl acetate fraction showed inhibitory activity compared to an untreated control (w/o). Values are indicated in % of the untreated control (w/o-ctrl).
b-d: chromatograms (obtained by HPLC) of the ethyl acetate fraction (b), the methanol fraction after partition with n-heptane (c) and the n-heptane fraction (d). Peaks of interest were detected at 210 nm and are indicated by black arrows.

e,f: Fractions of RC 23 (e) and RC 24 (f) were tested in a plasminogen activation assay. The methanol fraction (RC 23) (e) and the n-heptane fraction (RC 24) respectively (f) served as positive controls and are indicated with white bars. Values are indicated as absorption at 405 nm ($A_{405\ nm}$).
e: Fractions RC 23.8 and RC 23.9 showed good inhibitory activity and are indicated by white bars.
f: Fractions RC 24.5-24.9 showed good activity as well and are indicated by white bars.

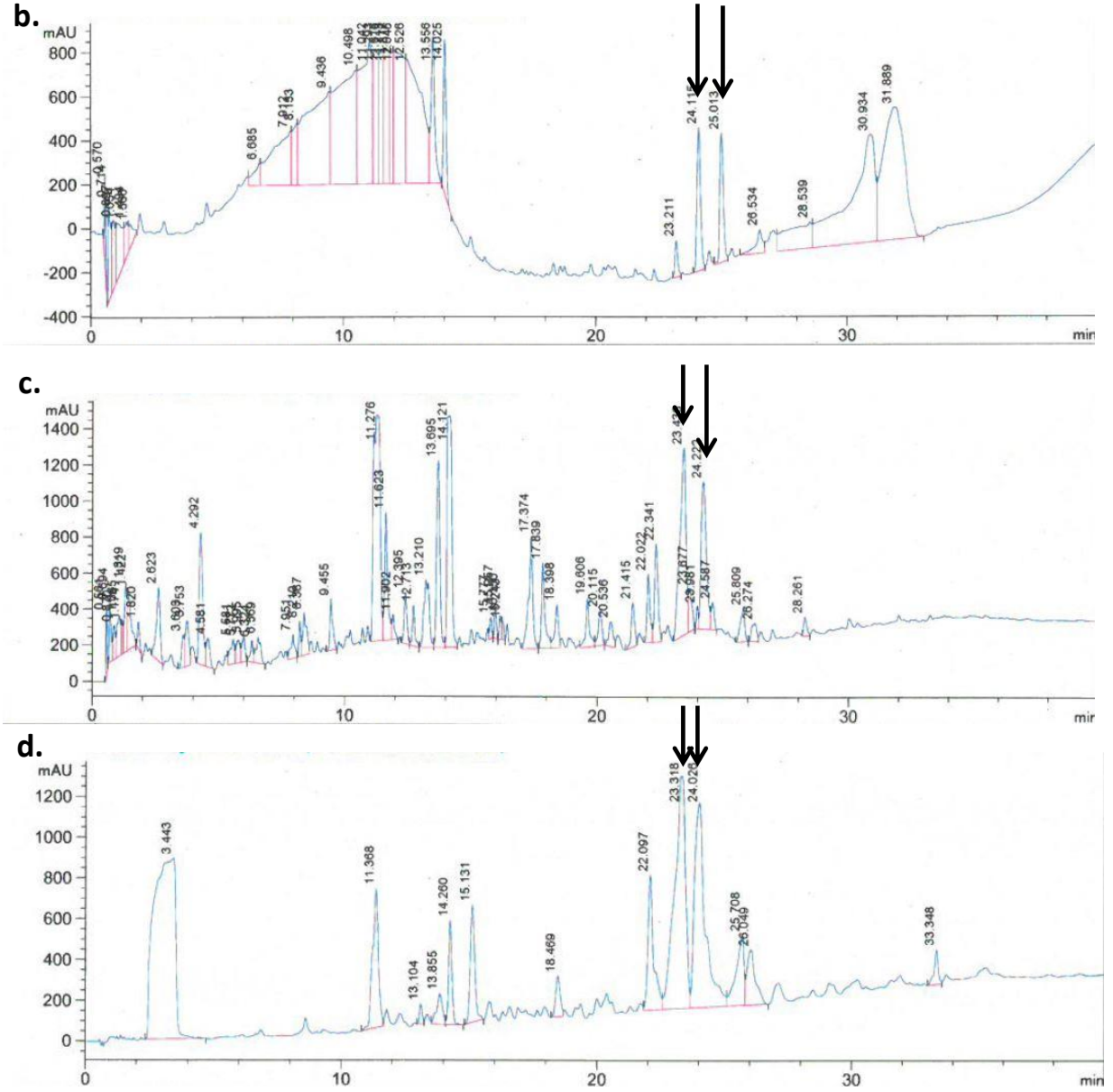

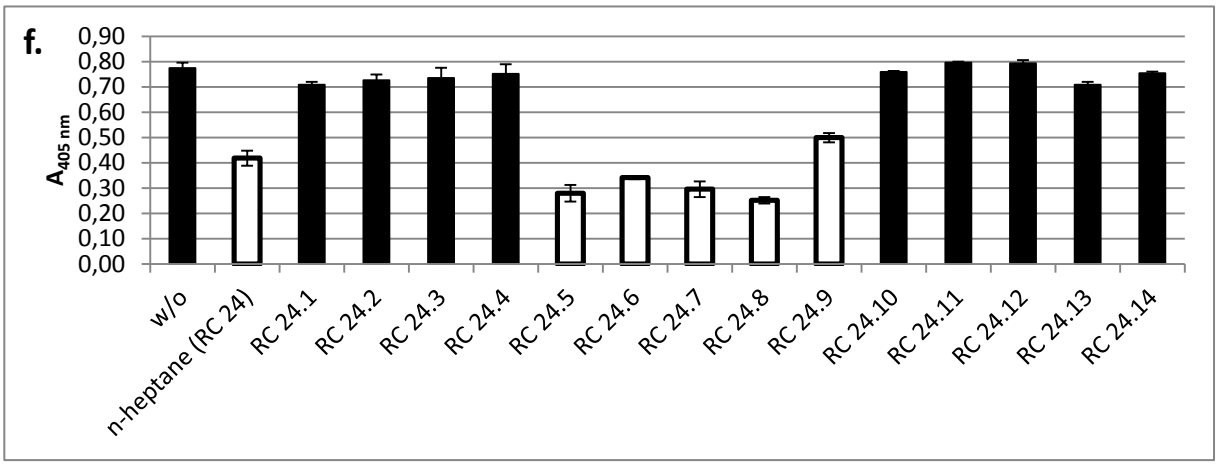

As the chromatograms of all inhibitory fractions contained the twin peaks, one fraction was chosen for further purification: RC 23.8 was separated by RP-MPLC. The fractions were collected according to peaks at 210 nm in the chromatogram. As an example, the detail in the MPLC-chromatogram depicted in fig. 3.3-4a shows the peaks which were collected as fractions RC 25.1-25.3. Next, these fractions were tested for their bioactivity (fig. 3.3-4b). Fractions RC 25.1-25.5 showed excellent inhibitory activity. However, as RC 25.1 and RC 25.3 were the purest fractions with regard to analytical RP-HPLC, these were chosen for further purification by Si-flash-LC.

Fig. 3.3-4c-e show the results of the bioactivity assay: after separation of RC 25.1 several active fractions were detected (RC 26.2-RC 26.6; RC 26.8). Separation of RC 25.3 revealed several active fractions as well (RC 27.5-27.7; RC 27.12-27.13; RC 27.15-27.16; RC 27.19-27.21).

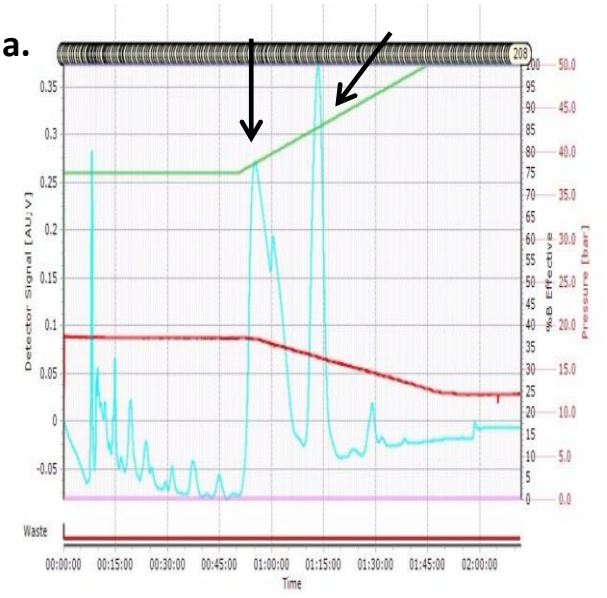

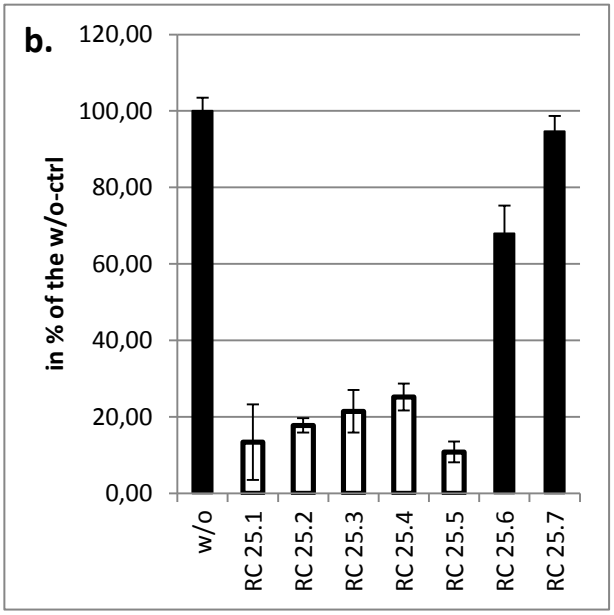

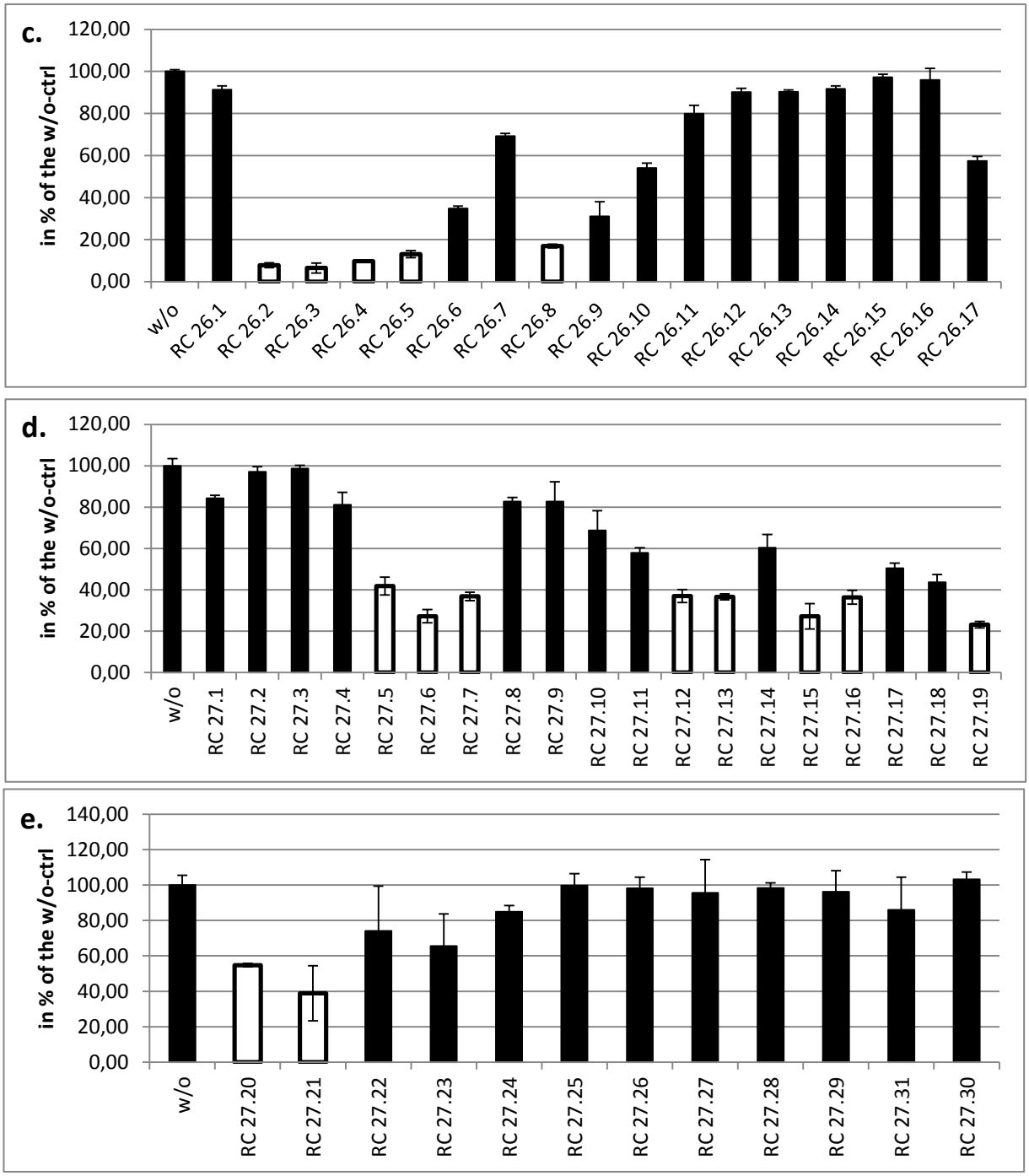

Figure 3.3-4: Purification of active compounds via RP-MPLC and Si-flash-LC.
a,c-e: Plasminogen activation assay of RC 25.1-25.7 (a), RC 26.1-26.17 (c), RC 27.1-27.19 (d) and RC 27.20-27.30 (e). Values are indicated in % of the untreated control (w/o-ctrl). White bars indicate fractions with good activity and were unified and renamed (vide table 3.3-1).
a: RP-MPLC of fraction RC 23.8. Black arrows indicate peaks which were collected as fractions RC 25.1-25.3. Peaks were detected at 210 nm.
b--e: Fractions RC 25.1-25.5 (b), RC 26.2-26.5 (c), RC 26.8 (c), RC 27.5-27.7 (d), RC 27.12-27.13 (d), RC 27.15-27.16 (d) and RC 27.19-27.21 (d,e) showed good activity in comparison to the untreated control (w/o).

As indicated in table 3.3-1, several fractions belonging to the same peak in the chromatogram were united and were renamed afterwards. The fractions RC 28.1-RC 28.6 were analyzed by UPLC to

detect impurities. Two additional fractions, RC 36.1 and RC 36.2, were also obtained by subsequent purification of RC 23.8 as indicated above. RC 36.1 and RC 28.1 are identical as well as RC 28.5 and RC 36.2. RC 28.1, RC 28.5, RC 36.1 and RC 36.2 were sufficiently pure (fig. 3.3-5a,b). Therefore, they were used for characterization in additional bioassays as well as for structure elucidation.

Table 3.3-1: New names of united fractions. The table shows the fractions that were united and the corresponding new name.

fractions that were united	new fraction name
RC 26.2-26.5	RC 28.1
RC 26.8	RC 28.2
RC 27.5-27.7	RC 28.3
RC 27.12-27.13	RC 28.4
RC 27.19-27.21	RC 28.5
RC 27.15-27.16	RC 28.6

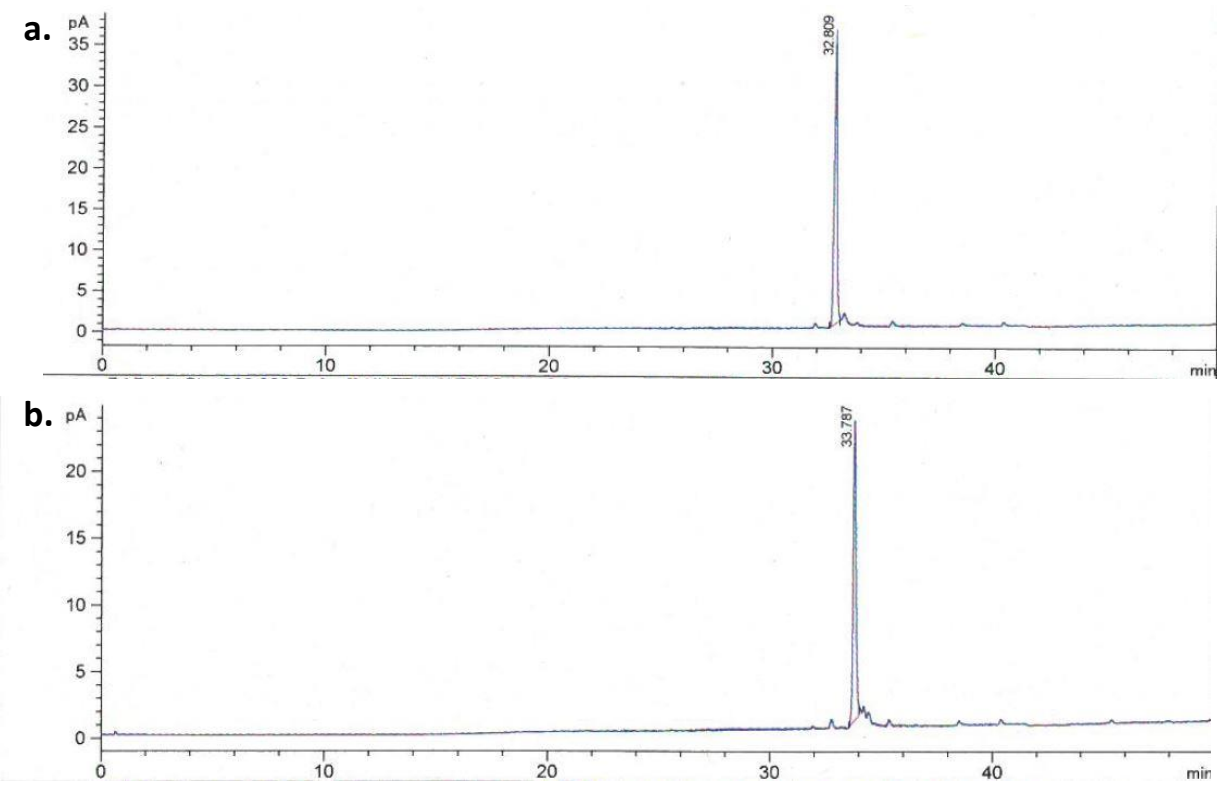

Figure 3.3-5: HPLC-chromatograms of purified compounds.
a-b: HPLC-chromatograms of RC 36.1 (a) and RC 36.2(b). Peaks were detected by a Corona detector.

3.3.3 Structure elucidation of purified compounds reveals fatty acids

A ^{1}H-NMR spectrum had already been recorded of two enriched fractions that contained the abovementioned twin peaks. In these, a fatty acid type was assigned to each peak (performed by Dr. Rolf Jansen, MWIS, HZI).

However, to assess that the purified compounds RC 28.1 and RC 28.5 were fatty acids as well, HR-ESIMS data and more NMR spectra were recorded.

According to the MS data RC 28.1 had the elemental formula $C_{16}H_{30}O_2$ ($[M+H]^+$ *m/z* 255.2327; calcd. 255.2319) whereas the one of RC 28.5 was $C_{18}H_{32}O_2$ ($[M+H]^+$ *m/z* 281.2477; calcd. 281.2475).

Fig. 8-1a,b (section 8.1) show the ^{1}H- and ^{13}C-NMR spectra of RC 28.1. The ^{13}C-NMR spectrum supported the assumption that RC 28.1 is a C_{16}-carboxylic acid: signals for 16 carbon atoms were found, among those a characteristic signal of a terminal carboxylic acid (δ_{COOH} = 178.3 ppm) and several signals neighboring the acid carbon (tab. 3.3-2). Furthermore, two signals for double bond C atoms were detected (tab. 3.3-2) beside several signals of C atoms in an unbranched carbon chain (fig. 8-1b).

In the ^{1}H NMR spectrum of RC 28.1 signals of a terminal methyl group and two protons at double bond C atoms were detected. Additionally, methylene protons in vicinity of the double bond were assigned as well as further methylene protons of the carbon chain (tab. 3.3-2; fig. 8-1a). These findings indicated that RC 28.1 is an unsaturated C_{16}-carboxylic acid with one double bond that is located neither near the terminal acid nor the methyl group.

Table 3.3-2: NMR data of RC 28.1 in $CDCl_3$ (containing traces of CD_3OD). The table shows chemical shifts (δ) given in ppm for C atoms and protons and correlates them with structural elements.

δ_C [ppm]	type	δ_H [ppm]	type
178.3	-**C**OOH	**5.3 (2H)**	**H**-C=C- / -C=C-**H**
130.1	-**C**=C-	**2.3 (2H)**	-C**H$_2$**-COOH
129.8	-C=**C**-	**2.0 (4H)**	-C=C-C**H$_2$**-C / -C-C**H$_2$**-C=C-
33.8	-**C**-COOH	**1.6 (4H)**	-C**H$_2$**-C-COOH
14.1	-**C**H$_3$	**1.3 (14H)**	-C-C**H$_2$**-C-
22.7-31.8 (11C)	-**C**-	**0.9 (3H)**	-C**H$_3$**

Fig. 8-1c,d (section 8.1) show the ^{1}H- and ^{13}C-NMR spectra of RC 28.5. The ^{13}C-NMR spectrum revealed that RC 28.5 is a C_{18}-carboxylic acid: signals for 18 carbon atoms were found including a signal for a terminal carboxylic acid (δ_{COOH} = 176. 3 ppm). Furthermore, four signals were assigned as double bond C atoms (tab. 3.3-3) as well as a signal of a methyl group. Fig. 8-1d also shows several signals for C atoms in a carbon chain.

In the ^{1}H-NMR spectrum of RC 28.5 signals of a methyl group and of four methine protons at double bonds were assigned. Further signals for methylene groups neighboring double bonds were detected

together with signals of several methylene protons in an unbranched carbon chain. In addition, protons of a methylene group neighboring both double bonds were detected (tab. 3.3-3; fig. 8-1c). These spectra indicate that RC 28.5 is an unsaturated C_{18}-carboxylic acid containing two double bonds that are located neither near the carboxylic acid nor the methyl group.

Table 3.3-3: NMR data of RC 28.5 in $CDCl_3$ (containing traces of CD_3OD). The table shows chemical shifts (δ) given in ppm for C atoms and protons and correlates them with structural elements.

δ_C [ppm]	type	δ_H [ppm]	type
176.3	-**C**OOH	**5.4 (2H)**	**H**-C=C- / -C=C-**H**
130.03	-**C**=C-	**5.3 (2H)**	**H**-C=C- / -C=C-**H**
130.01	-**C**=C-	**2.75 (2H)**	-C=C-C**H$_2$**-C=C-
128.1	-C=**C**-	**2.35 (2H)**	-C**H$_2$**-COOH
127.9	-C=**C**-	**2.00 (4H)**	C-C**H$_2$**-C=C- / -C=C-C**H$_2$**-C
14.1	-**C**H_3	**1.6 (2H)**	-C**H$_2$**-C-COOH
22.6-33.4 (12C)	-**C**-	**1.25-1.5 (14H)**	-C-C**H$_2$**-C-
		0.9 (3H)	-C**H$_3$**

Although HR-ESIMS and NMR spectroscopy revealed and confirmed that both compounds were fatty acids, the location of the double bonds was not determined from the spectra. Therefore, different GC-MS derivatization methods were used.

Initially, methyl esters of the respective compound were prepared. Fig. 8-2a (section 8.2) shows the gas-chromatogram (upper part) of the methyl ester of RC 28.1. One major peak at 15.60 min was observed while no major impurities were detected. The lower part of fig. 8-2a shows the MS spectrum of the peak at 15.58 min. The molecular ion $[M+H]^+$ of the methyl ester of RC 28.1 was detected at *m/z* 269.0. Consequently, RC 28.1 has a molecular mass of 254 Da (as also determined by HR-ESIMS, see above). Moreover, an alkyl fragmentation series was observed since *m/z* values were reduced by 14 Da (e.g. m/z 137 → 123 → 109 →95 → 81 → 67) indicating the presence of a carbon chain.

Fig. 8-2b (section 8.2) shows the gas-chromatogram (upper part) of the methyl ester of RC 28.5. Beside the major peak at 19.04 min no significant impurities were detected. The lower part of fig. 8-2b shows the MS spectrum of the peak at 19.02 min. The molecular ion $[M+H]^+$ of the methyl ester of RC 28.5 was observed at *m/z* 295.0. As a result, RC 28.5 has a molecular weight of 280 Da (as already assessed by HR-ESIMS, see above). Furthermore, an alkyl fragmentation series was observed (e.g. m/z 109 → 95→ 81 → 67 and 149 → 135 → 121).

The initial loss of 32 Da for both RC 28.1 and RC 28.5 indicates the elimination of methanol. Moreover, the presence of double bond(s) for both compounds might be the reason for the interruption of the alkyl series for RC 28.5 and the incomplete alkyl series for RC 28.1. However, the

location of a double bond cannot be determined precisely by formation of methyl esters since double bond(s) can change their positions during fragmentation.

Therefore, further derivatization methods were applied. One such method is the derivatization with dimethyl disulfide (DMDS). Fig. 3.3-6 shows the reaction scheme. Upon addition of DMDS, thiomethyl groups are generated at the position of the former double bond. Therefore, the exact location of a double bond can be determined (Dunkelblum *et al.*, 1985; Leonhardt and DeVilbiss, 1985). This method is more suitable for monounsaturated fatty acids because polyunsaturated fatty acids can form thiophen or thiopyran rings which can be substituted by methyl groups as well.

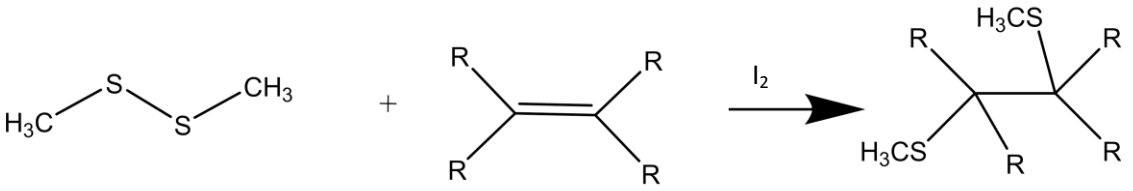

Figure 3.3-6: Schematic reaction of DMDS with a double bond.
DMDS is added to a double bond. Then thiomethyl groups can be found where the double bond was located. Iod serves as a catalyst.

Fig. 8-3 (section 8.2) shows the MS spectrum of the DMDS derivative of RC 28.1. The molecular ion $[M+H]^+$ was detected at *m/z* 361.9 and represents the methyl ester of RC 28.1 with two thiomethyl groups added to the double bond. A fragment ion was detected at *m/z* 217.0 corresponding to fragment **1** (fig. 3.3-7). However, a fragment **2** was not observed in the mass spectrum. Thus, evidence supports the assumption that the double bond of RC 28.1 is located at position 9.

Figure 3.3-7: Possible fragments of the DMDS derivative of RC 28.1
Fragment 1: *m/z* 217; Fragment 2: *m/z* 145 or if positively charged *m/z* 146.

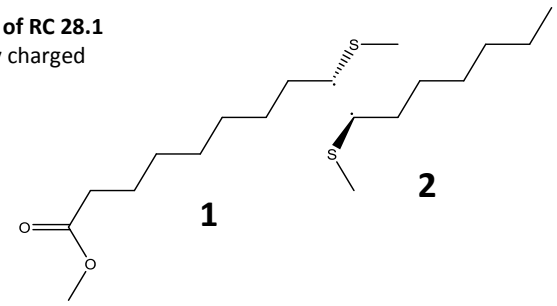

As the location of the double bonds of RC 28.5 could not be analyzed by derivatization with DMDS and as fragment **2** (fig. 3.3-7) was missing in the MS spectrum of the DMDS derivative of RC 28.1, another derivatization was applied: the formation of DMOX (dimethyloxazoline) derivatives. By derivatization of (poly)unsaturated fatty acids to DMOX derivatives, double bonds can be located

because they are disabled to change positions during fragmentation (Fay and Richli, 1991). Fig. 3.3-8 shows the reaction schematically.

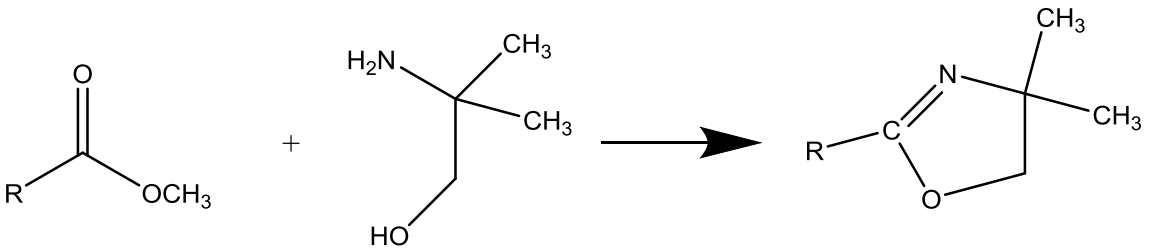

Figure 3.3-8: Schematic formation of DMOX derivatives.
Upon reaction of 2-amino-2-methyl-propan-1-ol with a methyl ester a DMOX derivative is formed.

Fig. 8-4 (section 8.2) shows the GC-chromatograms of the derivatives of RC 36.1 and RC 36.2. It was observed that shortly after the main peak a smaller peak eluted which showed the same MS fragmentation pattern as the main peak (fig. 8-4a,c, marked by black arrows). Possibly, both compounds were mixtures of two fatty acids with different configurations. Though, the later eluting one was only present in small amounts. A blank sample was run as well. It was observed that several impurities were present on the column which were also observed in the chromatogram of RC 36.2 (fig. 8-4b,c).

To determine the location of the double bond(s), DMOX derivatives of RC 36.1 and RC 36.2 were analyzed by GC-MS. For comparison, linoleic acid (LA), linoelaidic acid (LEA), palmitoleic acid (PA) and palmitelaidic acid (PEA) were derivatized as well. These are commercially available C_{18}- and C_{16}-fatty acids, respectively, with double bond(s) in different configurations: LA is a (9*Z*,12*Z*)-octadecadienoic acid whereas LEA is a (9*E*,12*E*)-octadecadienoic acid. PA is a (9*Z*)-hexadecenoic acid whereas PEA is a (9*E*)-hexadecenoic acid.

As depicted in fig. 8-5a (section 8.2) the molecule ion of the DMOX derivative of RC 36.1 was found at *m/z* 307. Characteristic fragments were found as well: fragmentation occurs at the site of the double bond or next to the double bond (*m/z* 196 and 208) indicating that the double bond was located at position 9. Fig. 3.3-9a shows a fragmentation scheme of the DMOX derivative of RC 36.1. The molecule ion of the DMOX derivative of RC 36.2 was detected at *m/z* 333. In addition, characteristic fragments (representing fragmentation next to a double bond or at the site of a double bond) of the derivative of RC 36.2 were observed as well (*m/z* 196, 208, 222, 238 and 262; fig. 8-5b) indicating that the double bonds are located at positions 9 and 12. Fig. 3.3-9b shows the fragmentation scheme of the DMOX derivative of RC 36.2.

As shown in fig. 8-6 (section 8.2) identical MS spectra were recorded for the DMOX derivatives of RC 36.1, PEA and PA as well as for those of RC 36.2, LEA and LA. Therefore, the double bond of

RC 36.1 was assigned to position 9. This result supported the determination by DMDS derivatization (see above). Furthermore, the double bonds of RC 36.2 were assigned to positions 9 and 12.

Moreover, (in the run displayed) PA eluted at 19.54 min whereas PEA eluted at 19.74 min. The main peak of the DMOX derivative of RC 36.1 eluted at 19.55 min and the smaller one at 19.72 min. Therefore, RC 36.1 most likely contained mainly (9*Z*)-hexadecenoic acid and a smaller amount of (9*E*)-hexadecenoic acid (fig. 8-6a; section 8.2).

Furthermore, (in the run displayed) LA eluted at 25.39 min whereas LEA eluted at 25.70 min. The main peak of the DMOX derivative of RC 36.2 eluted at 25.38 min and a smaller peak at 25.71 min. Consequently, one could assume that RC 36.2 contained mainly (9*Z*,12*Z*)-octadecadienoic acid and a smaller amount of (9*E*,12*E*)-octadecadienoic acid (fig. 8-6b,c; section 8.2).

To investigate these assumptions, preliminary experiments regarding plasminogen activation were performed with the commercially available fatty acids (LA, LEA, PA and PA). These data are found in the supplemental information (vide section 6.2).

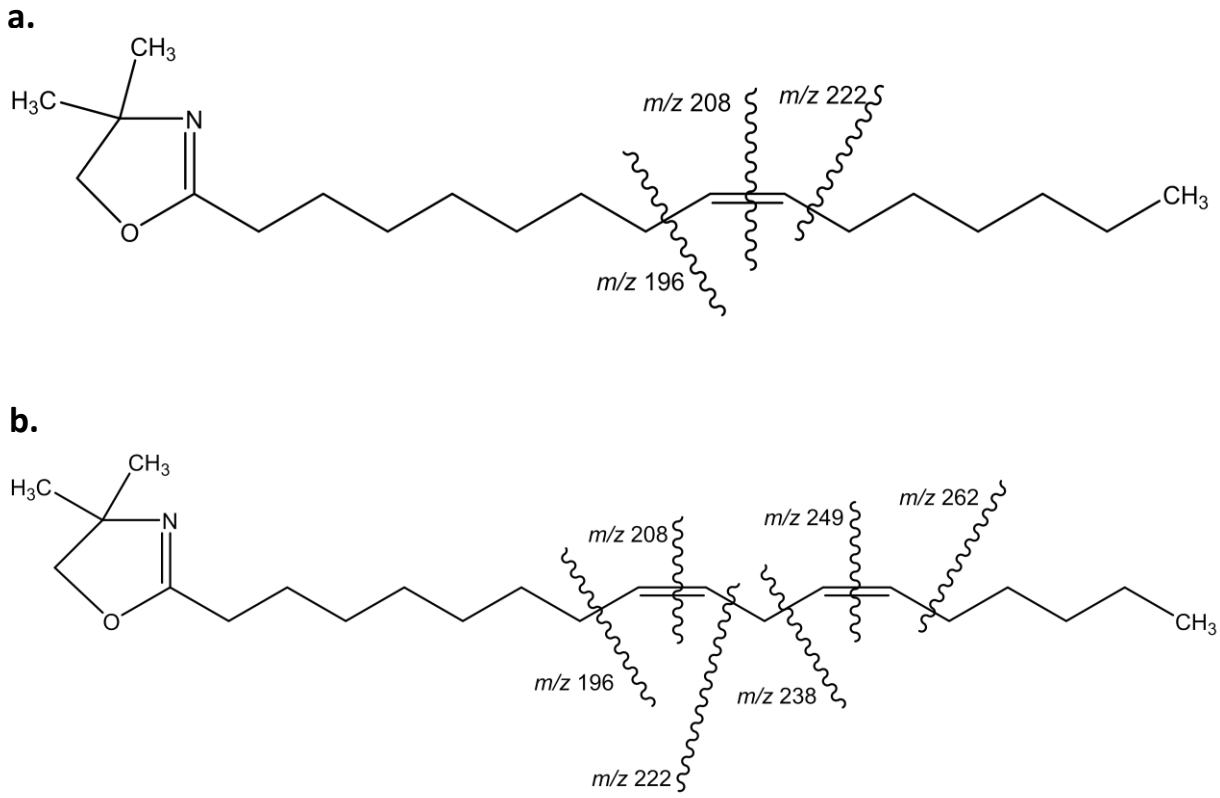

Figure 3.3-9: Indicated fragmentation pattern of DMOX derivatives of RC 36.1 and RC 36.2.
a,b: Upon fragmentation characteristic fragments of DMOX derivatives of RC 36.1 (a) and RC 36.2 (b) can be detected. *m/z* values are indicated next to a wiggled line. These lines indicate the fragmentation pattern.

3.3.4 Isolated fatty acids inhibit the activation of plasminogen

After isolation, purification and structure elucidation the fatty acids (RC 36.1 and RC 36.2) were tested for their inhibitory activity with regard to plasminogen activation.

First, it was assessed if both compounds (RC 36.1 and RC 36.2; molecular structures (in one possible configuration) are displayed in fig. 3.3-10) were able to inhibit plasminogen activation mediated by different cluster types of streptokinase.

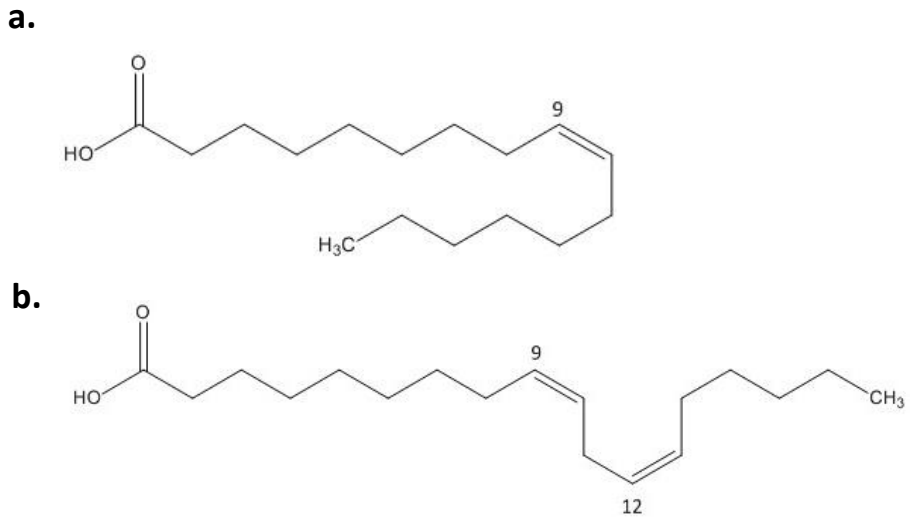

Figure 3.3-10: Molecular structures of RC 36.1 and RC 36.2.
The figure displays the molecular structures of RC 36.1 (a) and RC 36.2 (b) in one possible configuration. a: RC 36.1 is a hexadec-9-enoic acid which is displayed here in the possible (9*Z*)-configuration. b: RC 36.2 is a octadeca-9,12-dienoic acid which is displayed here in the possible (9*Z*,12*Z*)-configuration.

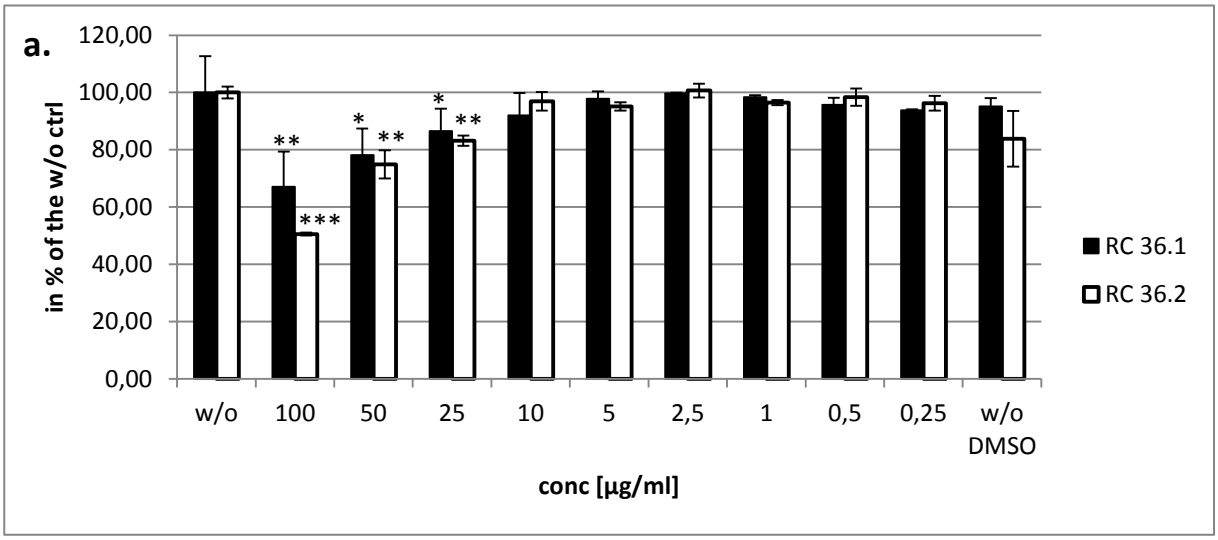

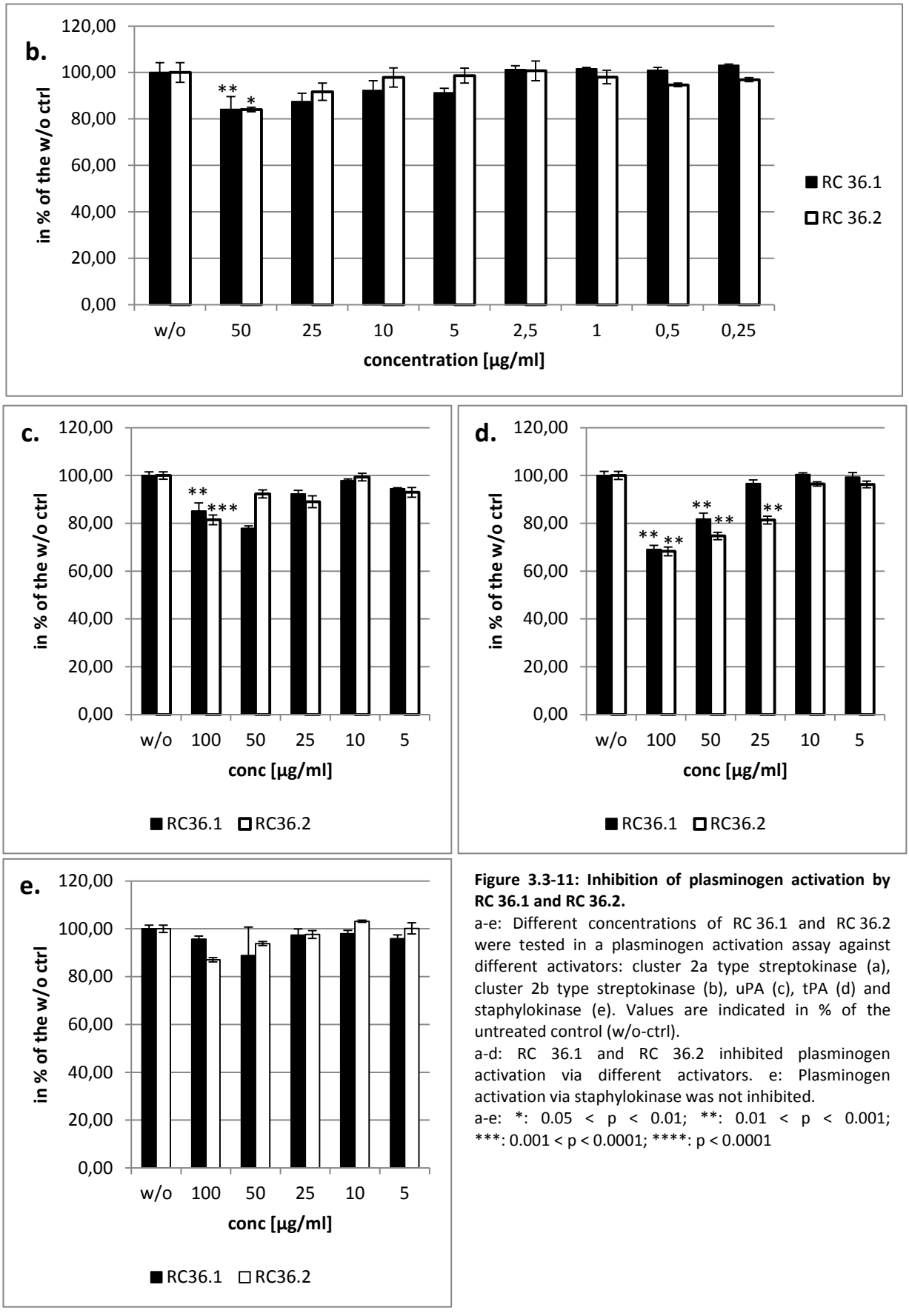

Figure 3.3-11: Inhibition of plasminogen activation by RC 36.1 and RC 36.2.

a-e: Different concentrations of RC 36.1 and RC 36.2 were tested in a plasminogen activation assay against different activators: cluster 2a type streptokinase (a), cluster 2b type streptokinase (b), uPA (c), tPA (d) and staphylokinase (e). Values are indicated in % of the untreated control (w/o-ctrl).

a-d: RC 36.1 and RC 36.2 inhibited plasminogen activation via different activators. e: Plasminogen activation via staphylokinase was not inhibited.

a-e: *: 0.05 < p < 0.01; **: 0.01 < p < 0.001; ***: 0.001 < p < 0.0001; ****: p < 0.0001

Both compounds (RC 36.1 and RC 36.2) inhibited plasminogen activation mediated by cluster 2a type streptokinase (for a detailed elaboration on the cluster type of the different strains used in this study, vide section 6.1): At a concentration of 100 µg/ml (approx. 357 µM) RC 36.1 inhibited plasminogen activation by 20-40 %. Therefore, the IC_{50} of RC 36.1 is higher than the concentrations used in this assay. By contrast, RC 36.2 had an IC_{50} of 100 µg/ml (approx. 357 µM) (fig. 3.3-11a). At first sight, these IC_{50}-values seem to be quite high and therefore, possibly, of no relevance. However, in correlation to those of EACA and TA (fig. 3.2-3, section 3.2), it is clear that the abovementioned IC_{50}-values were still much lower than the one of EACA and in the same range as the IC_{50}-value of TA.

In contrast to the inhibition of cluster 2a type streptokinase, the inhibition of cluster 2b type streptokinase was not efficient: RC 36.1 and RC 36.2 inhibited activation of plasminogen by 20 % at a concentration of 50 µg/ml (approx. 197 µM (RC 36.1) and 179 µM (RC 36.2); fig. 3.3-11b). An inhibition of only 20 % was achieved at concentrations of 250 µM for TA and 1 mM for EACA, either (fig. 3.2-4b, section 3.2). Hence, both RC 36.1 and RC 36.2 were more active than EACA and TA concerning inhibition of plasminogen activation mediated by different types of streptokinase.

Furthermore, both compounds were tested for their inhibitory properties of activation of plasminogen mediated by different activators. First, they were tested against staphylokinase as activator. No significant inhibition of plasminogen activation was observed (fig. 3.3-11e). By contrast, EACA and TA were able to inhibit plasminogen activation mediated by staphylokinase at low concentrations (Fig. 3.2-5c, section 3.2).

Then, RC 36.1 and RC 36.2 were tested against uPA as activator. Both substances showed a slight inhibition of plasminogen activation: RC 36.2 showed an inhibition of 20 % at a concentration of 100 µg/ml (approx. 357 µM) whereas RC 36.1 inhibited plasminogen activation by 20 % at a concentration of 50 µg/ml (approx. 197 µM; fig. 3.3-11c). Compared to EACA and TA which were not able to inhibit plasminogen activation mediated by uPA in this assay (fig. 3.2-5a, section 3.2), both compounds were able to inhibit plasminogen activation – although high concentrations were necessary and the inhibition was not sufficient (fig. 3.3-11c).

Moreover, RC 36.1 and RC 36.2 were tested against tPA as activator of plasminogen. Both compounds inhibited plasminogen activation by 30 % at a concentration of 100 µg/ml (approx. 394 µM (RC 36.1) and 357 µM (RC 36.2); fig. 3.3-11d). As already described in section 3.2, EACA and TA were not able to inhibit tPA in this assay (fig. 3.2-5b).

As a result, RC 36.1 and RC 36.2 inhibited several activators of plasminogen. Whereas only a slight inhibition was observed for uPA, tPA and cluster 2b type streptokinase, they were most effective in inhibiting activation of plasminogen mediated by cluster 2a type streptokinase.

The plasminogen activation assay mimics basic processes of the physiological situation. Nevertheless, it does not represent all factors involved – above all, it does not mirror the situation in an infection

context. Therefore, another model was used: When streptococci access the tissue after e.g. a skin infection, the contact activation system is activated which results in entrapment of streptococci in clots. Though, streptococci are able to escape these clots: by secretion of streptokinase plasminogen gets activated to plasmin which is able to lyse fibrin clots. Therefore, streptokinase plays an important role in the escape of streptococci from this entrapment (Loof *et al.*, 2014). Hence, it was investigated if the fatty acids inhibited plasminogen activation during entrapment of streptococci in a clot.

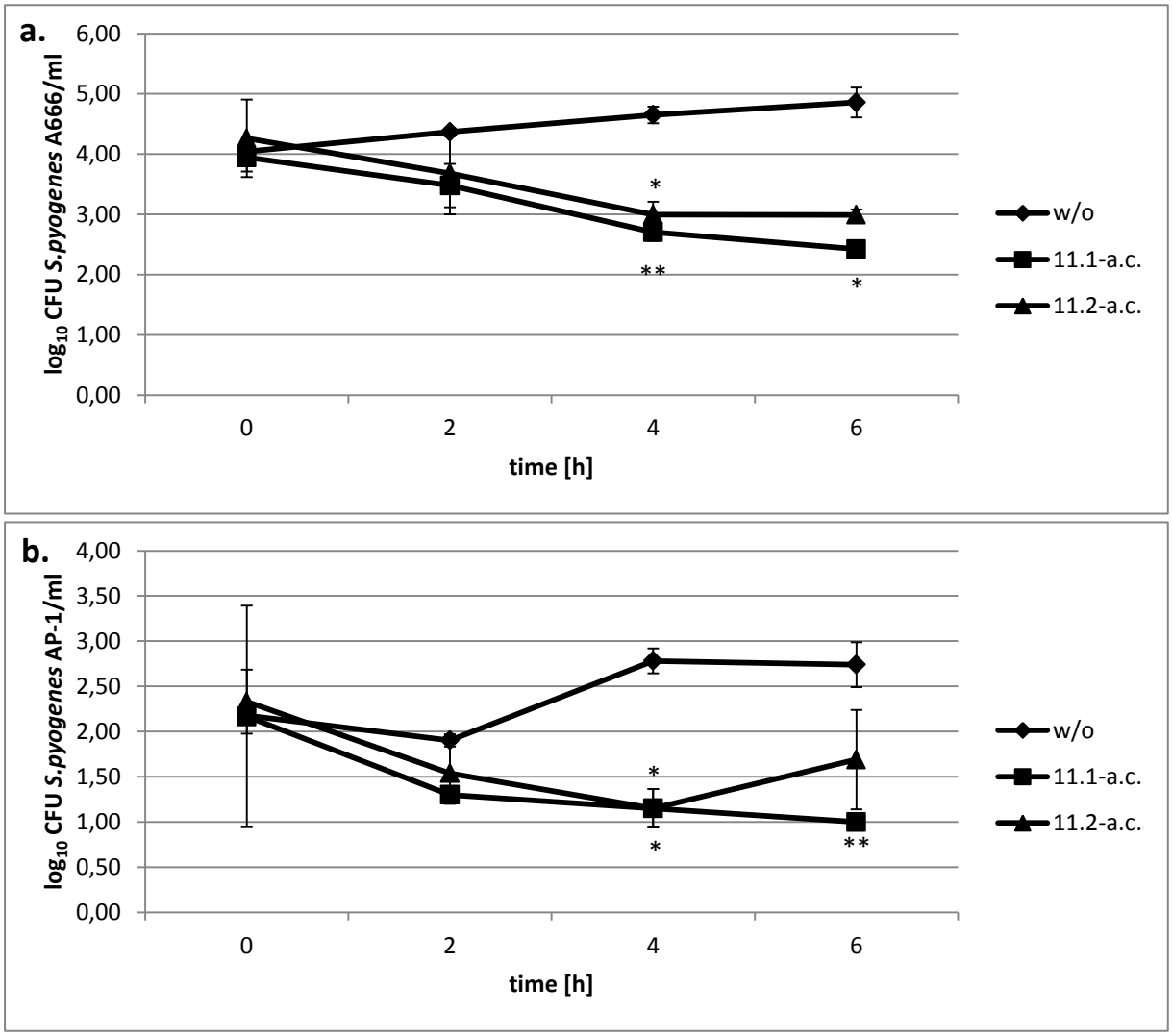

Figure 3.3-12: Treatment with RC 11.1 and RC 11.2 prolongs entrapment of *S.pyogenes* within clots.
a,b: *S.pyogenes* strain A666 (a) or AP1 (b) were entrapped within a clot. After clot formation RC 11.1 or RC 11.2 was added or the clot remained untreated (w/o). Streptococci in the supernatant were plated every 2 h. Values are indicated as $\log_{10}$ CFU of the respective *S.pyogenes* strain.
a, b: In samples treated with a compound fewer streptococci outside the clot were detected.
a,b: *: $0.05 < p < 0.01$; **: $0.01 < p < 0.001$

The fatty acids were added after clot formation. Furthermore, two enriched fractions (RC 11.1 corresponding to RC 25.1 and RC 11.2 corresponding to RC 25.3) of the fatty acids were used (obtained from Dr. Rolf Jansen, MWIS, HZI). RC 11.1 contained only minor impurities and RC 11.2 contained another substance which was not active in the plasminogen activation assay (for an elaboration of the characterization of RC 11.1 and RC 11.2 vide section 6.3). Two different strains of *S.pyogenes* were used: A666 which has a cluster 2b type streptokinase and AP1 harboring a cluster 2a type streptokinase (for determination of the cluster type vide section 6.1). 4 h after clot induction, significantly less streptococci of the strain A666 were detected outside the clot upon treatment with either RC 11.1 or RC 11.2 (concentration used: 60 µg/ml). This effect remained significant for RC 11.1 until 6 h (fig. 3.3-12a). Similarly, treatment with either RC 11.1 or RC 11.2 (concentration used: 30 µg/ml) led to significantly fewer streptococci of the strain AP1 4 h after clot induction. In addition, this effect remained significant for RC 11.1 until 6 h after clot induction (fig. 3.3-12b).

After all, upon treatment fewer streptococci were detected outside clots. Thereby, entrapment of two different strains was prolonged significantly. Beside other virulence factors, both strains differed in their cluster type of streptokinase and, thereby, by their mode of plasminogen activation.

The mechanisms underlying plasminogen activation by different activators are distinct. Plasminogen activation by different activators was hampered upon treatment (fig. 3.3-11; fig. 3.3-12). Additionally, the effects of a longer entrapment can be attributed to inhibition of either plasminogen activation or plasmin activity. However, inhibition of other bacterial factors could also contribute to the observed effects. Further assays were needed to exclude the involvement of other bacterial factors and to investigate the question if either plasminogen or plasmin were targeted.

3.3.5 Plasmin as one target of the isolated fatty acids

To answer the question if plasmin activity was inhibited, a fibrinolysis assay was performed. In this assay a clot was formed by addition of thrombin and fibrinogen and then lysed by plasmin. The isolated fatty acids (RC 36.1 and RC 36.2) were added after clot formation. 120 min after clot induction 80 % of the untreated clot was lysed. In contrast to this, only 65 % of a clot treated with 100 µg/ml (approx. 394 µM) of RC 36.1 was lysed indicating that RC 36.1 inhibited clot lysis. Nevertheless, RC 36.2 (concentration used: 100 µg/ml; approx. 357 µM) inhibited clot lysis significantly: only 22 % of the clot was lysed upon treatment (fig. 3.3-13a).

To assess if both compounds were able to inhibit plasmin activity directly, an assay was used which measures plasmin activity by activation of the plasmin-specific substrate S-2251 (vide 2.4.6).

As described in section 3.2, EACA and TA targeting plasminogen did not inhibit plasmin activity (fig. 3.2-7b). In contrast to that, both fatty acids (RC 36.1 and RC 36.2) inhibited plasmin activity: the IC_{50} of RC 36.2 was determined at around 2.5 µg/ml (approx. 9 µM) whereas the one of RC 36.1 was detected at 10-25 µg/ml (approx. 39-98 µM; fig. 3.3-13b). Compared to e.g. the IC_{50}-values obtained by plasminogen activation mediated by cluster 2a type streptokinase (fig. 3.3-11a), the IC_{50}-values from inhibition of plasmin activity were lower.

Hence, the results obtained by the fibrinolysis and by the plasmin activity assay provided evidence that both compounds RC 36.1 and RC 36.2 target plasmin and inhibit its activity.

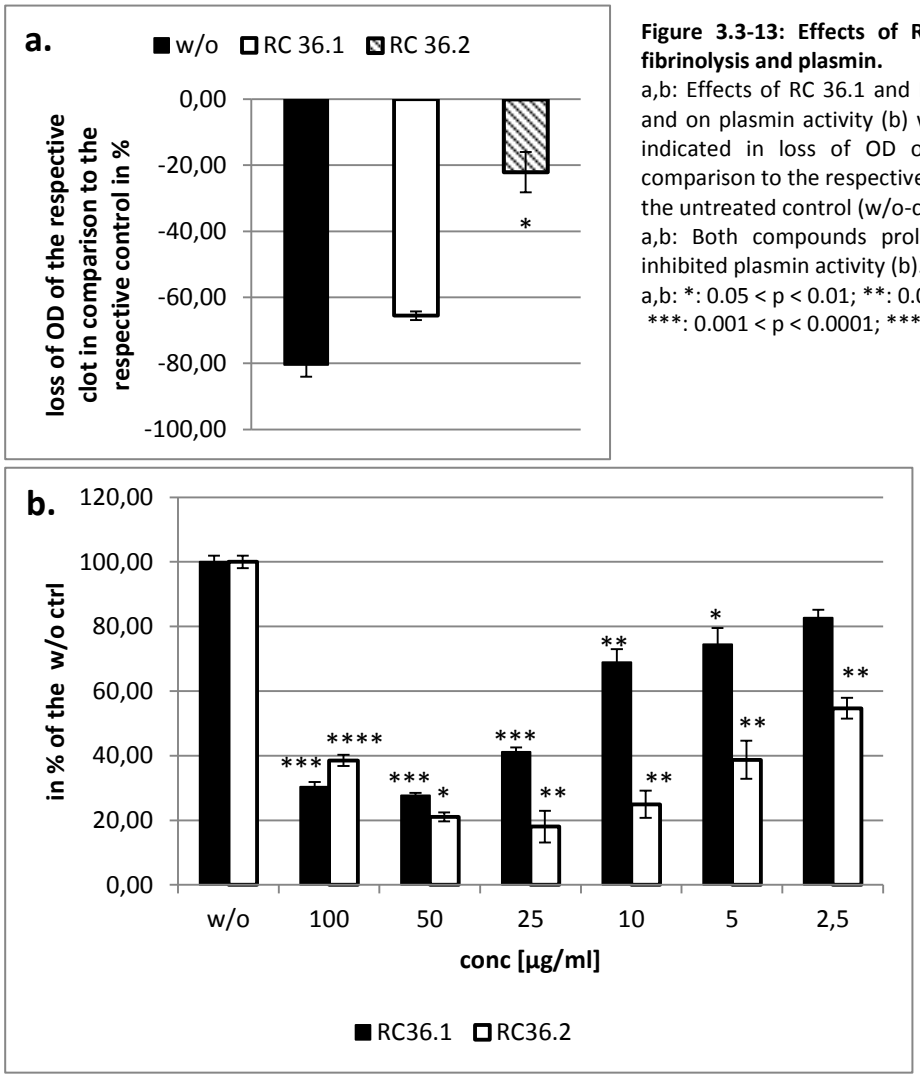

Figure 3.3-13: Effects of RC 36.1 and RC 36.2 on fibrinolysis and plasmin.
a,b: Effects of RC 36.1 and RC 36.2 on fibrinolysis (a) and on plasmin activity (b) were assessed. Values are indicated in loss of OD of the respective clot in comparison to the respective control in % (a) or in % of the untreated control (w/o-ctrl).
a,b: Both compounds prolonged clot lysis (a) and inhibited plasmin activity (b).
a,b: *: 0.05 < p < 0.01; **: 0.01 < p < 0.001;
***: 0.001 < p < 0.0001; ****: p < 0.0001

3.3.6 Effects of isolated fatty acids on survival in experimental murine infection models with *S.pyogenes*

A subcutaneous murine infection model using huPlg transgenic C57BL6/J mice was used for testing the effects of RC 36.1 and RC 36.2 as potential therapeutics. Thereby, two different streptococcal strains were used: infection with the strain 5448 resulted in an overall survival rate of 40-50 % whereas infection with the strain AP1 resulted in a lethality rate of 100 %. Additional information about a possible cause for the different survival rates of these two strains (both harboring a cluster 2a type streptokinase) is given in the supplemental information (section 6.4).

First, the substances were tested for toxicity. As both substances are very similar in structure, only one enriched fraction (RC 11.1) was used for initial toxicity tests. No toxicity was observed *in vivo* when RC 11.1 (dose 50 µg) was administered s.c. once (fig. 3.3-14a) or daily for 7 days (fig. 3.3-14b).

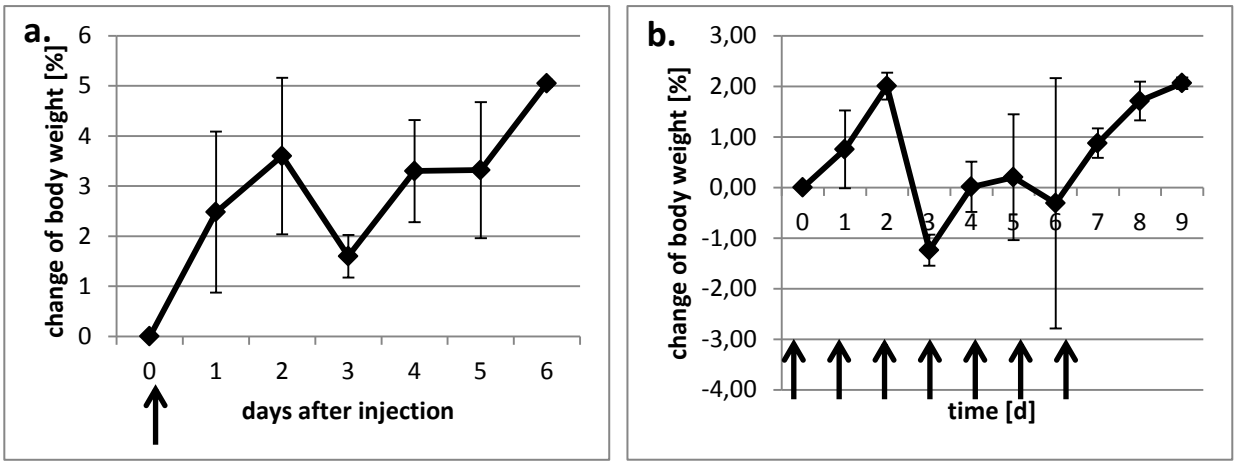

Figure 3.3-14: Assessment of possible toxic effects of RC 11.1 on huPlg transgenic mice.
a,b: huPlg transgenic C57Bl6/J mice were treated s.c. with RC 11.1 once (a) or up to six days (b). Black arrows indicate days of treatment with RC 11.1 (dose: 50 µg s.c.). Numbers of mice used for the trial: a: n =5; b: n=3.

Then, both substances were tested in a subcutaneous *in vivo* infection model using the strain 5448. Mice were treated or left untreated on the day of infection and on day 2 after challenge. Treated mice received a dose of 50 µg s.c. (approx. 2 mg/kg, average weight of mice 23 g). By day 10 untreated mice regained their initial weight whereas treated mice still had a weight loss of about 2 g (approx. 5 %, fig. 3.3-15a). The survival rate for untreated mice was 46 % after 10 days. The survival rates for animals with 'treatment regimen one' (RC 36.1/RC 25.1) or 'treatment regimen two' (RC 36.2/RC 25.3) were 53.8 % and 66.7 %, respectively (fig. 3.3-15c). Though, no significance was observed for treated mice. A slight tendency towards a longer survival was detected.

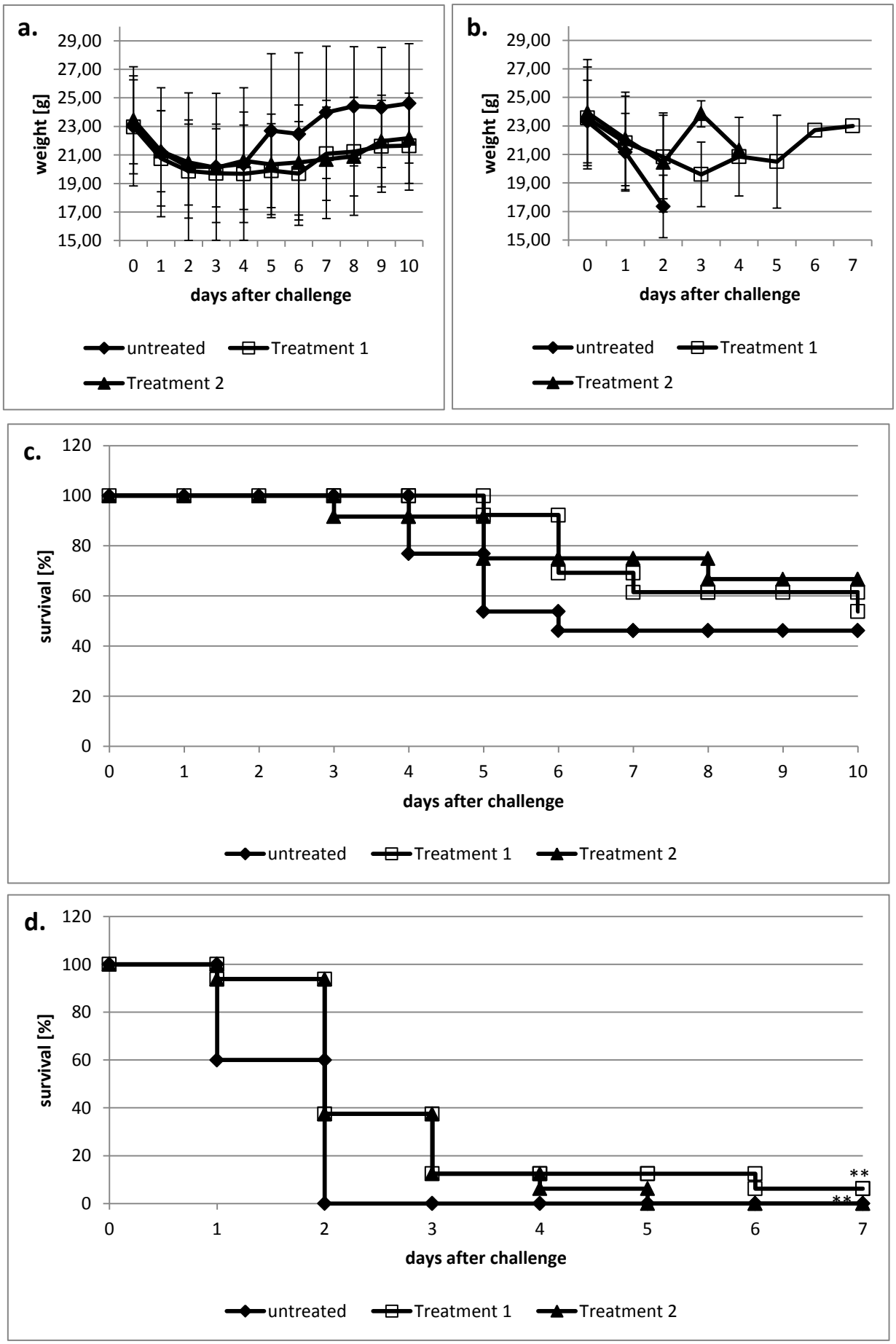
a.
weight [g]
29,00
27,00
25,00
23,00
21,00
19,00
17,00
15,00
0 1 2 3 4 5 6 7 8 9 10
days after challenge
untreated
Treatment 1
Treatment 2
b.
weight [g]
29,00
27,00
25,00
23,00
21,00
19,00
17,00
15,00
0 1 2 3 4 5 6 7
days after challenge
untreated
Treatment 1
Treatment 2
c.
survival [%]
120
100
80
60
40
20
0
0 1 2 3 4 5 6 7 8 9 10
days after challenge
untreated
Treatment 1
Treatment 2
d.
survival [%]
120
100
80
60
40
20
0
**
**
0 1 2 3 4 5 6 7
days after challenge
untreated
Treatment 1
Treatment 2

Figure 3.3-15: Effects of isolated fatty acids on survival in two *in vivo* infection models.
a-d: huPlg transgenic C57Bl6/J mice were infected s.c. with *S.pyogenes* strain 5448 (a,c; infection dose 3-5x10^7 cfu) or with the strain AP1 (b,d; infection dose: 1x10^7 cfu). Mice were untreated (with PBS) or treated with treatment regimen one (RC 25.1/RC 36.1) or two (RC 25.3/RC 36.1). Mice infected with AP1 (b,d) were treated on the day of infection. Mice infected with 5448 (a,c) were treated on the day of infection and received a boost on day 2 after infection. Treated mice received a dose of 50 µg s.c. (corresponding to approx. 2 mg/kg).
a,b: No significant differences in weight after challenge were observed within the different treatment groups.
c,d: A slight tendency towards a prolonged survival was detected for 5448. Prolongation of survival upon treatment is significant for AP1.
d: **: p = 0.0021 for treatment regimen one as well as for treatment regimen two compared to untreated (Mantel-Cox-Test).
a,c: untreated: n =13; treatment 1: n=13; treatment 2: n=12. Data were pooled from four independent experiments.
b,d: untreated: n=15; treatment 1: n=16; treatment 2: n=16. Data were pooled from three independent experiments.

In addition, both substances were tested in a subcutaneous *in vivo* infection model using the strain AP1: mice were treated or left untreated only on the day of infection and received the same dose as in the trial that was performed using the strain 5448. Untreated mice lost more weight than treated mice (weight loss on day 2: untreated: 25 % vs. regimen 1: 11 % and regimen 2: 15 %). Those mice receiving 'treatment regimen one' nearly regained their initial weight by day 6 (fig. 3.3-15b). By day 2, all untreated mice were dead. By contrast, mice treated with 'treatment regimen one' or 'regimen two' still reached a survival rate of 40 % on day 2. All mice treated with 'treatment regimen two' were dead by day 5. Most of the mice treated with 'treatment regimen one' died by day 6. However, one mouse also survived the trial (fig. 3.3-15d). As a result, both fatty acids prolonged survival significantly in the trial with the strain AP1.

Although superiority was not detected for the infection model with the strain 5448, it was assessed using the model with the strain AP1. The latter showed undoubtedly that administration of each isolated fatty acid improved the outcome in the infection model leading to systemic severity.

4 Discussion

4.1 Inhibitors of group A streptococcal invasion

4.1.1 Disorazoles as inhibitors of group A streptococcal invasion

The disorazoles have been investigated for their effects in cancer therapy: they target the paclitaxel binding site within microtubules. Thereby, they inhibit tubulin polymerization which leads to apoptosis (Elnakady *et al.*, 2004; Hopkins and Wipf, 2009). In addition, they are currently under investigation as antibody-drug-conjugates against triple-negative breast cancer (Seitz *et al.*, 2014). Up to now, they have never been tested in an infection context. In this study, it is shown that disorazoles inhibit the invasion of *S.pyogenes* into host epithelial cells. Furthermore, disorazoles were the only active compounds inhibiting streptococcal invasion in a screen with 300 myxobacterial extracts and 200 myxobacterial compounds (fig. 3.1-1 and 3.1-2). After all, this obviously unique feature of the disorazoles with regard to the other tested myxobacterial compounds was investigated in more detail.

S.pyogenes has evolved three different mechanisms to invade host cells: (a) invasion via a zipper-like mechanism (M protein-mediated); (b) invasion via formation of caveolae (SfbI-mediated) or (c) invasion via formation of membrane ruffles as a result of cytoskeletal rearrangements (Rohde and Chhatwal, 2013). Invasion into epithelial cells has a significant benefit for *S.pyogenes*: by doing so, an efficient eradication by antibiotic treatment is impossible. A reason for that is that penicillin cannot (fully) penetrate into the cells. Therefore, by invading epithelial cells, streptococci can escape antibiotic killing and hide intracellulary. This intracellular reservoir might be the cause for persistence of and recurrent infections with streptococci (Österlund *et al.*, 1997; Neeman *et al.*, 1998). Consequently, inhibition of invasion facilitates eradication of streptococci by antibiotics.

The amount of intracellular viable streptococci was decreased significantly upon treatment with disorazoles. Moreover, this inhibition of invasion was concentration-dependent. Double-immunofluorescence staining and SEM pictures showed that streptococci remained extracellularly. Therefore, it is unlikely that streptococci were killed intracellulary. In fact, disorazoles efficiently inhibited invasion via formation of caveolae (SfbI-mediated) and via formation of membrane ruffles (cytoskeletal rearrangements). Though, invasion via formation of membrane ruffles was inhibited at lower concentrations than the one via formation of caveolae. This was observed in two distinct epithelial cell types (fig. 3.1-2-3.1-8).

It had not been investigated before whether the disorazoles interfere with the eukaryotic host cell or influence the streptococci. In this study, a minimal inhibitory concentration for disorazole Z on

different group A streptococcal strains could not be determined. In addition, supplementation of streptococci with disorazole Z during cultivation did not influence the amount of viable bacteria compared to an untreated control (vide section 3.1.4). Streptococci supplemented with disorazole Z during cultivation were subjected to infection of HEp2-cells which had not been treated with disorazoles prior to infection. If streptococci were supplemented with disorazoles during cultivation, invasion was not inhibited (fig. 3.1-9). It was shown clearly that invasion was only hampered when epithelial cells were treated with disorazoles before or during infection with *S.pyogenes*. This leads to the hypothesis that disorazoles did not influence the regulation of streptococcal invasive factors like the SfbI protein. However, to exclude that e.g. streptococcal surface molecules were affected by treatment with disorazoles, it will be necessary to evaluate expression levels of treated and untreated streptococci. As streptococci (supplemented with disorazole Z during cultivation) were not hindered to invade into epithelial cells when HEp2-cells were left untreated, most probably disorazoles did not affect streptococcal viability or the expression of streptococcal surface proteins involved in the invasion process (fig. 3.1-9). Therefore, affection of streptococcal surface proteins upon disorazole treatment was not relevant or likely in the infection assay. Consequently, there is strong evidence that disorazoles interfere directly with the eukaryotic host cells and influence downstream signaling processes after adherence of streptococci.

As disorazoles are well known cytotoxic drugs acting on tubulin (Elnakady *et al.*, 2004), one could assume that their inhibitory properties were a result of cytotoxicity: if the cytoskeleton of eukaryotic cells, e.g. the actin cytoskeleton, had been affected fatally, cytoskeletal rearrangements or actin recruitment would not have been possible anymore. Thus, streptococci would not induce their uptake into eukaryotic cells.

Indeed, the tubulin matrix was slightly altered upon treatment with disorazoles (fig. 3.1-11). This could be a hint for early cytotoxic effects as the tubulin fragments appeared to be shorter in comparison to an untreated and uninfected control. However, it should not be overlooked that also the untreated control infected with the *S.pyogenes* strain A40 or A8 showed alterations with regard to the tubulin matrix (fig. 3.1-11b,h). In addition, slight alterations concerning the cytoskeleton were detected by double-immunofluorescence. However, it cannot be ignored that these alterations were detected in both untreated and treated cells (fig. 3.1-11). Although, double-immunofluorescence staining is suitable to detect alterations compared to uninfected cells, it is not appropriate to state that these effects are a result of cytotoxicity.

Therefore, other methods have to be used to assess cell viability: several methods are eligible to detect metabolic activity. The measurement of lactate dehydrogenase (LDH) is an indicator of cytotoxicity and cell lysis: LDH is present in the cytoplasm and only found extracellularly when the plasma membrane is damaged. Another assay involves MTT as a substrate: only metabolically active

cells reduce MTT to a formazan. In a study that tested different assays to assess cytotoxic effects, the MTT assay proved to be more sensitive than the LDH assay when cells were treated with a toxic substance (Fotakis and Timbrell, 2006). In this study here an MTT assay was used. Although treatment with disorazoles for 24 h resulted in a survival of HEp2-cells of only 40-50 %, there is no significant cytotoxicity for infected HEp2-cells treated with disorazoles compared to untreated and uninfected controls under the conditions used in the infection assay. Both untreated and treated HEp2-cells infected with the strain A8 did not show cytotoxic effects compared to the untreated and uninfected control. In contrast to that, HEp2-cells infected with the strain A40 showed statistically significant lower cell viability compared to the untreated and uninfected control. However, HEp2-cells treated with disorazoles and infected with the strain A40 did not show significantly less cell viability compared to the infected control (fig. 3.1-10). Consequently, infection with the strain A40 per se results in less cell viability compared to uninfected cells. Therefore, possible alterations in the cell shape detected in double-immunofluorescence images of cells treated with disorazoles cannot be attributed to cytotoxic effects of the disorazoles under assay conditions. It was not determined why *S.pyogenes* reduces cell viability during infection. In this study a high MOI of around 40 was used. This high ratio of bacteria to eukaryotic cells is not physiological. However, it is suitable to stress the model maximally to test protective or inhibitory effects of compounds; in this case of the disorazoles. Possibly, this high bacterial load resulted in a higher rate of cell death leading to the observed effects. In addition, one might think that cytotoxicity of the disorazoles had to be detected under infection assay conditions as it was published that the disorazoles have an IC_{50} lower than 100 pM (Elnakady *et al.*, 2004). However, recent studies revealed that the IC_{50}-values of the disorazoles are even higher than the published ones. The reason for the low IC_{50}-values is that disorazoles stick to pipette tips which results in inaccurate dilution. To avoid this, special pipette tips have to be used to determine the correct IC_{50} (Dr. Jennifer Herrmann, personal communication; the correct IC_{50} for disorazole A_1 is 310 pM for inhibition of cellular proliferation of A549-cells (Hearn *et al.*, 2006); the IC_{50} published by Elnakady *et al.*, 2004, was 2.3 pM). These special pipette tips were also used in this study.

As there are no significant cytotoxic effects of the disorazoles under the conditions used in the infection assay, inhibition of invasion was not the result of cytotoxicity. Ozeri and colleagues demonstrated that tubulin is not recruited to the site of entry during infection with *S.pyogenes*. Therefore, tubulin is not directly involved in streptococcal invasion (Ozeri *et al.*, 2001). However, the target of the disorazoles is tubulin polymerization (Elnakady *et al.*, 2004). Vinblastine and tubulysin A are cytotoxic drugs targeting tubulin. Like the disorazoles, they bind to the (paclitaxel) binding site (Zeino *et al.*, 2013). If tubulin played a role in streptococcal invasion and if inhibition of invasion was a result of cytotoxic effects, vinblastine and tubulysin A as cytotoxic drugs would also inhibit invasion.

Though, both compounds did not hamper invasion of streptococci into epithelial cells. At first sight, vinblastine seemed to reduce invasion of the strain A8 at high concentrations. However, analysis of double-immunofluorescence pictures revealed that there was no difference compared to an untreated control. This observation proves that vinblastine does not inhibit streptococcal invasion (fig. 3.1-12). Therefore, it is very unlikely that inhibition of invasion was a result of side effects on tubulin. These results are in accordance with the ones of Ozeri and colleagues (Ozeri *et al.*, 2001).
Consequently, it is clear that disorazoles target a different process during invasion of streptococci. This implies that the disorazoles have a potential second target not related to tubulin.
A functional actin cytoskeleton is necessary especially for invasion by cytoskeletal rearrangements (Molinari *et al.*, 2000). The actin cytoskeleton did not appear to be affected upon treatment with disorazoles (fig. 3.1-13). Hence, hindrance of invasion was not expected as, e.g. in the case of the strain A8, actin could still be recruited to the site of entry. Moreover, an apparently functional actin cytoskeleton was another indicator for non-toxicity under the conditions used in the infection assay.
In the SfbI-mediated pathway of streptococcal invasion a signaling cascade involving *inter alia* β_1-integrins leads to uptake of streptococci (Wang *et al.*, 2006). However, analysis of known downstream signaling processes of the SfbI-mediated pathway did not reveal the putative, second target of the disorazoles: recruitment of integrins and integrin clustering was not hindered (fig. 3.1-14). Another important factor in downstream signaling is vinculin. It links integrins to the actin cytoskeleton (Critchley, 2000). Upon treatment with disorazoles, there was no difference in the distribution of vinculin. Vinculin still took part in formation of focal adhesions (fig 3.1-15). Finally, vinculin and integrins are not involved in the mechanism of uptake via cytoskeletal rearrangements (Molinari *et al.*, 2000). As disorazoles also inhibited the latter pathway of invasion, the target has to play a role in both invasion pathways.

4.1.2 Ezrin as a potential novel factor in group A streptococcal invasion into epithelial cells is inhibited by disorazoles

SEM images showed clearly that HEp2-cells infected with *S.pyogenes* harbored shorter and fewer microvilli on their cell surface upon treatment with disorazoles (fig. 3.1-4d-f). Several factors are involved in the regulation of microvilli. One of the major regulators is ezrin (Berryman *et al.*, 1993; Viswanatha *et al.*, 2014). It consists of an N-terminal globular domain, an extended α-helical domain, a poly-proline region and a charged C-terminal domain (Tsukita *et al.*, 1997b). The N-terminal domain is able to bind membrane proteins whereas the C-terminal domain binds F-actin (Bretscher *et al.*, 2002; Viswanatha *et al.*, 2014). Ezrin does not only play an important role with regard to microvilli, but also in signal transduction of several receptors and protein kinases. Among these is *inter alia* PI_3-

kinase which is an important factor in the SfbI-mediated pathway (Hirao *et al.*, 1996; Schoenwaelder and Burridge, 1999; Bretscher *et al.*, 2002). Therefore the effects on ezrin upon treatment with disorazoles were investigated.

Double-immunofluorescence pictures demonstrated undoubtedly that ezrin appeared to be altered in infected cells upon treatment with disorazoles compared to untreated cells (fig. 3.1-16). So far, ezrin has not been described as a factor in streptococcal invasion into epithelial cells via the SfbI-mediated pathway or via cytoskeletal rearrangements. Therefore, its potential role still has to be elucidated. However, two publications mention a possible role of ezrin in the pathogenesis of streptococci.

It was shown by Cywes and Wessels that *S.pyogenes* invaded keratinocytes by CD44-mediated signaling. Signal transduction by CD44 involves *inter alia* ezrin. In that publication the authors proved that *S.pyogenes* colocalized with ezrin. Furthermore, it was hypothesized that ezrin was responsible for induction of membrane ruffling resulting in the uptake of group A streptococci. It has to be emphasized that this signaling cascade was induced by binding of the hyaluronic acid capsule of *S.pyogenes* to the receptor CD44 (Tsukita *et al.*, 1997a; Cywes and Wessels, 2001). In contrast to that, internalization via CD44-mediated signaling is not relevant for the invasion assays performed in this study: Molinari and colleagues demonstrated that both strains used in this study kept their invasive properties upon treatment with hyaluronidase. This treatment resulted in a loss of the hyaluronic acid capsule for both strains (Molinari *et al.*, 2000).

In addition, Hoe and colleagues showed that a streptococcal factor usually binding to complement factors (streptococcal inhibitor of complement; Sic) was able to bind ezrin. As a result of this binding, group A streptococcal strains carrying Sic were disabled to invade into epithelial cells. The authors hypothesized that invasion was diminished as ezrin was not able to bind to actin anymore. Though, strains carrying Sic do usually also harbor an M1 protein. Furthermore, it was observed that *S.pyogenes* strains carrying an M1 protein, but not Sic, were able to invade into epithelial cells. However, it was not demonstrated that ezrin was needed for uptake of *S.pyogenes* – the authors did only detect that Sic bound ezrin and inhibited the uptake (Hoe *et al.*, 2002; Binks *et al.*, 2005). Both strains used in this study were taken up by epithelial cells independently of the M protein-mediated pathway as they invaded the cells by the SfbI-mediated pathway (strain A40) or by cytoskeletal rearrangements (strain A8). It has not been tested yet whether disorazoles are able to inhibit invasion mediated by the M protein. However, all three mechanisms of streptococcal invasion are distinct: whereas actin rearrangements play a role in the zipper-like mechanism (M protein-mediated) (Wang *et al.*, 2006), formation of caveolae (independent of actin recruitment to the site of entry) is predominant in the SfbI-mediated pathway and formation of membrane ruffles is important in the pathway via cytoskeletal rearrangements (Molinari *et al.*, 2000). Therefore, it is unlikely that

ezrin exhibits exactly the same function in all distinct mechanisms. It has been shown that ezrin is involved in several cellular processes (Bretscher *et al.*, 2002). As a result, ezrin may be involved in all three mechanisms, although it might exert different functions.

So far, ezrin has not been described as a factor in streptococcal invasion mediated by one of the abovementioned pathways (vide 4.1.1). The aforementioned publications only showed that ezrin was involved in non-common pathways of invasion. A side glance to mechanisms of other invasive pathogens might aid in the quest for the role of ezrin during streptococcal invasion:

Jung and colleagues reported the requirement of ezrin in the invasion process of *Listeria monocytogenes*. In that case *Listeria* invaded epithelial cells via the CD44-mediated signaling pathway (Jung *et al.*, 2009) which was also described by Cywes and Wessels and which had already been shown before (Vaheri *et al.*, 1997; Cywes and Wessels, 2001).

In contrast, enteropathogenic *E.coli* showed a more complex mechanism for invasion into epithelial cells. Whereas Finlay and colleagues demonstrated that ezrin was localized to adherent enteropathogenic *E.coli* (Finlay *et al.*, 1992), Berger and colleagues gave insights into possible mechanisms: they described that an effector protein from a type III secretion system interacts with another protein (NHERF1, an ERM-binding protein) leading to recruitment of activated ezrin (Berger *et al.*, 2009). Although streptococci do not have a type III secretion system as they are gram-positive bacteria (Saier, 2006), a similar factor or effector protein could exist leading to the recruitment of ezrin.

Takahashi and colleagues observed that ezrin was accumulated at the site of entry during infection with a *Neisseria meningitidis* strain harboring a certain pilin protein (Takahashi *et al.*, 2012). However, no accumulation at the entry port could be detected in this study: treatment with disorazoles altered the distribution and perhaps the structure of ezrin. Furthermore, it is possible that ezrin is not directly involved in internalization, but is necessary for mediating it. This explains why no recruitment of ezrin to the site of entry is observed in the infected untreated controls (fig. 3.1-15).

In contrast to the publications cited above, Korotkova and colleagues described an internalization mechanism for *E.coli* that has some similarities with the SfbI-mediated pathway: a factor of *E.coli* bound to $\alpha_5\beta_1$-integrin receptors. Binding to this receptor led to phosphorylation of PI_3-kinase and of ezrin (Korotkova *et al.*, 2008). In addition, Berger and colleagues showed that ezrin was phosphorylated upon activation of the RhoGTPase Cdc42 (Berger *et al.*, 2004). In the SfbI-mediated pathway, SfbI binds to fibronectin which then binds to $\alpha_5\beta_1$-integrin receptors. Analogously, also PI_3-kinase is phosphorylated (Wang *et al.*, 2006). Adjacent to the PI_3-kinase, Cdc42 is also involved in the SfbI-mediated pathway of streptococcal invasion (Ozeri *et al.*, 2001). Therefore, it is possible that

ezrin gets phosphorylated, either by Cdc42 or PI_3-kinase, and that it is directly involved into rearranging the cytoskeleton by binding to actin.

The side glance to other invasive pathogens sheds some light on the potential part of ezrin during streptococcal invasion, but further studies are needed to elucidate the role of ezrin in this process. To gain some more information about ezrin, it is necessary to highlight its role in cell biology and cancer. In these interrelations, it has been studied intensively: several pathways in which ezrin plays a crucial role have been elucidated (Bretscher *et al.*, 2002). By linking known functions of ezrin to an infection context, elucidation of underlying mechanisms of ezrin in streptococcal invasion will be more facile.

It has been shown that ezrin exists in a so-called dormant or in a non-dormant/activated state: in the dormant state the binding site for e.g. F-actin is masked. It is proposed that an intramolecular interaction between the N- and the C-terminal region results in conformational dormancy. In contrast, several proteins (*inter alia* CD44) are able to bind to dormant ezrin leading to subsequent activation (Bretscher, 1999). Furthermore, it was shown that phosphoinositide binding to ezrin is able to activate it, either. In general, ezrin gets activated by phosphorylation. If ezrin is not activated, it cannot fulfil its cellular functions (Fievet *et al.*, 2004). Some of these functions shall be discussed below with regard to the invasion pathways mediated by SfbI or by cytoskeletal rearrangements.

Ezrin is an integral part of microvilli and of membrane ruffles (Vaheri *et al.*, 1997): in the late 80ies Bretscher observed that phosphorylated ezrin is involved in formation of membrane ruffles and of microvillar-like surface structures (Bretscher, 1989). To be completely functional, microvilli require a dynamic phosphorylation and dephosphorylation of ezrin. If they lack a certain co-factor binding to dormant ezrin, short aberrant microvilli are detected (Reczek and Bretscher, 1998; Viswanatha *et al.*, 2014). In addition, immunofluorescence images of Korotkova and colleagues revealed that phosphorylated ezrin exhibited a punctuated pattern (Korotkova *et al.*, 2008). Similarly, such a punctuated pattern of ezrin was observed for HEp2-cells infected with *S.pyogenes* strain A40 or A8 (fig. 3.1-16a,d). By contrast, HEp2-cells infected with the strain A40 and treated with disorazoles did not show this pattern. In fact, they showed diffuse fluorescence and a possible cluster formation (fig. 3.1-16b,c). Though, HEp2-cells treated with disorazoles and infected with the strain A8 still showed a punctuated pattern beside diffuse fluorescence and possible cluster formation (fig. 3.1-16e,f). This punctuated pattern of ezrin which can be detected in infected, but untreated HEp2-cells could represent phosphorylated ezrin: as shown by Korotkova and colleagues phosphorylated ezrin represented a punctuated pattern (Korotkova *et al.*, 2008). By contrast, this would imply that ezrin is dephosphorylated upon treatment with disorazoles. Dephosphorylation of ezrin leads to its dormant state resulting in the disability of binding to actin (Tsukita *et al.*, 1997b; Bretscher, 1999). However, in this study, the phosphorylation status of ezrin was not determined.

Future research will have to elucidate the phosphorylation status of ezrin upon treatment with disorazoles. In addition, it could be tested if disorazoles bind to recombinant ezrin by using biophysical methods.

Moreover, ezrin is involved in signal transduction cascades: phosphorylated ezrin is able to activate PI_3-kinase in epithelial cells (Gautreau *et al.*, 1999). In addition, ezrin is able to activate focal adhesion kinase (FAK) (Poullet *et al.*, 2001). Both focal adhesion kinase and PI_3-kinase play an important role in signal transduction of the SfbI- and the M protein-mediated pathways of streptococcal invasion: after binding of *S.pyogenes* to the $\alpha_5\beta_1$-integrin receptor the integrin-linked kinase (ILK) is activated leading to subsequent phosphorylation of FAK and Src. In addition, PI_3-kinase is involved in the activation of ILK. Especially in the SfbI-mediated pathway, activation of Src is important as it leads to formation of caveolae. Then, streptococci are taken up by them (Sargiacomo *et al.*, 1995; Li *et al.*, 1996; Rohde *et al.*, 2003; Wang *et al.*, 2007). Additionally, it has been shown that Src phosphorylates ezrin. Furthermore, Srivastava and colleagues revealed a positive feedback mechanism: if ezrin was phosphorylated by Src, ezrin sustained the activity of Src (Srivastava *et al.*, 2005). Besides, it has been observed in a certain cancer cell line that ezrin colocalizes with caveolin-1 and actin. This suggests a connection between caveolae and the actin cytoskeleton mediated by ezrin (Lugini *et al.*, 2006).

Based on the observations of the aforementioned publications, the following mechanism can be proposed for the involvement of ezrin in the SfbI-mediated pathway of invasion (fig. 4.1-1): after binding of *S.pyogenes* to $\alpha_5\beta_1$-integrin receptors the integrin-linked kinase (ILK) becomes activated under involvement of PI_3-kinase. However, the latter is activated *inter alia* by phosphorylated ezrin. Furthermore, ILK leads to activation of FAK and Src. Again ezrin might aid in activation of FAK. By its positive feedback on Src, caveolae are formed. The transport of these to the cell surface might be mediated by ezrin. If ezrin is involved in central processes of the SfbI-mediated pathway, alterations on ezrin will affect the uptake of *S.pyogenes*. Treatment with disorazoles resulted in cluster formation of ezrin (fig. 3.1-16). In addition, treatment with disorazoles did not lead to alterations in integrin clustering and did neither affect vinculin (as a cytoskeletal linker between integrins and actin) nor the formation of focal adhesions nor the actin cytoskeleton (fig. 3.1-13-3.1-15). If treatment with disorazoles leads to alteration, inhibition or to dephosphorylation of ezrin and if ezrin is involved in central processes of the SfbI-mediated pathway, the hindrance/inhibition of invasion of streptococci is to be expected.

Additionally, phosphorylated ezrin might also be involved in the uptake of *S.pyogenes* via membrane ruffles by cytoskeletal rearrangements. Treatment with disorazoles led to shorter microvilli on the cell surface and to alterations on ezrin (fig. 3.1-4 and 3.1-16). If ezrin or an adjacent protein is inhibited, microvilli appear to be shorter as described by Viswanatha and colleagues (Viswanatha *et al.*, 2014). In addition, formation of membrane ruffles will be hampered as ezrin is

central in this process (Vaheri *et al.*, 1997): rearrangements of the actin cytoskeleton will be impaired if ezrin is not able to bind to actin. Consequently, inhibition of invasion via cytoskeletal rearrangements upon treatment with disorazoles could be explained by inhibition of ezrin and its various biological activities.

It was not investigated if disorazoles inhibit invasion mediated by the M protein, but it is likely that they do so. The M protein- and the SfbI-mediated pathway share some similarities concerning their signaling cascades (Wang *et al.*, 2007).

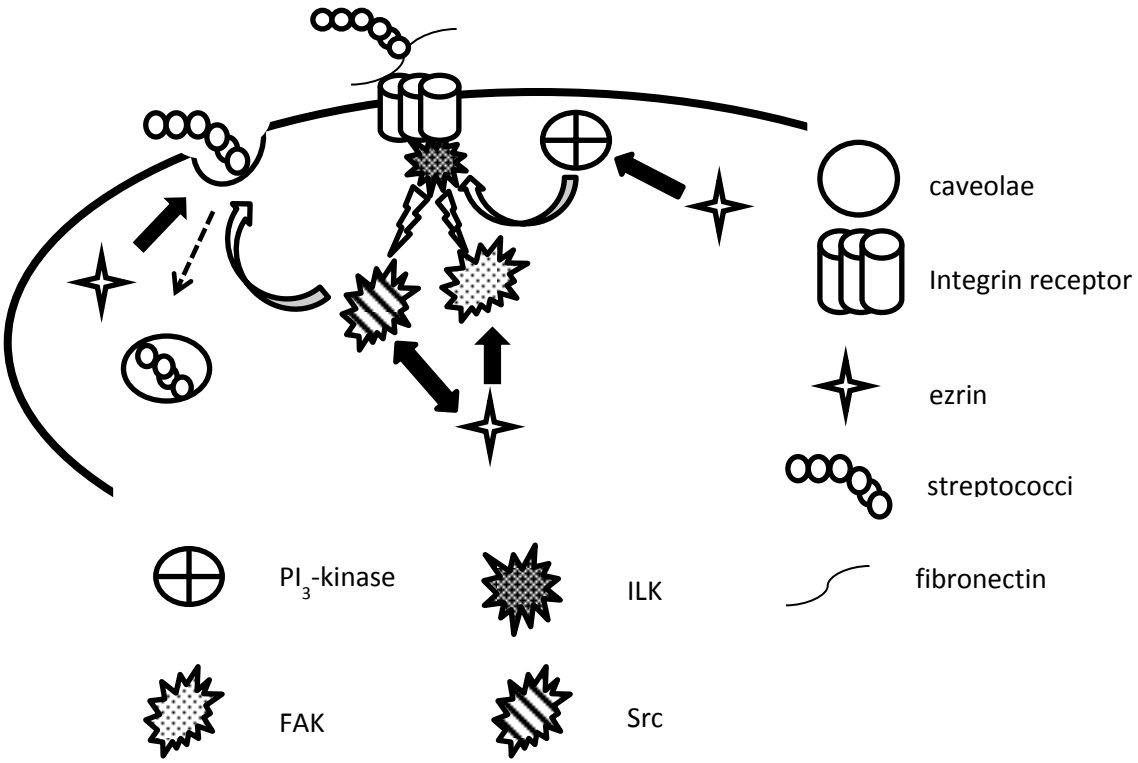

Figure 4.1-1: Proposed involvement of ezrin in the SfBI-mediated pathway.
The figure displays where ezrin might be involved in the SfBI-mediated pathway of streptococcal invasion. After streptococci bind to fibronectin, they bind to the integrin receptor. This results in activation of ILK with subsequent activation of FAK and Src. Activation of Src leads to formation of caveolae at the cell surface. PI_3-kinase is involved in activation of ILK. Ezrin is involved in activation of PI_3-kinase, FAK and associated with caveolae. Furthermore, it positively regulates Src.

It will have to be investigated if other proteins involved in the formation of focal adhesions and in linking integrin signals to the actin cytoskeleton are affected by disorazoles. One such candidate is talin: this protein has an N terminal domain that is homologue to the one of ezrin (Critchley, 2009). If the disorazoles target ezrin at its N terminal domain, it is likely that they will also target talin. Talin links the integrins to actin: the talin head promotes integrin clustering. In addition, talin also plays a role in the energy-dependent activation of β_1-integrins (Critchley, 2009). Although integrin clustering did not appear to be affected in this study (fig. 3.1-14), it has to be proven that talin is not inhibited

by disorazoles. Additionally, talin is also involved in ruffling of membranes (Burridge and Connell, 1983). Therefore, it could also take part in the streptococcal invasion pathway via cytoskeletal rearrangements.

In summary, there is significant evidence that the disorazoles have a second target: ezrin. Possibly, ezrin is a novel factor involved in streptococcal invasion. Further studies will have to highlight the role of ezrin in the invasion process of bacteria into eukaryotic cells in general and of streptococcal invasion in particular. However, subsequent research will have to elucidate the binding site of the disorazoles on ezrin. Furthermore, it will have to be shown that the disorazoles indeed target ezrin directly as indirect interactions via e.g. tyrosine kinases involved in activation of ezrin may also be influenced by these secondary metabolites.

4.1.3 Ezrin as the potential second target of the disorazoles – implications and possible applications

Disorazoles efficiently inhibit/hamper invasion mediated by cytoskeletal rearrangements and by SfbI. Although the disorazoles did not show significant cytotoxic effects under the conditions used in the infection assay, they reduced cell viability by 50-60 % after 24 h of treatment (fig. 3.1-10). Thus, the cytotoxic effect after 24 h is not deniable. However, they are able to block an important pathogenic mechanism of streptococci: invasion into epithelial cells. Due to their cytotoxicity after 24 h, it is not likely that they hold the potential to be developed as 'pathoblockers' of streptococcal infections. Nevertheless, partial structures of the disorazoles could be tested for their inhibitory properties: possibly, they show less or no cytotoxic effects and could then be used as 'pathoblockers'. Potential candidates for testing could be precursors of the chemical synthesis of disorazoles (Schäckel *et al.*, 2010). In addition, synthetic analogues could be tested as well (Wipf *et al.*, 2006). Once the target site of the disorazoles is known, structural information can be gained which could be used as a starting point to synthetize disorazole surrogates without tubulin binding activity and thus largely lacking cytotoxicity.

So far, no 'pathoblocker' targeting the invasion process is on the market or in development. Cue and colleagues discovered a β_1-integrin-antagonist and proposed this one as a remedy to enhance the efficacy of treatment in streptococcal infections: if streptococci cannot bind to β_1-integrin receptors anymore, they will remain extracellularly assuming that they would have invaded epithelial cells via the M protein- or the SfbI-mediated pathway. It was hypothesized that treatment with conventional antibiotics like penicillin would be more effective when streptococci remained extracellularly because penicillin cannot kill streptococci efficiently if they are located in an intracellular reservoir (Österlund *et al.*, 1997; Neeman *et al.*, 1998; Cue *et al.*, 2000). However, the authors did not provide

any data about cytotoxicity: as integrin receptors have key roles in eukaryotic cells, it is expected that inhibition of integrin receptors and the resulting signaling cascade might lead to cell death. A side glance to the field of cancer research confirms these considerations: $\alpha_5\beta_1$-integrin receptor antagonists are under investigation for treatment of solid tumors and for anti-angiogenesis as blocking of these receptors leads to cell death and reduces formation of new blood vessels in tumors (Schaffner *et al.*, 2013). However, if it can be managed to develop a β_1-integrin-antagonist that is e.g. specific for pharyngeal cells and does not exhibit cytotoxicity, this kind of antagonist will be a good option to combat persistence of streptococci. The same considerations can be applied to the disorazoles.

Although the disorazoles will probably not be developed as 'pathoblockers' of streptococcal infections, one should not overlook the potential they hold. Currently, they are under investigation as antibody-drug-conjugates in cancer assuming that tubulin polymerization is their sole target (Seitz *et al.*, 2014). This study showed that disorazoles also have an influence on ezrin (fig. 3.1-16) which implies that ezrin is a potential second target of the disorazoles.

As ezrin is involved in several cellular processes, it is an interesting target for cancer therapy. In particular ezrin plays a central role in three mechanisms frequently exploited by tumor cells: (1) Expression of ezrin is upregulated in two metastatic cancer types: rhabdomyosarcoma and osteosarcoma. Both cancer types are most common in children and adolescents, but rare in general. It is assumed that ezrin is necessary for metastatic tumor cells to interact with surrounding cells because ezrin mediates cell-cell junctions. It was observed that ezrin expression correlated with metastasis in a mouse model: an upregulation of ezrin led to a higher rate of metastasis. In addition, it was detected that silencing of ezrin decreased metastasis (Khanna *et al.*, 2004; Hunter, 2004; Yu *et al.*, 2004; Zhang *et al.*, 2014). (2) Metastatic tumor cells exhibit phagocyte-like behavior: lymphocytes that try to render metastatic tumor cells innocuous are ingested and digested by the latter. Phagocyte-like behavior of metastatic tumor cells is ezrin-dependent: ingested non-tumor-cells are found in caveolae. These have been shown to be associated with ezrin (Lugini *et al.*, 2006; Fais, 2007). (3) The expression of (drug) efflux pump p-glycoprotein (p-gp) is often highly upregulated in multi-drug-resistant tumor cell types. As a result, cytotoxic drugs cannot act against the tumor cell as they are rapidly exported by p-gp. Ezrin colocalizes with p-gp. Furthermore, silencing of ezrin resulted in restoration of drug susceptibility of multi-drug-resistant tumors. Therefore, ezrin is a key player in multi-drug-resistant tumors (Luciani *et al.*, 2002; Fais, 2004).

In this study, it was shown that disorazoles altered the cellular organization of ezrin in an infection context (fig. 3.1-16). By doing so, they inhibited streptococcal invasion mediated by cytoskeletal rearrangements and by SfbI. The alteration of the cellular organization of ezrin could be a result of a

direct influence of the disorazoles on ezrin or on upstream effectors of ezrin. Future research will have to investigate this.

Therefore, there is rising evidence that disorazoles have a second target which might be connected to ezrin or ezrin itself. Furthermore, this study suggests that ezrin is involved in streptococcal invasion. If the disorazoles are too toxic to be used as 'pathoblockers', there is a possibility to test them as agents against metastatic cancer types: so far, the aforementioned cancer types are related with a poor outcome as metastasis cannot be treated well (Zhang *et al.*, 2014). In addition, no inhibitor of ezrin is currently under investigation or has been published. As the cause for the aforementioned mechanisms exploited by tumor cells is an upregulation of ezrin, a targeted therapy with disorazoles could be beneficial: metastasis could be decreased, phagocyte-like behavior could be impaired and drug-sensitivity in multi-drug-resistant cancer types could be restored. Thus, future investigations should be directed towards the potential second target of the disorazoles in the context of metastatic cancers.

4.2 Inhibitors of plasmin(ogen)

The salinimyxantins and the two isolated fatty acids have the same target: they both inhibit plasmin(ogen). First, the salinimyxantins and the fatty acids will be discussed separately in the context of group A streptococcal diseases. Then, their potential application as antifibrinolytics and in the combat against infectious diseases caused by *S.pyogenes* will be elaborated.

4.2.1 Salinimyxantins as inhibitors of plasmin(ogen)

Recently, myxobacterial compounds termed 'salimyxins' have been identified. Although the names are related, the salinimyxantins should not be confounded with the salimyxins. The latter are structurally completely different metabolites which only exhibit weak antibiotic activity and have not been tested as anti-virulence agents (Felder *et al.*, 2013). The salinimyxantins also exhibited only weak to moderate antibiotic activity (weak activity against *S.pneumoniae* and moderate activity against *S.aureus*; data from the myxobase; assays performed by Victoria Schmitt and Dr. Jennifer Herrmann, MINS, HIPS). As the salinimyxantins feature completely new chemical scaffolds, they were investigated for their potential activity as anti-virulence agents or 'pathoblockers'.

First, all salinimyxantins were tested for their inhibition of plasminogen activation mediated by cluster 2a type streptokinase. Salinimyxantin sAP01 proved to be the most effective compound in the inhibition of plasminogen activation. sAP02 had an equal potential compared to sAP01. Therefore, the hydroxyl-group located close to the right aryl-ring can be substituted by a keto-group (fig. 3.2.1). Moreover, the loss in activity of the compound sAP03 suggests that the phenyl-ethyl-group is necessary. In case of the salinimyxantin sAP04, meta-substituents with a -I-effect led to a decrease in activity. Exchange of the hydroxyl-group in para-position in the right aryl moiety led to a slight decrease in activity. To sum up, both the phenyl-ethyl-ring and meta-substituents with a -I-effect decrease activity (fig. 3.2-1-3.2-2). However, the initial structure-activity relationship (SAR)-studies performed so far might be extended: as substituents with a +I- or +M-effect were necessary for good activity, it should be tested if additional substituents in ortho-position of the aryl-ring of the right moiety lead to a higher activity. These substituents should also have a +I- or a +M-effect and could be hydroxyl-, methoxy- ethoxy - or amino-groups. Furthermore, one could try to substitute the aryl-rings of the left moiety and of the lower moiety in ortho- and para-position with additional groups with a +I- or a +M-effect. As the exchange of the hydroxyl-group to a keto-group in the carbon chain did not lead to a decrease in activity, it should be investigated whether analogous groups like amino-groups

will lead to an increase or decrease in activity. Fig. 4.2-1 summarizes the aforementioned considerations.

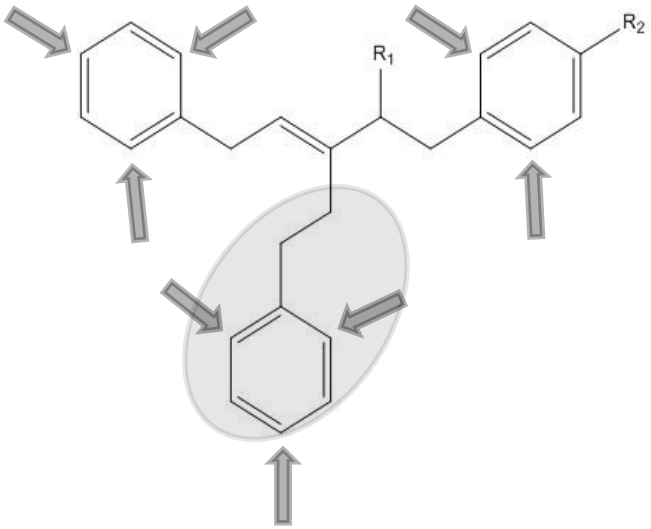

Figure 4.2-1: Possibilities for further SAR-studies of the salinimyxantins.
The basic chemical scaffold of the salinimyxantins is shown. Arrows indicate substitutions with +I- or +M-effect ligands. The phenyl-ethyl-moiety is highlighted in grey as it is necessary for activity. R_1 can be a keto-, hydroxyl- or amino-group. R_2 can be a methoxy-, hydroxyl-, amino- or ethoxy-group.

ε-amino caproic acid (EACA) and tranexamic acid (TA) (fig. 3.2-3) are known inhibitors of plasminogen activation. They are lysine-analogues and interact with kringle domains of plasminogen. Consequently, the latter cannot be activated to plasmin (Alkjaersig *et al.*, 1959; Markus *et al.*, 1979; Mathews *et al.*, 1996). In addition, EACA interacts with the streptokinase-plasminogen-complex by a kringle-dependent mechanism and is thereby able to inhibit this complex (Lin *et al.*, 2000).

Compared to the known inhibitors of plasminogen activation, the salinimyxantins sAP01 and sAP05 are more effective: EACA and TA have an IC_{50} of 1 mM and 250 µM, respectively (fig. 3.2-4). These IC_{50}-values are much higher than the IC_{50}-values of sAP01 (25-50 µM) and sAP05 (approx. 134 µM).

By contrast with other potent natural compounds (Baumann *et al.*, 2014), the IC_{50}-values of the salinimyxantins appear to be quite high. However, in the context of inhibition of plasminogen activation the salinimyxantins are potential new promising agents or lead compounds as their IC_{50}-values are much lower than those of the known inhibitors (EACA and TA).

As different cluster types of streptokinase activate plasminogen in different ways (McArthur *et al.*, 2008), the salinimyxantins were tested for their inhibitory properties against plasminogen activation of cluster 2b type streptokinase. The salinimyxantin sAP01 as well as the known inhibitors EACA and TA did not inhibit plasminogen activation mediated by cluster 2b type streptokinase efficiently: sAP01 inhibited plasminogen activation by only 20 % at a concentration of 50 µM. For the same range of inhibition 1 mM of EACA and 250 µM of TA were necessary (fig. 3.2-5). It cannot be stated that the salinimyxantins are good inhibitors of plasminogen activation mediated by cluster 2b type streptokinase. Though, the same applies to EACA and TA. As EACA and TA target plasminogen and interact with its lysine-binding sites, it is expected that inhibition of plasminogen activation is

independent of the respective activator. However, it can be hypothesized that the poor inhibition of all tested substances is a result of the different activation mechanism: as cluster 2b type streptokinase forms a tri-molecular complex involving fibrinogen (Cook *et al.*, 2014), potentially, EACA and TA are not able to access the kringles of plasminogen and to interact with them. Thus, they were not able to inhibit the activation of plasminogen to plasmin effectively. The target of the salinimyxantins is not known yet. The fact that these substances did also not inhibit the activation of plasminogen to plasmin to a greater extent suggests that they cannot interfere with the tri-molecular complex. This proposes two possible interaction partners for the salinimyxantins: streptokinase on the one hand or plasminogen on the other.

uPA and tPA are endogenous activators of plasminogen within the human host. Both cleave the Arg_{561}-Val_{562} bond of plasminogen proteolytically and thereby, activate plasminogen to plasmin (Parry *et al.*, 2000). Staphylokinase is another activator of plasminogen. Similarly to streptokinase, it forms a stoichiometric complex with plasminogen and thereby, activates plasminogen to plasmin (Coleman and Benach, 1999). TA and EACA did not inhibit activation of plasminogen mediated by tPA or uPA in concentrations ranging up to 25 µM. Activation of plasminogen mediated by staphylokinase was slightly inhibited by EACA and TA. By contrast, sAP01 inhibited plasminogen activation mediated by uPA, tPA and staphylokinase, but differed in efficiency resulting in different IC_{50}-values. sAP05 only inhibited plasminogen activation mediated by staphlyokinase. At low concentrations of sAP05 plasminogen activation mediated by uPA was accelerated (fig. 3.2-6). As sAP01 inhibited plasminogen activation mediated by all tested activators, there is strong evidence that it does not target a specific activator, but plasminogen. This explains the differences in the IC_{50}-values for the tested activators. Conversion from plasminogen to plasmin is a result of different modes of activation (see above). Depending on the respective activator, the plasminogen molecule might not be easily accessible resulting in unequal efficiency in inhibition of activation. The same explanation can be applied to EACA and TA. In addition, sAP05 which differs from sAP01 only in one substituent in para-position of the aryl-ring (fig. 3.2-1) did not inhibit plasminogen activation mediated by uPA and tPA in the tested concentrations (fig. 3.2-6): possibly, the methoxy-substituent led to decreased interaction with plasminogen. It can be assumed that low concentrations of sAP05 stabilized the conformation of two-chain-uPA resulting in accelerated plasminogen conversion. This cannot be observed at higher concentrations of sAP05 as possibly, plasminogen inhibition by sAP05 is more effective than activation of two-chain-uPA. However, these hypotheses need to be validated by e.g. docking studies of sAP05 with uPA and plasminogen.

sAP05 and sAP01 inhibited plasminogen activation mediated by several activators. As a result of the aforementioned thread, it is very likely that the salinimyxantins target plasminogen. The exact region of interaction between the salinimyxantins and the plasmin(ogen) molecule needs to be elucidated.

However, an involvement of lysine-binding sites within the kringle-domains of the plasmin(ogen) molecule is unlikely due to the fact that the salinimyxantins lack amino-groups like EACA and TA. Though, it could still be possible that they interact with them. Future investigations will have to determine the binding region of the salinimyxantins within the plasmin(ogen) molecule.

As the salinimyxantins are taken into account as 'pathoblockers', their cytotoxic effects had to be investigated in more detail. In this study, sAP01 and sAP03 were tested: sAP01 is considered as the most active compound and sAP03 lacks the phenyl-ethyl-moiety. At concentrations up to 50 µM both compounds were found to be cytotoxic. Though, at concentrations of about 5 µM, they did not exhibit cytotoxic effects. In addition, the lack of the phenyl-ethyl-group resulted in lower cytotoxicity (fig. 3.2-7). As a result, the structure should be optimized to reduce cytotoxic effects: possibly, substitutions in ortho- and para-position of the aryl-rings of the left and right moiety with groups harboring a +I- or a +M-effect could compensate the loss of the phenyl-ethyl-group with regard to the inhibitory activity. Moreover, amino-groups as substituents could be beneficial: possibly, a stronger inhibitory effect will be observed as the compounds will interact with lysine-binding sites within the kringle-domains of plasminogen then.

EACA and TA inhibit plasminogen exclusively, but not plasmin activity (fig. 3.2-8). As it is most likely that the salinimyxantins have a different target in the plasminogen molecule, the same region could also be targeted in the plasmin molecule. Both tested salinimyxantins inhibited plasmin activity in two different assays: in a clot lysis assay and in an assay measuring the activity of plasmin directly. Clot lysis is a dynamic process: if a clot is not destroyed, thrombin will continue to activate fibrinogen to fibrin. This results in a clot with increased stability towards lysis by plasmin: the more fibrin fibers exist within a clot (as a result of thrombin activity), the less rapidly the clot will be destroyed by plasmin. As plasmin activity was inhibited by sAP01, thrombin was enabled to rebuild the clot. This fact explains the change in the inhibition rates of sAP01: after an initial inhibition of only 40 % of clot lysis, clot lysis was inhibited up to 60 %. Since EACA and TA cannot inhibit plasmin activity because they only target plasminogen, the clot was lysed (fig. 3.2-8a). In addition, sAP01 and sAP05 inhibited plasmin activity directly. sAP05 was even more effective in inhibition of plasmin than sAP01 (fig. 3.2-8). Therefore, optimization of the structure of the salinimyxantins with substituents with a +I- or +M-effect could be worthwhile. It has to be emphasized that the IC_{50}-value of sAP05 for plasmin was lower than 13 µM (fig. 3.2-8). Assuming that sAP05 will have similar cytotoxic effects as sAP01 (as they differ only in one substituent), it is likely that no cytotoxic effects will be observed at concentrations around 5-10 µM (fig. 3.2-7). At these concentrations sAP05 already exhibited a significant inhibitory activity with regard to plasmin. Nevertheless, sAP05 has to be tested for its cytotoxic effects as it is a good candidate for further development as a 'pathoblocker'. However, it

has to be underlined that without structural modifications, the therapeutic window will be quite small.

The salinimyxantins appear to be a promising new group of natural products derived from myxobacteria that target plasmin(ogen) - an important host factor deployed as a virulence factor of bacteria like *S.pyogenes* (Walker *et al.*, 2005). Nevertheless, the binding of the salinimyxantins has to be proven by either biophysical methods or by co-crystallization. The latter method will also give insights into the precise binding site within the plasmin(ogen) molecule.

4.2.2 Isolated fatty acids as inhibitors of plasmin(ogen)

In contrast to the salinimyxantins which are clearly secondary metabolites, the fatty acids discovered here could be part of the primary or secondary metabolism. They were found in several myxobacterial extracts (fig. 3.3-1), but not in the myxobacterial compound library. In addition, they were already produced after day one of cultivation and their production did not decline over time (fig. 3.3-2). By contrast, production of secondary metabolites starts (often) only after several days of cultivation. Sometimes myxobacterial strains stop producing their secondary metabolites when they are cultivated for a longer time. This is often attended by a different morphology and faster growth rates of the respective producing strain (Dr. Kathrin I. Mohr, personal communication). This did not apply to the fatty acids: extracts from the different myxobacterial strains prepared in different intervals within three years did not lose their activity (data not shown), although some strains adapted to cultivation conditions by growing faster and changing their morphology. Future investigations should clarify if the fatty acids belong to the primary or secondary metabolism and uncover how they are produced within myxobacteria.

The isolated fatty acids (RC 36.1 and RC 36.2) only harbored one or two double bond(s), respectively. Therefore, the UV-detection was only possible at 210 nm. At that wavelength, some detectors are not sensitive enough and often solvents absorb the UV-light. As a result, peaks harboring active substances can be overlooked. The Corona detector used in this study is based on the charged aerosol technology. Like detection by mass or NMR, the Corona is a (universal) detector which also tracks substances that do not have UV-active structural elements (Górecki *et al.*, 2006). Though, the Corona detector was only used in conjunction with an analytical HPLC, but not with preparative liquid chromatography. Therefore, an activity-guided-strategy for purification and isolation of the compounds was applied: fractions obtained by preparative LC were tested in the plasminogen activation assay and only active fractions were used for further purification (fig. 3.3-3 and 3.3-4). To assure that the fatty acids were protonated and quantitatively extracted with organic solvents, acidic conditions were used.

After isolation, the exact mass and the elemental composition of both fatty acids were determined by using HR-ESIMS. ^{1}H- and ^{13}C-NMR spectra of both fatty acids were recorded. However, these could not aid in the exact localization of the double bond(s) due to the presence of too many methylene signals (fig. 8-1). Two-dimensional NMR methods like HSQC, HMBC or COSY-spectra (data not shown) could not elucidate the exact position of the double bond(s): the resolution was not sufficient to clearly assign the methylene signals.

Therefore, different derivatizations for GC-MS were used. Derivatization to methyl esters was not suitable to detect the location of a double bond. The fragmentation pattern of the respective molecule gave a hint (fig. 8-2), but did not determine the possible location definitely: double bonds change their positions upon fragmentation as they delocalize the charge. Therefore, methods preventing this double bond migration like derivatization with DMDS or 2-amino-2-methyl-propan-1-ol had to be used. Derivatization with DMDS was only suitable for monounsaturated fatty acids like RC 36.1 (fig. 8-3). Polyunsaturated fatty acids like RC 36.2 can form more complex products with DMDS: thiopyran or thiophen rings can be built. Furthermore, a partial thio-methyl-substitution at the position of one double bond is possible as well as formation of di- or tri-adducts that are not sufficiently volatile anymore. As a result, these adducts will not elute from the GC-column (Dunkelblum *et al.*, 1985; Leonhardt and DeVilbiss, 1985). To determine the location of a double bond without a reference spectrum deposited in a database, it is necessary to know the potential products of a reaction. Then, it is possible to gain an idea of the fragmentation pattern and reveal characteristic fragments. As this procedure does not apply to polyunsaturated fatty acids, another derivatization method had to be used.

If fatty acids are derivatized with 2-amino-2-methyl-propan-1-ol to become DMOX-derivatives, the respective double bond is not involved in the reaction with the reagent and remains ‘untouched’. But the respective double bond is disabled to migrate during fragmentation. Instead, fragmentation occurs in α-position and in the middle of the double bond(s). The latter fragmentation is unlikely to occur in mass spectrometry. However, it can be observed in some cases - as well as in the case of the DMOX-derivatives (Fay and Richli, 1991). Consequently, this derivatization method is suitable for both fatty acids, RC 36.1 and RC 36.2. Mild reaction conditions had to be used as the double bond(s) are oxidized easily under harsh reaction conditions. By derivatization with 2-amino-2-methyl-propan-1-ol under mild reaction conditions, the location of the double bond(s) of the respective fatty acid was determined undoubtedly (fig. 8-5).

Nevertheless, no reliable information on the exact configuration of the respective double bond(s) was obtained. To get a first idea of the configuration of the respective fatty acid, commercially available fatty acids with different configurations of the double bond(s) were subjected to GC-MS analysis after derivatization with 2-amino-2-methyl-propan-1-ol and observed to elute slightly

differently. Comparison of these elution profiles to those of RC 36.1 and RC 36.2 led to the hypothesis that both compounds, RC 36.1 and RC 36.2, are mixtures of two configurations: RC 36.1 mainly consisted of (9*Z*)-hexadecenoic acid with a very small amount of (9*E*)-hexadecenoic acid whereas RC 36.2 was essentially composed of (9*Z*,12*Z*)-octadecadienoic acid with a smaller proportion of (9*E*,12*E*)-octadecadienoic acid (fig. 8-3 and 8-6). Preliminary experiments with regard to plasminogen activation with the commercially available fatty acids were performed. Although, the corresponding commercially available fatty acids inhibited plasminogen activation, higher concentrations were needed to obtain the same effects compared to experiments with RC 36.1 or RC 36.2 (fig. 6-2). Possibly, the commercially available fatty acids were not as pure as RC 36.1 and RC 36.2. Acidic extractions (vide 2.1.4) were performed to assure that the commercially available fatty acids were protonated similarly: as there is no information available about their preparation process, it is conceivable that they were partially supplied in their salt forms. However, acidic extraction might have led to a lower yield of the respective commercially available fatty acid: the extraction process itself did not guarantee a completely quantitative extraction. In addition, double bond(s) may get oxidized resulting in a loss of activity. As only two configurations for RC 36.1 were possible, one commercially available fatty acid or the combination of both should have had the same effects as RC 36.1. Therefore, the extraction process still has to be optimized. If the commercially available fatty acids can be extracted quantitatively, inhibition of plasminogen activity by one of these commercially available fatty acids might indicate the configuration of the double bond(s) within the isolated fatty acids (RC 36.1 and RC 36.2).

In addition, other analytical methods can assist in the determination of the exact configuration: GC-MS with a chiral stationary phase in correlation with known fatty acids for every possible configuration (i.e. (9*Z*)-hexadecenoic acid, (9*E*)-hexadecenoic acid, (9*Z*,12*Z*)-octadecadienoic acid, (9*E*,12*Z*)-octadecadienoic acid, (9*Z*,12*E*)-octadecadienoic acid, (9*E*,12*E*)-octadecadienoic acid) as ‘standards’ will determine the configuration of RC 36.1 and RC 36.2: elution profiles will be clearly distinguishable.

RC 36.1 and RC 36.2 (fig. 3.3-10) inhibit plasminogen activation mediated by uPA, tPA, cluster 2a and 2b type streptokinase. Plasminogen activation mediated by staphylokinase was not inhibited (fig. 3.3-11). The cluster types of the streptokinases of the respective strains were determined unequivocally by sequence analysis of the β-domain (fig. 6-1). For inhibition of plasminogen activation mediated by cluster 2a type streptokinase similar concentrations of RC 36.1 and RC 36.2 as for inhibition by EACA and TA were needed. Though, inhibition of plasminogen activation by cluster 2b type streptokinase was not achieved completely. Compared to EACA and TA, lower concentrations of RC 36.1 and RC 36.2 were needed to achieve the same effects. In addition, RC 36.1 and RC 36.2 inhibited plasminogen activation mediated by uPA and tPA whereas EACA and TA were

not able to do so. As RC 36.1 and RC 36.2 inhibited plasminogen activation mediated by several activators with different modes of action, there is evidence that they target plasminogen. The differences in the ranges of inhibition can be a result of the different modes of activation of the different activators (as already elaborated in section 4.2.1). Although EACA, TA, RC 36.1 and RC 36.2 are all fatty acids, it is not likely that they have the same target within the plasminogen molecule: as RC 36.1 and RC 36.2 do not harbor amino-groups, it is unlikely that they will interact with lysine-binding sites within the kringle domains of plasmin(ogen). However, this interaction cannot be excluded. Presumably, the salinimyxantins (section 4.2.1) and the fatty acids (RC 36.1 and RC 36.2) also have different targets within the plasminogen molecule: the salinimyxantins were more effective in the inhibition of plasminogen and also inhibited plasminogen activation mediated by staphylokinase. The activation of plasminogen by staphylokinase was not inhibited by RC 36.1 and RC 36.2. Although, RC 36.1 and RC 36.2 were not as potent as the salinimyxantins concerning inhibition of plasminogen activation, they still have an advantage: they are not toxic (as they are fatty acids) and, therefore, will have a larger therapeutic window.

Moreover, differences in the inhibition of plasminogen activation mediated by different streptococcal strains harboring a cluster 2a type streptokinase were detected: both compounds, RC 36.1 and RC 36.2, inhibited plasminogen activation mediated by the cluster 2a type streptokinase of the strain AP1 not as efficiently as the activation mediated by the streptokinase of the strain A614 (fig. 3.3-11 and fig. 6-2). As culture supernatants were used for the plasminogen activation assay mediated by cluster 2a type streptokinase, these supernatants do not only consist of streptokinase, but harbor also other secreted streptococcal proteins. Potentially, these secreted factors interfere with the fatty acids and lead to a decrease of their activity. The use of recombinant proteins excludes these interference factors. However, in a clinical situation, fatty acids will also have to assert themselves against other secreted streptococcal proteins. Although both tested strains harbor a cluster 2a type streptokinase, they might differ significantly in other virulence factors. Therefore, it should be considered that higher concentrations of the fatty acids might be necessary for an efficient inhibition of plasminogen activation depending on the respective streptococcal strain.

In addition to their inhibitory properties with regard to plasminogen activation, the fatty acids prolonged entrapment of two different streptococcal strains significantly (fig. 3.3-12). These strains (AP1 and A666) harbor a cluster 2a and a cluster 2b type streptokinase, respectively (fig. 6-1). Although other virulence factors like SpeB might play a role as well, clot lysis is mainly a result of activation of plasminogen to plasmin. Streptococci escape from clots by activating plasminogen by secretion of streptokinase or by binding plasmin to their cell surface (Tapper and Herwald, 2000; McArthur *et al.*, 2012; Loof *et al.*, 2014). By inhibition of plasminogen activation, streptococcal

escape from clots is hampered. Although treatment with the fatty acids was beneficial (fig. 3.3-12), it was not determined if they target only plasminogen or plasmin directly.

If they have a binding site distinct from the one of EACA and TA, then this binding site could still be present in the plasmin molecule (similar to the salinimyxantins). Both compounds, RC 36.1 and RC 36.2, inhibited plasmin activity directly. In addition, RC 36.2 was more efficient in the inhibition of plasmin than RC 36.1: this finding was supported by its inhibiting activity against clot lysis and plasmin (fig. 3.3-13). RC 36.1 and RC 36.2 do not differ significantly in their chemical scaffold: RC 36.2 harbors an additional double bond and two additional C-atoms in its carbon chain compared to RC 36.1. Therefore, RC 36.2 has a slightly longer carbon chain than RC 36.1. As RC 36.2 is more active than RC 36.1, future SAR-studies could reveal even more potent candidates. Assumedly, another double bond in the carbon chain could lead to an additional increase in activity.

However, both compounds, RC 36.1 and RC 36.2, are promising with regard to their plasmin(ogen) inhibitory activities. In addition, testing of one of them *in vivo* for toxicity did confirm that they are not toxic (with respect to acute toxicity; fig. 3.3-14). The only slight gain of weight (around 2 %) during a 7-day-treatment can be attributed to anesthesia: mice have to be anesthetized every time they receive a s.c. injection (this is not necessary for the German ethical approval, but for the Australian one). As a result, it was observed that the mice did not eat much after anesthesia. Thereby, they did not gain as much weight as they could have gained without being subjected to this procedure (gain of weight on day 6 after a single injection vs. daily injections: 5 % vs. 0 %; fig. 3.3-14).

The strain 5448 appeared in the late 80ies and is a globally disseminated M1T1 group A streptococcal clone being responsible for several cases of severe invasive diseases. It harbors a cluster 2a type streptokinase and has several additional virulence factors favoring an invasive phenotype after skin infection (Kansal *et al.*, 2000; Aziz *et al.*, 2004; Cole *et al.*, 2006; Walker *et al.*, 2007; Maamary *et al.*, 2012; Barnett *et al.*, 2013). In an animal infection model with the strain 5448, both treatment regimens with the fatty acids did not prolong survival significantly. Treatment regimen one contained RC 36.1 whereas treatment regimen two contained RC 36.2. However, a slight tendency towards a longer survival was observed. Moreover, there was no significant difference in weight loss concerning the three different groups (fig. 3.3-15).

By contrast, both treatment regimens with the fatty acids do prolong survival significantly in the animal infection model using the strain AP1. There were no significant differences in weight loss between the three different treatment groups (fig. 3.3-15). The strain AP1 harbors an M1 protein - similar to the strain 5448. Moreover, it has a cluster 2a type streptokinase like the strain 5448. However, both strains differ significantly in their invasiveness: whereas infection with the strain 5448 is attended by a survival rate of 40-50 %, the lethality rate of the infection with the strain AP1 is 100 % if mice are treated only with PBS (fig. 3.3-15). The reason is that both strains differ in the

expression and secretion of other virulence factors resulting, for instance, in a hyperinflammation caused by the strain AP1 (Herwald *et al.*, 2004; Pahlman *et al.*, 2006). Moreover, the strain AP1 has a mutation in its *covS* gene leading to a loss of expression of SpeB, a proteinase that degrades several host and bacterial proteins, among these streptokinase (fig. 6-4 and 6-5). It has been shown that complete or partial loss of *covS* results in severe disease outcomes. Besides, SpeB expression is inversely correlated with disease severity: if SpeB is expressed, the outcome of the disease is less severe. In addition, if streptokinase is not degraded by SpeB, streptokinase can exert its function and activate plasminogen to plasmin. By generation of plasmin, streptococci are enabled to disseminate into deeper tissue and become systemic (Kansal *et al.*, 2000; Aziz *et al.*, 2004; Liang *et al.*, 2013; Tatsuno *et al.*, 2013). Therefore, the loss of SpeB expression in the strain AP1 (fig. 6-4) can be an additional explanation for its higher lethality rate in murine infection models compared to infections with the strain 5448.

However, the two treatment regimens were more effective in handling infections with the strain AP1 compared to those with the strain 5448 as they prolonged survival significantly in trials with the strain AP1 (fig. 3.3-15). The strain AP1 starts disseminating immediately compared to the strain 5448 which causes first skin lesions before dissemination (Walker *et al.*, 2007). Therefore, an early treatment with the fatty acids inhibiting plasmin(ogen) might result in hindrance of dissemination of the strain AP1 leading to a less severe outcome.

Only slight differences in the survival curves of untreated and treated mice were detected in the 5448 trial. As only groups of 12-13 mice were used so far, usage of higher mouse numbers might reveal superiority of a certain treatment regimen as well.

In addition, the outcome of the infection could be improved by a daily treatment with the two regimens. However, for the animal model with the strain 5448, treatment should only start after skin lesions can be observed. Otherwise, also untreated mice (that receive PBS as 'placebo') will survive the trial (observations from trials at the University of Queensland, Brisbane, Australia; data not shown): lavage with PBS close to the injection site before the strain 5448 becomes systemic apparently improved the outcome of the infection. If mice do not have to be anaesthetized for injection, a daily application of the respective treatment in the animal model with the strain AP1 could be beneficial. Moreover, administration of higher doses of the respective regimen could result in better outcomes for both infection models.

Another group also pursuing the way to treat invasive group A streptococcal infections with anti-virulence agents is the one of David Ginsburg: Sun and colleagues found two streptokinase gene expression inhibitors which had an IC_{50} of around 100 µM in a plasminogen activation assay mediated by streptokinase. Only one of these inhibitors showed significant effects in an *in vivo* model with a survival rate of around 40 %. The strain used in this infection model had a *covRS* mutation and might

therefore be similar to a certain extent to the strain AP1 employed in this study. The higher survival rates in the model described in the publication might be attributed to lower infection doses compared to the ones for AP1 used in this study. Moreover, the authors applied the streptokinase gene expression inhibitor daily for 4-5 days. They also administered high and low doses of their compound (40 µg and 5 µg) and observed significant effects for both doses ($p < 0.04$ and $p < 0.011$). Though, they did not apply the Mantel-Cox- or the Wilcoxon-test for calculation of the p-values: they 'corrected' their data with the Bonferroni method and used a logrank-test afterwards (Sun *et al.*, 2012) without explaining the reasons for their choice. Even though the Mantel-Cox- and the Wilcoxon-tests were used for determination of significance in survival assays, the approach of Sun and colleagues is not entirely *lege artis*: the Bonferroni method can only be implemented to determine statistical difference between gene expression levels. For survival- or kaplan-meier-plots, either the Mantel-Cox- or the Wilcoxon-test have to be applied. Similarly, different groups comparing gene expression levels and then survival curves utilized the Bonferroni method for testing of statistical significance of gene expression levels as a first step and a suitable test for determination of significance in a survival assay afterwards (Evans *et al.*, 2012; Li *et al.*, 2015) which is different from the procedure chosen by Sun and colleagues. Consequently, it cannot be stated if their streptokinase gene expression inhibitor significantly prolongs survival. In addition, the survival curve with the pooled data can also not be considered as a proof for a significant prolonged survival: the data of different treatments consisting of different doses of their inhibitors with different application schemes were summarized. Additionally, the authors found out that their inhibitor did not only inhibit streptokinase gene expression, but that it also altered several other genes (Sun *et al.*, 2012). Therefore, their compound cannot be considered as a specific streptokinase gene expression inhibitor - but rather as an inhibitor interfering with the entire group A streptococcal gene expression.

In comparison, the fatty acids (RC 36.1 and RC 36.2) examined in this study have a different target. However, both compound groups can be considered as anti-virulence agents: the compound of Sun and colleagues targets *inter alia* streptokinase gene expression directly whereas the fatty acids inhibit the exploitation of plasmin(ogen) by streptococci. In addition, the fatty acids have similar or quite lower IC_{50}-values than the streptokinase gene expression inhibitor with regard to inhibition of plasminogen activation (Sun *et al.*, 2012). However, these IC_{50}-values cannot be compared as Sun and colleagues used a different streptococcal strain possibly harboring a distinct streptokinase cluster type. Moreover, the fatty acids prolong survival in the animal model with the strain AP1 significantly.

As a consequence, the fatty acids are auspicious with regard to their activity - especially in the *in vivo* model with the strain AP1. As a result of targeting plasmin(ogen), the further development of both

compound groups, fatty acids (RC 36.1 and RC 36.2) and salinimyxantins, as 'pathoblockers' or as new antifibrinolytics is suggested.

4.2.3 Inhibitors of plasmin(ogen) and their potential application as antifibrinolytics

Only three different antifibrinolytics made it into the market: aprotinin, ε-amino caproic acid (EACA) and tranexamic acid (TA). The latter two target plasminogen whereas aprotinin targets plasmin. EACA was never approved for the German market. In the case of aprotinin, the approval was suspended in 2007. Nevertheless, the suspension was lifted in 2013 on certain conditions (e.g. a risk management plan and registration of patients[1]), until now, no formulation for systemic antifibrinolysis containing aprotinin is on the (German) market. Though, several products used for local antifibrinolysis contain aprotinin (e.g. Artiss®, Beriplast®). Actually, only tranexamic acid remained on the market and is used as an antifibrinolytic for local and systemic therapy of bleeding (Cyklokapron®, film-coated tablets and injectable solution). However, a re-evaluation of tranexamic acid in conjunction with a resolution of the European Commission in 2012 led to cancellation of several indications. In addition, an analysis of the benefit-to-risk-profile resulted in the recognition of several adverse effects like severe sight disorders, seizures and severe gastrointestinal effects. But there was no proof for an elevated mortality rate under treatment with tranexamic acid assuming that it was administered as early as possible (in case of prevention of (severe) bleeding due to trauma, application of tranexamic acid was only beneficial when it was administered 3 h after injury). Moreover, contraindications comprise allergy or hypersensitivity against tranexamic acid and previous thromboembolic events[2] (Fergusson *et al.*, 2008; CRASH-2 collaborators *et al.*, 2011; Franchini and Mannucci, 2014). Consequently, in case of a contraindication, like allergy, there is no other drug on the market that can be used instead.

Furthermore, besides bleeding complications as a result of plasminogen activation by recombinant streptokinase or urokinase, or as a result of accidents or surgery, overdosing of the 'new generation' of anticoagulant drugs, like dabigatran (Pradaxa®), rivaroxaban (Xarelto®) or apixaban (Eliquis®), targeting FXa or thrombin (for the coagulation cascade vide fig. 1-7, section 1.1.2.2.2) can lead to severe bleeding complications, either, as there is no antidote on market so far (*nota bene*: antidotes for FXa-inhibitors as well as for thrombin inhibitors are under development (Lu *et al.*, 2013; Honickel *et al.*, 2015)). Treatment with tranexamic acid only was not able to prevent severe bleeding.

[1] "Risikobewertungsverfahren zu Aprotinin-haltigen Arzneimitteln für die intravenöse Anwendung" performed by "The Federal Institute for Drugs and Medical Devices" in Germany (Bundesinstitut für Arzneimittel und Medizinprodukte)

[2] "Durchführungsbeschluss der Kommission vom 10.10.2012, betreffend die Zulassungen der Humanarzneimittel mit dem Wirkstoff "Tranexamsäure" gemäß Artikel 31 der Richtlinie 2001/83/EG des Europäischen Parlaments und des Rates"

By contrast, only fibrinogen or FXIII concentrates with a low dose of tranexamic acid were able to reduce these bleeding complications (Tengborn *et al.*, 2015).

The fatty acids (RC 36.1 and RC 36.2) and the salinimyxantins can enrich the class of antifibrinolytics: as depicted in this section, tranexamic acid is the only antifibrinolytic used in the clinic to prevent severe systemic bleeding. Though, the use is also connected with severe adverse events. Certainly, the fatty acids and salinimyxantins will also have to be investigated *inter alia* for their respective drug-safety-profiles. They will not be developed to prevent overdosing with 'new generation' anticoagulant drugs as more specific antidotes are already under clinical investigation. Though, investigation of the fatty acids and salinimyxantins concerning the indication 'severe systemic bleeding' will be worthwhile: as these two groups of compounds inhibit plasminogen activation and plasmin activity directly, they can be used as plasmin inhibitors as well. Tranexamic acid does not have such a dual role. Therefore, the compounds found in this study could fill the gap that aprotinin has left. If they have a better benefit-to-risk-profile than aprotinin, they could replace aprotinin in countries where it is re-used nowadays.

4.2.4 Inhibitors of plasmin(ogen) - powerful new agents in the combat against infectious diseases

In addition to its role as an antifibrinolytic, aprotinin has also been tested in a streptococcal skin infection model. Mice infected with *S.pyogenes* and treated with aprotinin showed a significant reduction in size of skin lesions. The authors hypothesized that this can be attributed to two facts: (1) Streptococci were not able to acquire plasmin activity anymore. Consequently, plasmin was not used for dissemination into deeper tissue. (2) An endogenous antimicrobial peptide is not able to kill streptococci if these acquire surface plasmin activity as plasmin will degrade the peptide. By inhibition of plasmin by aprotinin, the antimicrobial peptide (human cathelicidin LL-37) is enabled to kill the streptococci (Hollands *et al.*, 2012).

The fatty acids (RC 36.1 and RC 36.2) improved survival of mice infected with the strain AP1 significantly (fig. 3.3-15). In addition, it was observed that mice infected with the strain 5448 and treated with the fatty acids showed skin lesions one or two days later than untreated mice infected with the same strain (data not shown). This fact can account for a slower onset of the infection with the strain 5448. Although the fatty acids target plasminogen activation and plasmin activity directly, it is possible that these are not the only effects leading to an improved outcome in the *in vivo* model. By inhibition of plasmin by the fatty acids, the host's immune defense is enabled to kill streptococci by secretion of the abovementioned antimicrobial peptide (human cathelicidin LL-37). Therefore,

future research can elaborate if this effect can be observed for salinimyxantins and the fatty acids as well.

Moreover, it has been described that the strain AP1 causes a hyperinflammation which contributes to severe outcomes *in vivo* (Pahlman *et al.*, 2006). Both fatty acids harbor at least one double bond. Unsaturated fatty acids can be oxidized which could result in anti-inflammatory effects by reducing oxidative stress. Preliminary studies in a cell-based assay indicated that RC 36.1 and RC 36.2 had slight anti-inflammatory effects. These effects were observed for 3 full hours after application of the fatty acids in a cell-based inflammation infection model. In this model translocation of NFκB (a transcription factor inducing factors involved in inflammatory responses) to the nucleus was measured. Nuclear translocation of NFκB can *inter alia* also be a result of oxidative stress (Morgan and Liu, 2011). This translocation occurred upon infection with *S.pyogenes*. Though, it was not determined if it occurred as a result of oxidative stress. However, this translocation was slightly reduced when infected cells were treated with RC 36.1 or RC 36.2 (data not shown). Therefore, it is possible that these (side-)effects also contribute to a better outcome in the *in vivo* infection model with the strain AP1. Potentially, they reduce an initial inflammation caused by this strain. As inflammation caused by streptococcal strains plays a role in invasive infections (Walker *et al.*, 2014) and as also molecules regardless of their double bonds could have anti-inflammatory effects and prevent nuclear translocation of NFκB (Lyß *et al.*, 1998), the salinimyxantins (although harboring one double bond) and the fatty acids should be tested in-depth for their anti-inflammatory properties.

In addition, plasmin can also be bound directly to surface receptors of streptococci, like SEN, or plasminogen can be bound to surface receptors, like PAM or GAPDH, and is then activated to plasmin (Pancholi and Fischetti, 1998; Pancholi and Chhatwal, 2003; Sanderson-Smith *et al.*, 2012). Acquisition of surface plasmin activity is advantageous for streptococci as it facilitates dissemination into deeper tissue (Cole *et al.*, 2006; Sanderson-Smith *et al.*, 2008). It was not assessed in this study if plasmin activity can be inhibited by the fatty acids or the salinimyxantins when plasmin is bound to one of these surface receptors. Though, the significant prolongation of entrapment of streptococci by the fatty acids can be a hint for inhibition of surface-bound plasmin activity (fig. 3.3-12): possibly streptococci safe themselves not only by secretion of streptokinase, but also by direct destruction of the fibrin clot by surface-bound plasmin. Therefore, future investigations should address the question if surface-bound plasmin activity can also be inhibited by salinimyxantins and the fatty acids.

However, streptococci are not the only bacteria exploiting the host's plasminogen activation system: besides staphylococci that secrete staphylokinase for activation of plasminogen, *Yersinia pestis* and *Salmonella enterica* also interfere with the coagulation and fibrinolysis equilibrium (Lähteenmäki *et al.*, 2005). In contrast to streptococci, staphylokinase is not responsible for

dissemination into deeper tissue: by using a skin infection animal model, it was shown that staphylokinase assists in the establishment of an infection, but does not lead to spreading into deeper tissue. However, disease severity was reduced. Peetermans and colleagues hypothesized that this fact was due to α_2-antiplasmin (an endogenous inhibitor of plasmin) inhibiting the plasmin(ogen)/staphylokinase-complex. As α_2-antiplasmin is not able to inhibit plasmin(ogen)/streptokinase-complexes of two clusters of streptokinase, this is a possible explanation for the differences in dissemination between staphylococci and streptococci (Kwiecinski *et al.*, 2013; Peetermans *et al.*, 2014). By contrast, the Pla protease of *Yersinia pestis* leads to invasiveness: Pla cleaves plasminogen at the same site as uPA (Sodeinde *et al.*, 1992). In addition, it activates single-chain to two-chain uPA and inactivates *inter alia* α_2-antiplasmin. However, it also inactivates the tissue factor pathway inhibitor. Therefore, *Yersinia* alters the hemolytic balance (Korhonen *et al.*, 2013). Recently, it was discovered that infection of human cells by *Salmonella enterica* serovar Typhimurium resulted in an increased presence of uPA. As a consequence, plasminogen was activated and dissemination was favored. Furthermore, the increased presence of uPA upon infection with Salmonella was a result of the protein PgtE which is structurally similar to Pla. This one inhibited the inhibitor of active uPA and at the same time activated single-chain to two-chain (i.e. active) uPA (Järvinen *et al.*, 2013).

It is likely that both, salinimyxantins and fatty acids, counteract the mechanisms exhibited by the aforementioned pathogens: both, salinimyxantins and fatty acids, inhibit plasminogen activation mediated by uPA and tPA (fig. 3.2-6 and 3.3-11). As Pla and PgtE activate plasminogen similarly to uPA, it is very likely that both compound groups will also interfere with these two activators. In addition, salinimyxantins inhibit plasminogen activation mediated by staphylokinase (fig. 3.2-6). Beside the aforementioned pathogens, there are several others interacting with the host's plasminogen/plasmin system (Bergmann and Hammerschmidt, 2007). As the salinimyxantins and the fatty acids target a host's component, there is rising evidence that they can be used not only to combat invasive streptococcal diseases, but also to fight against other severe bacterial infections.

4.3 Pathoblockers targeting virulence: the beginning of a new success story?

Within recent years, the concept of targeting virulence by blocking conserved pathogenic mechanisms of bacteria has been developed: with this concept of anti-virulence inhibitors or 'pathoblockers', clinicians shall be provided with new weapons to fight against bacteria who have found a loophole for most of the currently used antibiotics. In addition, these agents shall help to improve the outcome of severe diseases not sufficiently treatable up to now (Carapetis *et al.*, 2005; Clatworthy *et al.*, 2007; Cegelski *et al.*, 2008; Waddington *et al.*, 2014). Several screening strategies have been implemented to find potent new drugs (O'Connell *et al.*, 2013; Beckham and Roe, 2014). To date, most of these anti-virulence agents target quorum-sensing, especially of *Pseudomonas aeruginosa*, but also of *Streptococcus mutans*. These anti-virulence agents are of synthetical or natural origin, i.e. coumarin (Rasko *et al.*, 2008; Jansen *et al.*, 2010; Kunze *et al.*, 2010; Zender *et al.*, 2013; Pistorius *et al.*, 2011; Lu *et al.*, 2012, 2014; Starkey *et al.*, 2014; Gutiérrez-Barranquero *et al.*, 2015). One of these synthetical anti-virulence agents has recently been licensed by a pharmaceutical company (press release 5th March 2015, HZI, Braunschweig). In addition, so-called 'pilicides' were found that target pili of e.g. *E.coli* resulting in a decreased adhesion and biofilm formation (Chorell *et al.*, 2012). Moreover, some groups also found inhibitors of virulence gene expression of *Staphylococcus aureus* (Ma *et al.*, 2012) and *Streptococcus pyogenes* (Sun *et al.*, 2012). For the latter pathogen it was intended to target streptokinase gene expression specifically (Yestrepsky *et al.*, 2013, 2014). However, so far, there are no inhibitors published or on the market that target the invasion process or the exploitation of the plasminogen system directly. Targeting the invasion process with the disorazoles on the eukaryotic side is not entirely desirable: if cellular functions are altered, these agents can prevent invasion (fig. 3.3-1), but there is also the risk to damage the cells fatally. Therefore, targeting the bacterial side similarly to the abovementioned 'pilicides' or 'PqsR-antagonists' is more preferable. By contrast, interference with the host's plasminogen/plasmin system by application of the salinimyxantins and the fatty acids can be a possible treatment not only for invasive group A streptococcal diseases, but also for streptococcal diseases in which streptokinase plays a putative role, e.g. APSGN. Although again the host side is targeted, the *in vivo* model with the strain AP1 and the fatty acids showed that treatment improves the outcome of the disease (fig. 3.3-15). However, possible side effects which were not detected so far will have to be investigated.

5 Concluding remarks

In this thesis, it is shown that essential virulence pathways of *S.pyogenes* like adhesion and invasion or the exploitation of the host's plasminogen/plasmin system can be successfully blocked by natural compounds.

Inhibition of the host's plasminogen/plasmin system may improve the outcome of invasive group A streptococcal diseases like sepsis or necrotizing fasciitis as plasmin is deployed as a virulence factor (Walker *et al.*, 2014). In addition, specific fatty acids described here and the salinimyxantins could be a treatment option for acute poststreptococcal glomerulonephritis as streptokinase is thought to play a crucial role in the pathogenesis by activation of plasminogen (Nordstrand *et al.*, 1998, 2000). Besides, they can also be developed as antifibrinolytics. As a result, the fatty acids and the salinimyxantins are promising new compounds in the combat against group A streptococcal diseases.

Although the disorazoles exhibit cytotoxic effects after 24 h, they can be used as a model substance for inhibition of group A streptococcal invasion and might be modified for further application. The effects on ezrin reveal another target of the disorazoles which could uncover unknown indications of the disorazoles in cancer therapy. The alterations of ezrin upon treatment with the disorazoles lead to the hypothesis that ezrin is a potential new factor involved in - at least two different - group A streptococcal invasion pathways.

All activities of natural compounds discovered in this thesis may enrich the new class of 'pathoblockers' to improve the outcome of severe group A streptococcal diseases and open a new chapter in the combat against infectious diseases.

6 Supplemental information

6.1 Determination of the streptokinase cluster types of *S.pyogenes* strains A614, AP1 and A666

Different cluster types of streptokinase exist resulting in different plasminogen activation mechanisms (McArthur *et al.*, 2008). Therefore, the cluster type for each strain used in this study was determined. Thereby, the sequences of each strain were mapped against the β-domain of strains representing the different clusters.

The strains A614 and AP1 both have a cluster 2a type streptokinase as their β-domains are 100 % identical to the β-domain of the strain 5448 which also has a cluster 2a type streptokinase (fig. 6-1a,b (McArthur *et al.*, 2008)). In addition, the strain A666 harbors a cluster 2b type streptokinase as no insertions or deletions and only minor exchanges of bases were found in contrast to the strain NS59, a representative strain of a cluster 2b streptokinase (fig. 6-1c, (McArthur *et al.*, 2008)).

Figure 6-1: *ska* gene sequences of the *S.pyogenes* strains A614, AP1 and A666 in comparison to the ones of the strains 5448 and NS59.

a-c: The *ska* gene sequences of the strains A614 (a), AP1 (b) and A666 (c) were mapped against the β-domain of the strain 5448 (a,b,) or the strain NS59 (c). Identity is displayed as a dot. Differences in the bases are shown as the respective different base.

a,b: β-domains of the strains A614 and AP1 are 100 % identical with the one of the strain 5448.

c: Some minor base exchanges can be detected in the strain A666 with regard to the strain NS59.

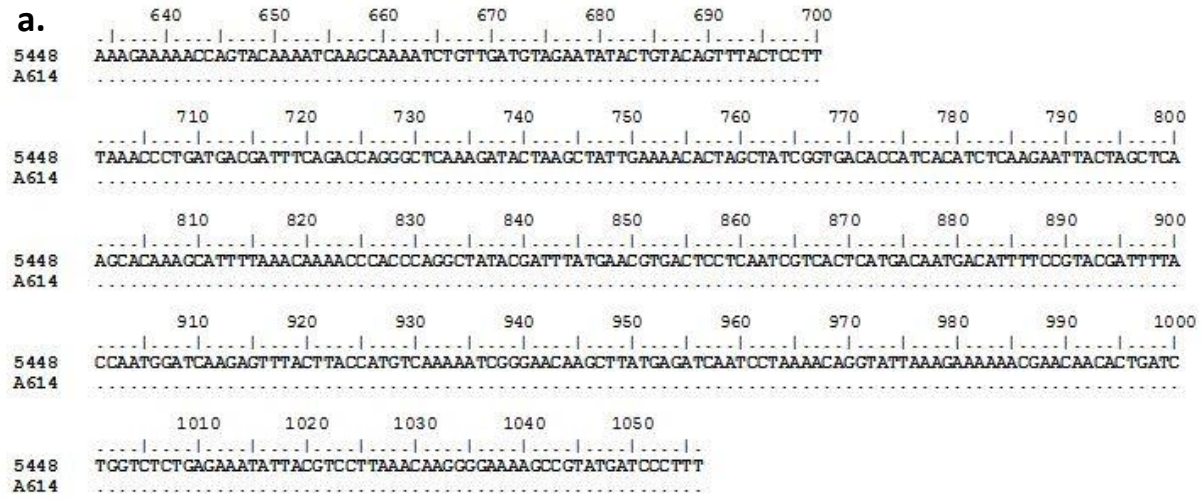

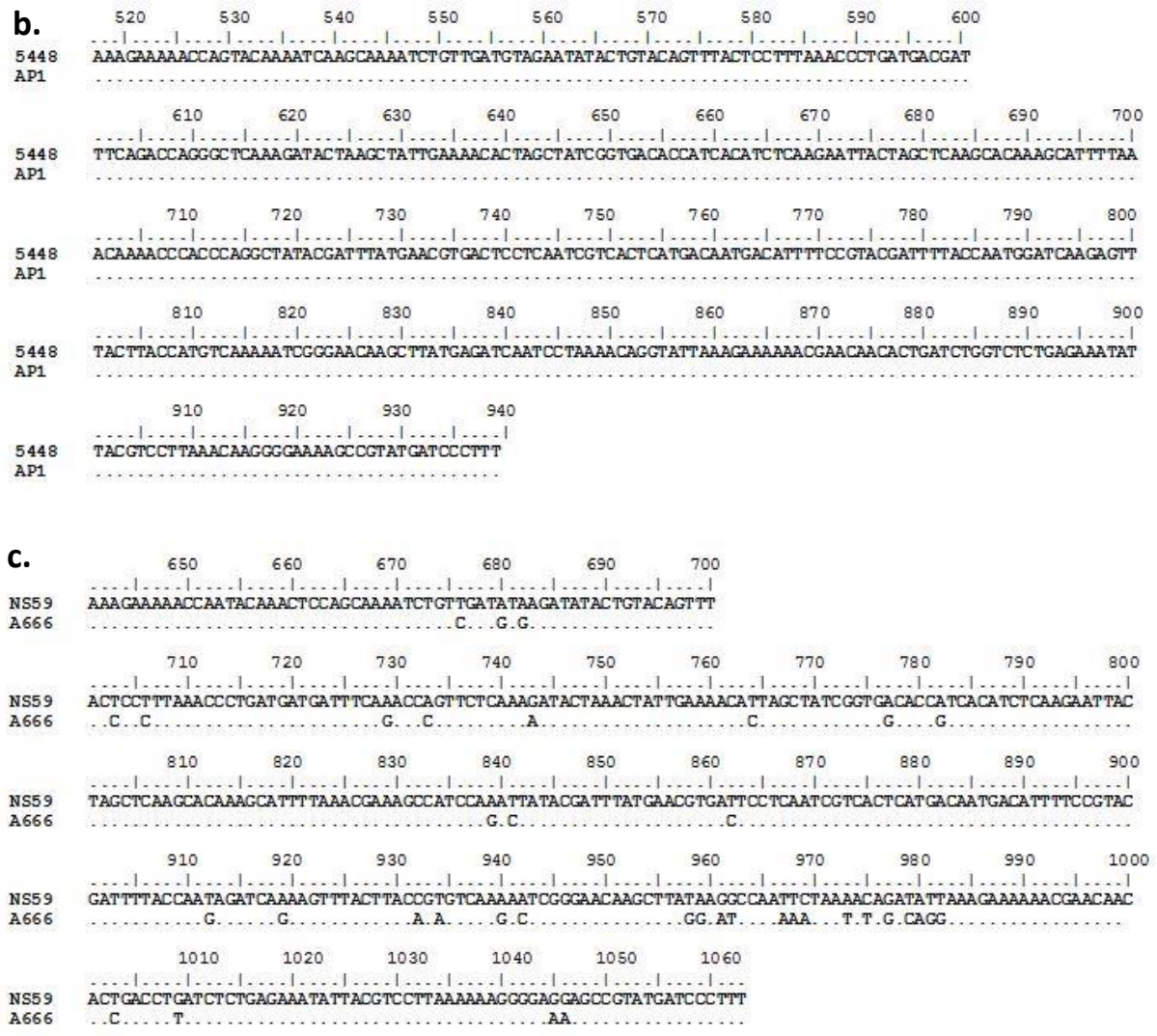

6.2 Commercially available fatty acids inhibit plasminogen activation

The commercially available fatty acids (LEA, PEA, PA and LA; corresponding to RC 36.1 and RC 36.2; vide section 3.3.3) were tested for their inhibitory properties of plasminogen activation. As RC 36.1 is a hexadec-9-enoic acid, two unsaturated C_{16}-fatty acids with the two possible *E*- and *Z*-configurations of the double bond, palmitoleic acid (PA) and palmitelaidic acid (PEA), were tested. Moreover, two unsaturated C_{18}-fatty acids (linoleic acid (LA) and linoelaidic acid (LEA)) with two possible configurations of the double bonds corresponding to RC 36.2 were tested as well. The GC-data (vide sections 3.3.3 and 8.2) of RC 36.1 and RC 36.2 suggested that both substances contained the respective C_{16}- or C_{18}-fatty acid with two different configurations. Therefore, combinations of the commercially available fatty acids (LEA/LA and PEA/PA) were tested as well. Inhibition of plasminogen activation was tested with two different strains harboring both a cluster 2a type streptokinase: A614 and AP1. The strain A614 was used both for the standard plasminogen activation

assay and for screening of active compounds (vide section 3.3.1). The strain AP1 was chosen in addition to the strain A614 as it is known that the strain AP1 exhibits high virulence in murine infection models (Shannon *et al.*, 2010).

The combination of LEA/LA and PEA/PA was most effective in inhibition of plasminogen activation for both tested strains (fig. 6-2a,b,d,e). PEA/PA and LEA/LA inhibited plasminogen activation mediated by the strain A614 by only 20-30 % at a concentration of 250 µg/ml of each fatty acid. In addition, PEA inhibited plasminogen activation by 20 % at a concentration of 250 µg/ml (approx. 984 µM). LA, LEA and PA alone did not inhibit plasminogen activation significantly (fig. 6-2a,b).

Both isolated fatty acids RC 36.1 and RC 36.2 were tested for inhibition of plasminogen activation mediated by streptokinase of the strain AP1 as well. Thereby, the activity of the isolated and the commercially available fatty acids was compared. Both RC 36.1 and RC 36.2 inhibited plasminogen activation by only 25-30 % (fig. 6-2c). They exhibited a lower activity against the strain AP1 compared to the strain A614 (fig. 3.3-11a; section 3.3.4). The combinations of the commercially available fatty acids (LEA/LA and PEA/PA) as well as PEA, PA and LA alone showed significant inhibitory effects. Though, these effects resulted only in an inhibition of plasminogen activation by 20-30 % at concentrations of 250 µg/ml (fig. 6-2d,e).

Consequently, inhibition mediated by commercially available fatty acids was not as efficient as by RC 36.1 and RC 36.2. A possible reason could be that the commercially available fatty acids were not sufficiently pure or could not be recovered quantitatively after acidic extraction (vide 2.1.4). As a result, RC 36.1 and RC 36.2 were used for additional assays.

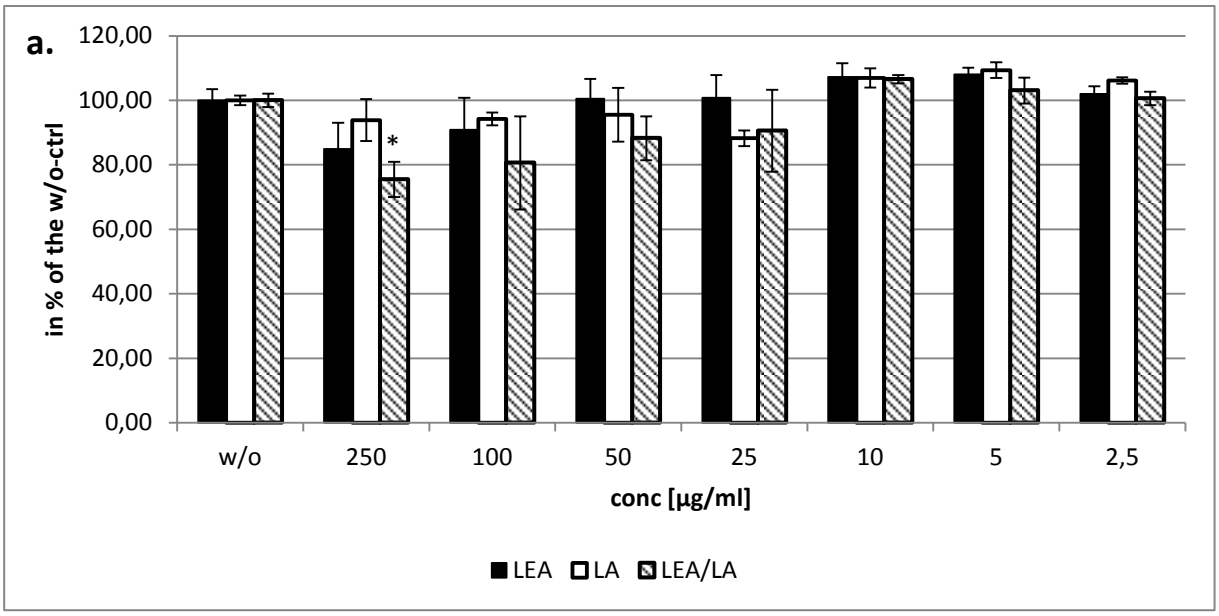

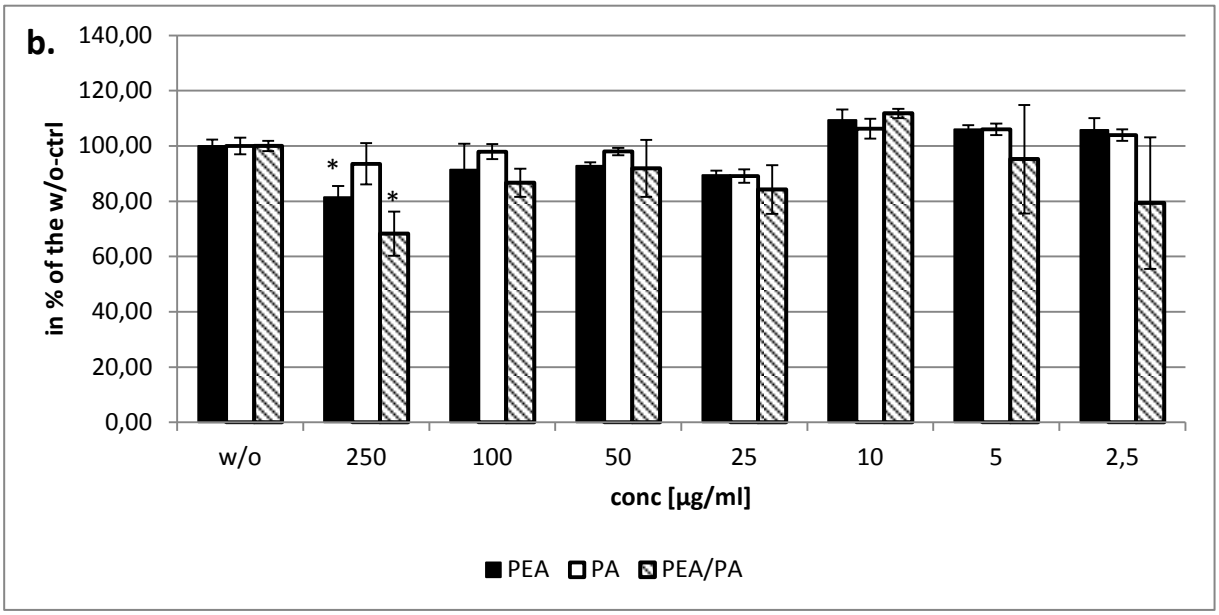
b.
140,00
120,00
100,00
80,00
60,00
40,00
20,00
0,00
in % of the w/o-ctrl
*
*
w/o
250
100
50
25
10
5
2,5
conc [µg/ml]
PEA
PA
PEA/PA

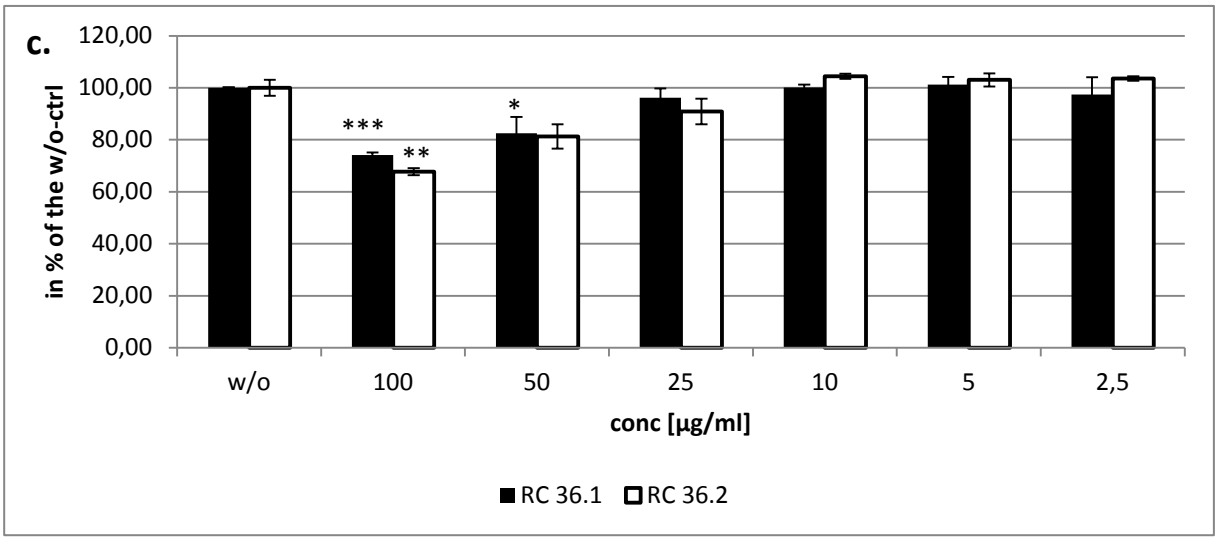
c.
120,00
100,00
80,00
60,00
40,00
20,00
0,00
in % of the w/o-ctrl
***
**
*
w/o
100
50
25
10
5
2,5
conc [µg/ml]
RC 36.1
RC 36.2

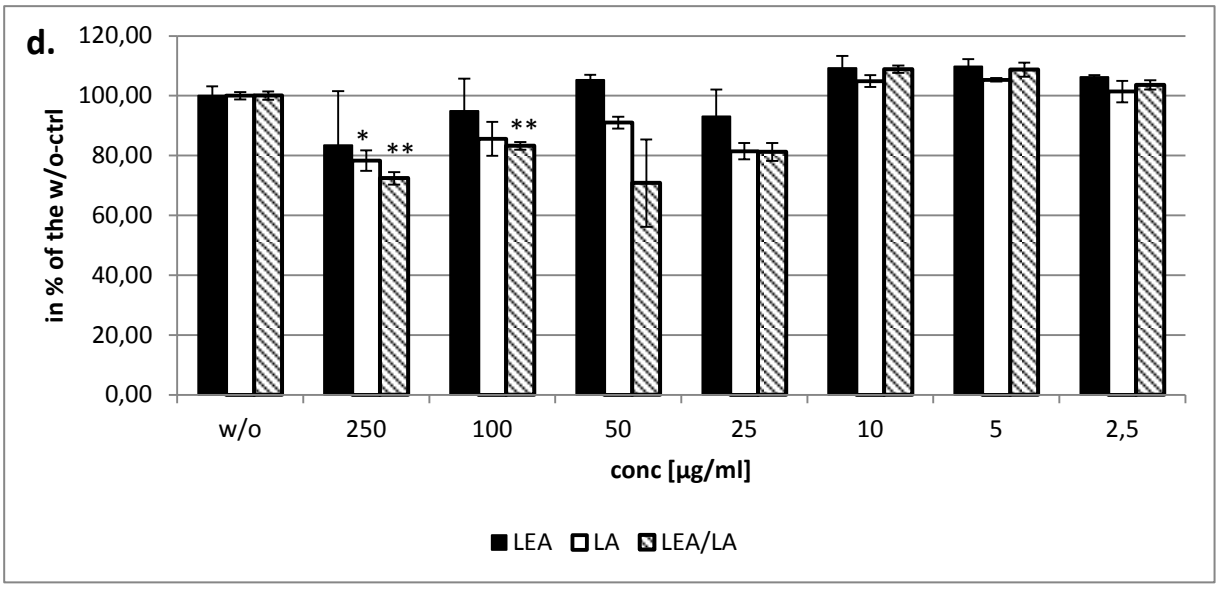
d.
120,00
100,00
80,00
60,00
40,00
20,00
0,00
in % of the w/o-ctrl
*
**
**
w/o
250
100
50
25
10
5
2,5
conc [µg/ml]
LEA
LA
LEA/LA

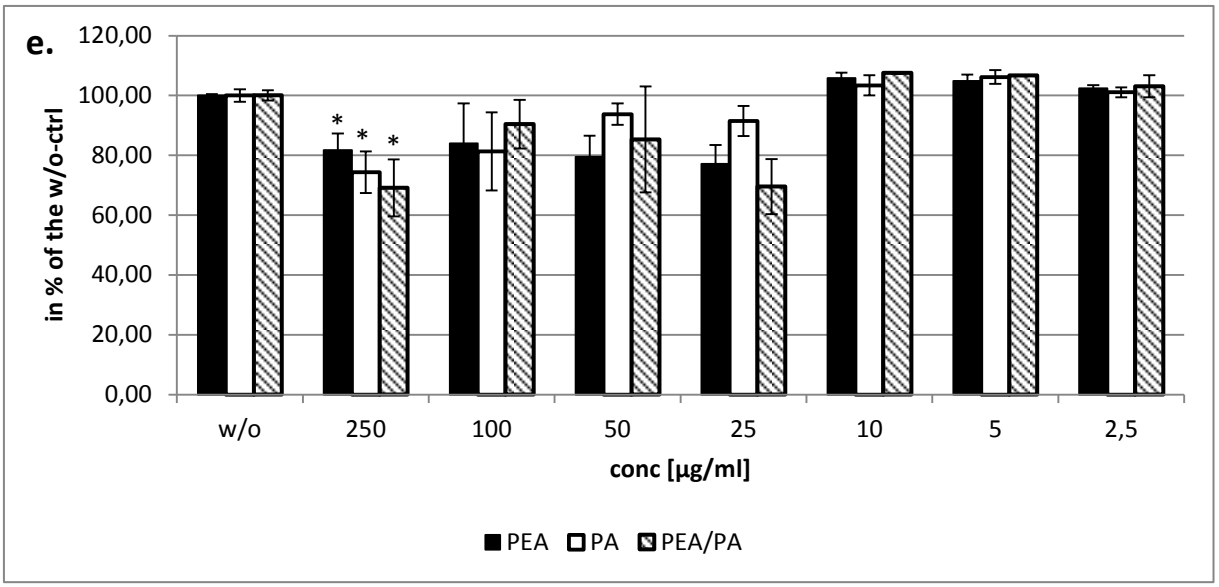

Figure 6-2: Characterization of commercially available fatty acids compared to RC 36.1 and RC 36.2.
a-e: A plasminogen activation assay was performed. Plasminogen was activated via cluster 2a type streptokinase from strain A614 (a,b) or AP1 (c-e). PEA, PA or a combination thereof (50% PEA and 50% PA) were tested (b,e). LA, LEA or a combination thereof (50 % LEA and 50 % LA) were tested as well (a,d). In addition, RC 36.1 and RC 36.2 were tested, either (c). Values are indicated in % of the untreated control (w/o-ctrl).
a-e: Commercially available fatty acids (LEA, LA, PEA and PA) inhibit plasminogen activation via cluster 2a type streptokinase in high concentrations. Combinations of LEA/LA or PEA/PA seem to be more effective (a,b,d,e). RC 36.1 and RC 36.2 inhibit plasminogen activation via cluster 2a type streptokinase of the strain AP1 as well (c).
a-e: *: $0.05 < p < 0.01$; **: $0.01 < p < 0.001$; ***: $0.001 < p < 0.0001$

6.3 HPLC-chromatograms and bioactivity of RC 11.1 and RC 11.2

To determine possible impurities of RC 11.1 and RC 11.2, both enriched fractions were subjected to an analytical HPLC. It was detected that RC 11.1 harbored only minor impurities (fig. 6-3a) whereas another peak was detected in RC 11.2 in addition to the main peak at 26.1 min (fig.6-3b).

To exclude that impurities were responsible for inhibition of plasminogen activation, both enriched fractions were fractionated by HPLC and the obtained fractions were tested in a plasminogen activation assay (vide sections 3.2 and 3.3). For RC 11.1 the fraction at 25-25.5 min showed inhibitory activity in the same range as the entire enriched fraction of RC 11.1 (fig. 6-3c). Consequently, activity was assigned to the main peak at 25.1 min (fig. 6-3a).

The fraction at 26-26.5 min of RC 11.2 showed also inhibitory activity comparable to the entire enriched fraction of RC 11.2. Furthermore, no activity was detected in the fractions 19-20.5 min corresponding to the additional peak in the chromatogram (fig. 6-3d). As a result, activity was assigned to the main peak at 26.1 min whereas the peaks at 19.1 and 20 min did not exhibit inhibitory activity (fig. 6-3b).

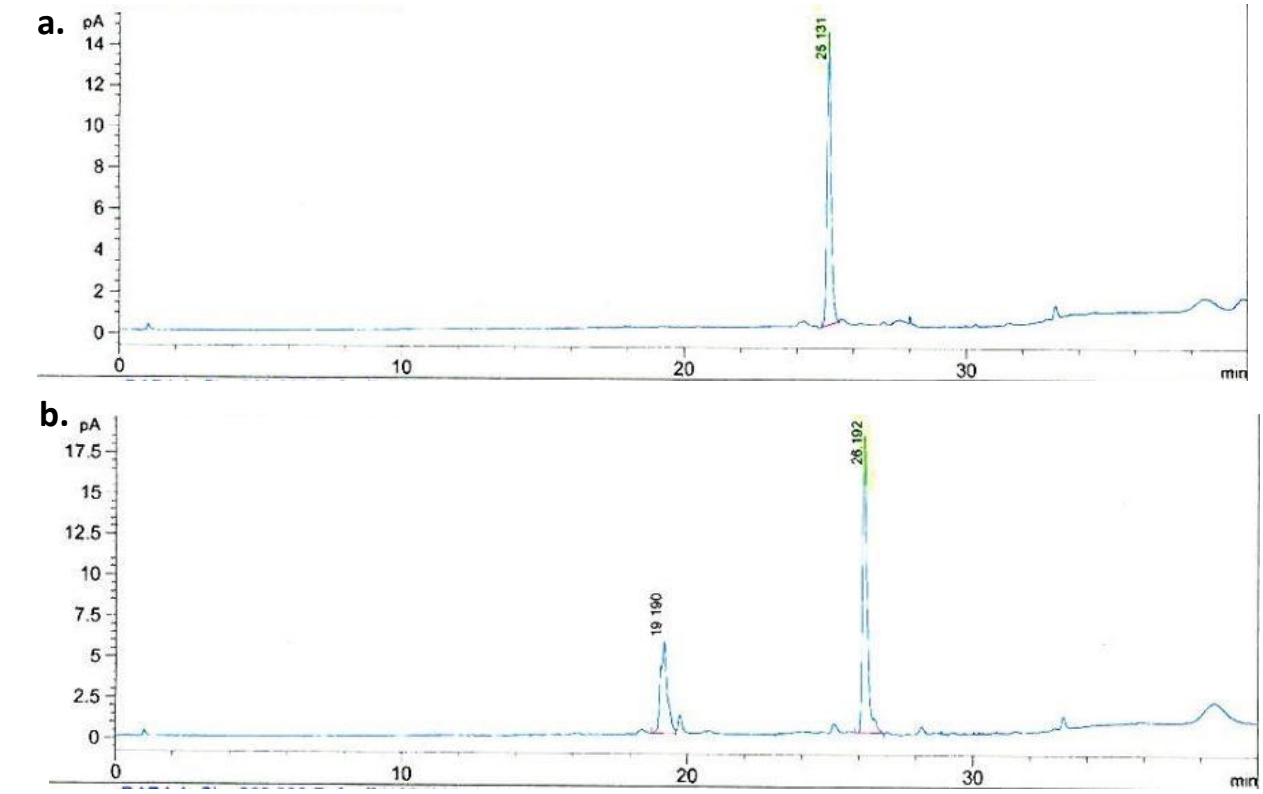

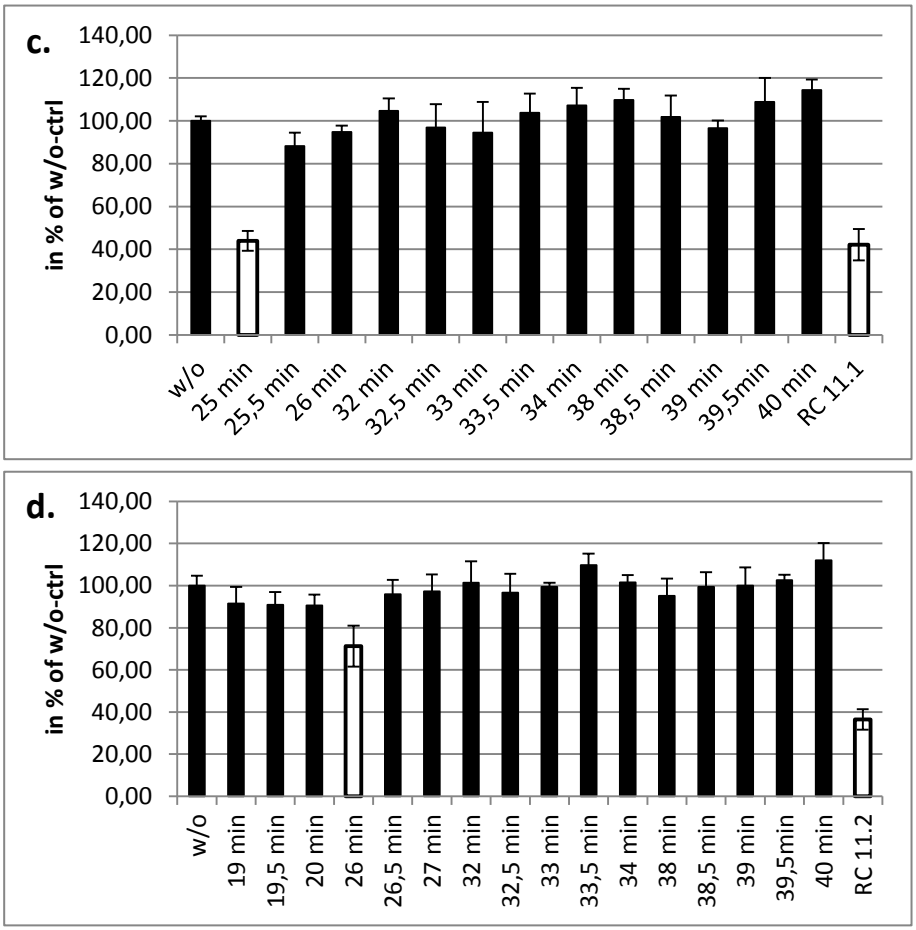

Figure 6-3: Characterization of RC 11.1 and RC 11.2.
a,b: HPLC-chromatograms were recorded of RC 11.1 and RC 11.2. A Corona detector was used for peak detection.
c,d: A plasminogen activation assay was performed for fractions of RC 11.1 and RC 11.2. Plasminogen was activated by cluster 2a type streptokinase. Values are indicated in % of the untreated control (w/o-ctrl).
a,b: Only minor impurities were detected for RC 11.1 (a) whereas two peaks were detected in the chromatogram of RC 11.2 (b).
c,d: Activity was found in the fraction at 25-25.5 min for RC 11.1 (c, marked by a white bar). For RC 11.2 activity was found at 26-26.5 min (d, marked by a white bar). RC 11.1 and RC 11.2 were tested as well as controls (c,d), marked by white bars.

6.4 Mutations in the *covRS* gene of *S.pyogenes* strain AP1 - a cause for elevated virulence in *in vivo* models?

Two animal models were used in this study that mimic a skin infection leading to systemic severity: the first one relies on the *S.pyogenes* strain 5448 (cluster 2a type streptokinase, SpeB positive (McArthur *et al.*, 2008)) whereas the latter relies on the *S.pyogenes* strain AP1 (cluster 2a type streptokinase, vide section 6.1). In both *in vivo* models, mice were infected subcutaneously. The outcome of the infection was different, although both strains harbor a cluster 2a type streptokinase: mice infected with strain 5448 had a survival rate of about 40 % (Walker *et al.*, 2007), infection with the strain AP1 resulted in a lethality rate of 100 % after 2-3 days (Loof, unpublished; Shannon *et al.*, 2010). As a result, the strain AP1 led to the same outcome of the animal model compared to strains with a cluster 1 type streptokinase (Cook *et al.*, 2012).

To investigate the potential cause for this fact, the strain AP1 was compared to the strain 5448 with regard to its SpeB expression. As SpeB is the adversary of streptokinase, differences in SpeB expression could result in differences in virulence: if streptokinase is not degraded, development of invasive disease is favored (Sun *et al.*, 2004).

AP1 did not express SpeB (fig. 6-4). The potential reason for this could be a mutation in the *covRS* gene as this regulates SpeB expression (Cole *et al.*, 2011). In comparison, the strain 5448 has an intact *covRS* gene and expresses SpeB (fig. 6-4) (Aziz *et al.*, 2004; Walker *et al.*, 2007; Hollands *et al.*, 2010). Consequently, the *covRS* gene of the strain AP1 was analyzed: several point mutations, insertions and deletions were found in comparison to a reference strain with an intact *covR* gene (fig. 6-5a). Furthermore, the *covRS* gene of the strain AP1 was compared to the one of the strain MGAS 5005 which also has a completely functional *covRS* gene (Sumby *et al.*, 2005). Furthermore, the strain MGAS 5005 was chosen as it is similar to the strain 5448 (Maamary *et al.*, 2012). No mutations were detected in the *covR* gene of the strain AP1 in comparison to MGAS 5005 (fig. 6-5b). Though, several deletions and base exchanges were detected in the *covS* gene (fig. 6-5c).

Therefore, there is strong evidence that the enhanced virulence of the strain AP1 in comparison to the strain 5448 is - at least partially - a result of mutations in the *covRS* gene leading to a loss of SpeB expression. Furthermore, this accounts for non-degradation of streptokinase as SpeB is not present.

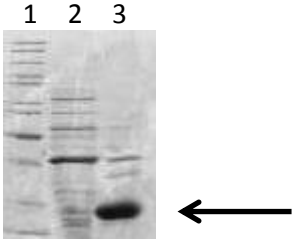

Figure 6-4: SpeB expression of different *S.pyogenes* strains.
Lane 1: Marker; Lane 2: *S.pyogenes* strain AP1; Lane 3: *S.pyogenes* strain 5448
Secreted proteins were precipitated and subjected to an SDS-Gel-electrophoresis.
SpeB was not expressed by the strain AP1 whereas it was expressed by the strain 5448. A black arrow points to the 40 kDa protein.

a.

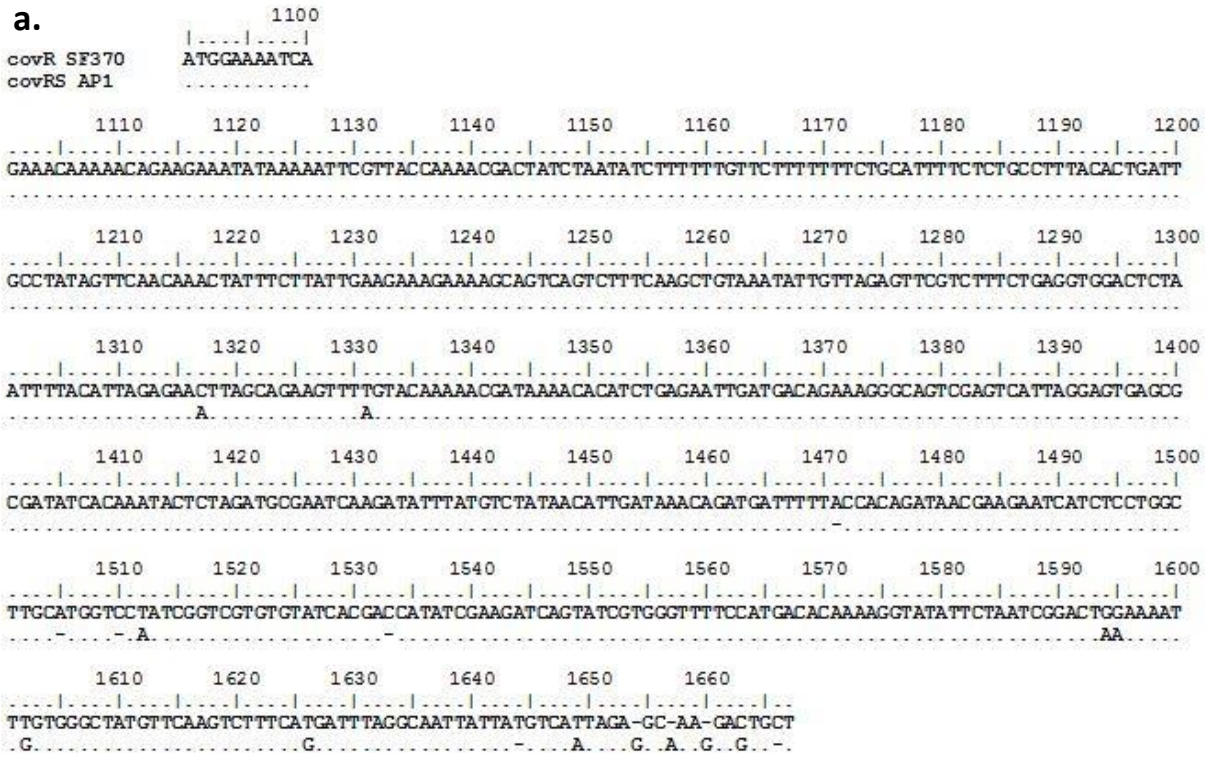
1100
covR SF370 ATGGAAAATCA
covRS AP1 ....
1110 1120 1130 1140 1150 1160 1170 1180 1190 1200
GAAACAAAAACAGAAGAAATATAAAAATTCGTTACCAAAACGACTATCTAATATCTTTTTTGTTCTTTTTTTCTGCATTTTCTCTGCCTTTACACTGATT
1210 1220 1230 1240 1250 1260 1270 1280 1290 1300
GCCTATAGTTCAACAAACTATTTCTTATTGAAGAAAGAAAAGCAGTCAGTCTTTCAAGCTGTAAATATTGTTAGAGTTCGTCTTTCTGAGGTGGACTCTA
1310 1320 1330 1340 1350 1360 1370 1380 1390 1400
ATTTTACATTAGAGAACTTAGCAGAAGTTTTGTACAAAAACGATAAAACACATCTGAGAATTGATGACAGAAAGGCAGTCGAGTCATTAGGAGTGAGCG
1410 1420 1430 1440 1450 1460 1470 1480 1490 1500
CGATATCACAAATACTCTAGATGCGAATCAAGATATTTATGTCTATAACATTGATAAACAGATGATTTTTACCACAGATAACGAAGAATCATCTCCTGGC
1510 1520 1530 1540 1550 1560 1570 1580 1590 1600
TTGCATGGTCCTATCGGTCGTGTGTATCACGACCATATCGAAGATCAGTATCGTGGGTTTTCCATGACACAAAAGGTATATTCTAATCGGACTGGAAAAT
1610 1620 1630 1640 1650 1660
TTGTGGGCTATGTTCAAGTCTTTCATGATTTAGGCAATTATTATGTCATTAGA-GC-AA-GACTGCT

b.

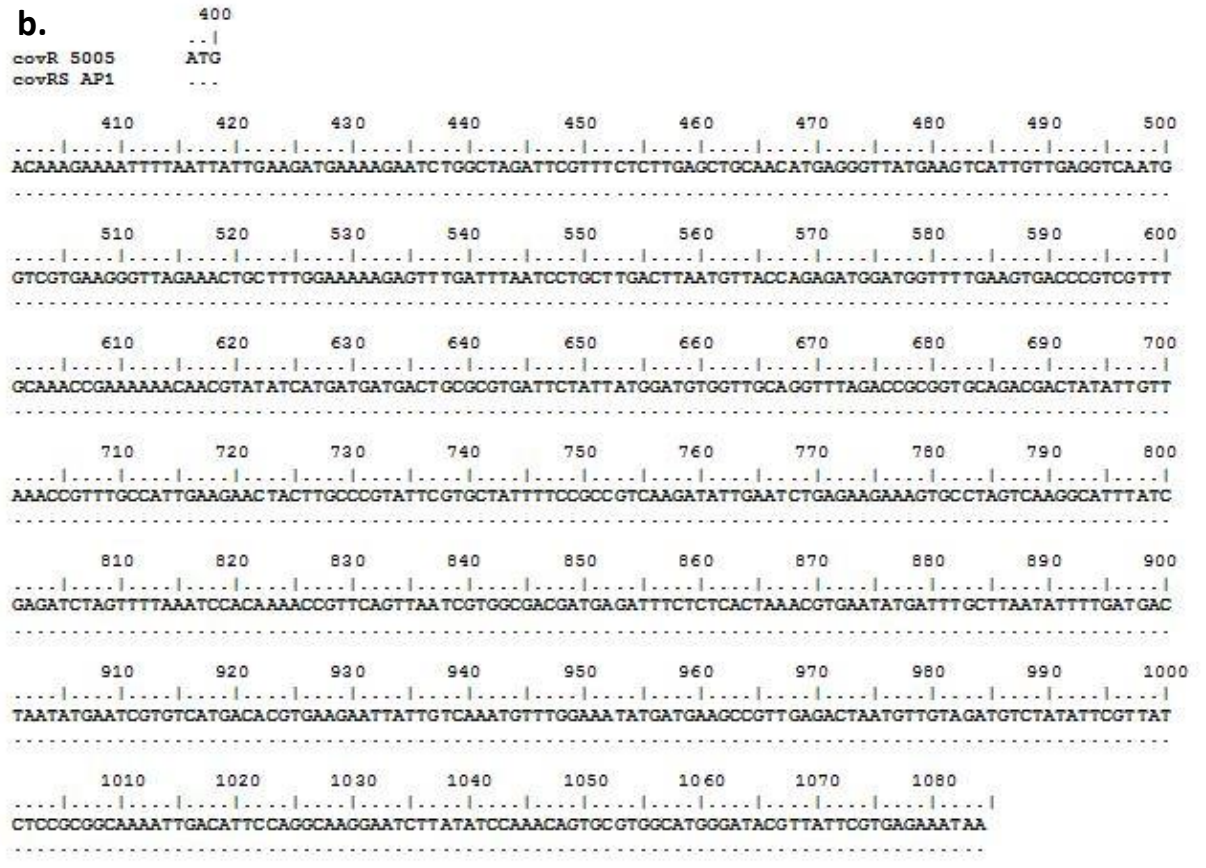
400
covR 5005 ATG
covRS AP1 ...
410 420 430 440 450 460 470 480 490 500
ACAAAGAAAATTTTAATTATTGAAGATGAAAAGAATCTGGCTAGATTCGTTTCTCTTGAGCTGCAACATGAGGGTTATGAAGTCATTGTTGAGGTCAATG
510 520 530 540 550 560 570 580 590 600
GTCGTGAAGGGTTAGAAACTGCTTTGGAAAAAGAGTTTGATTTAATCCTGCTTGACTTAATGTTACCAGAGATGGATGGTTTTGAAGTGACCCGTCGTTT
610 620 630 640 650 660 670 680 690 700
GCAAACCGAAAAAACAACGTATATCATGATGATGACTGCGCGTGATTCTATTATGGATGTGGTTGCAGGTTTAGACCGCGGTGCAGACGACTATATTGTT
710 720 730 740 750 760 770 780 790 800
AAACCGTTTGCCATTGAAGAACTACTTGCCCGTATTCGTGCTATTTTCCGCCGTCAAGATATTGAATCTGAGAAGAAAGTGCCTAGTCAAGGCATTTATC
810 820 830 840 850 860 870 880 890 900
GAGATCTAGTTTTAAATCCACAAAACCGTTCAGTTAATCGTGGCGACGATGAGATTTCTCTCACTAAACGTGAATATGATTTGCTTAATATTTTGATGAC
910 920 930 940 950 960 970 980 990 1000
TAATATGAATCGTGTCATGACACGTGAAGAATTATTGTCAAATGTTTGGAAATATGATGAAGCCGTTGAGACTAATGTTGTAGATGTCTATATTCGTTAT
1010 1020 1030 1040 1050 1060 1070 1080
CTCCGCGGCAAAATTGACATTCCAGGCAAGGAATCTTATATCCAAACAGTGCGTGGCATGGGATACGTTATTCGTGAGAAATAA

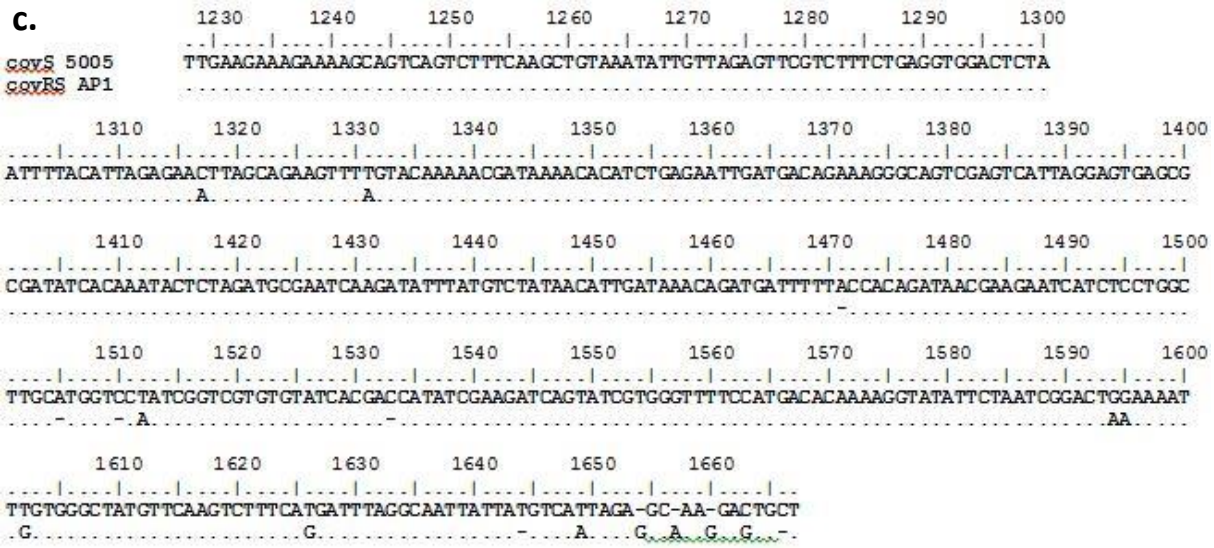

Figure 6-5: *covRS* gene sequence of the *S.pyogenes* strain AP1 in comparison to the ones of the strains SF370 and MGAS 5005.

a-c: The *covRS* gene sequence of the strain AP1 was mapped against the *covR* gene sequence of the strain SF370 (a), the *covR* gene of MGAS 5005 (b) and the *covS* gene of MGAS 5005 (c). Differences (insertions/deletions) are displayed as a dash. Differences in the bases are shown as the respective different base.

a,c: Several insertions, deletions and mutations were detected. Identity is displayed as a dot.

b: The *covR* gene of the strain AP1 was 100 % identical to the *covR* gene of MGAS 5005.

7 References

Abbot EL, Smith WD, Siou GPS, Chiriboga C, Smith RJ, Wilson JA *et al.* (2007). Pili mediate specific adhesion of *Streptococcus pyogenes* to human tonsil and skin. *Cell Microbiol* **9**: 1822–1833.

Aigle B, Corre C. (2012). Waking up *Streptomyces* secondary metabolism by constitutive expression of activators or genetic disruption of repressors. In: *Methods in Enzymology*, Vol. 517, Elsevier, pp 343–366.

Alekshun MN, Levy SB. (2007). Molecular mechanisms of antibacterial multidrug resistance. *Cell* **128**: 1037–1050.

Alkjaersig N, Fletcher AP, Sherry S. (1959). ε-aminocaproic acid: an inhibitor of plasminogen activation. *J Biol Chem* **234**: 832–837.

Amara U, Rittirsch D, Flierl M, Bruckner U, Klos A, Gebhard F *et al.* (2008). Interaction between the coagulation and complement system. *Adv Exp Med Biol* **632**: 71–79.

Andersson BA, Holman RT. (1974). Pyrrolidides for mass spectrometric determination of the position of the double bond in monounsaturated fatty acids. *Lipids* **9**: 185–190.

Anonick PK, Vasudevan J, Gonias SL. (1992). Antifibrinolytic activities of alpha-N-acetyl-L-lysine methyl ester, epsilon-aminocaproic acid, and tranexamic acid. Importance of kringle interactions and active site inhibition. *Arterioscler Thromb Vasc Biol* **12**: 708–716.

Arêas GP, Schuab RB, Neves FP, Barros RR. (2014). Antimicrobial susceptibility patterns, *emm* type distribution and genetic diversity of *Streptococcus pyogenes* recovered in Brazil. *Mem Inst Oswaldo Cruz* **109**: 935–939.

Arpin M, Chirivino D, Naba A, Zwaenepoel I. (2011). Emerging role for ERM proteins in cell adhesion and migration. *Cell Adhes Migr* **5**: 199–206.

Aziz RK, Pabst MJ, Jeng A, Kansal R, Low DE, Nizet V *et al.* (2004). Invasive M1T1 group A *Streptococcus* undergoes a phase-shift *in vivo* to prevent proteolytic degradation of multiple virulence factors by SpeB. *Mol Microbiol* **51**: 123–134.

Baker DD, Chu M, Oza U, Rajgarhia V. (2007). The value of natural products to future pharmaceutical discovery. *Nat Prod Rep* **24**: 1225.

Baltz RH. (2014). Combinatorial biosynthesis of cyclic lipopeptide antibiotics: a model for synthetic biology to accelerate the evolution of secondary metabolite biosynthetic pathways. *ACS Synth Biol* **3**: 748–758.

Barnett TC, Liebl D, Seymour LM, Gillen CM, Lim JY, LaRock CN *et al.* (2013). The globally disseminated M1T1 clone of group A *Streptococcus* evades autophagy for intracellular replication. *Cell Host Microbe* **14**: 675–682.

Baumann S, Herrmann J, Raju R, Steinmetz H, Mohr KI, Hüttel S *et al.* (2014). Cystobactamids: myxobacterial topoisomerase inhibitors exhibiting potent antibacterial activity. *Angew Chem Int Ed* **53**: 14605–14609.

Beckham KSH, Roe AJ. (2014). From screen to target: insights and approaches for the development of anti-virulence compounds. *Front Cell Infect Microbiol* **4**. doi:10.3389/fcimb.2014.00139.

Ben Nasr A, Herwald H, Sjobring U, Renne T, Müller-Esterl W, Bjorck L. (1997). Absorption of kininogen from human plasma by *Streptococcus pyogenes* is followed by the release of bradykinin. *Biochem J* **326**: 657–660.

Berge A, Sjöbring U. (1993). PAM, a novel plasminogen-binding protein from *Streptococcus pyogenes*. *J Biol Chem* **268**: 25417–25424.

Berger CN, Billker O, Meyer TF, Servin AL, Kansau I. (2004). Differential recognition of members of the carcinoembryonic antigen family by Afa/Dr adhesins of diffusely adhering Escherichia coli (Afa/Dr DAEC). *Mol Microbiol* **52**: 963–983.

Berger CN, Crepin VF, Jepson MA, Arbeloa A, Frankel G. (2009). The mechanisms used by enteropathogenic Escherichia coli to control filopodia dynamics. *Cell Microbiol* **11**: 309–322.

Bergmann R, van der Linden M, Chhatwal GS, Nitsche-Schmitz DP. (2014). Factors that cause trimethoprim resistance in *Streptococcus pyogenes*. *Antimicrob Agents Chemother* **58**: 2281–2288.

Bergmann S, Hammerschmidt S. (2007). Fibrinolysis and host response in bacterial infections. *Thromb Haemost*. doi:10.1160/TH07-02-0117.

Berryman M, Franck Z, Bretscher A. (1993). Ezrin is concentrated in the apical microvilli of a wide variety of epithelial cells whereas moesin is found primarily in endothelial cells. *J Cell Sci* **105 (Pt 4)**: 1025–1043.

Binks MJ, Fernie-King BA, Seilly DJ, Lachmann PJ, Sriprakash KS. (2005). Attribution of the various inhibitory actions of the Streptococcal Inhibitor of Complement (SIC) to regions within the molecule. *J Biol Chem* **280**: 20120–20125.

Bisno AL, Brito MO, Collins CM. (2003). Molecular basis of group A streptococcal virulence. *Lancet Infect Dis* **3**: 191–200.

Bode HB, Bethe B, Höfs R, Zeeck A. (2002). Big effects from small changes: possible ways to explore nature's chemical diversity. *Chembiochem Eur J Chem Biol* **3**: 619–627.

Bode HB, Müller R. (2005). The impact of bacterial genomics on natural product research. *Angew Chem Int Ed* **44**: 6828–6846.

Boxrud PD, Fay WP, Bock PE. (2000). Streptokinase binds to human plasmin with high affinity, perturbs the plasmin active site, and induces expression of a substrate recognition exosite for plasminogen. *J Biol Chem* **275**: 14579–14589.

Boxrud PD, Verhamme IM, Bock PE. (2004). Resolution of conformational activation in the kinetic mechanism of plasminogen activation by streptokinase. *J Biol Chem* **279**: 36633–36641.

Boyle MD, Lottenberg R. (1997). Plasminogen activation by invasive human pathogens. *Thromb Haemost* **77**: 1–10.

Breton RC, Reynolds WF. (2013). Using NMR to identify and characterize natural products. *Nat Prod Rep* **30**: 501–524.

Bretscher A. (1989). Rapid phosphorylation and reorganization of ezrin and spectrin accompany morphological changes induced in A-431 cells by epidermal growth factor. *J Cell Biol* **108**: 921–930.

Bretscher A. (1999). Regulation of cortical structure by the ezrin-radixin-moesin protein family. *Curr Opin Cell Biol* **11**: 109–116.

Bretscher A, Edwards K, Fehon RG. (2002). ERM proteins and merlin: integrators at the cell cortex. *Nat Rev Mol Cell Biol* **3**: 586–599.

Brodin P, Christophe T. (2011). High-content screening in infectious diseases. *Curr Opin Chem Biol* **15**: 534–539.

Brown AG, Butterworth D, Cole M, Hanscomb G, Hood JD, Reading C *et al.* (1976). Naturally-occurring β-lactamase inhibitors with antibacterial activity. *J Antibiot (Tokyo)* **29**: 668–669.

Bucar F, Wube A, Schmid M. (2013). Natural product isolation - how to get from biological material to pure compounds. *Nat Prod Rep* **30**: 525–545.

Bull AT, Stach JEM. (2007). Marine actinobacteria: new opportunities for natural product search and discovery. *Trends Microbiol* **15**: 491–499.

Burns EH, Marciel AM, Musser JM. (1996). Activation of a 66-kilodalton human endothelial cell matrix metalloprotease by *Streptococcus pyogenes* extracellular cysteine protease. *Infect Immun* **64**: 4744–4750.

Burridge K, Connell L. (1983). A new protein of adhesion plaques and ruffling membranes. *J Cell Biol* **97**: 359–367.

Butler MS, Buss AD. (2006). Natural products — The future scaffolds for novel antibiotics? *Biochem Pharmacol* **71**: 919–929.

Camacho C, Coulouris G, Avagyan V, Ma N, Papadopoulos J, Bealer K *et al.* (2009). BLAST+: architecture and applications. *BMC Bioinformatics* **10**: 421.

Campbell EA, Pavlova O, Zenkin N, Leon F, Irschik H, Jansen R *et al.* (2005). Structural, functional, and genetic analysis of sorangicin inhibition of bacterial RNA polymerase. *EMBO J* **24**: 674–682.

Cantón R, Loza E, Morosini MI, Baquero F. (2002). Antimicrobial resistance amongst isolates of *Streptococcus pyogenes* and *Staphylococcus aureus* in the PROTEKT antimicrobial surveillance programme during 1999-2000. *J Antimicrob Chemother* **50 Suppl S1**: 9–24.

Carapetis JR. (2004). Current issues in managing group A streptococcal infections. *Adv Exp Med Biol* **549**: 185–190.

Carapetis JR, Steer AC, Mulholland EK, Weber M. (2005). The global burden of group A streptococcal diseases. *Lancet Infect Dis* **5**: 685–694.

Carlsson F, Sandin C, Lindahl G. (2005). Human fibrinogen bound to *Streptococcus pyogenes* M protein inhibits complement deposition via the classical pathway. *Mol Microbiol* **56**: 28–39.

Cegelski L, Marshall GR, Eldridge GR, Hultgren SJ. (2008). The biology and future prospects of antivirulence therapies. *Nat Rev Microbiol* **6**: 17–27.

Chain E, Florey HW, Gardner AD, Heatley NG, Jennings MA, Orr-Ewing J *et al.* (1940). Penicillin as a chemotherapeutic agent. *The lancet* **236**: 226–228.

Chang H-H, Cohen T, Grad YH, Hanage WP, O'Brien TF, Lipsitch M. (2015). Origin and proliferation of multiple-drug resistance in bacterial pathogens. *Microbiol Mol Biol Rev* **79**: 101–116.

Chaussee MS, Phillips ER, Ferretti JJ. (1997). Temporal production of streptococcal erythrogenic toxin B (streptococcal cysteine proteinase) in response to nutrient depletion. *Infect Immun* **65**: 1956–1959.

Chorell E, Pinkner JS, Bengtsson C, Banchelin TS-L, Edvinsson S, Linusson A *et al.* (2012). Mapping pilicide anti-virulence effect in *Escherichia coli*, a comprehensive structure–activity study. *Bioorg Med Chem* **20**: 3128–3142.

Clatworthy AE, Pierson E, Hung DT. (2007). Targeting virulence: a new paradigm for antimicrobial therapy. *Nat Chem Biol* **3**: 541–548.

Cole JN, Barnett TC, Nizet V, Walker MJ. (2011). Molecular insight into invasive group A streptococcal disease. *Nat Rev Microbiol* **9**: 724–736.

Cole JN, McArthur JD, McKay FC, Sanderson-Smith ML, Cork AJ, Ranson M *et al.* (2006). Trigger for group A streptococcal M1T1 invasive disease. *FASEB J* **20**: 1745–1747.

Coleman JL, Benach JL. (1999). Use of the plasminogen activation system by microorganisms. *J Lab Clin Med* **134**: 567–576.

Cook SM, Skora A, Gillen CM, Walker MJ, McArthur JD. (2012). Streptokinase variants from *Streptococcus pyogenes* isolates display altered plasminogen activation characteristics - implications for pathogenesis. *Mol Microbiol* **86**: 1052–1062.

Cook SM, Skora A, Walker MJ, Sanderson‐Smith ML, McArthur JD. (2014a). Site-restricted plasminogen activation mediated by group A streptococcal streptokinase variants. *Biochem J* **458**: 23–31.

Cook SM, Skora A, Walker MJ, Sanderson‐Smith ML, McArthur JD. (2014b). Site-restricted plasminogen activation mediated by group A streptococcal streptokinase variants. *Biochem J* **458**: 23–31.

Cortina NS, Krug D, Plaza A, Revermann O, Müller R. (2012). Myxoprincomide: a natural product from *Myxococcus xanthus* discovered by comprehensive analysis of the secondary metabolome. *Angew Chem Int Ed* **51**: 811–816.

Courtney HS, von Hunolstein C, Dale JB, Bronze MS, Beachey EH, Hasty DL. (1992). Lipoteichoic acid and M protein: dual adhesins of group A streptococci. *Microb Pathog* **12**: 199–208.

Cragg GM, Newman DJ. (2013). Natural products: A continuing source of novel drug leads. *Biochim Biophys Acta BBA - Gen Subj* **1830**: 3670–3695.

CRASH-2 collaborators, Roberts I, Shakur H, Afolabi A, Brohi K, Coats T *et al.* (2011). The importance of early treatment with tranexamic acid in bleeding trauma patients: an exploratory analysis of the CRASH-2 randomised controlled trial. *Lancet* **377**: 1096–1101, 1101.e1–2.

Critchley DR. (2009). Biochemical and structural properties of the integrin-associated cytoskeletal protein talin. *Annu Rev Biophys* **38**: 235–254.

Critchley DR. (2000). Focal adhesions–the cytoskeletal connection. *Curr Opin Cell Biol* **12**: 133–139.

Cue D, Dombek PE, Lam H, Cleary PP. (1998). *Streptococcus pyogenes* serotype M1 encodes multiple pathways for entry into human epithelial cells. *Infect Immun* **66**: 4593–4601.

Cue D, Lam H, Cleary PP. (2001). Genetic dissection of the *Streptococcus pyogenes* M1 protein: regions involved in fibronectin binding and intracellular invasion. *Microb Pathog* **31**: 231–242.

Cue D, Southern SO, Southern PJ, Prabhakar J, Lorelli W, Smallheer JM *et al.* (2000). A nonpetide integrin antagonist can inhibit epithelial cell ingestion of *Streptococcus pyogenes* by blocking formation of integrin α5β1-fibronectin-M1 protein complexes. *Proc Natl Acad Sci* **97**: 2858–2863.

Cunningham MW. (2000). Pathogenesis of group A streptococcal infections. *Clin Microbiol Rev* **13**: 470–511.

Cunningham MW. (2008). Pathogenesis of group A streptococcal infections and their sequelae. In: *Hot Topics in Infection and Immunity in Children IV*, Springer, pp 29–42.

Cywes C, Wessels MR. (2001). Group A *Streptococcus* tissue invasion by CD44-mediated cell signalling. *Nature* **414**: 648–652.

Dale JB, Fischetti VA, Carapetis JR, Steer AC, Sow S, Kumar R *et al.* (2013). Group A streptococcal vaccines: Paving a path for accelerated development. *Vaccine* **31**: B216–B222.

Dalton TL, Hobb RI, Scott JR. (2006). Analysis of the role of CovR and CovS in the dissemination of *Streptococcus pyogenes* in invasive skin disease. *Microb Pathog* **40**: 221–227.

Dalton TL, Scott JR. (2004). CovS inactivates CovR and is required for growth under conditions of general stress in *Streptococcus pyogenes*. *J Bacteriol* **186**: 3928–3937.

Dawid W. (2000). Biology and global distribution of myxobacteria in soils. *FEMS Microbiol Rev* **24**: 403–427.

Dawid W, Gallikowski CA, Hirsch P. (1988). 3.8 Psychrophilic myxobacteria from antarctic soils. *Polarforschung* **58**: 271–278.

Derbise A, Song YP, Parikh S, Fischetti VA, Pancholi V. (2004). Role of the C-terminal lysine residues of streptococcal surface enolase in glu- and lys-plasminogen-binding activities of group A streptococci. *Infect Immun* **72**: 94–105.

Dietrich W, Ebell A, Busley R, Boulesteix A-L. (2007). Aprotinin and anaphylaxis: analysis of 12,403 exposures to aprotinin in cardiac surgery. *Ann Thorac Surg* **84**: 1144–1150.

Dinkla K, Nitsche-Schmitz DP, Barroso V, Reissmann S, Johansson HM, Frick I-M *et al.* (2007). Identification of a streptococcal octapeptide motif involved in acute rheumatic fever. *J Biol Chem* **282**: 18686–18693.

Dombek PE, Cue D, Sedgewick J, Lam H, Ruschkowski S, Finlay BB *et al.* (1999). High-frequency intracellular invasion of epithelial cells by serotype M1 group A streptococci: M1 protein-mediated invasion and cytoskeletal rearrangements. *Mol Microbiol* **31**: 859–870.

Dunkelblum E, Tan SH, Silk PJ. (1985). Double-bond location in monounsaturated fatty acids by dimethyl disulfide derivatization and mass spectrometry: Application to analysis of fatty acids in pheromone glands of four lepidoptera. *J Chem Ecol* **11**: 265–277.

Eison TM, Ault BH, Jones DP, Chesney RW, Wyatt RJ. (2011). Post-streptococcal acute glomerulonephritis in children: clinical features and pathogenesis. *Pediatr Nephrol* **26**: 165–180.

Ellis NMJ, Kurahara DK, Vohra H, Mascaro-Blanco A, Erdem G, Adderson EE *et al.* (2010). Priming the immune system for heart disease: a perspective on group A streptococci. *J Infect Dis* **202**: 1059–1067.

Elnakady YA, Sasse F, Lünsdorf H, Reichenbach H. (2004). Disorazol A1, a highly effective antimitotic agent acting on tubulin polymerization and inducing apoptosis in mammalian cells. *Biochem Pharmacol* **67**: 927–935.

Engelmann B, Massberg S. (2013). Thrombosis as an intravascular effector of innate immunity. *Nat Rev Immunol* **13**: 34–45.

Evans JJ, Crist HS, Durvesh S, Bruggeman RD, Goldenberg D. (2012). A comparative study of cell cycle mediator protein expression patterns in anaplastic and papillary thyroid carcinoma. *Cancer Biol Ther* **13**: 776–781.

Facklam R. (2002). What happened to the streptococci: overview of taxonomic and nomenclature changes. *Clin Microbiol Rev* **15**: 613–630.

Facklam RF, Martin DR, Marguerite L, Dwight RJ, Efstratiou A, Thompson TA *et al.* (2002). Extension of the Lancefield classification for group A streptococci by addition of 22 new M protein gene sequence types from clinical isolates: *emm103* to *emm124*. *Clin Infect Dis* **34**: 28–38.

Fairbrother RW, Williams BL. (1956). Two new antibiotics; antibacterial activity of novobiocin and vancomycin. *Lancet* **271**: 1177–1178.

Fais S. (2004). A role for ezrin in a neglected metastatic tumor function. *Trends Mol Med* **10**: 249–250.

Fais S. (2007). Cannibalism: A way to feed on metastatic tumors. *Cancer Lett* **258**: 155–164.

Fay L, Richli U. (1991). Location of double bonds in polyunsaturated fatty acids by gas chromatography-mass spectrometry after 4,4-dimethyloxazoline derivatization. *J Chromatogr A* **541**: 89–98.

Felder S, Kehraus S, Neu E, Bierbaum G, Schäberle TF, König GM. (2013). Salimyxins and enhygrolides: antibiotic, sponge-related metabolites from the obligate marine myxobacterium *Enhygromyxa salina*. *ChemBioChem* **14**: 1363–1371.

Fergusson DA, Hébert PC, Mazer CD, Fremes S, MacAdams C, Murkin JM *et al.* (2008). A comparison of aprotinin and lysine analogues in high-risk cardiac surgery. *N Engl J Med* **358**: 2319–2331.

Fiebig A, Loof TG, Babbar A, Itzek A, Koehorst JJ, Schaap PJ *et al.* Comparative Genomics of Streptococcus pyogenes M1 isolates differing in virulence and propensity to cause systemic infection in mice. *Int J Med Microbiol*. doi:10.1016/j.ijmm.2015.06.002.

Fievet BT, Gautreau A, Roy C, Del Maestro L, Mangeat P, Louvard D *et al.* (2004). Phosphoinositide binding and phosphorylation act sequentially in the activation mechanism of ezrin. *J Cell Biol* **164**: 653–659.

Finlay BB, Rosenshine I, Donnenberg MS, Kaper JB. (1992). Cytoskeletal composition of attaching and effacing lesions associated with enteropathogenic *Escherichia coli* adherence to HeLa cells. *Infect Immun* **60**: 2541–2543.

Firn RD, Jones CG. (2003). Natural products - a simple model to explain chemical diversity. *Nat Prod Rep* **20**: 382.

Fischetti VA. (1989). Streptococcal M protein: molecular design and biological behavior. *Clin Microbiol Rev* **2**: 285–314.

Fischetti VA, Horstmann RD, Pancholi V. (1995). Location of the complement factor H binding site on streptococcal M6 protein. *Infect Immun* **63**: 149–153.

Fotakis G, Timbrell JA. (2006). In vitro cytotoxicity assays: comparison of LDH, neutral red, MTT and protein assay in hepatoma cell lines following exposure to cadmium chloride. *Toxicol Lett* **160**: 171–177.

Franchini M, Mannucci PM. (2014). Adjunct agents for bleeding. *Curr Opin Hematol* **21**: 503–508.

Franck Z, Gary R, Bretscher A. (1993). Moesin, like ezrin, colocalizes with actin in the cortical cytoskeleton in cultured cells, but its expression is more variable. *J Cell Sci* **105**: 219–231.

Fudou R, Jojima Y, Iizuka T, Yamanaka S. (2002). *Haliangium ochraceum* gen. nov., sp. nov. and *Haliangium tepidum* sp. nov.: novel moderately halophilic myxobacteria isolated from coastal saline environments. *J Gen Appl Microbiol* **48**: 109–116.

Fujimoto H, Kinoshita T, Suzuki H, Umezawa H. (1970). Studies on the mode of action of althiomycin. *J Antibiot (Tokyo)* **23**: 271–275.

Gaffney PJ, Urano T, de Serrano VS, Mahmoud-Alexandroni M, Metzger AR, Castellino FJ. (1988). Roles for chloride ion and fibrinogen in the activation of [Glu^1]plasminogen in human plasma. *Proc Natl Acad Sci U S A* **85**: 3595–3598.

Ganesan A. (2004). Natural products as a hunting ground for combinatorial chemistry. *Curr Opin Biotechnol* **15**: 584–590.

Ganesan A. (2008). The impact of natural products upon modern drug discovery. *Curr Opin Chem Biol* **12**: 306–317.

Garcia R, Müller R. (2014a). The family *Haliangiaceae*. In: *The Prokaryotes*, Rosenberg, E, DeLong, EF, Lory, S, Stackebrandt, E, & Thompson, F (eds), Springer Berlin Heidelberg, pp 173–181.

Garcia R, Müller R. (2014b). The family *Myxococcaceae*. In: *The Prokaryotes*, Rosenberg, E, DeLong, EF, Lory, S, Stackebrandt, E, & Thompson, F (eds), Springer Berlin Heidelberg, pp 191–212.

Garcia R, Müller R. (2014c). The family *Nannocystaceae*. In: *The Prokaryotes*, Rosenberg, E, DeLong, EF, Lory, S, Stackebrandt, E, & Thompson, F (eds), Springer Berlin Heidelberg, pp 213–229.

Garcia R, Müller R. (2014d). The family *Phaselicystidaceae*. In: *The Prokaryotes*, Rosenberg, E, DeLong, EF, Lory, S, Stackebrandt, E, & Thompson, F (eds), Springer Berlin Heidelberg, pp 239–245.

Garcia R, Müller R. (2014e). The family *Polyangiaceae*. In: *The Prokaryotes*, Rosenberg, E, DeLong, EF, Lory, S, Stackebrandt, E, & Thompson, F (eds), Springer Berlin Heidelberg, pp 247–279.

Garcia RO, Krug D, Müller R. (2009). Chapter 3 Discovering natural products from myxobacteria with emphasis on rare producer strains in combination with improved analytical methods. In: *Methods in Enzymology*, Vol. 458, Elsevier, pp 59–91.

Garcia RO, Reichenbach H, Ring MW, Müller R. (2009). *Phaselicystis flava* gen. nov., sp. nov., an arachidonic acid-containing soil myxobacterium, and the description of *Phaselicystidaceae* fam. nov. *Int J Syst Evol Microbiol* **59**: 1524–1530.

Gautreau A, Poullet P, Louvard D, Arpin M. (1999). Ezrin, a plasma membrane–microfilament linker, signals cell survival through the phosphatidylinositol 3-kinase/Akt pathway. *Proc Natl Acad Sci* **96**: 7300–7305.

Gerber MA. (1996). Antibiotic resistance: relationship to persistence of group A streptococci in the upper respiratory tract. *Pediatrics* **97**: 971–975.

Gerth K, Bedorf N, Höfle G, Irschik H, Reichenbach H. (1996). Epothilons A and B: antifungal and cytotoxic compounds from *Sorangium cellulosum* (Myxobacteria). Production, physico-chemical and biological properties. *J Antibiot (Tokyo)* **49**: 560–563.

Gerth K, Müller R. (2005). Moderately thermophilic myxobacteria: novel potential for the production of natural products isolation and characterization. *Environ Microbiol* **7**: 874–880.

Gillen CM, Towers RJ, McMillan DJ, Delvecchio A, Sriprakash KS, Currie B *et al.* (2002). Immunological response mounted by Aboriginal Australians living in the Northern Territory of Australia against *Streptococcus pyogenes* serum opacity factor. *Microbiology* **148**: 169–178.

Gnosspelius G. (1978). Myxobacterial slime and proteolytic activity. *Arch Microbiol* **116**: 51–59.

Goldman BS, Nierman WC, Kaiser D, Slater SC, Durkin AS, Eisen JA *et al.* (2006). Evolution of sensory complexity recorded in a myxobacterial genome. *Proc Natl Acad Sci U S A* **103**: 15200–15205.

Górecki T, Lynen F, Szucs R, Sandra P. (2006). Universal response in liquid chromatography using charged aerosol detection. *Anal Chem* **78**: 3186–3192.

Gutiérrez-Barranquero JA, Reen FJ, McCarthy RR, Dobson ADW, O'Gara F. (2015). Deciphering the role of coumarin as a novel quorum sensing inhibitor suppressing virulence phenotypes in bacterial pathogens. *Appl Microbiol Biotechnol*. doi:10.1007/s00253-015-6436-1.

Halabalaki M, Vougogiannopoulou K, Mikros E, Skaltsounis AL. (2014). Recent advances and new strategies in the NMR-based identification of natural products. *Curr Opin Biotechnol* **25**: 1–7.

Hall A. (1998). Rho GTPases and the actin cytoskeleton. *Science* **279**: 509–514.

Hall SW, Humphries JE, Gonias SL. (1991). Inhibition of cell surface receptor-bound plasmin by alpha 2-antiplasmin and alpha 2-macroglobulin. *J Biol Chem* **266**: 12329–12336.

Hasty DL, Ofek I, Courtney HS, Doyle RJ. (1992). Multiple adhesins of streptococci. *Infect Immun* **60**: 2147.

Hayes ML, Castellino FJ. (1979a). Carbohydrate of the human plasminogen variants. I. Carbohydrate composition, glycopeptide isolation, and characterization. *J Biol Chem* **254**: 8768–8771.

Hayes ML, Castellino FJ. (1979b). Carbohydrate of the human plasminogen variants. III. Structure of the O-glycosidically linked oligosaccharide unit. *J Biol Chem* **254**: 8777–8780.

Hayes ML, Castellino FJ. (1979c). Carbohydrate of the human plasminogen variants. II. Structure of the asparagine-linked oligosaccharide unit. *J Biol Chem* **254**: 8772–8776.

Hearn BR, Arslanian RL, Fu H, Liu F, Gramajo H, Myles DC. (2006). Methanolysis products of disorazole A1. *J Nat Prod* **69**: 148–150.

Held J, Gebru T, Kalesse M, Jansen R, Gerth K, Müller R *et al.* (2014). Antimalarial activity of the myxobacterial macrolide chlorotonil A. *Antimicrob Agents Chemother* **58**: 6378–6384.

Henningham A, Barnett TC, Maamary PG, Walker MJ. (2012). Pathogenesis of group A streptococcal infections. *Discov Med* **13**: 329–342.

Herwald H, Cramer H, Mörgelin M, Russell W, Sollenberg U, Norrby-Teglund A *et al.* (2004). M protein, a classical bacterial virulence determinant, forms complexes with fibrinogen that induce vascular leakage. *Cell* **116**: 367–379.

Hirao M, Sato N, Kondo T, Yonemura S, Monden M, Sasaki T *et al.* (1996). Regulation mechanism of ERM (ezrin/radixin/moesin) protein/plasma membrane association: possible involvement of phosphatidylinositol turnover and Rho-dependent signaling pathway. *J Cell Biol* **135**: 37–51.

Hoe NP, Ireland RM, DeLeo FR, Gowen BB, Dorward DW, Voyich JM et *al.* (2002). Insight into the molecular basis of pathogen abundance: group A *Streptococcus* inhibitor of complement inhibits bacterial adherence and internalization into human cells. *Proc Natl Acad Sci* **99**: 7646–7651.

Hoffmann T, Krug D, Hüttel S, Müller R. (2014). Improving natural products identification through targeted LC-MS/MS in an untargeted secondary metabolomics workflow. *Anal Chem* **86**: 10780–10788.

Hollands A, Gonzalez D, Leire E, Donald C, Gallo RL, Sanderson-Smith M *et al.* (2012). A bacterial pathogen co-opts host plasmin to resist killing by cathelicidin antimicrobial peptides. *J Biol Chem* **287**: 40891–40897.

Hollands A, Pence MA, Timmer AM, Osvath SR, Turnbull L, Whitchurch CB *et al.* (2010). Genetic switch to hypervirulence reduces colonization phenotypes of the globally disseminated group A *streptococcus* M1T1 clone. *J Infect Dis* **202**: 11–19.

Honickel M, Treutler S, van Ryn J, Tillmann S, Rossaint R, Grottke O. (2015). Reversal of dabigatran anticoagulation *ex vivo*: Porcine study comparing prothrombin complex concentrates and idarucizumab: *Thromb Haemost* **113**. doi:10.1160/TH14-08-0712.

Hopkins CD, Wipf P. (2009). Isolation, biology and chemistry of the disorazoles: new anti-cancer macrodiolides. *Nat Prod Rep* **26**: 585.

Horstmann RD, Sievertsen HJ, Knobloch J, Fischetti VA. (1988). Antiphagocytic activity of streptococcal M protein: selective binding of complement control protein factor H. *Proc Natl Acad Sci* **85**: 1657–1661.

Horstmann RD, Sievertsen HJ, Leippe M, Fischetti VA. (1992). Role of fibrinogen in complement inhibition by streptococcal M protein. *Infect Immun* **60**: 5036–5041.

Hufsky F, Scheubert K, Böcker S. (2014). New kids on the block: novel informatics methods for natural product discovery. *Nat Prod Rep* **31**: 807.

Hunter KW. (2004). Ezrin, a key component in tumor metastasis. *Trends Mol Med* **10**: 201–204.

Irschik H, Jansen R, Gerth K, Höfle G, Reichenbach H. (1995). Disorazol A, an efficient inhibitor of eukaryotic organisms isolated from myxobacteria. *J Antibiot (Tokyo)* **48**: 31–35.

Irschik H, Jansen R, Gerth K, Höfle G, Reichenbach H. (1987). The sorangicins, novel and powerful inhibitors of eubacterial RNA polymerase isolated from myxobacteria. *J Antibiot (Tokyo)* **40**: 7–13.

Irschik H, Reichenbach H, Höfle G, Jansen R. (2007). The thuggacins, novel antibacterial macrolides from Sorangium cellulosum acting against selected gram-positive bacteria. Production, antimicrobial activity and mechanism of action. *J Antibiot (Tokyo)* **60**: 733.

Jansen R, Irschik H, Huch V, Schummer D, Steinmetz H, Bock M *et al.* (2010). Carolacton - A macrolide ketocarbonic acid that reduces biofilm formation by the caries- and endocarditis-associated bacterium *Streptococcus mutans*. *Eur J Org Chem* **2010**: 1284–1289.

Jansen R, Irschik H, Reichenbach H, Wray V, Höfle G. (1994). Antibiotics from gliding bacteria, LIX. Disorazoles, highly cytotoxic metabolites from the sorangicin-producing bacterium *Sorangium cellulosum*, strain So ce12. *Liebigs Ann Chem* **1994**: 759–773.

Jansen R, Mohr KI, Bernecker S, Stadler M, Müller R. (2014). Indothiazinone, an indolyl thiazolyl ketone from a novel myxobacterium belonging to the *Sorangiineae*. *J Nat Prod* **77**: 1054–1060.

Janssen GR, Wireman JW, Dworkin M. (1977). Effect of temperature on the growth of *Myxococcus xanthus*. *J Bacteriol* **130**: 561–562.

Janssen MEW, Kim E, Liu H, Fujimoto LM, Bobkov A, Volkmann N *et al.* (2006). Three-dimensional structure of vinculin bound to actin filaments. *Mol Cell* **21**: 271–281.

Järvinen HM, Laakkonen L, Haiko J, Johansson T, Juuti K, Suomalainen M *et al.* (2013). Human single-chain urokinase is activated by the omptins PgtE of *Salmonella enterica* and Pla of *Yersinia pestis* despite mutations of active site residues: Activation of human urokinase by enteric bacteria. *Mol Microbiol* **89**: 507–517.

Johansson L, Norrby-Teglund A. (2013). Immunopathogenesis of streptococcal deep tissue infections. *Curr Top Microbiol Immunol* **368**: 173–188.

Johnsson E, Thern A, Dahlbäck B, Heden L-O, Wikström M, Lindahl G. (1996). A highly variable region in members of the streptococcal M protein family binds the human complement regulator C4BP. *J Immunol* **157**: 3021–3029.

Jones CG, Firn RD. (1991). On the evolution of plant secondary chemical diversity. *Philos Trans R Soc Lond B Biol Sci* **333**: 273–280.

Jung C, Matzke A, Niemann HH, Schwerk C, Tenenbaum T, Orian-Rousseau V. (2009). Involvement of CD44v6 in InlB-dependent *Listeria* invasion. *Mol Microbiol* **72**: 1196–1207.

Kaddoum RN, Chidiac EJ, Zestos MM, Rajan SD, Baraka A. (2007). An anaphylactic reaction after primary exposure to an aprotinin test dose in a child with a severe milk allergy. *J Cardiothorac Vasc Anesth* **21**: 243–244.

Kalia A, Bessen DE. (2004). Natural selection and evolution of streptococcal virulence genes involved in tissue-specific adaptations. *J Bacteriol* **186**: 110–121.

Kansal RG, McGeer A, Low DE, Norrby-Teglund A, Kotb M. (2000). Inverse relation between disease severity and expression of the streptococcal cysteine protease, SpeB, among clonal M1T1 isolates recovered from invasive group A streptococcal infection cases. *Infect Immun* **68**: 6362–6369.

Kaplan EL, Chhatwal GS, Rohde M. (2006). Reduced ability of penicillin to eradicate ingested group A streptococci from epithelial cells: clinical and pathogenetic implications. *Clin Infect Dis* **43**: 1398–1406.

Kaplan EL, Johnson DR. (2001). Unexplained reduced microbiological efficacy of intramuscular benzathine penicillin G and of oral penicillin V in eradication of group a streptococci from children with acute pharyngitis. *Pediatrics* **108**: 1180–1186.

Kapur V, Topouzis S, Majesky MW, Li LL, Hamrick MR, Hamill RJ *et al.* (1993). A conserved *Streptococcus pyogenes* extracellular cysteine protease cleaves human fibronectin and degrades vitronectin. *Microb Pathog* **15**: 327–346.

Katerov V, Andreev A, Schalén C, Totolian AA. (1998). Protein F, a fibronectin-binding protein of *Streptococcus pyogenes*, also binds human fibrinogen: isolation of the protein and mapping of the binding region. *Microbiology* **144**: 119–126.

Kefalides NA, Pegg MT, Ohno N, Poon-King T, Zabriskie J, Fillit H. (1986). Antibodies to basement membrane collagen and to laminin are present in sera from patients with poststreptococcal glomerulonephritis. *J Exp Med* **163**: 588–602.

Kelly DF, Taylor DW, Bakolitsa C, Bobkov AA, Bankston L, Liddington RC *et al.* (2006). Structure of the α-actinin–vinculin head domain complex determined by cryo-electron microscopy. *J Mol Biol* **357**: 562–573.

Khalil MW, Sasse F, Lünsdorf H, Elnakady YA, Reichenbach H. (2006). Mechanism of action of tubulysin, an antimitotic peptide from myxobacteria. *ChemBioChem* **7**: 678–683.

Khanna C, Wan X, Bose S, Cassaday R, Olomu O, Mendoza A *et al.* (2004). The membrane-cytoskeleton linker ezrin is necessary for osteosarcoma metastasis. *Nat Med* **10**: 182–186.

Khil J, Im M, Heath A, Ringdahl U, Mundada L, Engleberg NC *et al.* (2003). Plasminogen enhances virulence of group A streptococci by streptokinase-dependent and streptokinase-independent mechanisms. *J Infect Dis* **188**: 497–505.

Kirst HA. (2013). Developing new antibacterials through natural product research. *Expert Opin Drug Discov* **8**: 479–493.

Knupp dos Santos DF, Kyaw CM, Amabile De Campos T, Miller RNG, Noronha EF, da Cunha Bustamante MM et *al.* (2014). The family *Cystobacteraceae*. In: *The Prokaryotes*, Rosenberg, E, DeLong, EF, Lory, S, Stackebrandt, E, & Thompson, F (eds), Springer Berlin Heidelberg, pp 19–40.

Koehn FE, Carter GT. (2005). The evolving role of natural products in drug discovery. *Nat Rev Drug Discov* **4**: 206–220.

Korhonen TK, Haiko J, Laakkonen L, Järvinen HM, Westerlund-Wikström B. (2013). Fibrinolytic and coagulative activities of *Yersinia pestis*. *Front Cell Infect Microbiol* **3**. doi:10.3389/fcimb.2013.00035.

Korotkova N, Yarova-Yarovaya Y, Tchesnokova V, Yazvenko N, Carl MA, Stapleton AE *et al.* (2008). *Escherichia coli* DraE adhesin-associated bacterial internalization by epithelial cells is promoted independently by decay-accelerating factor and carcinoembryonic antigen-related cell adhesion molecule binding and does not require the DraD invasin. *Infect Immun* **76**: 3869–3880.

Kreikemeyer B, McIver KS, Podbielski A. (2003). Virulence factor regulation and regulatory networks in *Streptococcus pyogenes* and their impact on pathogen–host interactions. *Trends Microbiol* **11**: 224–232.

Krug D, Müller R. (2014). Secondary metabolomics: the impact of mass spectrometry-based approaches on the discovery and characterization of microbial natural products. *Nat Prod Rep* **31**: 768.

Krug D, Zurek G, Revermann O, Vos M, Velicer GJ, Müller R. (2008). Discovering the hidden secondary metabolome of *Myxococcus xanthus*: a study of intraspecific diversity. *Appl Environ Microbiol* **74**: 3058–3068.

Krzyściak W, Pluskwa KK, Jurczak A, Kościelniak D. (2013). The pathogenicity of the *Streptococcus* genus. *Eur J Clin Microbiol Infect Dis* **32**: 1361–1376.

Kunze B, Reck M, Dötsch A, Lemme A, Schummer D, Irschik H *et al.* (2010). Damage of *Streptococcus mutans* biofilms by carolacton, a secondary metabolite from the myxobacterium *Sorangium cellulosum*. *BMC Microbiol* **10**: 199.

Kwiecinski J, Jacobsson G, Karlsson M, Zhu X, Wang W, Bremell T *et al.* (2013). Staphylokinase promotes the establishment of *Staphylococcus aureus* skin infections while decreasing disease severity. *J Infect Dis* **208**: 990–999.

Laemmli UK. (1970). Cleavage of structural proteins during the assembly of the head of bacteriophage T4. *Nature* **227**: 680–685.

Lähteenmäki K, Edelman S, Korhonen TK. (2005). Bacterial metastasis: the host plasminogen system in bacterial invasion. *Trends Microbiol* **13**: 79–85.

Lamagni TL, Darenberg J, Luca-Harari B, Siljander T, Efstratiou A, Henriques-Normark B *et al.* (2008). Epidemiology of severe *Streptococcus pyogenes* disease in Europe. *J Clin Microbiol* **46**: 2359–2367.

Lamba D, Bauer M, Huber R, Fischer S, Rudolph R, Kohnert U et *al.* (1996). The 2.3 A crystal structure of the catalytic domain of recombinant two-chain human tissue-type plasminogen activator. *J Mol Biol* **258**: 117–135.

Lancefield RC. (1933). A serological differentiation of human and other groups of hemolytic streptococci. *J Exp Med* **57**: 571–595.

Lang E. (2014). The family *Kofleriaceae*. In: *The Prokaryotes*, Rosenberg, E, DeLong, EF, Lory, S, Stackebrandt, E, & Thompson, F (eds), Springer Berlin Heidelberg, pp 183–189.

LaPenta D, Rubens C, Chi E, Cleary PP. (1994). Group A streptococci efficiently invade human respiratory epithelial cells. *Proc Natl Acad Sci* **91**: 12115–12119.

Law RHP, Caradoc-Davies T, Cowieson N, Horvath AJ, Quek AJ, Encarnacao JA *et al.* (2012). The X-ray crystal structure of full-length human plasminogen. *Cell Rep* **1**: 185–190.

Lee JL, Naguwa SM, Cheema GS, Gershwin ME. (2009). Acute rheumatic fever and its consequences: A persistent threat to developing nations in the 21st century. *Autoimmun Rev* **9**: 117–123.

Leonhardt BA, DeVilbiss ED. (1985). Separation and double-bond determination on nanogram quantities of aliphatic monounsaturated alcohols, aldehydes and carboxylic acid methyl esters. *J Chromatogr A* **322**: 484–490.

Lewis K. (2013). Platforms for antibiotic discovery. *Nat Rev Drug Discov* **12**: 371–387.

Liang Z, Zhang Y, Agrahari G, Chandrahas V, Glinton K, Donahue DL *et al.* (2013). A natural inactivating mutation in the CovS component of the CovRS regulatory operon in a pattern D *Streptococcal pyogenes* strain influences virulence-associated genes. *J Biol Chem* **288**: 6561–6573.

Ligon BL. (2004). Penicillin: its discovery and early development. *Semin Pediatr Infect Dis* **15**: 52–57.

Lijnen HR, Collen D. (1982). Interaction of plasminogen activators and inhibitors with plasminogen and fibrin. *Semin Thromb Hemost* **8**: 2–10.

Lin L-F, Houng A, Reed GL. (2000). Epsilon amino caproic acid inhibits streptokinase−plasminogen activator complex formation and substrate binding through kringle-dependent mechanisms. *Biochemistry (Mosc)* **39**: 4740–4745.

Lipinski CA, Lombardo F, Dominy BW, Feeney PJ. (2001). Experimental and computational approaches to estimate solubility and permeability in drug discovery and development settings. *Adv Drug Deliv Rev* **64**: 3–26.

Li S, Seitz R, Lisanti MP. (1996). Phosphorylation of caveolin by Src tyrosine kinases. The α-isoform of caveolin is selectively phosphorylated by v-Src *in vivo*. *J Biol Chem* **271**: 3863–3868.

Li Y, Sun B, Pei B, Li C, Zhang Z, Yin Y *et al.* (2015). Osteopontin-expressing macrophages in non-small cell lung cancer predict survival. *Ann Thorac Surg*. doi:10.1016/j.athoracsur.2014.11.054.

Lizano S, Johnston KH. (2005). Structural diversity of streptokinase and activation of human plasminogen. *Infect Immun* **73**: 4451–4453.

Longstaff C. (1994). Studies on the mechanisms of action of aprotinin and tranexamic acid as plasmin inhibitors and antifibrinolytic agents. *Blood Coagul Fibrinolysis Int J Haemost Thromb* **5**: 537–542.

Loof TG, Deicke C, Medina E. (2014). The role of coagulation/fibrinolysis during *Streptococcus pyogenes* infection. *Front Cell Infect Microbiol* **4**. doi:10.3389/fcimb.2014.00128.

Loof TG, Mörgelin M, Johansson L, Oehmcke S, Olin AI, Dickneite G *et al.* (2011). Coagulation, an ancestral serine protease cascade, exerts a novel function in early immune defense. *Blood* **118**: 2589–2598.

Luciani F, Molinari A, Lozupone F, Calcabrini A, Lugini L, Stringaro A *et al.* (2002). P-glycoprotein-actin association through ERM family proteins: a role in P-glycoprotein function in human cells of lymphoid origin. *BLOOD-N Y-* **99**: 641–648.

Lu C, Kirsch B, Zimmer C, de Jong JC, Henn C, Maurer CK *et al.* (2012). Discovery of antagonists of PqsR, a key player in 2-alkyl-4-quinolone-dependent quorum sensing in *Pseudomonas aeruginosa*. *Chem Biol* **19**: 381–390.

Lu C, Maurer CK, Kirsch B, Steinbach A, Hartmann RW. (2014). Overcoming the unexpected functional inversion of a PqsR antagonist in *Pseudomonas aeruginosa* : An in vivo potent antivirulence agent targeting *pqs* quorum sensing. *Angew Chem Int Ed* **53**: 1109–1112.

Lu G, DeGuzman FR, Hollenbach SJ, Karbarz MJ, Abe K, Lee G *et al.* (2013). A specific antidote for reversal of anticoagulation by direct and indirect inhibitors of coagulation factor Xa. *Nat Med* **19**: 446–451.

Lugini L, Matarrese P, Tinari A, Lozupone F, Federici C, Iessi E *et al.* (2006). Cannibalism of live lymphocytes by human metastatic but not primary melanoma cells. *Cancer Res* **66**: 3629–3638.

Lyß G, Knorre A, Schmidt TJ, Pahl HL, Merfort I. (1998). The anti-inflammatory sesquiterpene lactone helenalin inhibits the transcription factor NF-κB by directly targeting p65. *J Biol Chem* **273**: 33508–33516.

Maamary PG, Ben Zakour NL, Cole JN, Hollands A, Aziz RK, Barnett TC *et al.* (2012). Tracing the evolutionary history of the pandemic group A streptococcal M1T1 clone. *FASEB J* **26**: 4675–4684.

Macarron R. (2006). Critical review of the role of HTS in drug discovery. *Drug Discov Today* **11**: 277–279.

Macris MH, Hartman N, Murray B, Klein RF, Roberts RB, Kaplan EL *et al.* (1998). Studies of the continuing susceptibility of group A streptococcal strains to penicillin during eight decades. *Pediatr Infect Dis J* **17**: 377–381.

Marjenberg ZR, Ellis IR, Hagan RM, Prabhakaran S, Hook M, Talay SR *et al.* (2011). Cooperative binding and activation of fibronectin by a bacterial surface protein. *J Biol Chem* **286**: 1884–1894.

Markus G, Priore RL, Wissler FC. (1979). The binding of tranexamic acid to native (Glu) and modified (Lys) human plasminogen and its effect on conformation. *J Biol Chem* **254**: 1211–1216.

Mathews II, Vanderhoff-Hanaver P, Castellino FJ, Tulinsky A. (1996). Crystal structures of the recombinant kringle 1 domain of human plasminogen in complexes with the ligands ε-aminocaproic acid and trans-4-(aminomethyl) cyclohexane-1-carboxylic acid. *Biochemistry (Mosc)* **35**: 2567–2576.

Ma Y, Xu Y, Yestrepsky BD, Sorenson RJ, Chen M, Larsen SD *et al.* (2012). Novel inhibitors of *Staphylococcus aureus* virulence gene expression and biofilm formation Bereswill, S (ed). *PLoS ONE* **7**: e47255.

McArthur JD, Cook SM, Venturini C, Walker MJ. (2012). The role of streptokinase as a virulence determinant of *Streptococcus pyogenes* - potential for therapeutic targeting. *Curr Drug Targets* **13**: 297–307.

McArthur JD, McKay FC, Ramachandran V, Shyam P, Cork AJ, Sanderson-Smith ML *et al.* (2008). Allelic variants of streptokinase from *Streptococcus pyogenes* display functional differences in plasminogen activation. *FASEB J* **22**: 3146–3153.

McArthur JD, Walker MJ. (2006). Domains of group A streptococcal M protein that confer resistance to phagocytosis, opsonization and protection: implications for vaccine development. *Mol Microbiol* **59**: 1–4.

McArthur J, Medina E, Mueller A, Chin J, Currie BJ, Sriprakash KS *et al.* (2004). Intranasal vaccination with streptococcal fibronectin binding protein Sfb1 fails to prevent growth and dissemination of *Streptococcus pyogenes* in a murine skin infection model. *Infect Immun* **72**: 7342–7345.

McCurdy HD. (1969). Studies on the taxonomy of the Myxobacterales. I. Record of Canadian isolates and survey of methods. *Can J Microbiol* **15**: 1453–1461.

McDonald JC. (1967). Studies on the genus *Archangium* (Myxobacterales). II. The effect of temperature and carbohydrates on some physiological processes. *Mycologia* **59**: 1059–1068.

McMillan DJ, Drèze P-A, Vu T, Bessen DE, Guglielmini J, Steer AC *et al.* (2013). Updated model of group A *Streptococcus* M proteins based on a comprehensive worldwide study. *Clin Microbiol Infect* **19**: E222–E229.

Medina E, Goldmann O, Toppel AW, Chhatwal GS. (2003). Survival of *Streptococcus pyogenes* within host phagocytic cells: a pathogenic mechanism for persistence and systemic invasion. *J Infect Dis* **187**: 597–603.

Medina E, Molinari G, Rohde M, Haase B, Chhatwal GS, Guzmán CA. (1999). Fc-mediated nonspecific binding between fibronectin-binding protein I of *Streptococcus pyogenes* and human immunoglobulins. *J Immunol* **163**: 3396–3402.

Medina E, Rohde M, Chhatwal GS. (2003). Intracellular survival of *Streptococcus pyogenes* in polymorphonuclear cells results in increased bacterial virulence. *Infect Immun* **71**: 5376–5380.

Mera RM, Miller LA, Daniels JJD, Weil JG, White AR. (2005). Increasing prevalence of multidrug-resistant *Streptococcus pneumoniae* in the United States over a 10-year period: Alexander Project. *Diagn Microbiol Infect Dis* **51**: 195–200.

Mohr KI, Garcia RO, Gerth K, Irschik H, Müller R. (2012). *Sandaracinus amylolyticus* gen. nov., sp. nov., a starch-degrading soil myxobacterium, and description of *Sandaracinaceae* fam. nov. *Int J Syst Evol Microbiol* **62**: 1191–1198.

Molinari G, Rohde M, Guzmán CA, Chhatwal GS. (2000). Two distinct pathways for the invasion of *Streptococcus pyogenes* in non-phagocytic cells. *Cell Microbiol* **2**: 145–154.

Molinari G, Talay SR, Valentin-Weigand P, Rohde M, Chhatwal GS. (1997). The fibronectin-binding protein of *Streptococcus pyogenes*, SfbI, is involved in the internalization of group A streptococci by epithelial cells. *Infect Immun* **65**: 1357–1363.

Monea S, Lehti K, Keski-Oja J, Mignatti P. (2002). Plasmin activates pro-matrix metalloproteinase-2 with a membrane-type 1 matrix metalloproteinase-dependent mechanism. *J Cell Physiol* **192**: 160–170.

Montes M, Tamayo E, Orden B, Larruskain J, Perez-Trallero E. (2010). Prevalence and clonal characterization of *Streptococcus pyogenes* clinical isolates with reduced fluoroquinolone susceptibility in Spain. *Antimicrob Agents Chemother* **54**: 93–97.

Morgan MJ, Liu Z. (2011). Crosstalk of reactive oxygen species and NF-κB signaling. *Cell Res* **21**: 103–115.

Mosmann T. (1983). Rapid colorimetric assay for cellular growth and survival: application to proliferation and cytotoxicity assays. *J Immunol Methods* **65**: 55–63.

Müller R, Wink J. (2014). Future potential for anti-infectives from bacteria – How to exploit biodiversity and genomic potential. *Int J Med Microbiol* **304**: 3–13.

Mullis KB, Faloona FA. (1987). Specific synthesis of DNA in vitro via a polymerase-catalyzed chain reaction. *Methods Enzymol* **155**: 335–350.

Nawrath T, Gerth K, Müller R, Schulz S. (2010). Volatile methyl esters of medium chain length from the bacterium *Chitinophaga* Fx7914. *Chem Biodivers* **7**: 2228–2253.

Neeman R, Keller N, Barzilai A, Korenman Z, Sela S. (1998). Prevalence of internalisation-associated gene, prtF1, among persisting group-A *streptococcus* strains isolated from asymptomatic carriers. *Lancet* **352**: 1974–1977.

Nerlich A, Rohde M, Talay SR, Genth H, Just I, Chhatwal GS. (2009). Invasion of endothelial cells by tissue-invasive M3 type group A streptococci requires Src kinase and activation of Rac1 by a phosphatidylinositol 3-kinase-independent mechanism. *J Biol Chem* **284**: 20319–20328.

Newman DJ, Cragg GM. (2012). Natural products as sources of new drugs over the 30 years from 1981 to 2010. *J Nat Prod* **75**: 311–335.

N.N. (1952). Erythromycin: another antibiotic. *Lancet* **2**: 232–233.

Nobbs AH, Lamont RJ, Jenkinson HF. (2009). *Streptococcus* adherence and colonization. *Microbiol Mol Biol Rev* **73**: 407–450.

Nordstrand A, McShan WM, Ferretti JJ, Holm SE, Norgren M. (2000). Allele substitution of the streptokinase gene reduces the nephritogenic capacity of group A streptococcal strain NZ131. *Infect Immun* **68**: 1019–1025.

Nordstrand A, Norgren M, Ferretti JJ, Holm SE. (1998). Streptokinase as a mediator of acute post-streptococcal glomerulonephritis in an experimental mouse model. *Infect Immun* **66**: 315–321.

Nordstrand A, Norgren M, Holm SE. (1999). Pathogenic mechanism of acute post-streptococcal glomerulonephritis. *Scand J Infect Dis* **31**: 523–537.

Norrby-Teglund A, Kaul R, Low DE, McGeer A, Newton DW, Andersson J *et al.* (1996). Plasma from patients with severe invasive group A streptococcal infections treated with normal polyspecific IgG inhibits streptococcal superantigen-induced T cell proliferation and cytokine production. *J Immunol* **156**: 3057–3064.

Ochel A, Rohde M, Chhatwal GS, Talay SR. (2014). The M1 protein of *Streptococcus pyogenes* triggers an innate uptake mechanism into polarized human endothelial cells. *J Innate Immun* **6**: 585–596.

O'Connell KMG, Hodgkinson JT, Sore HF, Welch M, Salmond GPC, Spring DR. (2013). Combating multidrug-resistant bacteria: current strategies for the discovery of novel antibacterials. *Angew Chem Int Ed* **52**: 10706–10733.

Ogawa T, Terao Y, Okuni H, Ninomiya K, Sakata H, Ikebe K *et al.* (2011). Biofilm formation or internalization into epithelial cells enable *Streptococcus pyogenes* to evade antibiotic eradication in patients with pharyngitis. *Microb Pathog* **51**: 58–68.

Ohkuni H, Todome Y, Yoshimura K, Yamamoto T, Suzuki H, Yokomuro K *et al.* (1991). Detection of nephritis strain-associated streptokinase by monoclonal antibodies. *J Med Microbiol* **35**: 60–63.

Okanya PW, Mohr KI, Gerth K, Jansen R, Müller R. (2011). Marinoquinolines A-F, pyrroloquinolines from *Ohtaekwangia kribbensis* (Bacteroidetes). *J Nat Prod* **74**: 603–608.

O'Loughlin RE, Roberson A, Cieslak PR, Lynfield R, Gershman K, Craig A *et al.* (2007). The epidemiology of invasive group A streptococcal infection and potential vaccine implications: United States, 2000-2004. *Clin Infect Dis* **45**: 853–862.

Olsen RJ, Musser JM. (2010). Molecular pathogenesis of necrotizing fasciitis. *Annu Rev Pathol Mech Dis* **5**: 1–31.

Olsen RJ, Shelburne SA, Musser JM. (2009). Molecular mechanisms underlying group A streptococcal pathogenesis. *Cell Microbiol* **11**: 1–12.

Österlund A, Popa R, Nikkilä T, Scheynius A, Engstrand L. (1997). Intracellular reservoir of *Streptococcus pyogenes* in vivo: a possible explanation for recurrent pharyngotonsillitis. *The Laryngoscope* **107**: 640–647.

Ozeri V, Rosenshine I, Ben-Ze'Ev A, Bokoch GM, Jou T-S, Hanski E. (2001). De novo formation of focal complex-like structures in host cells by invading Streptococci. *Mol Microbiol* **41**: 561–573.

Ozeri V, Rosenshine I, Mosher DF, Fässler R, Hanski E. (1998). Roles of integrins and fibronectin in the entry of *Streptococcus pyogenes* into cells via protein F1. *Mol Microbiol* **30**: 625–637.

Pahlman LI, Mörgelin M, Eckert J, Johansson L, Russell W, Riesbeck K *et al.* (2006). Streptococcal M Protein: A Multipotent and Powerful Inducer of Inflammation. *J Immunol* **177**: 1221–1228.

Pancholi V, Chhatwal GS. (2003). Housekeeping enzymes as virulence factors for pathogens. *Int J Med Microbiol IJMM* **293**: 391–401.

Pancholi V, Fischetti VA. (1992). A major surface protein on group A streptococci is a glyceraldehyde-3-phosphate-dehydrogenase with multiple binding activity. *J Exp Med* **176**: 415–426.

Pancholi V, Fischetti VA. (1997). A novel plasminogen/plasmin binding protein on the surface of group A streptococci. In: *Streptococci and the Host*, Springer, pp 597–599.

Pancholi V, Fischetti VA. (1998). α-Enolase, a novel strong plasmin(ogen) binding protein on the surface of pathogenic streptococci. *J Biol Chem* **273**: 14503–14515.

Pankov R, Yamada KM. (2002). Fibronectin at a glance. *J Cell Sci* **115**: 3861–3863.

Parry MA, Zhang XC, Bode I. (2000). Molecular mechanisms of plasminogen activation: bacterial cofactors provide clues. *Trends Biochem Sci* **25**: 53–59.

Pathak DT, Wei X, Wall D. (2012). Myxobacterial tools for social interactions. *Res Microbiol* **163**: 579–591.

Peetermans M, Vanassche T, Liesenborghs L, Claes J, Vande Velde G, Kwiecinksi J *et al.* (2014). Plasminogen activation by staphylokinase enhances local spreading of *S. aureus* in skin infections. *BMC Microbiol* **14**: 310.

Pelkmans L, Kartenbeck J, Helenius A. (2001). Caveolar endocytosis of simian virus 40 reveals a new two-step vesicular-transport pathway to the ER. *Nat Cell Biol* **3**: 473–483.

Pendleton JN, Gorman SP, Gilmore BF. (2013). Clinical relevance of the ESKAPE pathogens. *Expert Rev Anti Infect Ther* **11**: 297–308.

Pichichero ME. (1991). The rising incidence of penicillin treatment failures in group A streptococcal tonsillopharyngitis: an emerging role for the cephalosporins? *Pediatr Infect Dis J* **10**: S50–55.

Pistorius D, Müller R. (2012). Discovery of the rhizopodin biosynthetic gene cluster in *Stigmatella aurantiaca* Sg a15 by genome mining. *ChemBioChem* **13**: 416–426.

Pistorius D, Ullrich A, Lucas S, Hartmann RW, Kazmaier U, Müller R. (2011). Biosynthesis of 2-alkyl-4(1H)-quinolones in *Pseudomonas aeruginosa*: potential for therapeutic interference with pathogenicity. *ChemBioChem* **12**: 850–853.

Ponting CP, Marshall JM, Cederholm-Williams SA. (1992). Plasminogen: a structural review. *Blood Coagul Fibrinolysis Int J Haemost Thromb* **3**: 605–614.

Poole K. (2005). Efflux-mediated antimicrobial resistance. *J Antimicrob Chemother* **56**: 20–51.

Poullet P, Gautreau A, Kadare G, Girault J-A, Louvard D, Arpin M. (2001). Ezrin interacts with focal adhesion kinase and induces its activation independently of cell-matrix adhesion. *J Biol Chem* **276**: 37686–37691.

Projan SJ. (2003). Why is big Pharma getting out of antibacterial drug discovery? *Curr Opin Microbiol* **6**: 427–430.

Purushothaman SS, Wang B, Cleary PP. (2003). M1 protein triggers a phosphoinositide cascade for group A *Streptococcus* invasion of epithelial cells. *Infect Immun* **71**: 5823–5830.

Randel A, Infectious Disease Society of America. (2013). IDSA updates guideline for managing group A streptococcal pharyngitis. *Am Fam Physician* **88**: 338–340.

Rasko DA, Moreira CG, Li DR, Reading NC, Ritchie JM, Waldor MK *et al.* (2008). Targeting QseC signaling and virulence for antibiotic development. *Science* **321**: 1078–1080.

Reczek D, Bretscher A. (1998). The carboxyl-terminal region of EBP50 binds to a site in the amino-terminal domain of ezrin that is masked in the dormant molecule. *J Biol Chem* **273**: 18452–18458.

Reichenbach H. (1999). The ecology of the myxobacteria. *Environ Microbiol* **1**: 15–21.

Reichenbach H, Höfle G. (1993). Biologically active secondary metabolites from myxobacteria. *Biotechnol Adv* **11**: 219–277.

Rijken DC, Lijnen HR. (2009). New insights into the molecular mechanisms of the fibrinolytic system. *J Thromb Haemost* **7**: 4–13.

Rohde M, Chhatwal GS. (2013). Adherence and invasion of streptococci to eukaryotic cells and their role in disease pathogenesis. *Curr Top Microbiol Immunol* **368**: 83–110.

Rohde M, Müller E, Chhatwal GS, Talay SR. (2003). Host cell caveolae act as an entry-port for Group A streptococci. *Cell Microbiol* **5**: 323–342.

Royston D. (2015). The current place of aprotinin in the management of bleeding. *Anaesthesia* **70**: 46–e17.

Saier MH. (2006). Protein Secretion and Membrane Insertion Systems in Gram-Negative Bacteria. *J Membr Biol* **214**: 75–90.

Sanderson-Smith M, Batzloff M, Sriprakash KS, Dowton M, Ranson M, Walker MJ. (2006). Divergence in the plasminogen-binding group A streptococcal M protein family: functional conservation of binding site and potential role for immune selection of variants. *J Biol Chem* **281**: 3217–3226.

Sanderson-Smith M, De Oliveira DMP, Guglielmini J, McMillan DJ, Vu T, Holien JK *et al.* (2014). A systematic and functional classification of *Streptococcus pyogenes* that serves as a new tool for molecular typing and vaccine development. *J Infect Dis* **210**: 1325–1338.

Sanderson-Smith ML, De Oliveira DMP, Ranson M, McArthur JD. (2012). Bacterial plasminogen receptors: mediators of a multifaceted relationship. *J Biomed Biotechnol* **2012**: 1–14.

Sanderson-Smith ML, Dinkla K, Cole JN, Cork AJ, Maamary PG, McArthur JD *et al.* (2008). M protein-mediated plasminogen binding is essential for the virulence of an invasive *Streptococcus pyogenes* isolate. *FASEB J* **22**: 2715–2722.

Sanderson-Smith ML, Zhang Y, Ly D, Donahue D, Hollands A, Nizet V *et al.* (2013). A key role for the urokinase plasminogen activator (uPA) in invasive group A streptococcal infection Sullam, PM (ed). *PLoS Pathog* **9**: e1003469.

Sanford RA, Cole JR, Tiedje JM. (2002). Characterization and description of *Anaeromyxobacter dehalogenans* gen. nov., sp. nov., an aryl-halorespiring facultative anaerobic myxobacterium. *Appl Environ Microbiol* **68**: 893–900.

Sargiacomo M, Scherer PE, Tang Z, Kübler E, Song KS, Sanders MC *et al.* (1995). Oligomeric structure of caveolin: implications for caveolae membrane organization. *Proc Natl Acad Sci* **92**: 9407–9411.

Schaar V, Uddback I, Nordstrom T, Riesbeck K. (2014). Group A streptococci are protected from amoxicillin-mediated killing by vesicles containing β-lactamase derived from *Haemophilus influenzae*. *J Antimicrob Chemother* **69**: 117–120.

Schäberle TF, Lohr F, Schmitz A, König GM. (2014). Antibiotics from myxobacteria. *Nat Prod Rep* **31**: 953.

Schäckel R, Hinkelmann B, Sasse F, Kalesse M. (2010). The Synthesis of Novel Disorazoles. *Angew Chem Int Ed* **49**: 1619–1622.

Schaffner F, Ray A, Dontenwill M. (2013). Integrin α5β1, the fibronectin receptor, as a pertinent therapeutic target in solid tumors. *Cancers* **5**: 27–47.

Schatz A, Bugie E, Waksman SA. (2005). The classic: Streptomycin, a substance exhibiting antibiotic activity against gram-positive and gram-negative bacteria. *Clin Orthop* **&NA;**: 3–6.

Schlegel HG. (1992). Allgemeine Mikrobiologie. 7., überarb. Aufl. Thieme, Georg, Verlag KG: Stuttgart u.a.

Schneiker S, Perlova O, Kaiser O, Gerth K, Alici A, Altmeyer MO *et al.* (2007). Complete genome sequence of the myxobacterium *Sorangium cellulosum*. *Nat Biotechnol* **25**: 1281–1289.

Schoenwaelder SM, Burridge K. (1999). Bidirectional signaling between the cytoskeleton and integrins. *Curr Opin Cell Biol* **11**: 274–286.

Schottmüller H. (1903). Die Artunterscheidung der für den Menschen pathogenen Streptokokken durch Blutagar. *Münch Med Wochenschr* **50**: 849–853.

Schwarz-Linek U, Werner JM, Pickford AR, Gurusiddappa S, Kim JH, Pilka ES *et al.* (2003). Pathogenic bacteria attach to human fibronectin through a tandem β-zipper. *Nature* **423**: 177–181.

Scott JR, Barnett TC. (2006). Surface proteins of gram-positive bacteria and how they get there. *Annu Rev Microbiol* **60**: 397–423.

Seger C, Sturm S, Stuppner H. (2013). Mass spectrometry and NMR spectroscopy: modern high-end detectors for high resolution separation techniques - state of the art in natural product HPLC-MS, HPLC-NMR, and CE-MS hyphenations. *Nat Prod Rep* **30**: 970–987.

Seitz S, Buchholz S, Schally AV, Weber F, Klinkhammer-Schalke M, Inwald EC *et al.* (2014). Triple negative breast cancers express receptors for LHRH and are potential therapeutic targets for cytotoxic LHRH-analogs, AEZS 108 and AEZS 125. *BMC Cancer* **14**: 847.

Shannon O, Rydengard V, Schmidtchen A, Mörgelin M, Alm P, Sorensen OE *et al.* (2010). Histidine-rich glycoprotein promotes bacterial entrapment in clots and decreases mortality in a mouse model of sepsis. *Blood* **116**: 2365–2372.

Shi G-Y, Chang B-I, Chen S-M, Wu D-H, Wu H-L. (1994). Function of streptokinase fragments in plasminogen activation. *Biochem J* **304**: 235–241.

Shulman ST, Tanz RR, Dale JB, Steer AC, Smeesters PR. (2014). Added value of the *emm*-cluster typing system to analyze group A *Streptococcus* epidemiology in high-income settings. *Clin Infect Dis Off Publ Infect Dis Soc Am* **59**: 1651–1652.

Silva-Costa C, Friães A, Ramirez M, Melo-Cristino J. (2015). Macrolide-resistant *Streptococcus pyogenes*: prevalence and treatment strategies. *Expert Rev Anti Infect Ther* 1–14.

Smeesters PR, McMillan DJ, Sriprakash KS. (2010). The streptococcal M protein: a highly versatile molecule. *Trends Microbiol* **18**: 275–282.

Sodeinde OA, Subrahmanyam YV, Stark K, Quan T, Bao Y, Goguen JD. (1992). A surface protease and the invasive character of plague. *Science* **258**: 1004–1007.

Sood S, Awal RP, Wink J, Mohr KI, Rohde M, Stadler M *et al.* (2014). *Aggregicoccus edonensis* gen. nov., sp. nov., an unusually aggregating myxobacterium isolated from a soil sample. *Int J Syst Evol Microbiol* ijs.0.061176–0.

Spraggon G, Phillips C, Nowak UK, Ponting CP, Saunders D, Dobson CM *et al.* (1995). The crystal structure of the catalytic domain of human urokinase-type plasminogen activator. *Structure* **3**: 681–691.

Srivastava J, Elliott BE, Louvard D, Arpin M. (2005). Src-dependent ezrin phosphorylation in adhesion-mediated signaling. *Mol Biol Cell* **16**: 1481–1490.

Starkey M, Lepine F, Maura D, Bandyopadhaya A, Lesic B, He J *et al.* (2014). Identification of anti-virulence compounds that disrupt quorum-sensing regulated acute and persistent pathogenicity Whiteley, M (ed). *PLoS Pathog* **10**: e1004321.

Steer AC, Carapetis JR. (2009). Prevention and treatment of rheumatic heart disease in the developing world. *Nat Rev Cardiol* **6**: 689–698.

Stevens DL, Bisno AL, Chambers HF, Dellinger EP, Goldstein EJC, Gorbach SL *et al.* (2014). Practice guidelines for the diagnosis and management of skin and soft tissue infections: 2014 update by the Infectious Diseases Society of America. *Clin Infect Dis* **59**: 147–159.

Sticher O. (2008). Natural product isolation. *Nat Prod Rep* **25**: 517–554.

Stjernquist-Desatnik A, Samuelsson P, Walder M. (1993). Penetration of penicillin V to tonsillar surface fluid in healthy individuals and in patients with acute tonsillitis. *J Laryngol Otol* **107**: 309–312.

Stradal TB, Sechi AS, Wehland J, Rottner K. (2003). Chapter 12 The cytoskeleton. In: *Essential Cell Biology Vol 1: Cell Structure*, Davey, J & Lord, JM (eds), Practical Approach Series 262, pp 365–389.

Sumby P, Porcella SF, Madrigal AG, Barbian KD, Virtaneva K, Ricklefs SM *et al.* (2005). Evolutionary origin and emergence of a highly successful clone of serotype M1 group A *Streptococcus* involved multiple horizontal gene transfer events. *J Infect Dis* **192**: 771–782.

Sun H, Ringdahl U, Homeister JW, Fay WP, Engleberg NC, Yang AY *et al.* (2004). Plasminogen is a critical host pathogenicity factor for group A streptococcal infection. *Science* **305**: 1283–1286.

Sun H, Wang X, Degen JL, Ginsburg D. (2009). Reduced thrombin generation increases host susceptibility to group A streptococcal infection. *Blood* **113**: 1358–1364.

Sun H, Xu Y, Sitkiewicz I, Ma Y, Wang X, Yestrepsky BD *et al.* (2012). Inhibitor of streptokinase gene expression improves survival after group A *streptococcus* infection in mice. *Proc Natl Acad Sci* **109**: 3469–3474.

Surup F, Viehrig K, Mohr KI, Herrmann J, Jansen R, Müller R. (2014). Disciformycins A and B: 12-membered macrolide glycoside antibiotics from the myxobacterium *Pyxidicoccus fallax* active against multiresistant staphylococci. *Angew Chem Int Ed* **53**: 13588–13591.

Takada A, Makino Y, Takada Y. (1986). Effects of tranexamic acid on fibrinolysis, fibrinogenolysis and amidolysis. *Thromb Res* **42**: 39–47.

Takahashi H, Yanagisawa T, Kim KS, Yokoyama S, Ohnishi M. (2012). Meningococcal PilV potentiates *Neisseria meningitidis* type IV pilus-mediated internalization into human endothelial and epithelial cells. *Infect Immun* **80**: 4154–4166.

Talay SR, Valentin-Weigand P, Timmis KN, Chhatwal GS. (1994). Domain structure and conserved epitopes of Sfb protein, the fibronectin-binding adhesin of *Streptococcus pyogenes*. *Mol Microbiol* **13**: 531–539.

Talay SR, Zock A, Rohde M, Molinari G, Oggioni M, Pozzi G *et al.* (2000). Co-operative binding of human fibronectin to SfbI protein triggers streptococcal invasion into respiratory epithelial cells. *Cell Microbiol* **2**: 521–535.

Tapper H, Herwald H. (2000). Modulation of hemostatic mechanisms in bacterial infectious diseases. *Blood* **96**: 2329–2337.

Tatsuno I, Okada R, Zhang Y, Isaka M, Hasegawa T. (2013). Partial loss of CovS function in *Streptococcus pyogenes* causes severe invasive disease. *BMC Res Notes* **6**: 126.

Tengborn L, Blombäck M, Berntorp E. (2015). Tranexamic acid – an old drug still going strong and making a revival. *Thromb Res* **135**: 231–242.

Tillett WS, Garner RL. (1933). The fibrinolytic activity of hemolytic streptococci. *J Exp Med* **58**: 485–502.

Torres A, Cillóniz C, Ferrer M, Gabarrús A, Polverino E, Villegas S *et al.* (2015). Bacteraemia and antibiotic-resistant pathogens in community acquired pneumonia: risk and prognosis. *Eur Respir J*. doi:10.1183/09031936.00152514.

Trédan O, Campone M, Jassem J, Vyzula R, Coudert B, Pacilio C *et al.* (2015). Ixabepilone alone or with cetuximab as first-line treatment for advanced/metastatic triple-negative breast cancer. *Clin Breast Cancer* **15**: 8–15.

Tsukita S, Yonemura S, Tsukita S. (1997a). ERM (ezrin/radixin/moesin) family: from cytoskeleton to signal transduction. *Curr Opin Cell Biol* **9**: 70–75.

Tsukita S, Yonemura S, Tsukita S. (1997b). ERM proteins: head-to-tail regulation of actin-plasma membrane interaction. *Trends Biochem Sci* **22**: 53–58.

Vaheri A, Carpén O, Heiska L, Helander TS, Jääskeläinen J, Majander-Nordenswan P *et al.* (1997). The ezrin protein family: membrane-cytoskeleton interactions and disease associations. *Curr Opin Cell Biol* **9**: 659–666.

Violand BN, Byrne R, Castellino FJ. (1978). The effect of α-, ω-amino acids on human plasminogen structure and activation. *J Biol Chem* **253**: 5395–5401.

Viswanatha R, Bretscher A, Garbett D. (2014). Dynamics of ezrin and EBP50 in regulating microvilli on the apical aspect of epithelial cells. *Biochem Soc Trans* **42**: 189–194.

Wachsstock DH, Wilkins JA, Lin S. (1987). Specific interaction of vinculin with α-actinin. *Biochem Biophys Res Commun* **146**: 554–560.

Waddington CS, Snelling TL, Carapetis JR. (2014). Management of invasive group A streptococcal infections. *J Infect* **69**: S63–S69.

Walker MJ, Barnett TC, McArthur JD, Cole JN, Gillen CM, Henningham A *et al.* (2014). Disease manifestations and pathogenic mechanisms of group A *Streptococcus*. *Clin Microbiol Rev* **27**: 264–301.

Walker MJ, Hollands A, Sanderson-Smith ML, Cole JN, Kirk JK, Henningham A *et al.* (2007). DNase Sda1 provides selection pressure for a switch to invasive group A streptococcal infection. *Nat Med* **13**: 981–985.

Walker MJ, McArthur JD, McKay F, Ranson M. (2005). Is plasminogen deployed as a *Streptococcus pyogenes* virulence factor? *Trends Microbiol* **13**: 308–313.

Wang B, Li S, Dedhar S, Cleary PP. (2007). Paxillin phosphorylation: bifurcation point downstream of integrin-linked kinase (ILK) in streptococcal invasion. *Cell Microbiol* **9**: 1519–1528.

Wang B, Yurecko RS, Dedhar S, Cleary PP. (2006). Integrin-linked kinase is an essential link between integrins and uptake of bacterial pathogens by epithelial cells. *Cell Microbiol* **8**: 257–266.

Wang X, Lin X, Loy JA, Tang J, Zhang XC. (1998). Crystal structure of the catalytic domain of human plasmin complexed with streptokinase. *Science* **281**: 1662–1665.

Wardlaw JM, Murray V, Berge E, del Zoppo GJ. (2014). Thrombolysis for acute ischaemic stroke. *Cochrane Libr*. http://onlinelibrary.wiley.com/doi/10.1002/14651858.CD000213.pub3/full (Accessed March 13, 2015).

Weissman KJ, Müller R. (2010). Myxobacterial secondary metabolites: bioactivities and modes-of-action. *Nat Prod Rep* **27**: 1276.

Wenzel SC, Müller R. (2007). Myxobacterial natural product assembly lines: fascinating examples of curious biochemistry. *Nat Prod Rep* **24**: 1211.

Wenzel SC, Müller R. (2009a). Myxobacteria—'microbial factories' for the production of bioactive secondary metabolites. *Mol Biosyst* **5**: 567.

Wenzel SC, Müller R. (2009b). The impact of genomics on the exploitation of the myxobacterial secondary metabolome. *Nat Prod Rep* **26**: 1385.

Whitney CG, Farley MM, Hadler J, Harrison LH, Lexau C, Reingold A *et al.* (2000). Increasing prevalence of multidrug-resistant *Streptococcus pneumoniae* in the United States. *N Engl J Med* **343**: 1917–1924.

Wiman B, Collen D. (1978). On the kinetics of the reaction between human antiplasmin and plasmin. *Eur J Biochem* **84**: 573–578.

Winram SB, Lottenberg R. (1998). Site-directed mutagenesis of streptococcal plasmin receptor protein (Plr) identifies the C-terminal Lys^{334} as essential for plasmin binding, but mutation of the *plr* gene does not reduce plasmin binding to group A streptococci. *Microbiology* **144**: 2025–2035.

Wipf P, Graham TH, Vogt A, Sikorski RP, Ducruet AP, Lazo JS. (2006). Cellular analysis of disorazole C1 and structure-activity relationship of analogs of the natural product. *Chem Biol Drug Des* **67**: 66–73.

Wood CK, Turner CE, Jackson P, Critchley DR. (1994). Characterisation of the paxillin-binding site and the C-terminal focal adhesion targeting sequence in vinculin. *J Cell Sci* **107 (Pt 2)**: 709–717.

World Health Organization (ed). (2014). Antimicrobial resistance: global report on surveillance. World Health Organization: Geneva, Switzerland.

Yakovlev SA, Rublenko MV, Izdepsky VI, Makogonenko EM. (1995). Activating effect of the plasminogen activators on plasminogens of different mammalia species. *Thromb Res* **79**: 423–428.

Yamamoto E, Muramatsu H, Nagai K. (2014). *Vulgatibacter incomptus* gen. nov., sp. nov. and *Labilithrix luteola* gen. nov., sp. nov., two myxobacteria isolated from soil in Yakushima Island, and the description of *Vulgatibacteraceae* fam. nov., *Labilitrichaceae* fam. nov. and *Anaeromyxobacteraceae* fam. nov. *Int J Syst Evol Microbiol* **64**: 3360–3368.

Yayan J. (2014). The comparative development of elevated resistance to macrolides in community-acquired pneumonia caused by *Streptococcus pneumoniae*. *Drug Des Devel Ther* 1733.

Yestrepsky BD, Kretz CA, Xu Y, Holmes A, Sun H, Ginsburg D *et al.* (2014). Development of tag-free photoprobes for studies aimed at identifying the target of novel Group A *Streptococcus* antivirulence agents. *Bioorg Med Chem Lett* **24**: 1538–1544.

Yestrepsky BD, Xu Y, Breen ME, Li X, Rajeswaran WG, Ryu JG *et al.* (2013). Novel inhibitors of bacterial virulence: Development of 5,6-dihydrobenzo[h]quinazolin-4(3H)-ones for the inhibition of group A streptococcal streptokinase expression. *Bioorg Med Chem* **21**: 1880–1897.

Young MH, Engleberg NC, Mulla ZD, Aronoff DM. (2006). Therapies for necrotising fasciitis. *Expert Opin Biol Ther* **6**: 155–165.

Yu Y, Khan J, Khanna C, Helman L, Meltzer PS, Merlino G. (2004). Expression profiling identifies the cytoskeletal organizer ezrin and the developmental homeoprotein Six-1 as key metastatic regulators. *Nat Med* **10**: 175–181.

Zaffanello M, Cataldi L, Franchini M, Fanos V. (2010). Evidence-based treatment limitations prevent any therapeutic recommendation for acute poststreptococcal glomerulonephritis in children. *Ann Transplant* **16**: RA79–RA84.

Zanella F, Lorens JB, Link W. (2010). High content screening: seeing is believing. *Trends Biotechnol* **28**: 237–245.

Zarantonello P, Leslie CP, Ferritto R, Kazmierski WM. (2002). Total synthesis and semi-synthetic approaches to analogues of antibacterial natural product althiomycin. *Bioorg Med Chem Lett* **12**: 561–565.

Zeino M, Zhao Q, Eichhorn T, Herrmann J, Müller R, Efferth T. (2013). Molecular docking studies of myxobacterial disorazoles and tubulysins to tubulin. *J Biosci Med* **3**. doi:10.5780/jbm2013.

Zender M, Klein T, Henn C, Kirsch B, Maurer CK, Kail D *et al.* (2013). Discovery and biophysical characterization of 2-amino-oxadiazoles as novel antagonists of PqsR, an important regulator of *Pseudomonas aeruginosa* virulence. *J Med Chem* **56**: 6761–6774.

Zhang Y, Zhang L, Zhang G, Li S, Duan J, Cheng J *et al.* (2014). Osteosarcoma metastasis: prospective role of ezrin. *Tumor Biol* **35**: 5055–5059.

Ziegler WH, Liddington RC, Critchley DR. (2006). The structure and regulation of vinculin. *Trends Cell Biol* **16**: 453–460.

8 Appendix

8.1 NMR spectra of RC 28.1 and RC 28.5

a.

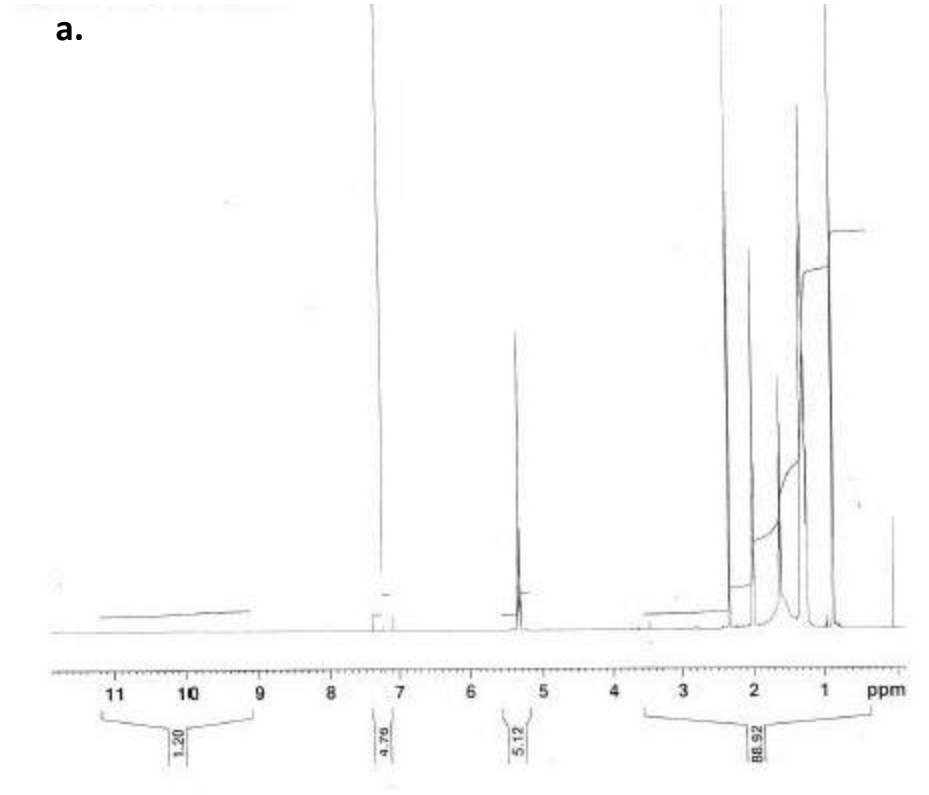

b.

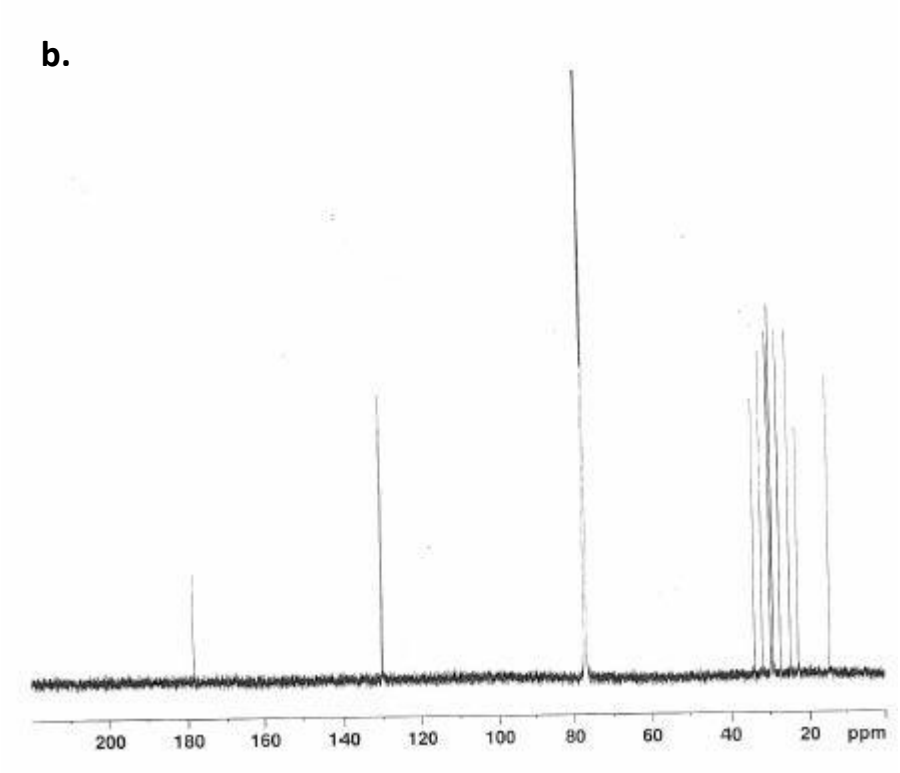

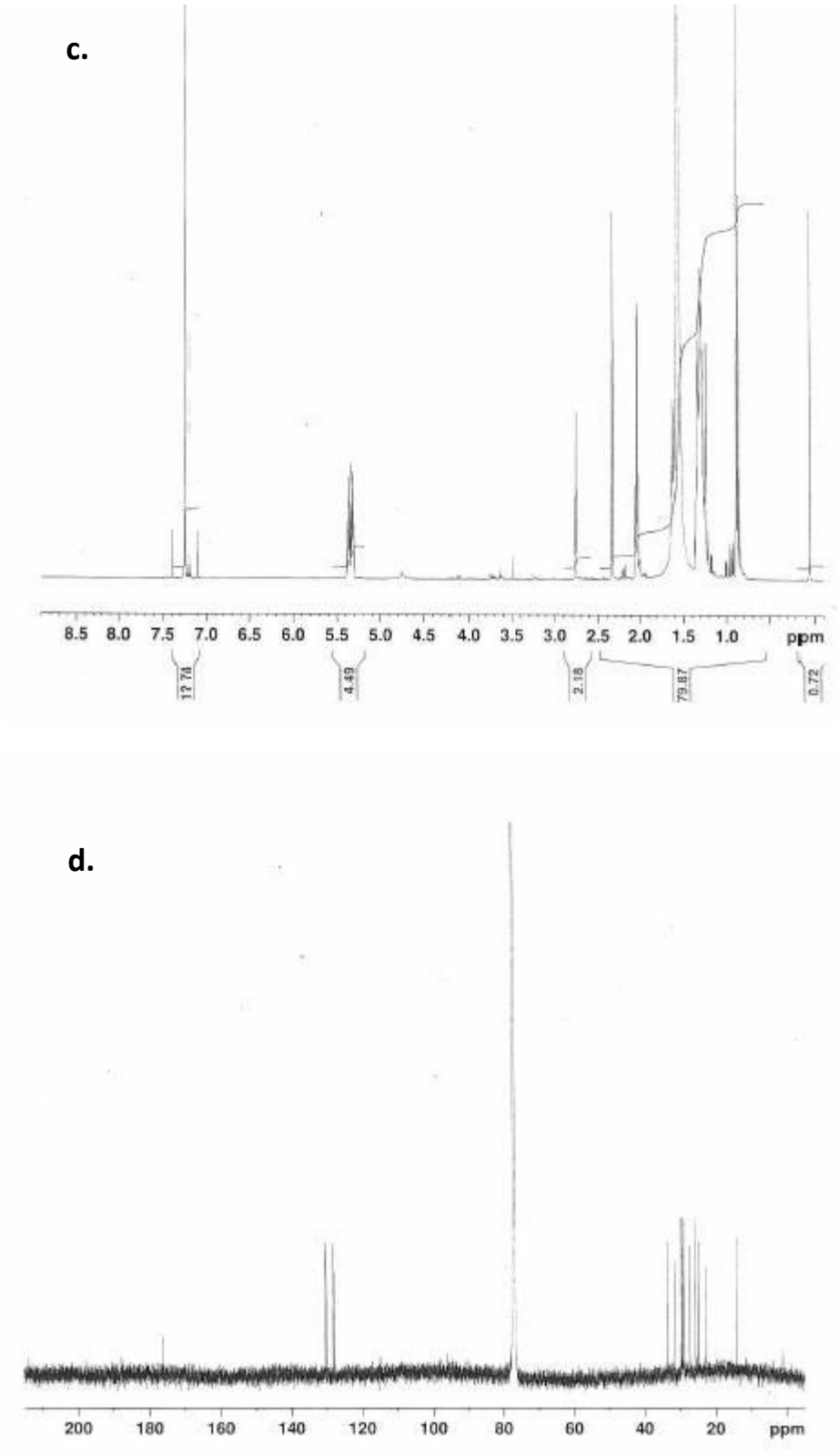

Figure 8-1: NMR spectra of RC 28.1 and RC 28.5.
Chemical shifts are given in parts per million (ppm). (a) ^{1}H-NMR spectrum of RC 28.1. (b) ^{13}C-NMR spectrum of RC 28.1. (c) ^{1}H-NMR spectrum of RC 28.5. (d) ^{13}C-NMR spectrum of RC 28.5.

8.2 GC-MS data

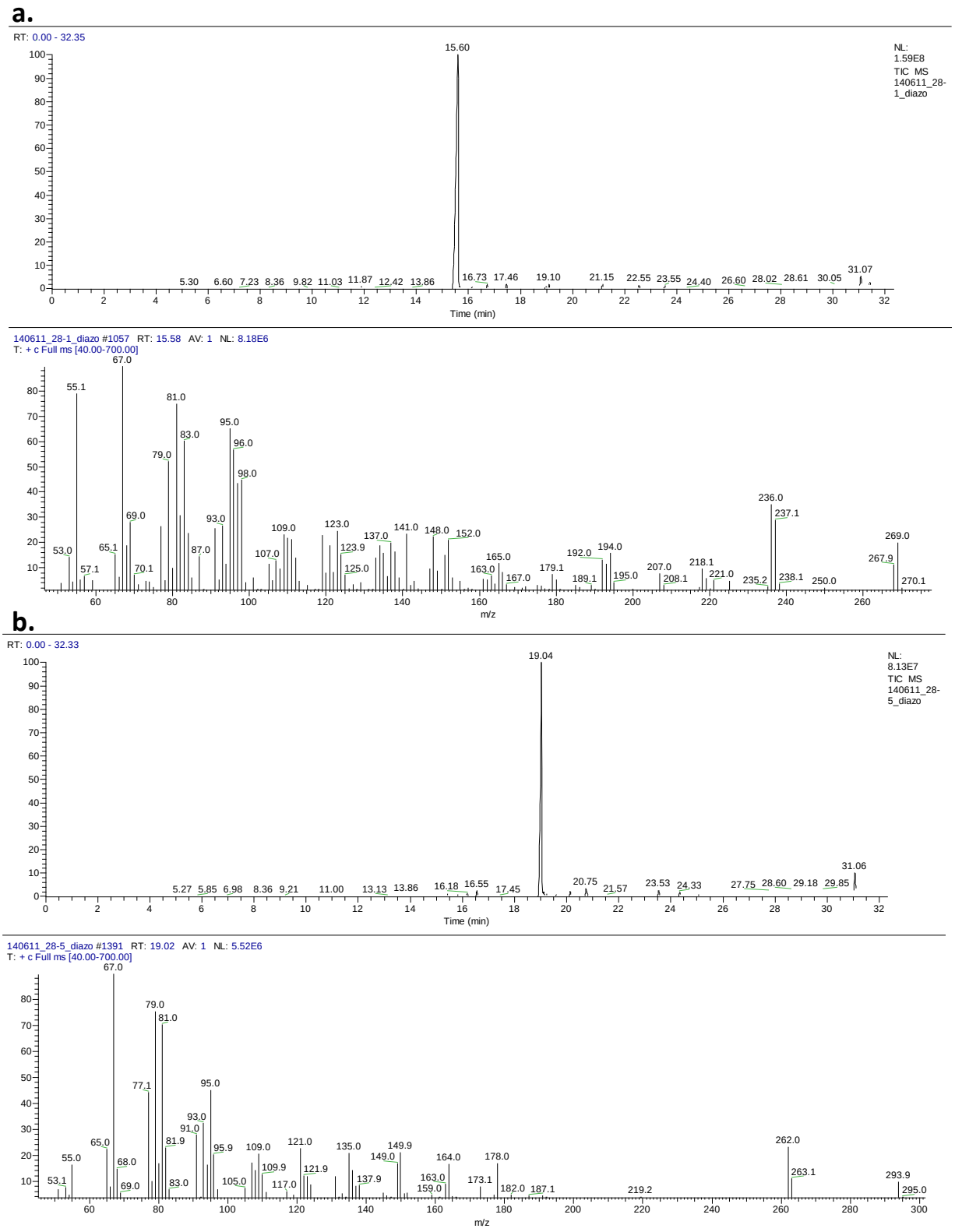

Figure 8-2: GC-MS of methyl ester derivatives of RC 28.1 and RC 28.5.
a,b: The upper part shows the GC-chromatogram of methyl ester derivatives of RC 28.1 (a) or RC 28.5 (b). Peaks were detected by MS. The lower part shows the MS-spectrum of the methyl ester derivative of RC 28.1 at 15.58 min (a) and of RC 28.5 at 19.02 min (b).

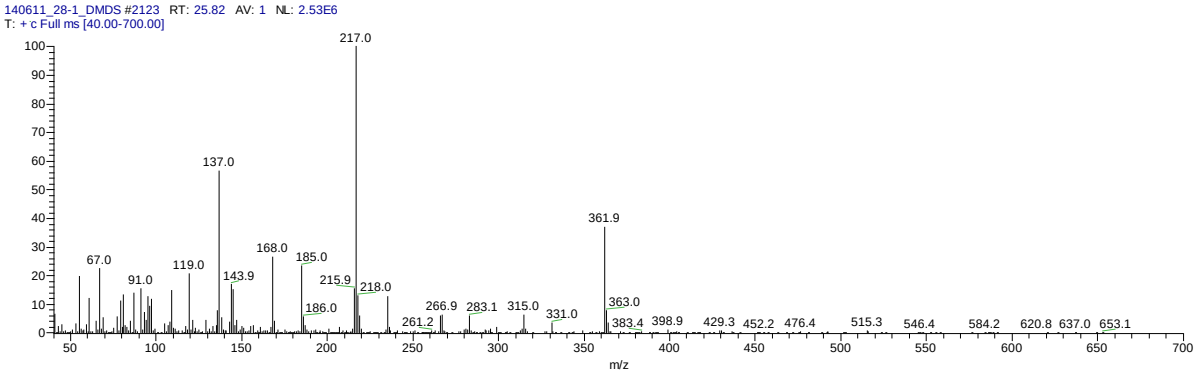

Figure 8-3: GC-MS of a DMDS derivative of RC 28.1
The MS spectrum of the DMDS derivative of RC 28.1 at 25.82 min is shown.

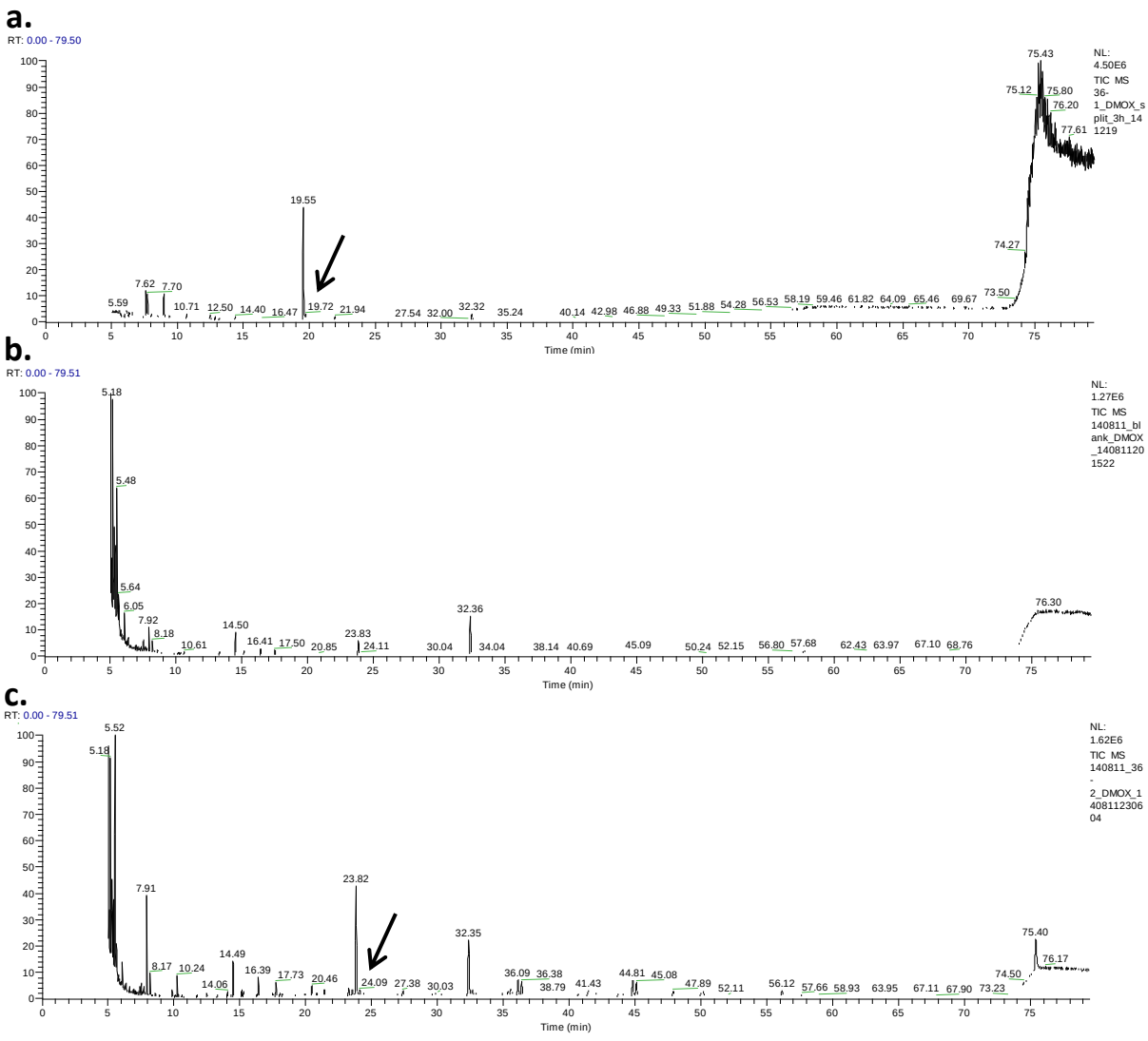

Figure 8-4: Gas-chromatograms of DMOX derivatives of RC 36.1 and RC 36.2.
a-c: Gas-chromatograms of DMOX derivatives of RC 36.1 (a) and RC 36.2 (c). As same impurities are present on the column a blank sample (b) was run as well. Peaks were detected by MS.
a,c: chromatograms show that samples might consist of mixtures of two fatty acids. Black arrows point to the respective peak.

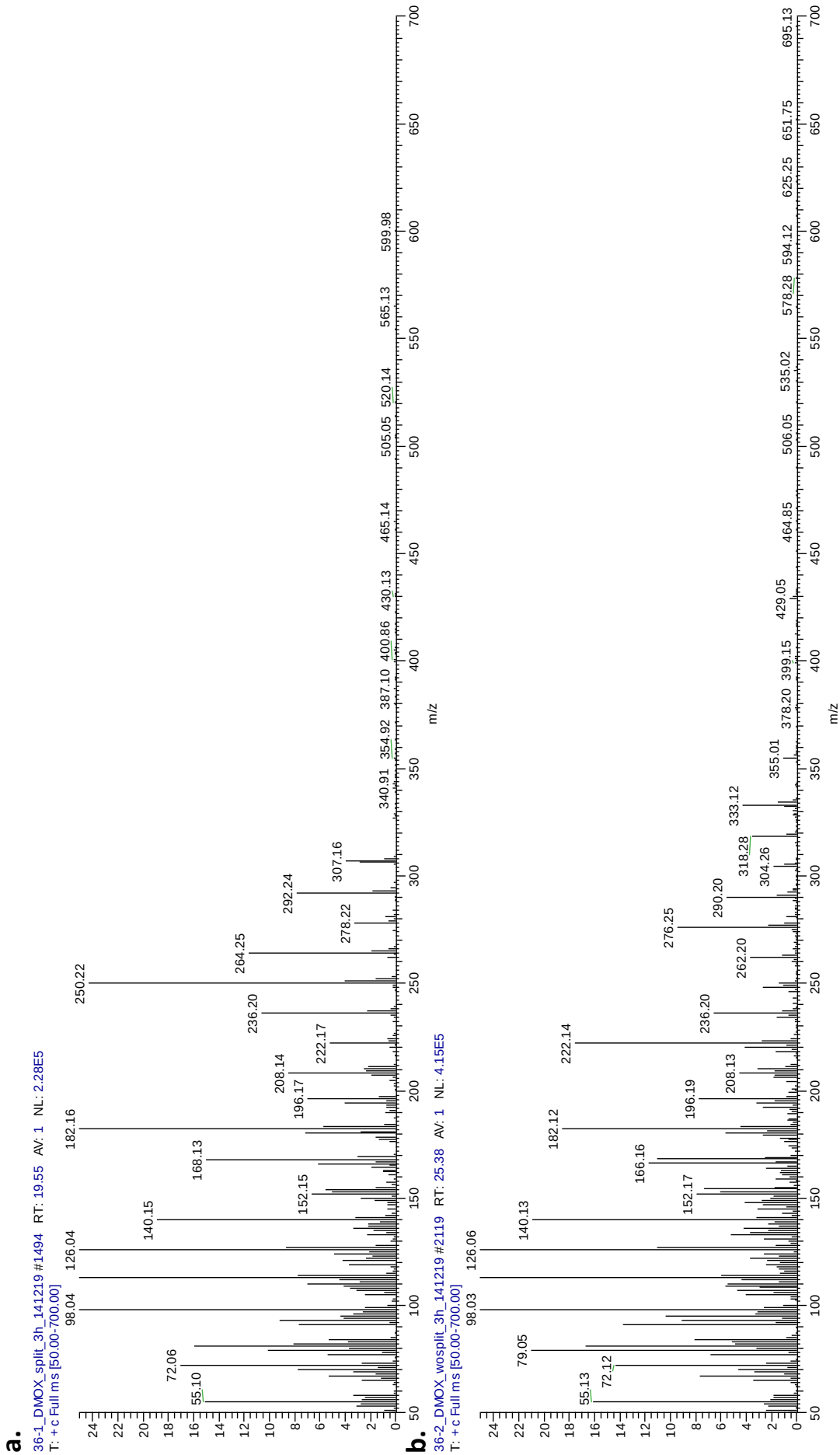

Figure 8-5: MS spectra of DMOX derivatives of RC 36.1 and RC 36.2.
a,b: MS spectra of DMOX derivatives of RC 36.1 (a) and RC 36.2 (b).

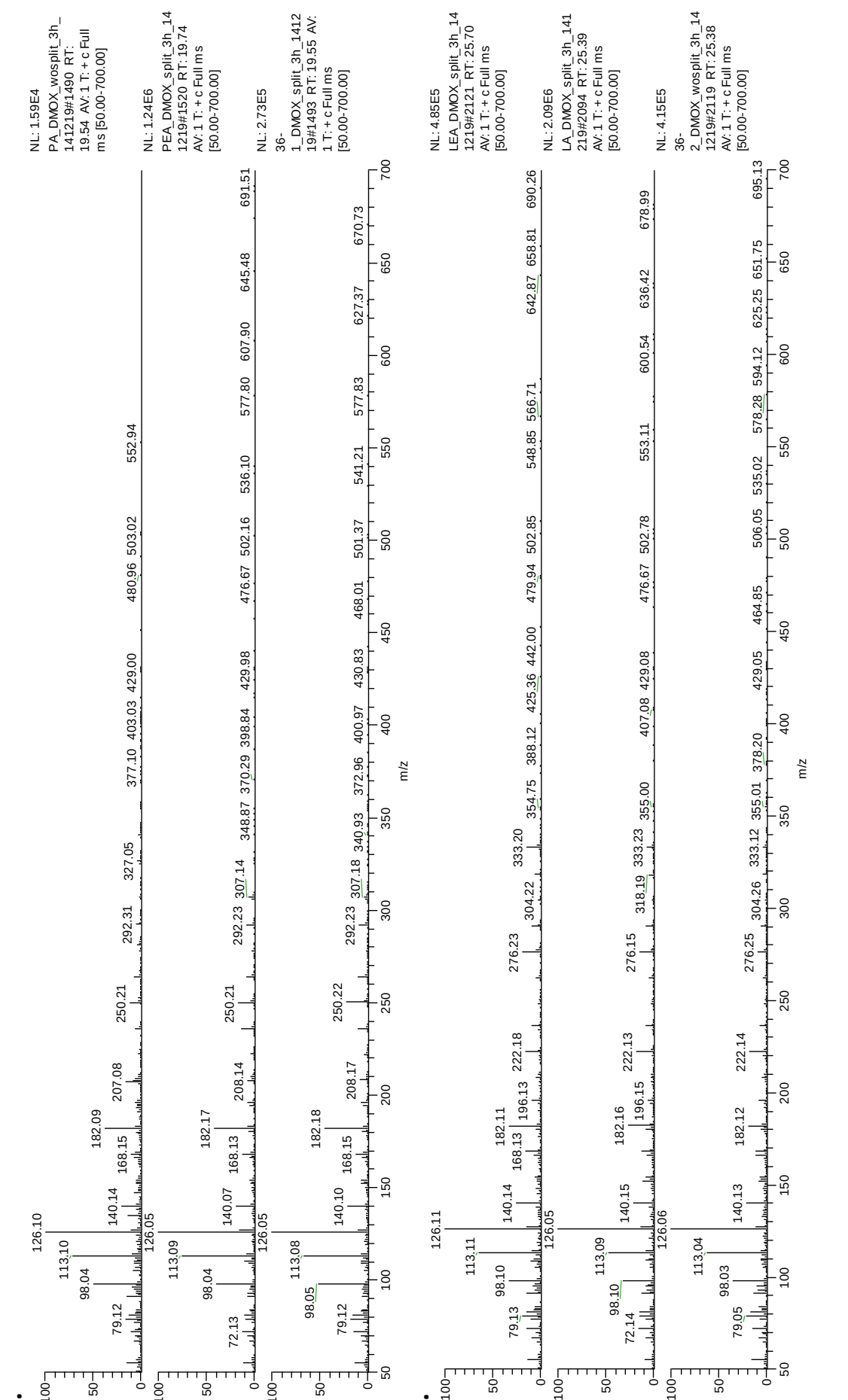
a.
NL: 1.59E4
PA_DMOX_wosplit_3h_141219#1490 RT: 19.54 AV: 1 T: + c Full ms [50.00-700.00]
NL: 1.24E6
PEA_DMOX_split_3h_141219#1520 RT: 19.74 AV: 1 T: + c Full ms [50.00-700.00]
NL: 2.73E5
36-1_DMOX_split_3h_141219#1493 RT: 19.55 AV: 1 T: + c Full ms [50.00-700.00]
b.
NL: 4.85E5
LEA_DMOX_split_3h_141219#2121 RT: 25.70 AV: 1 T: + c Full ms [50.00-700.00]
NL: 2.09E6
LA_DMOX_split_3h_141219#2094 RT: 25.39 AV: 1 T: + c Full ms [50.00-700.00]
NL: 4.15E5
36-2_DMOX_wosplit_3h_141219#2119 RT: 25.38 AV: 1 T: + c Full ms [50.00-700.00]
m/z

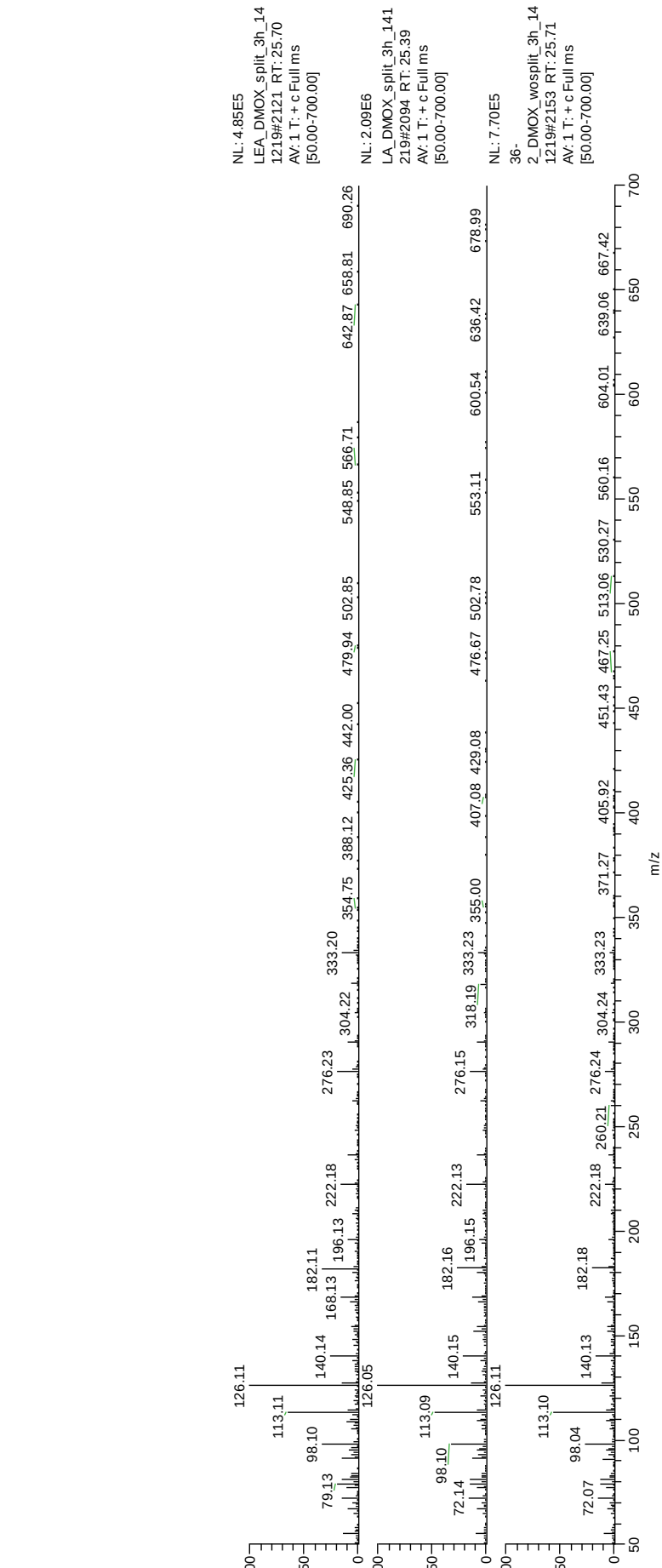

Figure 8-6: MS spectra of DMOX derivatives of RC 36.1 and RC 36.2 compared to those of commercially available fatty acids.
a: MS spectrum of DMOX derivatives of …
a: …PA at 19.54 min (upper), PEA at 19.74 min (middle) and RC 36.1 at 19.55 min (lower).
b: …LEA at 25.70 min (upper), LA at 25.39 min (middle) and RC 36.2 at 25.38 min (lower).
c: …LEA at 25.70 min (upper), LA at 25.39 min (middle) and RC 36.2 at 25.71 min (lower).

9 Conference contributions

Katharina Rox, Klaus Gerth, Manfred Rohde, Gursharan Singh Chhatwal, Rolf Müller (September 2014); poster presentation: **Targeting virulence: Inhibition of a streptococcal key pathogenic mechanism by bacterial natural compounds**. Annual Meeting of the German Pharmaceutical Society (DPhG) - Trends and Perspectives in Pharmaceutical Sciences, Frankfurt/Main, Germany

Katharina Rox, Klaus Gerth, Manfred Rohde, Gursharan Singh Chhatwal, Rolf Müller (October 2014); poster presentation: **Inhibition of streptococcal invasion by bacterial natural compounds - a possible way to encounter persistence and dissemination**. 4th Joint Conference of the German Society for Hygiene and Microbiology (DGHM) and Association for the General and Applied Microbiology (VAAM), Dresden, Germany

10 Acknowledgements

First of all, I sincerely thank Prof. Dr. Rolf Müller and Prof. Dr. Gursharan Singh Chhatwal for entrusting me with this interesting topic related to the possibility to combine several disciplines within one work.

I thank Prof. Dr. Rolf Müller for the faith he put in me, his willingness to give me plenty of rope in elaborating the subject without leaving me alone when problems and questions arose. I sincerely appreciated his scientific and personal advice. In addition, I am very thankful for the opportunity to broaden my network on the HZI- and HIPS-campus and to work and learn at three different spots and several distinct laboratories.

Equally, I thank Prof. Dr. Gursharan Singh Chhatwal for the trust he gave me and his support during the first 18 months of my thesis despite challenging conditions. I am grateful for the insights into his scientific way of thinking and for the initiative to apply for my visiting scholarship at the University of Queensland in Brisbane, Australia.

Furthermore, I thank Prof. Dr. Manfred Rohde for welcoming me in his group after closure of the Department of Medical Microbiology. I am grateful for his suggestions and for sharing his ideas with me during thesis committees and internal meetings. Furthermore, I thank him for acting as a second reviewer of my thesis.

Moreover, I sincerely thank Prof. Dr. Mark J. Walker for giving me the possibility to spend one month in his laboratory at the University of Queensland in Brisbane, Australia. I am grateful for all the ideas he shared with me concerning the plasminogen/fatty acid-project, especially for the opportunity to conduct so many mice experiments in his lab.

In addition, I thank his post-doc Dr. Christine M. Gillen for sharing her knowledge with regard to animal experiments with me and making my stay in Brisbane so enjoyable. Furthermore, I thank the whole Walker lab and people from related labs for welcoming me so warmly, especially Olga, Alvin and Tania.

I thank Prof. Dr. Rolf Hartmann for acting as my scientific advisor at the Saarland University and for his suggestions during my thesis committees.

I thank Dr. Torsten Loof for his idea to extend my project on *in vivo* experiments and for his assistance in the accomplishment. Moreover, I thank him both for interesting scientific and personal conversations.
I am grateful to Dr. Alberto Plaza for initiating the salinimyxantin-project with me and for good cooperation. In addition, I thank Suvd Nadmid and Dr. Alberto Plaza for providing me with salinimyxantins.

I am grateful to Dr. Rolf Jansen for sharing his knowledge concerning purification and isolation of compounds with me and for critically reading parts of my thesis. Moreover, I thank him for enriching scientific discussions.
I am also thankful to Kerstin Schober and Sabrina Wolpers with regard to technical advice and for a good working atmosphere in the chemical laboratory.
In addition, I thank Prof. Dr. Mark Stadler for giving me the opportunity to carry out some of my experiments in the MWIS lab and for his helpful (not only scientific) advice and discussions.
I thank Aileen Gollasch for HR-ESIMS- and Christel Kakoschke for NMR-measurements and Dr. Jutta Niggemann for taking part in my thesis committees and helping me with analytical questions in the beginning of the project.
Moreover, I thank Diana Telkemeyer for advice given during cultivation of myxobacteria and for the possibility to learn so much about myxobacteria from her.
Then I would like to acknowledge Yan-Yan Beer, Dr. Melanie Lüttge and PD Dr. Patric Nitsche-Schmitz for initial proof-of-concept studies and Stephanie Peter for assistance in preparation of recombinant streptokinase.
I am also thankful to Cäcilia Schwager and Dr. Matthias Keck who helped me when problems with the GC-MS arose. I also thank Dr. Klaus Gerth and PD Dr. Joachim Wink for good cooperation.
I am grateful to Steffen Bernecker and Reinhard Sterlinski who prepared the fermenter with me and took care for the technical issues during large-scale fermentation.
In addition, I thank Ina Schleicher for processing my samples for electron microscopy, her excellent technical assistance and Prof. Dr. Manfred Rohde for taking the SEM pictures.
Moreover, I am grateful to Dr. Oliver Goldmann for reading parts of my thesis and for his critical comments.

I would like to thank the members of the different labs (MMIK, ZEIM, INI, MINS, MWIS and MISG) for the pleasant working atmosphere and in particular Katja Mummenbrauer and Dr. Oliver Goldmann who gave me a hand whenever technical issues had to be solved. Moreover, I especially thank Jenni, Daniel, Ronald, Stephan, Simon, Ram, Uli and Angie for making my stays in Saarbrücken enjoyable in

several ways. In addition, I would like to thank my friends Christin, Anja, Matze, Robert, Fabio, Kathi, Aleyo and Diego for not only helping me with scientific and technical issues, but also for enriching my everyday life outside the lab.
In addition, I thank Sandra, Celina and Marius for their friendship since the beginning of our pharmacy studies until today.

I am grateful to the DAAD and the Go8-Initiative for funding my stay in Australia. Furthermore, I am thankful for funding by the President's Initiative and Networking Fund of the Helmholtz Association of German Research Centers under the contract number VH-GS-202. I also thank the HZI International Graduate School for enabling my attendance at interdisciplinary courses and conferences.

I also especially thank my sister Barbara for critically reading my thesis.
Finally, I sincerely thank my parents and my sister for their patience, their faith in me and for their support throughout my whole life.